CAPITAL UNIVERSITY OF SCIENCE AND TECHNOLOGY, ISLAMABAD

Molecular Characterization and Computational Analysis of Drug-Resistant Strains of *Mycobacterium tuberculosis*

by

Muhammad Tahir Khan

A thesis submitted in partial fulfillment for the degree of Doctor of Philosophy

in the

Faculty of Health and Life Sciences
Department of Bioinformatics and Biosciences

2020

Molecular Characterization and Computational Analysis of Drug-Resistant Strains of *Mycobacterium tuberculosis*

By

Muhammad Tahir Khan

(PI133001)

Dr. Yu-Juan Zhang, Professor

Chongqing Normal University, Shapingba, Chongqing, China

(Foreign Evaluator 1)

Dr. Neil Crickmore, Professor

School of Life Sciences, Sussex University, UK

(Foreign Evaluator 2)

Dr Shaukat Iqbal Malik

(Thesis Supervisor)

Dr. Sahar Fazal

(Head, Department of Bioinformatics and Biosciences)

Dr. Muhammad Abdul Qadir

(Dean, Faculty of Health and Life Sciences)

DEPARTMENT OF BIOINFORMATICS AND BIOSCIENCES

CAPITAL UNIVERSITY OF SCIENCE AND TECHNOLOGY

ISLAMABAD

2020

To My Mother, Father and Family

CERTIFICATE OF APPROVAL

This is to certify that the research work presented in the thesis, entitled "**Molecular Characterization and Computational Analysis of Drug-Resistant Strains of Mycobacterium Tuberculosis**" was conducted under the supervision of **Dr. Shaukat Iqbal Malik**. No part of this thesis has been submitted anywhere else for any other degree. This thesis is submitted to the **Department of Biosciences, Capital University of Science and Technology** in partial fulfillment of the requirements for the degree of Doctor in Philosophy in the field of **Bioinformatics**. The open defence of the thesis was conducted on **June 10, 2020**.

Student Name : Mr. Muhammad Tahir Khan
(PI-133001)

The Examination Committee unanimously agrees to award PhD degree in the mentioned field.

Examination Committee :

(a) External Examiner 1: Dr. Jamil Ahmed
Professor
University of Malakand, Chakdara,
Lower Dir, KPK

(b) External Examiner 2: Dr. Sajid Pervaiz Malik
Professor
QAU, Islamabad

(c) Internal Examiner : Dr. Samra Bashir
Professor
CUST, Islamabad

Supervisor Name : Dr. Shaukat Iqbal Malik
Professor
CUST, Islamabad

Name of HoD : Dr. Sahar Fazal
Associate Professor
CUST, Islamabad

Name of Dean : Dr. Muhammad Abdul Qadir
Professor
CUST, Islamabad

AUTHOR'S DECLARATION

I, **Mr. Muhammad Tahir Khan (Registration No. PI-133001),** hereby state that my PhD thesis titled, '**Molecular Characterization and Computational Analysis of Drug-Resistant Strains of Mycobacterium Tuberculosis**' is my own work and has not been submitted previously by me for taking any degree from Capital University of Science and Technology, Islamabad or anywhere else in the country/ world.

At any time, if my statement is found to be incorrect even after my graduation, the University has the right to withdraw my PhD Degree.

(Mr. Muhammad Tahir Khan)

Dated: 1 0 June, 2020

Registration No : PI-133001

PLAGIARISM UNDERTAKING

I solemnly declare that research work presented in the thesis titled **"Molecular Characterization and Computational Analysis of Drug-Resistant Strains of Mycobacterium Tuberculosis"** is solely my research work with no significant contribution from any other person. Small contribution/ help wherever taken has been duly acknowledged and that complete thesis has been written by me.

I understand the zero tolerance policy of the HEC and Capital University of Science and Technology towards plagiarism. Therefore, I as an author of the above titled thesis declare that no portion of my thesis has been plagiarized and any material used as reference is properly referred/ cited.

I undertake that if I am found guilty of any formal plagiarism in the above titled thesis even after award of PhD Degree, the University reserves the right to withdraw/ revoke my PhD degree and that HEC and the University have the right to publish my name on the HEC/ University Website on which names of students are placed who submitted plagiarized thesis.

(Mr. Muhammad Tahir Khan)

Dated:　　10　June, 2020

Registration No : PI-133001

List of Publications

It is certified that following publication(s) have been made out of the research work that has been carried out for this thesis:-

1. **Khan, MT** and Malik, S. I. (2019). *Structural dynamics behind variants in pyrazinamidase and pyrazinamide resistance.* Journal of Biomolecular Structure and Dynamics, pp. 1-15.

2. **Khan, MT**, Rehman, A. U., Junaid, M., Malik, S. I., and Wei, D. Q. (2018). *Insight into novel clinical mutants of RpsA-S324F, E325K, and G341R of Mycobacterium tuberculosis associated with pyrazinamide resistance.* Computational and Structural Biotechnology Journal, 16, pp. 379-387.

3. **Khan, MT**., Malik, S.I., Bhatti, A.I., Ali, S., Khan, A.S., Zeb, M.T., and Fazal, S. (2018). *Pyrazinamide-resistant Mycobacterium tuberculosis isolates from Khyber Pakhtunkhwa and rpsA mutations.* Journal of Biological Regulator and Homeostatic Agents, 32(3), pp. 705-709.

4. **Khan, MT**, Junaid, M., Mao, X., Wang, Y., Hussain, A., Malik, S. I., and Wei, D. Q. (2019). *Pyrazinamide resistance and mutations L19R, R140H, and E144K in Pyrazinamidase of Mycobacterium tuberculosis.* Journal of Cellular Biochemistry, 120(5), pp. 7154-7166.

5. **Khan, MT**., Malik SI., Ali S., Masood N., Nadeem T., Khan AS., Afzal MT (2019). *Pyrazinamide resistance and mutations in pncA among isolates of Mycobacterium tuberculosis from Khyber Pakhtunkhwa, Pakistan.* BMC Infectious Disease, 6;19(1), pp. 116-116.

6. **Khan, MT**., Khan A., Rehman, A.U., Wang, Y., Akhtar, K., Malik, S.I., and Wei, D.Q (2019). *Structural and free energy landscape of novel mutations in ribosomal protein S1 (rpsA) associated with pyrazinamide resistance.* Scientific Reports, 9(1), pp.1-2.

7. **Khan, MT**., Malik, S. I., Ali, S., Sheed Khan, A., Nadeem, T., Zeb, M. T., and Afzal, M. T. (2018). *Prevalence of pyrazinamide resistance in khyber Pakhtunkhwa, Pakistan.* Microbial Drug Resistance, 24(9), pp. 1417-1421.

Muhammad Tahir Khan

(PI133001)

Acknowledgements

(Muhammad Tahir Khan)

Abstract

Tuberculosis (TB) is one of the leading health problem caused by *Mycobacterium tuberculosis* (MTB). The standard new therapy of TB includes a six-month treatment of four recommended first-line drugs, isoniazid, rifampicin, pyrazinamide and ethambutol. However, the misuse of these drugs has led to the emergence of drug resistance MTB. Pyrazinamide (PZA) is an important component of first-line drugs because of its distinctive capability to kill subpopulations of persistent MTB under latent stage, where other drugs fail to work. The drug in initial stage requires a conversion into pyrazinoic acid (POA), an active form of PZA, by the activity of *pncA* encoded pyrazinamidase (PZase) enzyme. POA targets the ribosomal proteins S1 (RpsA) and aspartate decarboxylase (PanD). Mutations in *pncA* have been considered as the most common and primary cause of PZA-resistance. However, in minor cases, mutations in *rpsA* and *panD* have also been accounted in resistance. The major aims of this study was, to explore the prevalence of PZA-resistance in a geographically distinct region, Khyber Pakhtunkhwa province of Pakistan, molecular characterization, mechanisms of PZA-resistance behind mutations, and network analysis under latent stage. Samples have been taken and cultured from TB suspects, followed by PZA drug susceptibility testing on MTB positive samples. Genomic DNA was extracted and PCR products of *pncA*, *rpsA*, and *panD* was sequenced for mutations. To find the mechanism of PZA-resistance, the mutants and wild type proteins activities were analyzed through computational molecular dynamic simulations (MD simulation) at different time periods. Among 4518 TB samples, 754 (16.7%) subjects were detected as MTB positive. Out of total positive, 69 (14.8%) isolates were detected as PZA-resistance. The resistance isolate along with PZA-sensitive and one of each, H37Rv and *Mycobacterium bovis* as controls, were sequenced to analyze the mutations in the coding regions of *pncA*, *rpsA*, and *panD*. Thirty-six different mutation were identified in *pncA* of 51 PZA-resistant isolates. The sequences have been submitted to GeneBank (GeneBank Accession No. MH461111). Out of 36, fifteen mutations, including two deletion, 194-203delCCTCGTCGTG and 317-318-del-TC, have not been reported earlier. While, 18 resistance isolates lacked mutation in *pncA* (pncA$^{\text{WT}}$).

Mutations have not been detected in PZA sensitive isolates except, a single synonymous mutation at position C195T (Ser65Ser). Among 18 pncA^{WT} isolates, 11 have mutation in *rpsA* while seven were found as pncA^{WT} and rpsA^{WT} PZA-resistant. We identified 14 non-synonymous and one synonymous mutations in the coding region of *rpsA* gene. The remaining seven PZA-resistant isolates did not reveal any mutation. The sensitivity and specificity of the *pncA* sequencing method were 79.31% (95% CI, 69.29% to 87.25%) and 86.67% (95% CI, 69.28% to 96.24%). MD simulations analysis showed a significant variation in structures and activity between wild type and mutant PZase and RpsA proteins. Stability, flexibility, total energy, and drug binding pocket of these proteins also have been altered. Regulatory pathway analysis revealed that SigH and RshA are the major regulators under latent stage, receiving signals from PknB that might be an alternative drug target in PZA-resistance cases. In conclusion, mutation in the *pncA* is a major mechanism of PZA-resistance among circulating isolates. Molecular methods of investigating PZA-resistance are better to expose the cause of PZA resistant. In PZA-resistance, mutations in *pncA* and *rpsA* have been detected, altering the overall activity, causing a weak interactions with PZA and POA. Exploring alternative drug targets through investigation of regulatory pathways might be useful for alternative drug target identification and designing new drugs under latent stage of MTB. This study offers valuable information for better management of TB and drug resistance.

Contents

List of Figures

List of Tables

Abbreviations

AFB	Acid-Fast Bacilli
AIDS	Acquired Immunodeficiency Syndrome
AM	Alveolar Macrophage
AMK	Amikacin
ANIMO	Analysis of Networks with Interactive Modeling
APCs	Antigen Presenting Cells
BAL	Bronchoalveolar Lavage
BCNs	Boolean Control Networks
BLAST	Basic Local Alignemnt Search Tool
BNs	Boolean Networks
BSL-III	Biosafety Level-III
CAP	Capreomycin
CASTp	Computed Atlas of Surface Topography of proteins
CDC	Center for Disease Control
CIP	Ciprofloxacin
CRISPR	Clustered Regularly Interspaced Undersized Palindromic Repeat
CSF	Cerbrospinal Fluid
CTAB	Cetyltrimethylammonium Bromide
CUPSAT	Cologne University Protein Stability Analysis Tool
DCs	Dendritic Cells
DCCM	Dynamic Cross Correlation
DNA	Deoyribo Nucleic Acid
DST	Drug Susceptibility Testing
DTO	District Tuberculosis Office

EMB	Ethambutol
FR	Flanking Region
GMTV	Genome-wide *Mycobacterium tuberculosis* variation
GU	Growth Unit
HIV	Human Immunedeficiency Virus
HMC	Hayatabad Medical Complex
IDA	Intelligent Data Analysis
INH	Isoniazid
KAN	Kanamycin
KEGG	Koyoto Encyclopedia of Gene and Genome
KPK	Khyber Pakhtunkhwa
KTH	Khyber Teaching Hospital
LAM	Lipoarabinomannan
LEV	Levofloxacin
LM	Lipomannan
MDR	Multi-Drug Resistance
MD	Molecular Dynamics
MGIT	Mycobacterium Growth Indicator Tube
MMGBSA	Molecular Mechanics Generalized Born Solvent Accessibility
MMTH	Mufti Mehmood Teaching Hospital
MMFF94X	Merck Molecular Force Field 94x
MOE	Molecular Operating Environment
MOX	Moxifloxacin
MTB	*Mycobacterium tuberculosis*
MTBC	Mycobacterium tuberculosis Complex
MTs	Mutants
NAD	Nicotinamide Adenine Dinucleotide
NALC	NaOH/N-acetyl-L-cystein
NCBI	National Center for Biotechnology Information
NTP	National Tuberculosis Control Program
OFX	Ofloxacin

ORF	Open Reading Frame
PBN	Probabilistic Boolean Network
PCA	Principal Component Analysis
PCR	Polymerase Chain Reaction
PDB	Protein Data Bank
PIM	Phosphatidylinositol Mannosides
PMDT	Programmatic Management of Drug Resistant TB
POA	Pyrazinoic Acid
PROVEAN	Protein Variation Effect Analyzer
PZA	Pyrazinamide
PZase	Pyrazinamidase
QAPRTase	Quinolinic Acid Phosphoribosyl-Transferase
RefSeq	Reference Sequence
RIF	Rifampin
RMSD	Root Means Square Deviation
RMSF	Root Means Square Fluctuation
Rg	Radius of Gyration
RNA	Ribonucleic Acid
RPM	Rounds Per Minute
RpsA	Ribosomal Protein S1
SDM	Site Directed Mutator
SDS	Sodium Dodecyle Sulphate
SigH	Sigma Factor H
SIFT	Sorting Intolerant From Tolerant
STBs	Smooth Tuberculosis Bacilli
SVM	Support Vector Machine
TB	Tuberculosis
TBDRM	Tuberculosis Drug Resistance Mutation Database
TBE	Tris Borate EDTA Buffer
TLR	T-Lymphocyte Receptors
TNF	Tumor Necrosis Factor

TRs	Transcriptional Regulators
WGS	Whole Genome Sequences
WHO	World Health Organization
WT	Wild Type
XDR	Extensively Drug Resistance

Chapter 1

Introduction

1.1 Background

Tuberculosis (TB) is a worldwide communicable disease of human beings caused by *Mycobacterium tuberculosis* (MTB). It is now considered as one of the most shocking health problems, attacking the breathing system. However, in some cases the organism may spread to other body parts called extra-pulmonary TB. In 1950s and 1960s, a well-organized treatment was introduced with the hope to control the incidence worldwide, resulted in a significant reduction of TB incidence [1]. However, the disease still remains a major public health problem in most parts. WHO in 2012 announced Global Public Health Emergency because of a huge morbidity and mortality worldwide. The major causes of drug failure were accounted as the improper and incomplete use of drug, leading to the appearance of drug resistance. The disease was ranked second principal source of death among infectious diseases after HIV/AIDS [2]. Landry and Menzies in 2008 reported that about one third of the global population harboring MTB. In the light of previous reports, there are five high TB burden countries, India, Indonesia, China, Philippines, and Pakistan with 56 % of global TB [3]. Illiteracy, improper treatment, poverty accounted for drug resistant. Further, multi-drug resistance TB (MDR-TB) has been reported as 3.3% in new cases while 20% in previously treated cases [4].

1.1.1   WHO Global Report

According to the latest report 2018, TB caused 1.3 million deaths among HIV-negative in addition to 300000 deaths from TB and HIV-positive individuals. Globally, 10.0 million people developed TB disease: 5.8 million among men, 3.2 million among women, and 1.0 million among children. Overall 90% were adults (aged >15 years), 9% were HIV positive (72% in Africa). Two thirds of global TB incidence were reported from eight countries: India (27%), China (9%), Indonesia (8%), the Philippines (6%), Pakistan (5%), Nigeria and Bangladesh (4%), and South Africa (3%). Thirty high TB burden countries including these eight, accounted for 87% of global TB cases. The lowest incidence have been reported from WHO European Region (3%) and WHO Region of the Americas (3%) [5]. Drug-resistant TB remains a major problem in 2018. Worldwide 558,000 people were resistant to the most efective firstline drug, rifampicin (RR-TB), while 82% had MDR-TB. Globally, MDR have been reported in 3.5% of new (diagnostic) TB cases and 18% of previously treated cases.

In 2017, TB was the leading problem among infectious diseases from a single microorganism, ranked top leaving behind HIV/AIDS, while ninth in leading causes of death worldwide. Among HIV negative people, there were an estimated 1.3 million TB deaths excluding 374,000 among HIV-positive people (10%). Majority of the incidence reported here are; 45% from WHO South-East Asia Region, 25% WHO African Region, and 17% from WHO Western Pacific Region. WHO Eastern Mediterranean Region, the WHO European Region, and the WHO Region of the Americas has a smaller incidence of 7%, 3%, and 3% respectively. India, Indonesia, China, Philippines, and Pakistan are the top five countries with 56% of estimated cases [6]. Among the infected people, only 5-10% develop active TB in population. However, all the infected individuals do not eliminate MTB effectively. Such individual have persistent TB, where the MTB resides in macrophages of alveoli in non-replicative form known as latent stage. The risk to develop active TB is 10% [7] but may increases in case of HIV infections, immunosuppressive therapy and aging.

1.1.2 Etiology of Tuberculosis

Mycobacterium tuberculosis, the causative agent of TB, [8, 9] mainly found in the lungs where it resides in a round shaped nodule called tubercle, therefore, the bacterium is sometimes referred as tubercle bacillus. Mycobacteria can be categorized into numerous categories for reason of identification and cure. One of them is *M. tuberculosis* complex (MTBC), the causative agent of TB and *M. leprae* that causes leprosy. The second category called non-tubercle Mycobacteria (NTM), consists of all other mycobacteria, mostly non-pathogenic for humans, scattered in the surroundings. There are 140 species in this genus [10], in which a total of 50 species are human pathogenic [11]. Patients are most commonly affected by avium and intracellulare species [12, 13]. The MTBC is a collection of slow-growing organisms usually contains *M. tuberculosis*, *M. canettii*, and *M. africanum*, causing human TB in Africa; *M. microti* is the causative agent of TB in voles and *Mycobacterium bovis* infects diversity of mammalian species together with cattle and humans. Species of Caprae and pinnipedii are the two pathogens of animals [14]. Regardless of this genetically close connection, these organisms have different host priority and also phenotypically differ. Based on these observations, the researchers sometimes apply common species name instead of classifying them as one specie. In 1998 Cole and colleagues published the complete sequence of MTB H37Rv [15] where the G+C contents in the genome was detected as 65%, consisting of 4,411,532 base pairs (bp) genome. The last re-annotation recognized approximately 4,000 genes [16]. Plasmids have been found in a few species, but absent in MTB [17]. The genome also contains repetitive and insertion sequences (IS) in several mycobacterial species, including MTB. Molecular epidemiology of IS6110 and other clustered regularly interspaced undersized palindromic repeat (CRISPR) sequences have been paid special attention as they are used in spoligo-typing [18]. Further, IS6110 is also used as a marker for restriction fragment length polymorphism analysis [19]. MTB is rod-shaped bacterium with slow growth rate of 18-24 hours generation time [20]. Cell wall comprises of polysaccharides three layers and peptidoglycan containing mycolic acids, a type of complex fatty acid

making 30% of these components [21]. This property makes the envelope impermeable [22] also known as acid-fast bacilli (AFB) as the cell wall of mycobacteria impedes classical Gram staining [23]. The MTB cell wall consists of lower and upper two segments. Peptidoglycan (PG) layer is attached covalently with arabinogalactan (AG), connected with mycolic acids through short alpha-chain. Thus, mycolyl arabinogalactan peptidoglycan (mAGP) complex is called the core of cell wall. Longer and shorter fatty acids among free lipids are the major components of upper segment with shorter alpha-chains and longer chains respectively. Wall proteins, lipoarabinomannan (LAM), lipomannan (LM), phthiocerol containing lipids and phosphatidylinositol mannosides (PIMs) are embedded in these layers. Disruption of cell wall release LAM, proteins, PIMs, various solvents, and free soluble lipids, while insoluble residues are the mycolic acid arabinogalactan peptidoglycan complex [22].

1.1.3   Pathogenicity

In the human host, MTB normally find its way towards the alveolar passages of the lungs in the form of aerosols, where it encounters macrophages and dendritic cells of innate immune system, regarded as the major target cells of mycobacteria [24]. They need high concentration of oxygen (obligate aerobes), but may also stay alive in hypoxic conditions. Following infectivity, the host develops symptoms or it undergoes into latent stage. Within the body, MTB travel to the lungs and reaches the air sacs, where they are recognized as foreign and engulfed by body's macrophages followed by dissembling them under normal conditions. But in some cases of MTB infection, not all of the bacteria will be ruined by the immune system. In such case, the MTB take control of macrophages and multiply inside. The bacteria proliferate until macrophage burst, leading to additional illness and extracellular bacilli increase in number, give rise to granulomas. With the passage of time, granuloma's center necrotize, resulting in blood and sputum in the lungs [25]. The bacterium enters the alveolar macrophages by phagocytosis but possesses the power to run away from the macrophages eradication system and can survive

[26]. From phagocyte cell, the mycobacteria can spread to peripheral lymph nodes and other parts of lungs inspite of being responded by cell-mediated immune and humoral responses. Upon infection both, antigen-specific and innate immunity are elicited, inducing apoptosis in human alveolar macrophage (AM) by tumor necrosis factor (TNF) dependent mechanism [27]. The apoptotic response is postulated to be a defense mechanism, limiting the growth of MTB.

1.1.4   Tuberculosis and Human Immunodeficiency Virus

Tuberculosis pandemic is highly supported by HIV infections as it destroys the cell mediated immunity. TB and HIV co-infection significantly enhanced the incidence (12 to 14%) of TB worldwide. The highest rate was reported from African Region [4]. In Pakistan, the total TB-HIV co-infection was reported as 8.8 and 6.9 thousands in 2015 and 2016 WHO reports. A patient is more likely to suffer from TB because HIV kills T helper cells which are the effective weapons against MTB. HIV weakens the cellular immunity, leading to high incidence of TB [28]. At that moment the transmission risk of TB in community may also increases [29].

1.1.5   Drug Resistance

Drug resistance occurs whenever mutations, or chromosomal replication errors, arises in target or drug metabolic process. This results in the reduced effectiveness of antituberculosis therapies [30]. Resistant TB may be mono drug resistance when it resistant to a single drug or multi-drug resistance (MDR) when it shows resistance to INH and RIF. The third category of drug resistant TB is extensively drug resistant (XDR-TB). This group of MTB shows resistance to INH and RIF along with one of the fluoroquinolone and one injectable TB drugs. The standard time of TB treatment is six months while in case of multidrug and extremely drug resistance the duration of treatment may be extended upto two years or with more toxic and less potent. Further, the success rate of MDR and XDR is very low [30]. China, Russia, and India has a highest level of MDR-TB with 60% reported in

2013 data. XDR TB have been reported from 92 countries, showed 9.6% of MDR cases [4].

1.1.6 Mechanism of Drug Resistance

Very little information is available about the main mechanism that leads to the first-line drug resistance. However, mutations in the drug targets have been associated with drug resistance. RIF-Resistance in 96% of MTB isolates has been associated with mutation in the hot-spot region (rifampicin resistance-determining region) comprising 507-533 codons of *rpoB* gene [31]. Isoniazid (INH) resistance has been strongly linked with alteration in katG and inhA or its promoter region. The most common gene mutation identified so for in katG is S315T, results in lacking of isoniazid-NAD complex, required for its antimicrobial action [32]. Promoter region of inhA-15 is considered the next most frequent mutation site that results in low binding capability site of isoniazid-NAD adduct [33]. Further, inhA mutations may also affect the activity of structurally related drug, ethionamide as they have same target [34]. PZA is a structural analog of nicotinamide, discovered in 1952 [35]. It is a pro-drug, requiring the activity of PZase, a product of the 561-base-pairs *pncA* gene (Rv2043c) [36]. PZA is considered as a critical drug, playing a key role in reducing the treatment time from 9 to 6 months [37, 38]. The drug is recommended in combination with INH and RIF for short course chemotherapy [39]. The sterilizing activity of PZA, killing MTB persisters isolates, is the only drug among antituberculosis agents. In the 6 months treatment time, PZA is used in first 2-month intensive phase and the only drug that cannot be replaced without compromising treatment efficacy. Resistance to pyrazinamide (PZA) is associated with mutations in *pncA*. Most of the *pncA* mutation are dispersed in the entire gene of 561 base pair region in the ORF. Drug resistance to other first-line, RIF, INH, EMB, and OFX show connection between the phenotypic resistance and the target gene mutations in the drug resistance cases like katG (97%), inhA (3%), rpoB (95%), embB (65%), and gyrA/gyrB (94%) respectively [40]. However, PZA have several cellular targets where a disperse type of mutations are present in the

PZA activator, *pncA* gene. Approximately 70-97% of PZA-resistance emerges in the prodrug converting gene, *pncA* [41, 42] or putative regulatory isolates in MTB possess mutations in pyrazinamidase (PZase) region while 3-30% resistance have been linked with ribosomal proteins S1 (RpsA) and aspartate decarboxylase (panD) genes. PanD is involved in β-alanine biosynthesis, has been considered as new target of PZA. Mutations in this enzyme have been associated with resistance against PZA [43]. The enzyme is also involved in the synthesis of vitamin B5 (pantothenate), requiring for the synthesis of coenzyme "A" (CoA), that allows carbohydrates and fats to be burned to release energy.

1.2 Drug Resistance and Simulation

Computer simulations is an alternative of conventional experiments for exploring the properties of molecular structure and interactions among the atoms. Computer simulations of proteins and nucleic acid act as a bridge between microscopic length, time scales and experimental work in laboratory. We can deliver a deduction at the interactions among molecules and gain exact estimates of bulk properties. Simulations may act as a bridge between theoretical and experimental knowledge that may be tested by simulation of same model. Simulations on the computer are very useful in the sense when a test is difficult or impossible in the laboratory [44]. Molecular dynamics (MD) is a computer simulation procedure applied for studying the dynamics of a complex system of atoms and molecules. Under certain period of time, all the atoms and molecules interact and give a view of their interaction system. The trajectories of molecules are calculated for a system of interacting atoms and molecules by applying equations of motion where forces and potential energies are calculated using molecular force fields. Molecular systems consist of a bulk of molecules, therefore, analytical determination of properties of such systems is seemed to be impossible while MD simulation may solve this problem by using numerical procedures. MD is commonly applied for proteins 3D structure refinement obtained from NMR spectroscopy and X-ray crystallography. In structural biology, the method is frequently applied to study the motions of

atoms and molecules such as nucleic acids and proteins which may be important in protein structure modeling by simulating folding of the polypeptide chain and in ligand-receptor docking. The MD simulation results can be tested through laboratory experiments such as NMR spectroscopy. Advances in computational predictions and resources developed a hope for more and longer MD trajectories, in combination with more qualitative force field parameters, have resulted a large number of useful insight information in proteins structure prediction and receptors ligand interactions [45].

1.3 Regulatory Pathway Under Latent Stage

MTB faces a number of oxidoreductive stress generated by host defense in alveolar macrophages of lungs. These stress conditions include oxidative, acidic and nitrative, vital for the transition into dormant (non-replicative) state. MTB genomes has a diverse type of sensors, sensing stresses and switch to genetic program for transition into latency. A better understanding to explore these signaling pathways will help for control and designing potent drugs against non-replicative forms of MTB [46, 47]. Sigma (s) factors are the primary regulators of bacterial gene expression at primary level. There are 13 members of the sigma 70 family encoded by MTB genomes [15]. All these factors were categorized in four groups. Groups 1, 2, and 3 include SigA, SigB, and SigC respectively while the rest belong to group 4 that involved in signal sensing from extra-cytoplasmic location. They are also called 'S' factors involved in growth and stress response [48]. MTB sense redox by SigH, SigE, SigF and SigL, play important roles in the survival. Fernandes et al, was the first one that demonstrated the role of SigH in oxidative stress [49]. SigH is involved in regulating the expression of thioredoxins (trxB1 and trxC), thioredoxin reductase while SigE provide protection against oxidative stress. SigB expression is also regulated by SigE and SigH regulate stress-responders [50, 51]. Song et al. have verified the role of Rv3221a (RshA), anti-sigma factor of SigH present in the same operon as sigH [52]. RshA interacts with SigH in a 1:1 leading to the inhibition of SigH in vitro. During oxidative stress, phosphorylation of

RshA by PknB cause disruption of the interaction between RshA and SigH and thus regulates the induction of oxidative stress response by mycobacteria [53].

1.4   Modeling of Regulatory Pathway

The regulatory mechanism can be understood in more deep insight through mathematical and computational approaches for identifying the potential drug targets. One of these approach is Boolean Networks (BNs). The BNs consist of binary state variables with discrete-time dynamical systems. BNs have been applied as abstract modeling structures in various areas, including immune response, biological evolution, cell differentiation, neural networks, and gene regulation. The network provides a good framework for theoretical and qualitative analysis [54–57]. Inspite the simplicity of concept, complex biological systems can be modeled and understood for finding control strategies by the use of BN. To study the regulatory pathway, Boolean control networks (BCNs) are developed when a controls system is added. They takes one of the two values; 1 or 0. Here the value 1 indicate a particular entry is being made at that time point while value 0 indicate the effect of that entry has turned off. Such control system provides a deep understanding about the regulatory pathways of infectious agent under some specific conditions. BN modeling of stress regulatory pathway, sigH of *Mycobacterium tuberculosis* under the latent stage of TB is not reported. The pathway is activated in oxidative stress produced by host immune cells for eradication of MTB infection. Modeling of regulatory pathways will enable the clinicians for better insight understanding and developing effective TB management. One of the objective behind current investigation is to apply a system biology technique for modeling a signaling pathway of MTB under dormant conditions for better understanding and identification of alternative drug targets.

1.5   Tuberculosis in Pakistan

Pakistan has been ranked fifth among the top five high burden countries with 56% of global TB cases [6]. The WHO targets of TB control in Pakistan was adopted, detecting 70% of new cases every year, curing 85%. The incidence rate estimated in 2018 was 268 per 100000 population. Based on these estimates, the country reported a case detection rate of 64% for all types of TB [6, 58]. All these statistics are estimated one as there is no direct measures about the disease burden and how much these estimates are correct is still in question but the detection rate is encouraging one. The initial measures taken is to prevent the TB transmission, decreasing the TB burden in the country, and to increase the detection rate. Beside the National Tuberculosis Control Program (NTP), a large number of public and private health service practitioners are also attending a significant number of TB patients. These practitioner have already been informed to refer TB patient's to NTP but they do not follow the NTP guidelines regularly, leading to the emergence of drug resistant TB [59]. TB burden may be calculated by prevalence methods but such studies are costly and time-consuming. Pakistan has enhanced TB surveillance by introducing the Directly Observed Treatment Short course (DOTS). The DOTS has been found an affective approach in TB control, however, NTP still facing many challenges and did not got the full support of health care centers. Looking into the World Health Organization reports, tuberculosis and drug resistance in Pakistan has been remained a major public health problem [3, 60–62] (Table 1.1).

TABLE 1.1: Incidence of tuberculosis and drug resistance in Pakistan

Year	Incidence	Incidence/100000	Drug resistance
2011	410,000	231	3.4%
2012	410000	231	3.4%
2013	500,000	275	3.5%
2014	500,000	270	4.3%
2015	510,000	270	3.7%
2016	510,000	270	4.2%
2017	518,000	268	4.2%
2018	525,000	268	4.2%

1.6   Research Problem

PZA is a key first-line drug recommended by WHO along with RIF and INH to eliminate the persistant MTB under latent stage (Latent TB) in acdic and oxidative stress, where other drugs fail to work. In case of PZA-resistance there is no alternative drug which has been recommended by WHO. However, in other drug resistance, alternative second-line drugs have been made availble. PZA-resistance along with other drug resistance, is a major hurdle to achieve the goals of global TB control in high burden countries. The global report 2018 summarized that 56% of TB incidence have been reported from five high burden countries where Pakistan has been ranked fifth. Further, PZA is an important part of the first-line drug, recommended in short-course TB-treatment along with INH and RIF, shortened the treatment time from 9 to 6 months [63]. Due to high cidal effect at a low pH environment, PZA is also recommended in PZA-susceptible MDR-TB. An increasing number of PZA-resistant strains has been observed due to without precise knowledge of PZA DST, and its unstandardized usage in treatment may lead to develop resistance against other antibiotics. Majority of the geographic specific locations have not been able to explore the molecular level informations behind PZA-resistance. The lack of such information behind the PZA-resistance, further limit our knowledge about PZA-resistance in high burden countries that may further increase the incidence in geographic specifc location.

1.7   Research Philosophy

PZA is a pro-drug, activated by MTB encoded PZase, into pyrazinoic acid (POA), the active form of PZA. Mutations occurred in *pncA* gene are most commonly associated with PZA-resistance in vitro [64]. Therefore, sequencing of *pncA* gene in PZA-resistant isolates is better to identify mutations involved in resistance. Moreover, characterization and annotation is of particlular interest to identify the mutations of high, medium, and low level of resistance. For rapid analysis of such

mutations, numerous computational tools are available, where biological information are analyzed in a meaningful way. At a more integrative level, computational technologies have been found, useful in modeling of protein structures, predicting the effect of mutations on proteins properties, and molecular interactions. Further, pathways and network analysis of proteins might be useful for identification of some more potent drug targets for better management of drug resistance TB.

1.8   Problem in Focus

The estimated population of Khyber Pakhtunkhwa (KPK) province is about 26 million. A 51.6% increase has been detected in population since 1998 census, placing KPK above Islamabad, Punjab, and Azad Kashmir [65]. Geographically to the west, its borders touches the Tribal Areas, Gilgit Baltistan, to the northeast, Islamabad and Punjab to the east and southeast while it does not share border with Baluchistan, located in the southwest. It also shares an international border with Afghanistan through the historical Khyber Pass. Tuberculosis (TB) is a major public health problem in this province and unfortunately it has been one of the neglected health areas in the past. Now a TB control program has been established at Hayatabad Medical Complex Peshawar that regularly monitors the incidence and drug resistance in population. Multidrug resistance has been an emerging issue needed to be solved. In a previous study [66], 341 MDR follow up patients (previously treated) were enrolled to find the treatment outcomes. Results were alarming with elevated levels of first-line drug resistance (84.5%). MDR and XDR were found in 325 (95.3%) and 2(0.6%) cases, whereas 33 (99.4%), 326 (95.6%), and 31(93.5%) isolates were resistant to Isoniazid, Rifampicin, and pyrazinamide respectively. The appearance of large number of MDR cases shows that its transmission might be due to the improper treatment, illiteracy and poverty. Further, drug sensitivity testing is phenotypic, which is time consuming and their reliability is also an issue. Unfortunately, no molecular level study have been carried out that find the mutations of high level resistance. In our current study [67], a total of 1,075 MTB-positive isolates have been detected in one year screening of

TB suspects, in which 83 (7.7%) isolates have been detected as PZA-resistants. Among the resistant isolates, 76 (90%) and 67 (80%) were resistant to INH and RIF, whereas 63 (76%) were MDR. The resistance level of EMB, OFX, and SM among PZA-resistance were, 35 (42%), 40 (48%), and 41 (49-50%) respectively. More investigations are needed to find the actual incidence of drug resistance, prevalent in this geographical region.

1.9   Research Hypothesis

PZA-resistance have been commonly associated with mutations in *pncA*, with minor level in *rpsA* and *panD*. Screening of mutations in circulation isolates of geographically distinct region, KPK and computational analysis will extract some hidden informations about mechanism of resistance behind mutations in *pncA*, *rpsA*, *panD* and their association with PZA-resistance, present in MTB isolates, circulating in KPK population of Pakistan.

Analyzing the effect of these mutations on enzymes structure, functions, molecular interactions, dynamics, stability and the binding site (pocket size) might be useful to find the level and mechanism of resistance. Therefore, the current study was designed on screening of PZA-resistant strains from KPK province, Pakistan, a geographically different region, for characterization by sequencing of these genes.

MD simulations on wild types and mutants proteins and their comparison to study the effect on dynamics inclusing amino acid fluctuations, deviation, folding stability and ligand-receptor interactions and its distance will be useful to retrieve some meaningful informations behind PZA-resistance. These approaches are time efficient and offer less time for transmission. Regulation of MTB pathway under latent stage for more potent targets identification and the application of system biology approaches might be useful to unravel the regulatory network under latent stage. The foremost aim of this project was; to explore and understand the PZA-resistance and mechanism of resistance at molecular level.

1.10 Social and Economic Benefits of the Study

This is the first investigation on molecular scrutiny of PZA-resistance MTB isolates from KPK province of Pakistan. To the best of our knowledge, detailed information are not available regarding the molecular mechanism of PZA-resistance.

- This project will explore the data about prevalence of PZA-resistance among population of KPK for management of treatment in future.

- Secondly, geographically specific mutations will be useful in biomarkers development for rapid diagnosis of drug resistant TB.

- Thirdly, molecular dynamic simulations will explore the mechanism of PZA-resistance for better management of TB.

- The fourth, identification of new drug target under latent stage of TB, may be helpful in understanding the latent stage of MTB and its regulatory network.

Based on the literature search, the reserch gap was found which need to be filled through active investigations.

1.11 Objectives of the Study

The specific objectives behind the current study were:

- Identification of mutations in pyrazinamide resistant MTB isolates in KPK province.

- Molecular and functional characterization of mutations in PZA-resistance strains of KPK province, Pakistan.

- Pathway analysis of latent TB under oxidative stress.

1.12 Some Non-specific Objectives of the Study

- To explore the data about prevalence of PZA-resistance among TB patients of KPK for management of treatment in future.

- Secondly, the geographically specific mutations will be useful in biomarkers development for better and rapid diagnosis of PZA-resistance TB.

- Thirdly, characterization of mutations will extract some meaningful information behind resistance for better management of TB.

- The fourth, analysis of regulatory pathway will lead to some new target identification under latent stage of TB which might be helpful in understanding the regulatory network.

1.13 Research Methodology

The current research work has been carried out by adopting the four major steps, sample collection and processing, sequencing of PZA-resistance and sensitive isolate, computational analysis of novel mutations, and development of netwrok and pathways under latent TB.

The basic steps have been summarized as under.

1.13.1 Collection of Samples

Sample collections was performed in two phases with same protocoal.

- Ethical approval

- Sample collection

- Recording of TB suspects data

- Sample preservation

1.13.2 Processing and Culturing of Suspects Samples

- Processing of suspects samples

- Culturing of samples

- Identification of MTB

1.13.3 PZA Drug Susceptibility Testing (DST)

- Preparation of PZA-DST media

- Inoculum's preparation and inoculation of MGIT DST

- Interpretation of drug susceptibility testing

1.13.4 DNA Extraction

- Reagent preparation

- CTAB method

- Sonication method

1.13.5 Amplification of *pncA*, *rpsA*, and *panD*

- Reagent preparation

- Running of PCR

- Agarose gel electrophoresis

1.13.6 Sequencing of *pncA*, *rpsA*, and *panD*

- PCR products of *pncA*, *panD*, and *rpsA* genes were sequenced through 6 Applied Biosystems 3730xl (Macrogen Korea), Korean biotechnology company

1.13.7 Screening of Mutations in *pncA*, *rpsA*, and *panD*

- The sequence data of PZA-resistant and susceptible isolates of genes, *pncA*, *panD*, and *rpsA* were loaded into Mutation Surveyor V5.0.1 and BioEdit version 7.2.6.1, to analyze and compare with *pncA* (Rv2043c), *panD* (Rv3601c), and *rpsA* (Rv1630) gene of RefSeq database of NCBI (NC-000962).

1.13.8 Statistical Analysis

- Patient's data, location, age, treatment history, reason, sample-type, TB-type, HIV status, gender, and the drug resistant profile obtained after the drug susceptibility testing, was analyzed through Epi-Data.

1.13.9 Computational Analysis of Mutations

- MD simulation novel of mutants (MTs) and wild type (WT) PZase and RpsA.

- RMSD and RMSF of MTs and WT

- Principal component analysis of MTs and WT

- The Gibbs free energy calculation of WT and MTs

- Free energy calculation of WT and MTs

- Binding pocket measurement of WT and MTs

- Radius of gyration (Rg)

- Distance matrix

- Projection of motion (Eigenvectors)

- Fe^{+2} ion effect on MTs structure

- Prediction of mutation effect on PZase function

- Prediction of mutations effect on PZase stability

1.13.10 Pathway and Network Biology of Latent Stage

- Literature search for gene/proteins interacting under latent stage of MTB

- String network generation from gene/proteins

- Longest path identification among gene/proteins

1.14 Summary

We explored the prevalence of PZA-resistance in geographically distict location, Khyber Pakhtunkhwa province of Pakistan, molecular characterization of PZA-resistance isolates, and the mechanisms of PZA-resistance behind mutations in PZase and RpsA. The whole thesis has been structured in a systematic way into 6 chapters including chapter 1, describing the background of thesis title. Chapter 2 highlights the literature reviewed relevant to the field. Methodologies and materials have been described in Chapter 3, highlighting the major steps to complete PhD research work. Results and discussion have been explained in chapter 4 and 5 respectively. Chapter 6 describes the conclusion and recommendation followed by references and appendices section.

Chapter 2

Literature Review

2.1 Tuberculosis Burden

According to the world health organization report in 2017, 10.4 million TB cases occurred worldwide, including 5 millions (56%) men, 3.5 million (34%) women and, 1 millions (10%) children [60], where 58% incidence were reported from the South-East Asia and Western Pacific regions. Tuberculosis have been killed 1.5 million people (1.1 HIV-negative and 0.4 HIV-positive). The toll comprised 890 000 men, 480 000 women and, 140 000 children. Accordingly, 28% of the global incidence in 2014, African Region has reported the highest incidence rate (281/100 000), a double of worldwide average incidence (133/100,000). India has 23%, Indonesia 10%, and China has 10% of the global total. According to the WHO latest report 2017, WHO South-East Asia Region has been found on the top (45%) in TB incidence, followed by 25% and 17% from WHO African and WHO Western Pacific regions. WHO Eastern Mediterranean (7%) and European Region (3%) has a smaller proportion of TB incidence respectively. The annual incident of TB varied widely among countries in 2016, from under 10/100,000 population in developed countries to 150-300 in high TB burden countries, where as the Democratic People Republic of Korea, Lesotho, Mozambique, the Philippines and South Africa has an incidence of above 500 per 100,000 population.

WHO in 2017 established global report, according to which 56% of world TB have been reported from five high burden countries where Pakistan was ranked fifth [6]. MDR/RR-TB has been reported in twenty-six thousand individuals while the incidence rate of resistance cases per hundred thousand individuals was reported as fourteen among population. This provoke an alarming to the TB management in this high burden country.

2.2 Lineages

The Mycobacteria comprises a variety of closely linked organisms including *Mycobacterium bovis, caprae, microti, pinnipedii, origys, mungi, suricattae, the chimpanzee bacillus* [68] and also *M. africanum, M. tuberculosis sensu stricto* are adapted to humans. Inspite of these traditional species of MTBC, it also contains *M. canettii* and so-called smooth tuberculosis bacilli (STBs). The STBs are famous for their smooth colony formation as well some other important characteristics like horizontal gene transfer which differentiate it from other MTBC [69]. Further this group of bacterium rarely infects human and about sixty types have been characterized [70].

From evolutionary point of view, one group of MTBC have deleted genomic area called TbD1, also referred as evolutionary modern. While a group having no such deletion are known as the ancestral [71]. Based on the whole genome sequences (WGS) analyses, *Mycobacterium tuberculosis* complex (MTBC) have been classified into seven human-adapted lineages [72]. Lineage 2 and 4 are considered as the most prevalent groups. Lineage 2 widespread in Central and East Asia, South-Africa and Russia. Euro-American lineage 4 predominated in Europe, Asia, Africa and America. Lineages 1, 3 limited to East Africa, Central, South and South-East Asia. Lineages 5, 6 and 7 are restricted to only West Africa 1 and 2 also called *M. africanum* [73]. Lastly, two additional lineages inside the classical MTBC are adapted to diverse wild and household animal species. One of these two lineages comprise animal associated strains known as *M. bovis* (vaccinal strain BCG)[74].

2.3 Immunity

MTB is transmitted from person to person through aerosol and mainly resides in dendritic cells (DCs), antigen presenting cells (APCs), and macrophages as well in neutrophils and monocytes [75]. As a result, mycobacteria also infect these cells, resulting in granulomas formation, while in case of other infectious diseases, the APCs eliminate the disease causing organisms [76]. These bacteria have several mechanisms that add to their virulency for disseminations in the cells [77]. Further, there are multiple mechanisms of MTB for residing in host cell and stoping apoptosis [78]. Host has multiple recognition receptors that recognize MTB components for activation of innate immunity. Toll-like receptors, particularly TLR2 are most diverse in numbers, about 99 of recognized mycobacterial agonists, containing lipoproteins phosphatidyl inositol mannans and lipomannan. Further, MTB DNA is sensed by TLR9, causing the production of cytokines in mice [78].

2.4 Treatment of Tuberculosis

Drugs against TB are mainly classified into two major groups i.e. First-line drugs that include, Rifampicin (RIF), Isoniazid (INH), Pyrazinamide (PZA), Ethambutol (EMB), and Streptomycin (SM). These drugs are prescribed in the initial stage of TB while in case of resistance; second line drugs are prescribed which include, Fluoroquinolones: Levofloxacin (LEV), Ofloxacin (OFX), Ciprofloxacin (CIP), Moxifloxacin (MOX), and Injectable drugs: Amikacin (AMK), Capreomycin (CAP), and Kanamycin (KAN). The regular cure for fresh TB patients (defined as patients with no previous anti-TB treatment or with prior anti-TB treatment for less than 1 month) comprises of 2 months severe stage with daily INH/RIF/PZA/EMB followed by a 4 months nonstop period of daily INH/RIF (Table 2.1). These two drugs are the most effective agent for tuberculosis treatment. According to the a previous study [79], isoniazid (INH) is accountable for the early killing of around 95% bacteria in the initial days of cure, assisted

by rifampicin, regarded as the potent drug and pyrazinamide (PZA), which is effective against latent bacilli, uses during the rest of intensive phase. For drug resistant bacteria (MDR-TB), the treatment is complex with three groups of drugs i.e. injectable drugs, fluoroquinolone and oral bacteriostatic drugs. Injectable drug include aminoglycosides: streptomycin (STR), kanamycin (KAN), amikacin (AMK) which hinder protein synthesis, group 2 drugs (fluoroquinolone): ofloxacin, levofloxacin or moxifloxacin which effective against the DNA gyrase, involved in DNA replication and group 3 drugs (oral bacteriostatic drugs): Cycloserine which interferes with cell wall biosynthesis. The treatment regimen for MDR cases include of at least four effective drugs: one injectable drug (group 1, preferentially amikacin or kanamycin, since streptomycin STR resistance among MDR-TB is frequent), one fluoroquinolone (group 2), and one group 3 drug. Total period of treatment of drug-resistant TB is at least 18 months [80].

TABLE 2.1: Anti-tuberculosis first-line drugs and their targets

Drug	Effect on bacterial cell	Targets
Isoniazid	Bactericidal against replicating tubercle bacilli	Multiple targets e.g InhA
Rifampicin	Bacteriocidal activity	RNA polymerase β-subunit
Pyrazinamide	Bacteriostatic/bactericidal against non-replicating bacilli	Membrane energy Metabolism, RpsA, panD
Ethambutol	Bacteriostatic	Arabinosyl transferase
Streptomycin	Bactericidal	S12 protein (ribosomal) and 16S rRNA

2.5   Multidrug Resistant Tuberculosis

In clinical point of view, the enhancement in ability of bacterium to resist against drugs with high doses as compared to drug susceptible is called as drug resistance isolate. Resistant to isoniazid and rifampicin are termed as multidrug resistance (MDR). Strains which are MDR and also resistant to fluoroquinolone and at least one of three injectable second-line drugs (amikacin, kanamycin, capreomycin) are termed as XDR [81]. Some of the factors associated with drug resistance include,

the misuse, mismanage, wrong treatment, dosage or when the supply of drug is irregular. Resistance to drugs in MTBC may be primary or acquired in which patients infected with MTB strains, develop resistance inside patient body during the course of treatment. Primary resistance is considered difficult to control because approximately 20% of the drug resistant cases in the world are supposed to be correctly diagnosed, largely because of the reason that most of low income endemic areas have no suitable laboratory apparatus [82]. Another main cause of drug resistance are mutations, occuring in a particular locations of DNA, promoted through bacterial or extrinsic factors (environmental). The only possible reasons of these factors are either inappropriate treatment, patients non-adherence to treatment giudlines or delay diagnosis [83, 84] from side to side microbial cells that tolerate elevated levels of drug doses phenotypically (persisters), enhance the normal lifetime of bacteria exposed to drugs. The W.H.O estimated that there were 650,000 cases of MDR-TB worldwide in 2010 [58]. It expenses about 483,000 dollars to cure a single case of XDR-TB, and around 50% of this quantity is required for multi-drug resistant TB in the United States [85]. Drugs are selected with five groups on the basis of safety, efficacy and cost. The first category comprised of high-dose INH, RIF, PZA, and EMB. The 2nd category includes fluoroquinolone, in which high-dose levofloxacin is preferable. The 3rd category included the injectable drugs recommended in order of: capreomycin, kanamycin, and amikacin. The second-line TB drugs constitute the 4th group used in the following recommended order: thioamides, cycloserine, and aminosalicylic acid. The 5th group includes drugs whose efficacy is not yet fully determined and includes: amoxicillin with clavulanate, linezolid, carbapenems, clofazimine, thioacetazone, and clarithromycin [86].

2.6   Role of Pyrazinamide in Treatment

Among the first-line TB drugs, PZA possesses a unique property in reducing the TB treatment period from 9 to 6 months [87]. It is the only drug which is active against latent MTB under stress condition where other TB drugs fail [88]. This

behavior of PZA makes it an important drug for the treatment of susceptible as well as MDR-TB. Further, it has multiple targets, inhabiting the co-enzyme A, essential for persister survival, trans-translation and also energy production [42, 88, 89]. Resistance to PZA is frequently caused by mutations in *pncA* gene encoded, pyrazinamidase (PZase), involved in the conversion of pro-drug, PZA into active form pyrazinoic acid (POA). Phenotype based PZA susceptibility testing may give false result due to buffering issues, due to which the reliability is sometime low. Therefore, the most reliable method have been found as sequencing of *pncA* gene that is cost-effective, more rapid, and more reliable method. Molecular detection of PZA-resistance should be screened for better management of MDR/XDR-TB. In conclusion, PZA has been found essential component of front-line anti-TB agents inspiring new efforts to design novel kinds of antibiotics, targeting latent MTB [90].

2.7 PZA Activation and Mechanism of Action

PZA is a structural analog of nicotinamide, discovered in 1952 [35]. It is a pro-drug, requiring the activity of PZase, a product of the 561-base-pairs *pncA* gene (Rv2043c) [36], converting it into active form, pyrazinoic acid (POA) (Figure. 2.2) [91].
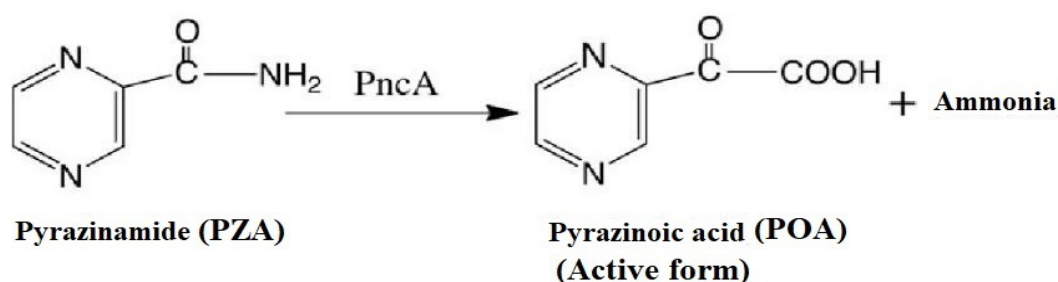
FIGURE 2.1: PZA Conversion into POA by PZase.
PZA conversion into POA, requires the activity of PZase enzyme, encoded by *pncA* [64].

Modern therapy of drug susceptible TB includes INH and RIF along with PZA for 6 months [63]. The drug has distinctive capability to kill the latent MTB
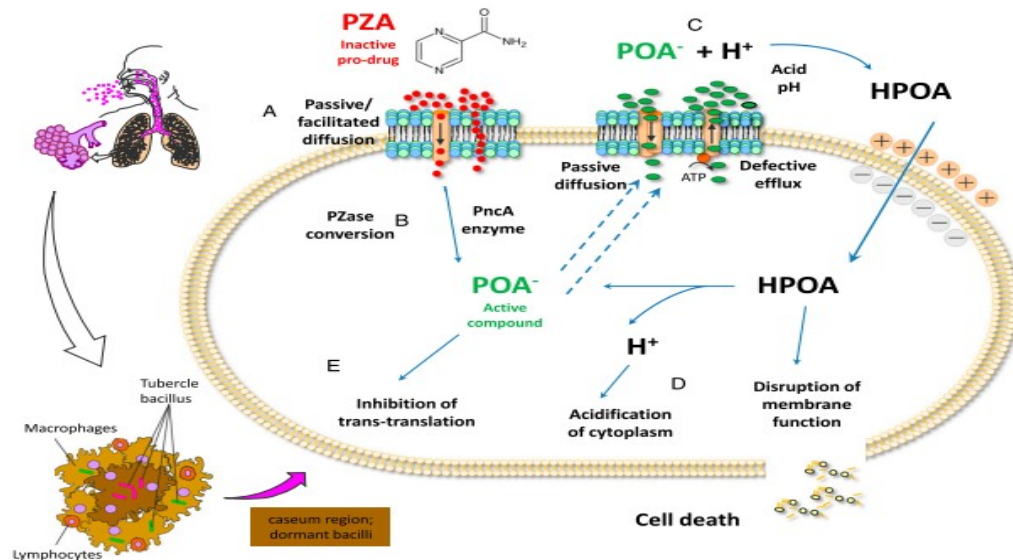
FIGURE 2.2: Mechanism of PZA action.
MTB residues in the macrophages of lungs in dormant stage. (A) PZA enters the bacterial cell through passive diffusion. (B) PZA is converted into active form, POA by MTB encoded PZase (*pncA*). (C) Some POA molecules are expelled ouside by weak efflux through passive diffusion. (D) POA causes acidic enviroment outside MTB cells and enter the cell along with H^+ ions (HPOA). This phenomena create acidic enviroment and causes disruption of MTB membrane. (E) POA also inhibite RpsA (trans-translation process) [92]

(semi-dormant bacilli) that continue its growth under acidic environments within macrophages [75], where the other drugs fail to act [93]. Mutations in *pncA* gene are strongly associated with PZA-resistance [74, 94–97] but not in all cases. These findings suggested that there may be multiple targets involved in PZA-resistance. Functionally important residues in PZase, Asp8, IIe133, Ala134 and Cys138, have been reported in the active site, might be altered by mutations, causing loss of function to convert the pro-drug PZA into active form POA. [98, 99]. The POA interferes with energy production which is the only source of its survival in host generated acidic environment [21]. Under host generated stress, the internal pH of phagolysosomes become weakly acidic and because of this change in pH, the drug lacks activity against such bacilli[26]. Further, a previous study reported that PZA has very poor bacteriostatic action against intracellular MTB in human monocytes-derived macrophages [100]. While Zhang et al. [101] reported that using an autoluminescent MTB reporter strain, the drug activity could be seen within three days of therapy, preliminary from the day following infection. The

drug enters bacilli through passive diffusion, converted into pyrazinoic acid (POA) by PZase where weak efflux pump causes the POA to be excreted, where the inefficient efflux pumps of MTB and acidic environment, the POA is reabsorbed and accumulated inside the cells, causing their damage. Some recent reports stated that PZA inhibits the catalytic activity of quinolinic acid phosphoribosyl-transferase (MtQAPRTase) [102], a key enzyme nicotinamide adenine dinucleotide (NAD) biosynthesis. PZA conversion into POA was [92, 103] observed as host-mediated in both TB patients and lab animals to model TB management. Further, they confirmed a good penetration of this pool circulating POA from plasma bacilli, residing in lung tissue and granulomas. They also found the oral bioavailability and revelation of POA in rabbits, guinea pigs, and mice. These findings suggested a medical investigation of oral POA as a remedial substitute to overcome *pncA*-mediated PZA-resistance.

2.8 Crystal Structures of PZase, RpsA, and PanD

The crystal structure of PZase encoded by *pncA* gene, was reported by Petrella [99] containing 185 amino acid, forming six β-sheets and four α-helix, resulting in a domain, consists of α/β structure (2.3-A). Cystein 138, an active site residue, located at N-terminal side of α-3 helix. Amino acids residues, Asp8, IIe133, Ala134 and Cys138 are most commonly associated with enzyme function and any mutations in this site will leads to loss of PZase activity. [99, 104–106]. However, diversed type of mutations present in whole PZase, away from active site but still they cause the loss of PZase activity because of their regulatory role in enzyme structure [107].

In MTB, there are four S1 domains of RpsA protein (2.3-C). Residues 292-363 are present in fourth S1 domain, also called C-terminus domain (MtRpsA$^{\text{CTD}}$) (2.3-B), capable of binding with POA. Amino acids F307, F310, H322, D352, and Arg357 forms RNA binding sites. PZA-resistance appears when mutations occurs in MtRpsA$^{\text{CTD}}$. Residues, Lys303, Phe307, Phe310, and Arg357 are present at

tmRNA binding site, involving in the interactions with two POA molecules [42, 89, 108]. Aspartate decarboxylase is a regulatory protein in the pantothenate pathway encoded by the panD gene [109]. The structure is predominantly consisting of seven B-strands, two alpha-helices, and two 3_{10} helices (2.3-D).

The PZase enzyme is encoded by *pncA* activate the PZA drug into active form pyrazinoic acid (POA) which has multiple target such as disrupting the membrane and its transport system, the RpsA and PanD. [90, 91, 110–112]. Consequently, mutations lead to alters the PZase, RpsA, and PanD activity, resulting PZA-resistance [36]. Non-synonymous mutations in *pncA* is the major cause of PZA-resistance [94]. Type of mutation and localization in PZase enzyme reduce the activity upto tenfold compared with native enzyme. [105, 106]. To explore the cause of resistance at molecular and atomic level, characterization of mutation is essential as its type, effect on enzymes structure, function, stability and also on the pocket size may be different.

2.9   PZA-resistance and PncA Mutations

The reported data of mutations in *pncA* gene shows two regions where alterations have been occurs i.e. open reading frame of 561 bp region and flanking region of 82 bp region [36]. According to the earlier reports, *pncA* has diverse type of mutations in different geographical regions [88, 113]. Looking to these findings, it seems difficult to develop molecular diagnostic tool for detection of gene mutations in PZA-resistance strains. Further, to find whether these mutations have any role in resistance, one should go back to the conventional method of DST whose reliability is also an issue. Tan [114] reported diverse types of mutations in *pncA* from different geographical regions. Southern Chinese isolates of MTB harbored mutations, more dispersed in the entire coding region. Moreover, some of the PZA-resistant isolates, were wild type *pncA*. These observations may raise the issues concerned with DST. In addition, a few strains show a low level of PZase activity, suggesting other targets of drug that might be involved in PZA-resistance
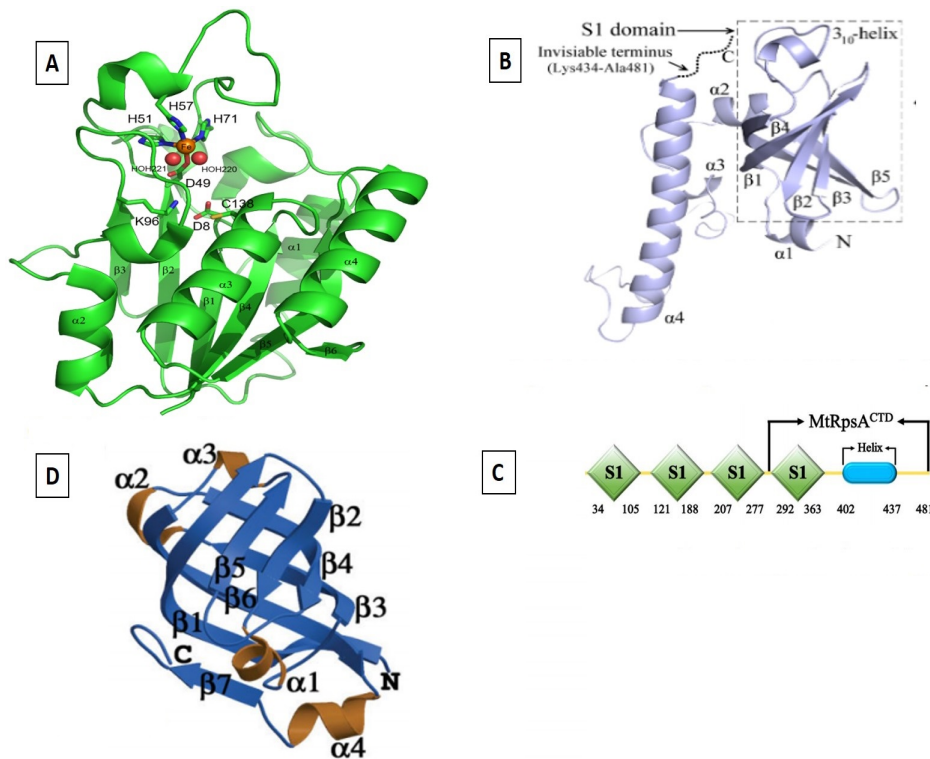
FIGURE 2.3: Crystal structures of drug targets

(A): PZase (B): RpsA (C): domain organization of RpsA and its C-terminal domain (MtRpsA$^{\text{CTD}}$) (D): PanD. PZase convert PZA into POA that inhibit the activity of PanD and RpsA

[95]. The drug has demonstrated a very specific activity against MTB but a very little against other mycobacteria, showing the variability in *pncA* of other species of mycobacteria i.e. *M. bovis* species has a natural substitution at position H57A in *pncA*, resulting no activity of PZase in these species [36]. Drug-resistance and mutations in the targets have been analyzed for different drugs, commonly used for the treatment of TB. Resistance against RIF, INH, ethambutol, and ofloxacin, have shown a capricious connection between the drug resistance phenotype and mutations in the genes, katG (97%), inhA (3%), rpoB (95%), embB (65%), and gyrA/gyrB (94%), respectively [40]. However, PZA seems to have several cellular targets, inlcuding RpsA and panD. But in majority (70-97%) of PZA-resistant isolates posses mutations in (*pncA*) gene or its regulatory region. The remaining 3% resistance have been associated with other targets. [115]. The resistant level of PZA in MDR cases have been calculated as 45.7% from Rio de Janeiro, Brazil [116], 67% from South Africa [117], 77% , 72% , 80% , 42% and 75% from Japan [118],

Brazil [119], Hong Kong, China [120], New Zealand [121] and Thailand respectively [122]. Similarly, a higher correlation (>90%) have been been reported from South Africa (92%) [123], China (91%) [124], Japan (97%) [125] and S. Korea (97%) [126]. These differences could be accredited to the limitation of phenotypic DST. False resistance may cause errors in the results of PZA DST which might be the results of ammonia production in metabolism, that could influence the process[127].

However, PZA-resistance is not confined to DST, as some studies have repeated their procedures to confirm the resistance and association with mutations in *pncA*. Therefore, studies from geographical distinct locations are need to investigate the PZA-resistance and mutation in *pncA* for better management of PZA-resistance TB in high burden countries.

2.10   PZA-resistance and RpsA Mutations

Shi et al. [111] identified ribosomal protein S1 (*rpsA*) a novel target of POA , an essential protein concerned in protein translation and the ribosome-sparing process of trans-translation. Mutations in *rpsA* (Rv1630, 1446 nucleotides), which encodes the S1 protein, result in changed POA binding and can thus intervene PZA-resistance in strains wild type for the *pncA* gene (*pncA* WT). They also sequenced the *rpsA* gene from strain and observed that it contained a DA438 deletion at the C-terminus of *rpsA* protein. This discovery that POA binds to *rpsA* and interferes the trans-translation activity assists to clarify how various stress environments, such as starvation, acid pH, hypoxia, energy inhibitors and other drugs could all potentiate PZA activity [128].

Alexander and colleagues [41] observed no mutations in *rpsA* of 11 PZA-resistant clinical samples that were genotypically wild type for the PZase gene. While a PZA-sensitive strain a single *rpsA* mutation (A364G) at the C-terminal was found. Their findings support the importance of *pncA* sequencing and tool of genetic value than *rpsA*. Simons and colleagues [127] found a single mutation in *rpsA* (V260I)

in 1 of 5 PZA-resistant isolates that support the Alexander suggestion. In a recent finding of , Akhmetova and colleagues [129] in Kazakhstan further supported the idea that gene sequencing of *pncA* and its FR, but not in *rpsA*, are frequent in PZA-resistant MTB. In conclusion from the above studies it appears that *rpsA* mutations are of no significant importance compared to PZA-resistance. More searches are needed that correlate specific mutations in *rpsA* that involved in drug resistance.

2.11   PZA-resistance and PanD Mutations

In MTB, *panD* gene code an enzyme called aspartate alpha-decarboxylase, the b-alanine synthesizer. This compound is a precursor for two important energy producer, pantothenate and co-enzyme 'A' biosynthesis. Although mutations in *pncA* have been associated with PZA-resistance but not in all cases. A few PZA-resistant strains have been detected as*pncA*$^{\text{WT}}$ and *rpsA*$^{\text{WT}}$ [90]. To invetigate that whether, there is any new mechanism of pyrazinamide resistance, Zhang et al. isolated 174, PZA-resistant and sequenced their whole genome. Five PZA-resistant strains have been detected as *pncA*$^{\text{WT}}$ and *rpsA*$^{\text{WT}}$ but these strains harboured *panD* mutations. Further, an amino acid substitution of P134S was identified in a multidrug resistant MTB strain, present naturally in PZA-resistant strains of *M. canettii*. Following the investigation of zhang, Shi et al [111] sequenced the genome of 3 pyrazinoic acid-resistant MTs. They also found mutations in *panD* gene of 3 MTs in vitro, while mutation *pncA* and *rpsA* gene have been found WT. Mutations, M117I was detected as most common (80%), effecting the C-terminus. In addition, they also found that POA inhibited the *panD* activity at therapeutical quantity but PZA lacked any effect on the inhibition of *panD* activity. These results demonstrated that POA also target PanD and mutations in PanD may cause POA-resistance in clinical isolates. Further the C-terminus residue, M117 of this protein may be involved with POA binding. These studies suggest that geographical diverse investigation should be performed to find the

role of PandD in different geographical regions. Further, these information will provide the level resistance in MTB isolates, prevalent in different geographies.

2.12   Role of Computational Biology

Proteomic deals with the methods of biochemistry, molecular biology and genetics to investigate the structure, function, and interactions of the proteins produced by the genes of a particular organism. This field is being developed constantly and new procedures are being announced. Now in the current age with the advent of computational biology it is likely to obtain the proteomic data. Bioinformatics makes it convenient to develop new algorithms to analyze large and diverse biological data sets to improve the processes. In present age, algorithms for image analysis of 2D gels have been established. Data analysis algorithms for peptide mass fingerprinting and peptide fragmentation fingerprinting have been developed.

2.13   Bioinformatics and Genomics

Genomics deals with complex sets of genes, where their expression under certain conditions are pivotal to infer their biological function. Human Genome Project was succesfully completed and about 30,000 genes were identified through the sequencing. Such a bulk of information were extracted from DNA through the application of bioinformatics. This enabled the researchers to dig out hidden knowledge about their functions they perform. Cures of major pubic health problems are being discovered through such inter-relation where bioinformatics, plays a major role.

2.13.1   Tools for Pocket Size Analysis

CASTp server is a good addition Computational Geometry [130] it calculates the pocketsize in proteins 3-D structure. The tool has the following advantage: 1)

recognition of and solvent 2) accurately measure the borders pocket solvent and 3) dot surface or the grid point is not used in parameters measurements. Further the interior and the accessible pockets both are calculated. The volume of solvent accessible area of molecular surface each one cavity, circumference and number is calculated which is important in drug interactions area and of pockets size are also calculated.

2.13.2 Sequence Editor Tools

Sequencher is a proficient tool for sequence analysis [131]. A user can simply paste the sequences without laborious work. However, for a large genome PHRED/PHRAP works perfectly [132]. Here, the search options and help functions are user friendly. The pDRAW is outstanding to paste your sequences, interpret and show; count the GC, open reading frame (ORF) and also the locations of primers. Another very handy tool, commonly used for editing sequences as well plasmid drawing is BioEdit [133]. It accepts a large number of different formats and bug free. ClustalW is very handy tool for sequence analysis and phylogeny [134]. It also BLASTs the sequences directly from the sequence alignment window and user friendly interface. However, Its limitation include the lack of support for XP-Windows. Mutation Surveyor have been found a very handy tool in Sanger sequencing, detecting sequence variations up to 400 lanes of sequencing data at a time with good sensitivity and accuracy [135].

2.13.3 Homology Modeling

Modeller is one of the most important tools in comparative modeling of proteins structures. The user provides an alignment of a sequence to be modeled with known related structures and Modeller automatically calculates a model containing all non-hydrogen atoms [137]. Molecular operating environment (MOE) is developed by a chemical computing group specialized in softwares development in bioinformatics, cheminformatics, docking, molecular simulation etc. It is a leading

Usability/ Functionality	Software and usability/functionality score						
Alignment	ClustalW	Sybyl	Insight	ICM	Prime	LOOK	Profit
• File formats		−		+	−	+	
• Annotation	−	−				+	+
• Generate			+	+	+	+	−
• Edit	−	−	+			+	
Score	−2	−3	2	2	0	4	0
Build	Swissmodel	Sybyl	DSModeler	ICM	Prime	LOOK	MOE
• Backbone			+	+		+	+
• Sidechain			+	+		+	+
• Disulfide bridge	−	+	+			−	+
• Loops			+	+			+
• Include ligand	−	−	+	−		−	+
Score	−2	0	5	2	0	0	5
Total		-3	7	4	0	4	

FIGURE 2.4: Performance of different software in homology modeling. '+' represent the ability to predict/perform while '-' means unable to predict/perform, MOE: Molecular operating environment, ICM: Internal Coordinate Mechanics [136].

drug discovery software platform for modeling and simulations with methodology development, in one package. It is most commonly used by biologists, medicinal chemists and computational chemists in academic research. The tool significantly more functional, superior and user friendly as compared to other softwares [136].

2.13.4 Tools for Functional Impact Calculation

Some commonly used bioinformatics tools has a good sensitivity and specificity in amino acid substitution and deletion in proteins are; Mutation Assessor, SIFT, PROVEAN (Protein Variation Effect Analyzer) and PolyPhen-2. (Table. 2.2) The relative performance is given in the previous study [138].

2.13.5 Proteins Stability Calculating Tools

The proteins may lose their functions because of alteration of a single amino acid residue can. To find such alteration in structure and function in proteins, bioinformatics tools are playing a very crucial role. In such cases, the change of amino acid and the effect on the stability of proteins is predicted. Here are

TABLE 2.2: Relative performance of tools in substitutions and function of proteins

Tool	Threshold	Ss*	Sp*	Ba*	NP*(%)
Human					
PROVEAN	22.3	78.4	79.1	78.8	0.0
Mutation Assessor	0.8	96.5	40.6	68.6	0.6
SIFT	0.1	85.0	77.0	69.0	2.0
PolyPhen-2	0.4	88.7	75.6	62.5	4.0
Non-Human					
		Ss*	Sp*	Ba*	NP*(%)
PROVEAN	22.3	80.2	75.3	77.8	0.0
Mutation Assessor	0.8	93.2	45.1	69.2	2.4
SIFT	0.1	87.5	78.4	69.3	5.0
PolyPhen-2	0.4	87.8	76.8	65.8	4.9

*:Ss; sensitivity, Sp; specificity, Ba; balance accuracy, NP; no prediction (sensitivity+ specificity)/2=balanced accuracy

some tools whose performance has been calculated and one could easily solve his problem. These predictor tools include i-Stable, I-Mutant2.0, MUPRO, AUTO-MUTE, PoPMuSiC2.0, and CUPSAT. The performance of each one is given in the (Table. 2.3)[139]. I-stable has a very good predicting power as compared to others. It predicts the stability of proteins when there is any change of amino acid by supporting the SVM (support vector machine) Proteins stability, structure and

TABLE 2.3: Relative performance of tools in proteins stability

Predictors	*Sn	*Sp	*Acc	*MCC
i-Stable	0.688	0.941	0.857	0.669
I-Mutant	0.377	0.916	0.736	0.357
I-Mutant	0.457	0.934	0.775	0.464
AUTO-MUTE	0.511	0.989	0.829	0.615
AUTO-MUTE	0.42	0.969	0.786	0.499
MUPRO	0.526	0.908	0.78	0.48
PoPMuSiC2.0	0.308	0.945	0.733	0.348
CUPSAT	0.474	0.78	0.678	0.261
Majority voting	0.425	0.98	0.795	0.527

*Accuracy (Acc), sensitivity (Sn), specificity (Sp), Matthews correlation coefficient (MCC).

function are most commonly affected by mutations. Therefore, the prediction of stability of these mutant proteins with precision is preferred for revealing the basic molecular aspects of diseases. Numerous innovative computational methods

have been established, to calculate the stability as well as the function of a mutated protein. These computational tools with good approaches based on sequence features, structure, and combined topographies (both structure and sequence features) deliver sensibly precise assessment of substitution of amino acid and effect of such mutations on protein's stability and function. Some bioinformatics tools that perform some special tasks in mutation analysis are given (Table. 2.4).

TABLE 2.4: Tools and their features prediction [140].

Tool	Remarks/Prediction
I-Mutant	Prediction of protein stability
nsSNPAnalyzer	Predict a nonsynonymous SNP has a phenotypic effect
PANTHER	Protein Analysis Through Evolutionary Relationships
MUpro	Prediction of Protein Stability from Sequences
PhD-SNP	Predictor of human deleterious SNPs
SNPs3D	Assigns molecular functional effects
Allign GVGD	Predicts deleterious to neutral
CUPSAT	Predicts changes in protein stability upon point mutations
iPTREE-STAB	decision tree based predicting protein stability
Eris	Predicts change in protein stability induced by mutation
SIFT	Predicts amino acid substitution affects
HOPE	Analyze the effect of certain mutation on protein structure
PolyPhen-2	Predicts change in structure and function
AUTO-MUTE	AUTOmated server for predicting functional consequences
MutationAssessor	Predicts the functional impact of substitutions
ProMaya	Predicts protein stability free energy difference

2.14 Bioinformatics and Simulation

Molecular dynamics simulations have been widely used technique to understand the dynamics of macromolecular. Present analysis in MD are close to biologically relevant ones. Information regarding macromolecules are collected about the dynamic properties are enough to study the effect of point mutation on proteins behavior and also shifting the paradigm of structural bioinformatics from single structures research to observe conformational ensembles. The internal motions and fluctuation in amino acids may effect the interaction of ligands with targets. The effect of mutations can be understand by the follwing methods.

2.14.1 Principal Component Analysis

Principal Component Analysis (PCA) is a mass-weighted Cartesian coordinates calculated in MD simulation. Movement in long trajectory is simplified and reduced [141, 142]. The variables which are transferred are call principal component (PCs). PC1 and PC2, the first two components, give the trajectories on initial two PCs of motion. Energies of proteins conformations is measured by Free Energy Landscape (FEL) [143]. The directions of motion is represented by a set of eigenvectors and eigenvalues.

2.14.2 Gibbs Free Energy Calculation

Gibbs free energy (G) is the energy available in the system [144]. The G of MTs proteins are plotted against WT at constant temperature and pressure, where reduction in G is an essential state because of its thermodynamic potential.

2.14.3 Free Energy Calculation

Drug and proteins relative binding affinity was estimated by Molecular Mechanics Generalized Born Solvent Accessibility (MMGBSA). A less negative scores shows strong binding. The proteins structure and drug free energy is originally MM-GBSA(G) binding energies, Van der Waals energy, hydrogen bonding energy, pi-pi packing energy, and total energy etc.

2.14.4 Binding Pocket Measurement

Mutations oftenly altere the pocket volume of protein. Changes in drug binding pocket size of proteins may result in weak binding affinity. The binding pocket volume of WT and MTs are measured using CASTp online server [145]. The server calculates the area and volume of pocket that might be useful in observation of any change in the size of pocket volume.

2.14.5   Metal Ion Effect

Catalytic proteins may contain some monovalent or divalent etc. Metal ions, confering functional properties. PZase contain Fe^{+2} coordinated by Asp49, His51, His57, and His71. Fe^{+2} ion effect of some MTs are also measured to observe the effect [146].

2.15   Current Research Work and Research Gap

In the view from the studies [93, 97, 129, 147] it appears that sequencing of *pncA* for mutations and resistance are more important than *rpsA* and *panD* mutations to analyze PZA-resistance. However, Sequencing *rpsA* and *panD* to screen mutations will further explore thier role involving in PZA-resistance in geographically different locations. For better managment of PZA-resistance, MTB regulatory pathways and network under latent are needed to investigate some more potent targets.

From the above review, it is obvious that *pncA* mutations coupled with in most of (upto 97%) PZA-resistance are discretized along the whole gene. However, in few cases, PZA-resistance has been linked with *rpsA* and *panD* genes mutations. For a rapid screening of PZA-resistance, it is possible to design probes that cover the most significant area of the *pncA* gene harboring mutations in those regions of most cases.

Prior to design geograpgic specific probes, screening of mutations in *pncA*, *rpsA*, and *panD* involved in PZA-resistance from different geographical regions are essential sort out and the sequencing technique smay be linked with suitable databases and algorithm that could differentiate mutations associated with resistance. In a study of Miotto and colleagues [92] from a multi-center found *pncA* variants on predictive value, involved in PZA-resistance. They found 28 mutations and were divided into: (i) Mutations with very high resistance found in *pncA* (85%). (ii) PZA-resistance mutations in less than 70% with high confidence resistance. (iii)

Genetic alterations having no linked with phenotypic resistance. Sharing of such information will improve the understanding and early diagnostic procedures for designing new strategies and ultimately better control of PZA-resistance in the course of treatment. Moreover, mehanism of PZA-resistance at molecular level behind geographic specific mutations could be explored using high throughput MD simulations technologies. In vivo experimental work, drug resistance could be investigated through the analysis of crystal structure while MD simulation has a unique advantage over experimental research, to explore the mechanisms of resistance at molecular level. Further, the residues level information and structural dynamics of protein and drug complexes can only be accessed through MD simulation which has been found difficult by experimental approaches. In molecular level research, MD simulation of drug-protein interactions have been widely applied to explain the mechanisms of drug resistance due to mutations. Here, we conducted this study to fill the gap of questions raised in the previous studies.

- The first question was; which mutations are prevalent in *pncA* of MTB isolates in Khyber Pakhtunkhwa, conferring PZA-resistance?

- The Second question, that, how these mutations effect the enzyme structure, interactions with drug, stability and, binding pocket that lead to PZA-resistance?

- The third question, was there any role of mutations in other genes like *rpsA* and *panD* in PZA-resistance?

- The fourth question was, how MTB regulates the major pathways under latent TB stage and survives in stress?

Exploring the mechanism of PZA-resistance behind mutations at molecular level will enable the researchers:

1) To develop more rapid and accurate molecular diagnostic test for screening of PZA-resistance in geographic specific regions.

2) To design novel anti-tuberculosis drugs by investigating regulatory network

under specific conditions.

3) To take measures against the drug resistance mechanisms.

2.15.1 Problem Statement

Molecular characterization offers better insight into the PZA-resistance which has not been investigated in our geography. PZA-resiatnce is most commonly associated with mutations in the drug activator, *pncA* (PZase) and targets *rpsA* and *panD*. Exploring the mechanism (conformational changes) of drug resistance behind mutations through computational approaches might be useful for better management of TB.

2.15.2 Possible Solution of the Problem

Geographic specific informations behind PZA-resistance may reduce TB burden. For the purpose, molecular and functional characterization of mutations behind PZA-resistance in locally circulated region is needed to be investigated at molecular level. Comparison of PZA-phenotypic and genotypic data will uncover specific polymorphism in the PZA target genes, *pncA*, *rpsA* and, *panD*. Moreover MD simulations of these mutations as alternative to wet lab experiments will explore the mechanism of resistance at molecular level. To identify some alternative potent drug targets, MTB regulatory pathways and network are also needed to be analyzed under latent stage of TB. In future, the genotypic data may be applied as molecular biomarkers in high burden countries for better management of drug resistance.

Chapter 3

Materials and Methods

This investigation was carried in the years from january 2016 to december 2017 in two phases, Phase-I and Phase-II with same protocol as following.

3.1 Ethical Considerations and Collection of Samples

The study was evaluated and approved by the CUST proposal committee and Ethical committee of TB Reference Laboratory of Khyber Pakhtunkhwa. Samples were taken from TB suspects along with data, location, gender, age, treatment history, sample type, HIV status, and disease type from suspects or their guardian and next care takers at Peshawar TB Reference Laboratory, Khyber Pakhtunkhwa (KPK). All the samples were subjected for further processing in Biosafety Level-III (BSL-III) Laboratory.

3.2 Processing and Culturing of Samples

TB suspects samples were digested and decontaminated to recover MTB. This process liquefies the mucus by applying NaOH/N-acetyl-L-cystein (NALC) to recover

the MTB and kill the normal flora.

3.2.1 Method

1. Samples were processed using NALC-NaOH equal volume concentration method [148] by transferring to falcon tube containing NaOH/N-acetyl-L-cystein (NALC). Samples were vortexed followed by incubation for 15 minutes to decontaminate at room temperature.

2. 50 ml phosphate buffer was transferred to tubes and centrifuged at 3000rpm for 15 minutes.

3. The supernatant was discarded in 5% phenol and the pellet was mixed with phosphate buffer and cultured on Lowenstein Jenson (LJ) media and mycobacterium growth indicator tube (MGIT), containing 7H9 media.

3.2.2 Culturing and Identification

To favour the growth of MTB, $800\mu l$ MGIT growth supplement and MGIT PANTA (polymyxin-B, amphotericin-B, nalidixic acid, trimethoprim, and azlocillin) was added to the MGIT tubes. A sample of $500\mu l$ from processed decontaminated specimen was also added to the tube. The MGIT tube was then kept in MGIT-960 machine which automatically sense the growths in the tube within recommended 17-22 days [149]. The instrument was checked for positive signal every day. In case of sample's positive indication, the tubes were analyzed under light which on shaking showed as small clumps, or cords like snowfall moving down towards the bottom of the tube. To confirm the growth is MTB, identification test (TBc ID, Ref: 245159) was performed which is a fast chromatographic immunoassay, detecting *M. tuberculosis* antigen. Approximately $100\mu l$ of sample was taken from positive tube and added the well in TBc ID device. Within 15 minutes, the emergence of pink to red at the Test 'T' and the control 'C' location showing the recognition of antigen, MPT64 of MTB in the samples [150]. All the confirmed MTB positive samples were subjected to PZA drug susceptibility testing (DST).

3.3 Drugs Susceptibility Testing

The MGIT-960 method is a fast system to measure the PZA drug susceptibility [151]. A sample was considered as drug resistant if 1% or more of the bacterial population showed growth in the presence of PZA critical concentration ($100\mu g/ml$).

3.3.1 Preparation of Drug Sensitivity Media

PZA drug was reconstituted with $2.5ml$ distilled water. Accurately $800\mu l$ PZA supplement was transferred to each MGIT tube. $100\mu l$ of PZA drug solution was also transferred to its correspondingly labeled MGIT PZA medium tube except controls.

3.3.2 Inoculum's Preparation and Inoculation

All the TB suspect samples incubated in BACTEC MGIT-960 system were observed for growth indication. A positive MTB tube on first day was considered day 0. These tubes were further left for 24 hours in MGIT known as day 1. For the preparation of PZA susceptibility test inoculum, samples were taken from day 1 tubes. A tube which has been positive longer than five days, was sub-cultured in a fresh 7 ml MGIT tube. All the MTB positive tubes were mixed by inversion two to four times.

- A 1:100 dilution of the MTB positive tubes were prepared using distilled water.

- A $500\mu l$ inoculum taken from a MGIT tube of 1:100 diluted specimen and inoculated in a MGIT tubes.

- These tubes were entered into instrument until positive indication.

- $500\mu l$ of inoculum was transferred to MGIT PZA tubes containing drug media and controls.

- The tubes were mixed gently by inversion three to four times.

- All the MGIT tubes were placed into the MGIT-960 and carefully observed on daily basis.

- PZA-resistant isolates were also tested through phenotypic DST of other first and second line drugs using MGIT 960 system, according to the policy guidelines of the WHO.

3.3.3 Interpretation of Drug Susceptibility Testing

MGIT susceptibility test completion signals are generated when the Growth Control (GC) indicated, the growth unit (GU) value of 400 or above. Susceptibility set of tubes were taken out from MGIT after scanning, and report of DST was observed. Susceptibility results were recorded as 'S' for susceptible and 'R' for resistance.

3.4 DNA Extraction and Polymerase Chain Reaction

Genomic DNA from pyrazinamide resistance isolates was extracted by cetyltrimethylammonium bromide (CTAB) [152] and sonication method [153, 154].

3.4.1 Isolation of Genomic DNA (CTAB Method)

Reagents

- Lysozyme

- 5M NaCl

- 24:1 chloroform/isoamyl alcohol

- 10% SDS

- CTAB/NaCl solution

- SDS/Proteinase 'K' mix

3.4.2   Method

- $1ml$ of MTB culture media from MGIT tubes was taken in microcentrifuge tube with $400\mu l$ of 1X TE buffer, vortexed for even mixing, treated at high temperature, 86° for 15 minutes followed by cooling to room temperature.

- A $50\mu l$ of lysozyme was added from 10 mg/ml solution and incubated for 1 hour at 37°.

- $75\mu l$ of Proteinase 'K' solution of 10% SDS was added and incubated at 65° for 10 minutes.

- $100\mu l$ NaCl of 5M was mixed, followed by the addition of $125\mu l$ of pre-warmed at 65° CTAB/NaCl mixture and incubated for 10 minutes at 65°.

- Chloroform/isoamyl in ratio of 24:1 was added and mixed in $750\mu l$ concentration and centrifuged at 12,000rpm for 5 minutes.

- A cold solution of isopropanol was mixed and stored for 20 minutes at -20°.

- The solution was then centrifuged at 14,000rpm for 15 minutes.

- Supernatant was removed and the pellet containing DNA was washed with 70% ethanol $1ml$, centrifuged for 15 minutes at 14,000rpm.

- Pellet was stored at -20° by re-suspending in 1X TE buffer for later use.

3.4.3   Sonication Method

- $1ml$ culture from MGIT tubes was transferred to microcentrifuge tube and centrifuged at 13000rpm for ten minutes.

- Supernatant was removed and molecular grade water was added to the pellet.

- Samples were heated at 86° for 30 minutes using Echotherm IC22 Digital, Chilling/Heating Dry Bath.

- The heated samples were sonicated for 15 minutes, using a sonicator (EL-MASONIC S30) followed by centrifugation at 10,000rpm for 5 minutes.

- Supernatant containing DNA was transferred to fresh tubes of $100\mu l$ molecular grade water and stored at -20°.

3.4.4 Polymerase Chain Reaction (PCR)

The *pncA* gene fragment was amplified as describe using GTQ Cycler 96 (HAIN Life Sciences) [155] through:

- *pncA*-Forward primer (5-GCGTCATGGACCCTATATC-3)

- *pncA*-Reverse primer (5-AACAGTTCATCCCGGTTC-3). The *rpsA* containing fragment was amplified through primers as described in previous study [155] through:

- *rpsA*-Forward (5-CGGAGCAACCCAACAATA-3)

- *rpsA*-Reverse (5-GTGGACAGCAACGACTTC-3). The *panD* gene fragment was amplified as described in previous study [43] through:

- *panD*-Forward: 5-TCAACGGTTCCGGTCGGCTGCT-3

- *panD*-Reverse:5-TATCCGCCACTGCTGCACGACCTT-3. A PCR mixture of $50\mu l$ contained:

- $0.1\mu l$ of each dNTPs

- $3\mu l$ $MgCl_2$

- $1\mu l$ of each forward and reverse primers

- $0.3\mu l$ tag Polymerase

- 34.6μl of molecular grade water

- 5μl of reaction buffer

- 3μl of genomic DNA. Conditions for PCR reaction were fixed to:

- 5 minutes at 94° for denaturation step followed by 30s at 94° of 30 cycles and 30s at 56°

- 72° for 1 minutes followed by 5 minutes at 72° as extension step [147, 155].

3.4.5 Agarose Gel Electrophoresis

Reagents

- Agarose

- 10X tris borate EDTA buffer (TBE)

- DNA loading dye

- Gel electrophoresis

- 1ml TBE buffer (1X) was taken in conical flask with 1g of agarose gel, for gel preparation.

- The mixture of TBE and agarose gel was boiled enough to clear transparent solution followed by cooling and addition of 2μl ethidium bromide.

- The solution of agarose gel was polymerized at room temperature and then placed in 1X TBE buffer electrophoresis chamber [156].

- 2μl of genomic DNA, mixed with loading dye, was loaded into the wells of gel.

- 2μl ladder DNA of 1kb was run as a positive control.

- All the samples in wells were run on 500 voltages, 120A currents for 30 minutes. The migration of DNA in the gel from cathode to anode was visualized in gel dock under UV-light (wavelength of 254 nm) and photographed using gel documentation system (Uvitec USA).

3.4.6   Sequencing

The purified PCR products of about $50\mu l$ of *pncA*, *panD*, and *rpsA* genes were preserved and the sequence part was run on 6 Applied Biosystems 3730xl (Macrogen Korea).

TABLE 3.1: List of instruments used in the current study

S.NO	Instrument Name	Brand	Country
1	GelBox	Syngene	U.K
2	Thermocycler	BD	Germany
3	Low temperature	Panasonic	Japan
4	Biosafety	Thermoscientific	U.S.A
5	MGIT	BD	Germany
6	Incubator	Memmert	Germany
7	Sonicator	BD	Germany
8	Centrifuge	Hettich	Germany
9	Ecotherm (Dry bath)	Torrey Pines Scientific	U.S.A
10	Autoclave	White Elephant HS-150	China
11	Digital Balance	Shimadzu	Germany
12	Hot Air Oven	Memmert	Germany

TABLE 3.2: List of chemicals

S.NO	Chemical Name
1	Reagents /Chemical
2	1% Virkon (virucidal disinfectant)
3	10 mg/mL lysozyme
4	CTAB/NaCl buffer (700 mM NaCl, 10% w/v CTAB)
5	SDS (10% in distilled H_2O, Sigma: 71736)
6	Proteinase K (20 mg/mL)
7	NaCl (5M)
8	Chloroform/Isoamyl alchohol (24:1 v/v)
9	Isopropanol (Molecular biology grade)
10	Ethanol (70% v/v in distilled H_2O, stored at -20°)
11	Tris-EDTA (TE) solution

3.4.7   Screening of Mutations in Sequences

The sequence data of PZA-resistant and susceptible isolates of genes, *pncA*, *panD*, and *rpsA* were loaded into Mutation Surveyor V5.0.1 and BioEdit version 7.2.6.1 [133, 157], to analyze and compare with RefSeq database of

NCBI (NC-000962) of *pncA* (Rv2043c), *panD* (Rv3601c), and *rpsA* (Rv1630) genes. The genes sequences of PZA-resistant and susceptible samples were compared with their RefSeq to find mutations in both, resistance and susceptible samples. Further, to find the effect of mutations on the structure and functions of proteins, all the mutations were structurally and functionally annotated at high performance computing Laboratory of Structural Bioinformatics, State Key Lab of Microbial Metabolism, Department of Bioinformatics and Biostatistics, School of life Sciences and Biotechnology, Shanghai Jiao Tong University, China.

3.5 Statistical Analysis

Epi-data is a good statistical software, developed by Lauritsen [158]. All the patient's data, location, age, treatment history, reason, sample type, TB type, HIV status, gender, and the drug resistant profile obtained after the drug susceptibility testing, was through Epi-Data entry version 3.1 through EPi-Data analysis software.

3.6 Computational Analysis of Mutations in PZA Resistance

3.6.1 Protein Structure Data

PZase and RpsA crystal structures (PDB ID: 3PL1, 4NNK, 4NNI) were downloaded from Protein Data Bank (PDB) [159]. The PDB contains large number of proteins structure, receiving structural data from scientists. All the water of crystallization was deleted from PZase and RpsA structures and mutations at a specific location were introduced by PYMOL [160] and mutate-model of Modeller. Modeller is used very commonly used for homology or comparative modeling [137].

Protein three-dimensional structures were also modeled by mutated model script. C:/ Program Files/ Modeller 9.19/bin/mutate-model>python mutate-model.py protein PDB-ID residue-position substituted residue three letter code chain>protein PDB ID.log.

The drug, PZA was downloaded from PubChem database (PubChem CID: 1046) [161]. Energy of the PZA, PZase, and RpsA were minimized using MMFF94X forcefield of Molecular Operation Environment (MOE) [162, 163].

- Forcefield=MMFF94x

- Gradient=0.05

- Option=calculate forcefield partial charges Hydrogen and partial charges were added with protonate 3D option with the following parameters:

- Temperature=310 K

- pH=6.5

- salt = 0.1

- electrostatics=Gb/VI

- Dielectric=1

- Van der Waals=800R3

- Cutoff= 15

- Solvent=80 The drug was saved in a database viewer for docking. Wild type (WT) and mutants (MTs) proteins were loaded one by one into MOE and partial charges were added to the system. Energy was minimized with forcefield AMBER99 as it is more suitable for proteins and nucleic acids. Energy minimized proteins and drug were docked with following parameters:

- placement = triangle matcher

- Rescoring = London dG

- Refinement = forcefield

- Retain option was set at 10 After docking, ligand and proteins interactions were observed with database browser option. All the modelled mutated proteins were loaded one by one in MOE in PDB format.

3.6.2 Molecular Dynamic Simulation

All the WT and MTs in two forms, apo and in complex with PZA and POA drug were subjected to MD simulations at high performanc computing center of Shanghai Jiao Tong University, China, using AMBER 14 [164]. To neutralize the systems, sodium and chloride ions were added into the cubic box by tleap [165, 166]. Equilibration was performed with moles, volume, and energy (NVT) ensemble followed by amount of substance, pressure, and temperature (NPT) at 1 bar for 2000ps for each. Principal Component Analysis (PCA) of WT and MTs was analyzed to compare the effect of mutations on proteins motion. Gibbs free energy (G) of WT and MTs were compared to infer the stability. The proteins structure and drug free energy is originally MM-GBSA(G) binding energies, Van der Waals energy, hydrogen bonding energy, pi-pi packing energy, and total energy. The binding pocket volume of WT and MTs were measured using CASTp online server [145]. The server calculates the area and volume of pocket that might be useful in observation of any change in the size of pocket volume.

3.6.3 Fe^{+2} Ion Effect

PZase contain Fe^{+2} coordinated by Asp49, His51, His57, and His71. Fe^{+2} ion effect of some MTs were also measured to observe the effect [146].

3.6.4 Prediction of Mutation Effect on Protein Function

Mutation Assessor and Provean online servers [138] are widely applied for biological functions annotation. For the further, confirmation, All the mutations detected

in this investigation were annotated through online servers, to find the effect on the biological function of proteins.

3.6.5 Effect of Mutations on Proteins stability

Stability of proteins during different environmental conditions is vital to perform the normal activity. All the mutated proteins were characterized, based on stability through I-stab, MuSTAB online server Site Directed Mutator (SDM) and CUPSAT (Cologne University Protein Stability Analysis Tool) tools [167, 168].

3.7 Pathway and Network Biology of Latent Tuberculosis

3.7.1 Literature Search

PZA is the only drug active against non-replicating MTB under the latent TB. To explore some more potent target under latent state, literature was searched for MTB major regulators, responding under the latent stage of TB using key words, latent stage TB, MTB survival under stress, role of sigma Factors, SigH of MTB, regulation of MTB pathway in stress condition, RshA role during stress, role of trxC, PknB and stress regulation. The relevant papers were manually searched for the genes and proteins functional under latent stage. All the genes interacting among each other, were extracted from the literature and mapped in UPPAAL tool, an integrated tool environment for modeling, in the form of sigH regulation network pathway.

3.7.2 String Network Generation

The pathway mapped from the literature was further confirmed for their interactions in string database [169]. The network file in TSV format was downloaded

from the string database and imported into Cytoscape v 3.5.1 [170]. The paths of network were analyzed through Pathlinker [171] plugin in cytoscape and searched for the longest path using background protein interaction network. Pathlinker computes several short paths efficiently from the receptors to transcriptional regulators (TRs) in a network. It can accurately rebuild an inclusive set of signaling pathways from the NetPath and KEGG databases. The longest path was analyzed using Analysis of Networks with Interactive Modeling (ANIMO) [172] plugin for better visualization purpose. SigH regulation was build to analyze some more drug target under latent stage of MTB.all
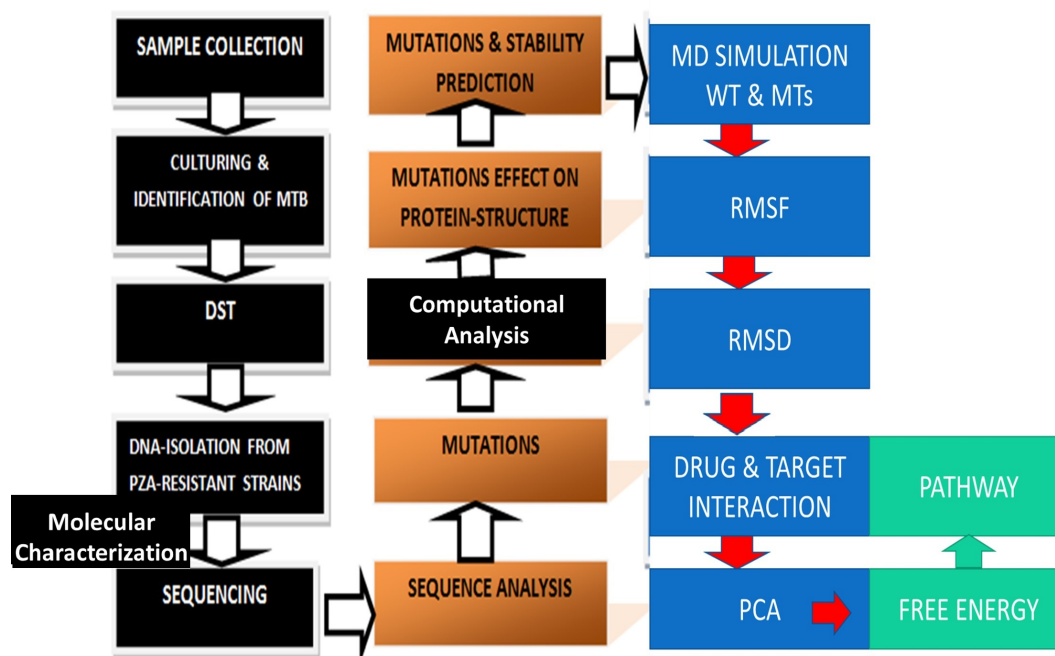

FIGURE 3.1: Flowchart methodology

Chapter 4

Results

The samples in the current investigation have been collected in two consecutive phases, phases-I and phase-II. However, due to some technical issues occured suddenly, phase-I samples have not been processed further for molecular analysis.

4.1   Phase-I Distribution of Suspect Data

A total of 8,119 TB suspects samples have been collected and processed from 17 District TB Control Officers (DTO) and Programmatic Management of Drug-resistance TB Units (PMDT). Out of total, 1075 were found MTB culture positive among which male and female were 587 (54.6%) and 488 (45.3%) respectively. Similarly, 410 (38%) and 665 (62%) were follow up (previously treated) and diagnostic (never treated) among TB positive samples (Table. 4.3). The number of resistance samples received from each TB units is given (Table. 4.1). The largest number of samples have been received from Mufti Mehmood Hospital (27) follwed by Lady reading hospital (10).

Sample type and age groups have been illustrated in table (4.2). Majority of the samples were collected from pulmonary origin (95%). The mean age of the patients was 36.5, ranging from 4 to 100 years. All the patients have been recorded HIV negative.

Table 4.1: Phase-I PZA-resistance samples collected from TB units

S.NO	Health Center	PZA-Resistance(No.)
1	DTO Bajawar	3
2	DTO Bunir	2
3	DTO Chitral	5
4	DTO Dir	4
5	DTO Hangu	4
6	DTO Kohat	3
7	DTO Mardan	1
8	DTO Noshehra	3
9	DTO Sawabi	3
10	DTO Swat	2
11	PMDT Hayatabad medical complex	3
12	PMDT Khyber teaching hospital	2
13	PMDT Ayub teaching hospital	2
14	PMDT Lady reading hospital	10
15	PMDT Mufti Mehmood hospital	27
16	PMDT Swat	9
	Total	83

*DTO: district tuberculosis officers, PMDT: programmatic management of drug resistance TB.

4.2 Phase-I Drug Susceptibility Pattern

Out of total MTB positive isolates, 83 (7.7%) were detected as PZA-resistance. The total number of samples received from each TB unit have been illustrated in the table (4.1). PMDT, ATH, and LRH have been shown, receiving majority of cases, where male to female ratios among PZA-resistance were 49 (59%) and 34 (41%) respectively (Table. 4.3). The resistance samples were further checked manually to confirm the growth of MTB against the critical concentration of drug. Out of total PZA-resistance, 76 (90% to 91.6%) and 67 (80 % to 80.7%) isolates shows resistance to INH and RIF respectively, where 63/83 (76%) were found as MDR. The resistance profile of the samples shows that a correlation between PZA and other drug-resistance might be existed, especially the two important first-line drug, INH and RIF. Morover, second-line drug resistance, OFX (48.20%) and SM (49.40%) were also detected in significant number (Table. 4.4). Further molecular study has not been performed on the phase-I PZA-resistance samples due to technical issue occured during their storage period.

TABLE 4.2: Phase-I characteristics of TB positive patients

A-Age group	Number
01-14	59
15-24	291
25-34	233
35-44	123
45-60	235
>60	134
B-Tuberculosis Type	
1. Extrapulmonary	
Acetic fluid	4
Cerebrospinal fluid	4
Bronchoalveolar lavage	1
Lymph node	1
Pericardial fluid	1
Pleural fluid	18
Tissue biopsy	7
Pus	14
Urine	1
Bone	1
Total	5%
2. Pulmonary	1023 (95%)

4.3   Phase-II Characteristics of TB Suspects

During the phase-II of the current study, 4518 TB suspects samples have been received from different TB units. All the patient's data was entered in CSV format. Gender wise male to female ratio was found as 1:1.05 (Male 2187, female 2300). Mean age of suspects were 32.55 years. The largest number of samples were received from Lady Reading Hospital (36.8%) followed by Hayatabad Medical Complex (15.6%).

A significant number of suspect samples have been also collected from other units including Combined Military Hospital (CMH) (3.1%), District Tuberculosis Officers (DTO) Peshawar (11.4%),Khyber Teaching Hospital (KTH) (9.6%), Programmatic Management of Drug Resistance TB (PMDT) Swat (6.6%), PMDT Mufti Mehmood Teaching Hospital (MMTH) (8.8%), and 180 (4%) from PMDT Ayub Teaching Hospital (Table. 4.5).   Characteristics of TB suspects has been given

TABLE 4.3: Phase-I Gender and treatment history of PZA-resistance

Gender-wise			
	Male	Female	Total
Culture positive	587 (54.6%)	488 (45.3%)	1075
PZA-resistance	49	34	83
Treatment history			
	Diagnostics	Follow up	Total
Culture positive	665 (62%)	410 (38%)	1075
PZA-resistance	55	28	83

TABLE 4.4: Phase-I Firstline drug resistance among PZA-resistance (%)

First-line drugs				
	RIF	INH	SM	EMB
Resistance	67	76	1	35
	80.70%	91.60%	1.20%	42.20%
Susceptible	16	7	82	48
	19.30%	8.40%	98.80%	57.80%
Second-line drugs				
	AMK	SM	CAP	OFX	KM
Resistance	14	41	12	40	17
	16.90%	49.40%	14.50%	48.20%	20.50%
Susceptible	69	42	71	43	66
	83.10%	50.60%	85.50%	51.80%	79.50%

RIF: Rifampicin, INH: Isoniazid, PZA: Pyrazinamide, EMB: Ethambutol,
SM:Streptomycin, LEV: Levofloxacin, OFX: Ofloxacin, CIP: Ciprofloxacin,
MOX:Moxifloxacin, AMK: Amikacin, CAP: Capreomycin KAN: Kanamycin.

(Tables. 4.3), (4.6), demonstrating that majority of patients were unknown to their HIV status (96.4%). However, HIV positive and negative has been recorded in 160 (3.5%) and 4 (0.1%) samples.Tuberculosis is basically of two types, pulmonary and extra pulmonary, based on the sample types. In the earlier case, the infectious agent resides in lungs or reaches the stomach in pediatric patients while in the latter case, the MTB spreads to other body parts like brain, bone, heart, and pleura etc. Among pulmonary, sputum and gastric aspirate samples have been found in highest i.e 3762 (83.3%) and 155(3.4%) respectively. Whereas, 145 (3.2%) were Bronchoalveolar Lavage (BAL), 152 (3.4%) of pleural fluid, and 85 (1.9%) were CSF respectively (Tables. 4.7). Lungs biopsy, synovial fluid, and bronchial aspirate were fewer in number.

TABLE 4.5: Phase-II Sample's detail collected from all TB units of KPK

S. No	*Health Center	Number	%
1.	ATO Khyber Agency	30	0.7
2.	CMH	141	3.1
3.	DTO Bajor Agency	8	0.2
4.	DTO Bannu	1	0
5.	DTO Buner	1	0
6.	DTO Charsadda	24	0.5
7.	DTO D.I.K	4	0.1
8.	DTO Dir Lower	4	0.1
9.	DTO Dir Upper	11	0.2
10.	DTO Hangu	1	0
11.	DTO Kohat	3	0.1
12.	DTO Kohistan	1	0
13.	DTO Lakki Marwat	1	0
14.	DTO Malakand	2	0
15.	DTO Mansehra	1	0
16.	DTO Mardan	8	0.2
17.	DTO Noshehra	19	0.4
18.	DTO Peshawar	515	11.4
19.	DTO Sawabi	16	0.4
20.	DTO Shangla	1	0
21.	HMC	707	15.6
22.	KTH	434	9.6
23.	Kuwait Hospital	7	0.2
24.	MMC Mardan	2	0
25.	PMDT ATH	180	4
26.	PMDT LRH	1661	36.8
27.	PMDT MMTH	399	8.8
28.	PMDT Swat	297	6.6
29.	Private	1	0
30.	PRL	17	0.4
31.	RMI	20	0.4
32.	Takht e Nusrati	1	0
	Total	4518	100

*ATH: Ayub Teaching Hospital, CMH: Complex Combined Military Hospital, DTO: District Tuberculosis Officers, HMC: Hayatabad Medical Complex, KTH: Khyber Teaching Hospital, LRH: Lady Reading Hospital, MMC: Mardan Medical Complex, RMI: Rehman Medical Institute. MMTH: Mufti Mehmood Teaching Hospital, PMDT: Programmatic Management of Drug Resistance TB, PRL: Peshawar Reference Laboratory.
Out of total number of cases reffered by PMDT, 54% have been sent by four units, Lady Reading Hospital, Mufti Mehmood Teaching Hospital, Ayub Teaching Hospital, and Swat.

4.4 Tuberculosis and HIV

TB and Human Immunodeficiency Virus (HIV) co-infection has also been found in significant number of cases in different countries. A person infected with HIV has a greater risk to develop TB where HIV destroys the T-cell that are regarded as the main defense system. Majority of TB suspect were unknown to their HIV status. Such patients do not conduct HIV test in routine checkup. Further, they may be living in remote areas, where TB and HIV test may not available. In the current study 160 (3.5%) were detected HIV$^+$ while 96.4% were of unknown to thier HIV status (Table. 4.6).

4.5 TB Suspects and Gender

Females have been found more likely at risk (50.9%) than male (48.4%). Sample type demonstared that, majority of the cases were never treated (diagnostics), 3908 (86.5%) as compared to follow-up (on treatment and previously treated), 3.1% and 10.4% (Table. 4.6). HIV known status (positive and negative) is very fewer in number (3% and 0.1%) where majority have unkwn status (96%).

TABLE 4.6: Phase-II characteristics of TB suspects

Gender	Number	%
Female	2300	50.9
Male	2187	48.4
Other	31	0.7
Total	4518	100
HIV-Status		
HIV +ve	160	3.5
HIV -ve	4	0.1
Unknown	4354	96.4
Total	4518	100
Treatment history		
Never Treated	3908	86.5
On Treatment	142	3.1
Previously Treated	468	10.4
Total	4518	100

TABLE 4.7: Sample types taken from TB suspects

Sample type	Number	%
Ascitic Fluid	52	1.2
BAL	145	3.2
Bronchial Aspirate	3	0.1
CSF	85	1.9
Gastric Aspirate	155	3.4
Gastric Lavage/Washing	15	0.3
Lung Biopsy	3	0.1
Lymph Node	6	0.1
Pericardial Fluid	17	0.4
Pleural Fluid	152	3.4
Pus	51	1.1
Sputum	3762	83.3
Synovial Fluid	8	0.2
Tissue Biopsy	42	0.9
Urine	22	0.5
Total	4518	100

BAL: Broncheoalveolar lavage, CSF: Cerbrospinal Fluid,
MTBC:Mycobacterium Tuberculosis Complex

4.6 Culture Result

All the TB suspects were grown on Mycobacterium Growth Indicator Tubes (MGIT) 7H9 and Lowenstein Jenson media (LJ). Out of 4518 samples, 754 (8.84%) were detected as MTB culture positive (Table. 4.8). The positive rate has been detected

TABLE 4.8: TB-positivity and patient data

Gender wise	MTBC	%	No growth	%	Total
Female	412	17.9	1888	82.1	2300
Male	337	15.4	1850	84.6	2187
Other	5	16.1	26	83.9	31
Total	754	16.7	3764	83.3	4518
Treatment history wise					
Never Treated	594	15.2	3314	84.8	3908
On Treatment	25	17.6	117	82.4	142
Previously-Treated	135	28.8	333	71.2	468
Total	754	16.7	3764	83.3	4518

higher in previously treated patient (Follow-up) (28.8%) as compared to never

TABLE 4.9: TB positivity rate in sample and disease types

Sample Type	MTBC	%	No growth	%	Total
Ascitic Fluid	4	7.7	48	92.3	52
BAL	30	20.7	115	79.3	145
Bronchial Aspirate	0	0	3	100	3
CSF	5	5.9	80	94.1	85
Gastric Aspirate	9	5.8	146	94.2	155
Gastric Lavage	1	6.7	14	93.3	15
Lung Biopsy	0	0	3	100	3
Lymph Node	1	16.7	5	83.3	6
Pericardial Fluid	1	5.9	16	94.1	17
Pleural Fluid	17	11.2	135	88.8	152
Pus	14	27.5	37	72.5	51
Sputum	664	17.7	3098	82.3	3762
Synovial Fluid	1	12.5	7	87.5	8
Tissue Biopsy	7	16.7	35	83.3	42
Urine	0	0	22	100	22
Total	754	16.7	3764	83.3	4518
Disease Type					
Extra Pulmonary	81	13.5	520	86.5	601
Pulmonary	673	17.2	3244	82.8	3917
Total	754	16.7	3764	83.3	4518

*BAL: Broncheoalveolar lavage, *CSF: Cerbrospinal Fluid

treated patients (diagnostics). Pulmonary samples are most common in comparison with extra-pulmonary. The highest number of positivity has been recorded in pus samples (27.5%) followed by BAL (20.7%), and sputum (17.7%) (Table. 4.9). MTB detection rate in pulmonary and extra-pulmonary samples were 17.2% and 13.5% respectively.

4.7 PZA-Resistance and Patient Data

The PZA-resistance rate and patients data has been shown (Table. 4.10). Majority of the resistance were detected in diagnostic patients. Pulmonary tuberculosis is more likely resistance than extra-pulmonary.

Out of total 754 culture positive, 69 (9.15%) were detected as PZA-resistance. These resistance samples were screened for mutations in the target genes.

4.8   PZA-resistance and Other Drugs

Among the PZA-resistance isolates, the resistance level of other first-line drugs were ; 29(41.2%) of SM, 64(92.8%) of INH, 58(84.1%) were RIF, and 35(50.7%) of EMB respectively, while second line drug resistance, AM, KAN, CAP, OFX, and MOX were 11(15.9%), 13(18.8%), 11(15.9%), 35(50.7%), and 2(2.9%) respectively as shown (Table. 4.11).

TABLE 4.10: PZA-resistance and socio-demographic data of patients.

Patient Data	Number (%)
Gender wise	
Female	44(63.8)
Male	25(36.2)
Total	69(100.0)
Treatment history wise	
Never Treated	44 (63.8)
On Treatment	21 (30.4)
Previously Treated	4(5.8)
Total	69(100.0)
Disease Type	
Extra Pulmonary	3(2.9)
Pulmonary	66(97.1)
Total	69(100.0)
Sample Type	
Bronchoalveolar Lavage	1(1.4)
Pus	2(2.9)
Sputum	66(95.7)
Total PZA-resistance	69

TABLE 4.11: First line drugs resistance among PZA-resistance isolates.

	*SM (%)	INH (%)	RIF (%)	EMB(%)
Resistance	29(41.2)	64(92.8)	58 (84.1)	35(50.7)
Susceptible	40(58.8)	5(7.2)	11(15.9)	34(49.3)

*SM: Streptomycin, INH: Isoniazid, RIF: rifampicin, EMB: Ethambutol

TABLE 4.12: Second line drugs resistance among PZA-resistance isolates

	AM	KAN	CAP	OFX	MOX
Resistance	11(15.9)	13(18.8)	11(15.9)	35(50.7)	2(2.9)
Susceptible	58(84.1)	56(81.2)	58(84.1)	34(49.3)	67(97.1)
Total	69	69	69	69	69
Type	**No. (%)**				
MDR	52(75.4)				
Mono Drug resistance	1(1.4)				
Poly Drug resistance	10(14.5)				
XDR	6(8.7)				

*(%), AMK: Amikacin, CAP: Capreomycin, KAN: Kanamycin,
MOX:Moxifloxacin, OFX: Ofloxacin.

4.9 PZA-resistance and Multidrug Resistance

Bacterial isolates exhibiting resistance to at least RIF and INH are called MDR while those which are MDR and also show resistance to one of the fluoro-quinilones (CAP, OFX) and one of the injectable drugs (KAN, AM) are termed as XDR. Resistance to any single or other than MDR are termed as mono and poly drug resistance. Here in both the cases, MDR and XDR are very hard to treat. Among PZA-resistance isolates, 52 (75.4%) and 8.7% were also MDR and XDR respectively (Table. 4.12).

4.10 PZA-resistance and PncA Mutations

On comparison of sequenced results among sensitive and resistance isolates, PZA-resistance harbored a large number of mutations within the coding region (561 bp) of *pncA* (Table.4.13). These mutations were dispersed type, scattering in the whole open reading frame (**Appendix-A**).

Out of 69 PZA-resistance isolates, 51(74%) harbored 36 mutations as shown (Table. 4.13). To find the novelity, all these were searched manually in TB drug resistance database (TBDReaMDB), Genome-wide *Mycobacterium tuberculosis* variation (GMTV), and also among the published literature. Variants

AAG96CAG (LYS96GLN) and AGC179TGC (SER179CYS) were found in 4 isolates each. Thirteen novel mutations including two deletion, 317-318delTC and 194-203delCCTCGTCGTG were not reported in previous studies. The most common mutations were detected at position 287(Lys96Thr), 423(Ser179Gly), and 535(Gln141 Arg). Majority of these were point mutations, however, deletions, 194-203 del CCTCGTCGTG (n=1), 317-318delTC (n=1), 530 del C (n=3) were also identified among PZA-resistance isolates. The most common synonymous mutation identified in both kinds, susceptible and resistance isolates was Ser65Ser at position 195C-T in 22 and 16 samples respectively. We did not detected any non-synonymous mutations in coding region of *pncA* of 26 PZA susceptible isolates. To estimate the performance of DST with *pncA* sequencing result of PZA-resistance isolates, the genotypic data for all 69 resistance was evaluated. Considering phenotypic as a reference, out of 69 resistance isolates, 51 (74%) have mutations in *pncA* with sensitivity 79.31% (95% CI,69.29% to 87.25%) and specificity 86.67% (95% CI,69.28% to 96.24%).

4.10.1 Mutation's Effect on Function

PROVEAN online server has been used to predict the effect of mutation's on PZase activity with cut-off value of -2.5. All the non-synonymous mutation in Pzase showed a deleterious effect on PZase function except Q141P, E144K, A170P, and S179G, where the effect has been predicted as neutral (Table. 4.14). This effect on function may cause PZA-resistance.

4.10.2 Mutation's Effect on Stability

The stability of mutations have been predicted through different online servers as given in the table (4.15). The stability has been found, decreasing due to these mutations except in a few cases (A46V, H71Y, T76P, A170P, S179G, and, S179C).

TABLE 4.13: *PncA* mutations in PZA-resistance isolates of *M. tuberculosis*

*N.T	Codon	A.A change	Mutation	DB-1	DB-2	Lit	No.
33C-A	AAC11AAA	ASN11LYS	Non-syn	nr	nr	nr	1
35A-C	GAC12GCC	ASP12ALA	Non-syn	r	r	r	2
53C-A	TCG12TAG	SER 53 STOP	Non-syn	nr	nr	nr	1
56T-G	CTG19CGG	LEU19ARG	Non-syn	r	nr	r	1
137C-T	GCA46GTA	ALA46VAL	Non-syn	r	r	r	1
161C-T	CCG54CTG	PRO54LEU	Non-syn	r	r	r	1
170A-C	CAC57CCC	HIS57PRO	Non-syn	r	nr	r	1
194_203	Del CCTCG TCGTG	FS	FS	nr	nr	nr	1
202T-C	TGG68CGG	TRP68ARG	Non-syn	r	r	r	1
205C-A	CCA69ACA	PRO69THR	Non-syn	nr	nr	nr	3
211C-T	CAT71TAT	HIS71TYR	Non-syn	r	r	r	3
212A-G	CAT71CGT	HIS71ARG	Non-syn	r	r	r	1
226A-C	ACT76CCT	THR76PRO	Non-syn	r	r	r	1
286A-C	AAG96CAG	LYS96GLN	Non-syn	r	nr	r	4
317-18	Del TC	FS	FS	nr	nr	nr	3
331G-T	GAG111TAG	STOP	Non-sen	nr	nr	nr	1
359T-G	CTG120CGG	LEU120ARG	Non-syn	nr	r	r	1
368G-C	CGC123CCC	ARG123PRO	Non-syn	nr	r	r	1
376G-A	GAT126AAT	ASP126ASN	Non-syn	nr	nr	nr	2
385G-A	GAT129AAT	ASP129ASN	Non-syn	nr	nr	r	1
391G-T	GTC131TTC	VAL131PHE	Non-syn	nr	r	r	1
398T-C	ATT133ACT	ILEU133THR	Non-syn	nr	r	nr	2
419G-A	CGC140CAC	ARG140HIS	Non-syn	nr	nr	r	2
422A-C	CAG141CCG	GLN141PRO	Non-syn	nr	r	r	3
430G-A	GAG144AAG	GLU144LYS	Non-syn	nr	nr	nr	1
437C-T	GCG146GTG	ALA146VAL	Non-syn	r	r	r	1
449G-C	GGC150GCC	GLY150ALA	Non-syn	nr	nr	nr	1
461G-C	AGG154ACG	ARG154THR	Non-syn	nr	nr	r	1
470T-G	GTG157GGG	VAL157GLY	Non-syn	nr	nr	r	2
508G-C	GCC170CCC	ALA170PRO	Non-syn	nr	nr	nr	1
519G-A	GAG173GAA	GLU173GLU	syn	nr	nr	nr	1
522G-A	GAG174GAA	GLU173GLU	syn	nr	nr	nr	1
530	DEL C	FS	FS	nr	nr	nr	3
535A-T	AGC179TGC	SER179CYS	Non-syn	nr	nr	r	4
535A-G	AGC179GGC	SER179GLY	Non-syn	nr	nr	r	1
538G-T	GTC180TTC	VAL180PHE	Non-syn	r	nr	r	1

(*Appendix-A), A.A; amino acid, DB-1; Tuberculosis Drug Resistance Mutation Database (TbDRM), DB-2; Genome-wide *Mycobacterium tuberculosis* variation (GMTV), Del; deleted, FS; frameshift, Lit; literature, Non-syn; Non synonymous, nr; not reported, N.T; nucleotide, r; reported, syn; synonymous. The appendix-A at the end shows the position of mutation.

TABLE 4.14: Effects of mutation on PZase function as predicted by PROVEAN

Variant	PROVEAN score	Prediction (cutoff= -2.5)
N11K	-5.577	Deleterious
D12A	-7.68	Deleterious
L19R	-5.654	Deleterious
A46V	-3.856	Deleterious
P54L	-9.651	Deleterious
H57P	-9.661	Deleterious
W68R	-13.64	Deleterious
P69T	-7.786	Deleterious
H71R	-7.867	Deleterious
H71Y	-5.9	Deleterious
T76P	-4.975	Deleterious
K96Q	-3.947	Deleterious
L120R	-5.552	Deleterious
R123P	-5.173	Deleterious
D126N	-2.578	Deleterious
D129N	-4.553	Deleterious
V131F	-4.535	Deleterious
I133T	-4.447	Deleterious
R140H	-4.164	Deleterious
Q141P	-1.031	Neutral
E144K	-0.238	Neutral
A146V	-3.606	Deleterious
G150A	-5.576	Deleterious
R154T	-4.294	Deleterious
V157G	-4.452	Deleterious
A170P	-1.75	Neutral
S179C	-2.754	Deleterious
S179G	4.38	Neutral
V180F	-4.266	Deleterious

4.10.3 Effect of Mutations on Protein Activity

To measure the effect of 15 novel mutations on PZase structure and function, insight properties including binding pocket, fluctuations in amino acids residues, hydrogen bonding, interaction energy, docking score was analyzed through MD simulation. Several analysis have been performed using High Performance Computing Center (HPC) at Bioinformatics and Biostatistics Department of Shanghai Jiao Tong University, China. We have detected many significant changes in activity and structure of PZase behind mutations, present in the active site and its

nearby residues that may produce an allosteric effect. The change may be seen in the

structure far residues. However, alteration can be analyzed in active site residues.

TABLE 4.15: Mutation effect on PZase stability, predicted through online servers

Variant	MutPDB	MutSEQ	MSVM	MUpro	CP*	iStable
N11K	*dec	dec	dec	dec	*incr	dec
D12A	dec	dec	dec	dec	incr	dec
L19R	dec	dec	dec	dec	dec	dec
A46V	dec	incr	dec	incr	incr	incr
P54L	dec	dec	dec	dec	incr	dec
H57P	dec	incr	dec	dec	dec	dec
W68R	dec	dec	incr	dec	dec	dec
P69T	dec	dec	dec	dec	dec	dec
H71R	dec	dec	dec	incr	incr	dec
H71Y	incr	incr	dec	incr	incr	incr
T76P	dec	incr	incr	dec	dec	incr
K96Q	dec	dec	dec	dec	dec	dec
L120R	dec	dec	dec	dec	dec	dec
R123P	dec	dec	dec	dec	dec	dec
D126N	dec	dec	dec	dec	incr	dec
D129N	dec	dec	dec	dec	dec	dec
V131F	dec	dec	dec	dec	dec	dec
I133T	dec	dec	dec	dec	dec	dec
R140H	dec	dec	dec	dec	dec	dec
Q141P	dec	dec	dec	incr	dec	dec
E144K	dec	dec	incr	dec	dec	dec
A146V	dec	dec	dec	incr	dec	dec
G150A	incr	dec	dec	dec	incr	dec
R154T	dec	dec	dec	incr	incr	dec
V157G	dec	dec	dec	dec	dec	dec
A170P	incr	incr	incr	dec	incr	incr
S179G	incr	null	incr	dec	incr	incr
S179C	incr	incr	incr	incr	dec	incr
V180F	dec	dec	dec	incr	dec	dec

*dec; decrease, incr; increase, CP; CUPSAT, *incr; increase,
CP; CUPSAT,*iStable; Integrated predictor for protein stability,
MutPDB; mutate protein databank, MutSEQ; mutate sequences,
MSVM; mutate protein support vector machine.

These tool may be applied for a quick access the affect in the ligand site residues and

surrounding. The overall results shows that these variants might be involved in loss or week interactions with PZA, resulting resistance.

4.10.3.1 PZase and Drug Interaction Energies

Total free energy depicts the stability of structures. PZA and PZase interaction energies is important to infer the function of enzymes. The role of electrostatics and Van der Waals (vdW) forces are important in protein bindings. In comparative analysis of total energies and other forces, between WT and MTs exhibit a significant variations. Polar solvation energy (PS), Solvent accessible surface area (SASA) has also been given (Table. 4.16). These findings clarify the affect of mutations on PZase activity. The strength of molecular and atomic interactions

TABLE 4.16: Characteristics and binding free energy of the WT and MTs PZase

PZase	Pocket	AD	MMGBSA				
	($\mathring{A}^3$)	(kcal/M)	vdWa	elec	ps	SASA	GTotal
WT	585.74	-5.8	-21.27	-19.88	25.65	-2.90	-18.40
N11K	551.92	-2.5	-17.78	-3.04	14.89	-2.63	-8.56
L19R	556.24	-5.4	-21.73	-25.46	35.88	-2.96	-14.28
A46V	404.68	-4.3	-20.13	-22.03	34.25	-2.78	-13.38
P69T	445.41	-2.7	-20.95	-25.08	35.51	-2.94	-13.46
D126N	494.56	-3	-21.06	-24.89	36.44	-2.92	-12.43
D129N	481.24	-3.1	-20.34	-23.68	33.79	-2.78	-11.45
V131F	406.76	-2.6	-18.55	-20.99	35.67	-2.45	-15.35
R140H	437.97	-5.2	-21.13	-23.37	35.36	-2.92	-12.05
Q141P	400.85	-3.9	-19.65	-22.56	32.23	-2.88	-13.23
E144K	552.83	-4.7	disso	0.67	1.61	-0.36	-
G150A	376.38	-5.1	-21.10	-21.45	34.32	-1.99	-14.33
R154T	480.48	-3.2	-17.23	-23.43	31.82	-2.76	-12.78
A170P	405.86	4.7	-19.88	-20.67	33.65	-2.65	-15.23
S179G	401.48	3.8	-20.43	-22.34	31.37	-2.45	-14.79
V180F	404.71	4.5	-18.35	-19.79	35.25	-2.91	-11.76

AD; Autodock score, disso; Dissociated, elec; Electrostatic energy, G-Total; Total binding free energy, MMGBSA; Molecular mechanics generalized born and surface area.

can be estimated by measuring the docking score. A significant variations in term of docking score have been observed between WT and MTs. A more negative value represent strong interactions (Table. 4.16). Although there is no significant

difference in Van der Waals (vdWa) and electrostatic energies among the MTs and WT, but MTs, E144K was dissociated and vdWa could not be calculated. The total energy of WT and MTs also shows significant differences. (Table. 4.16). Similarly, the drug binding pocket of MTs have been shown, decreasing in most cases by mutations.

4.10.3.2 Drug Binding Pocket

A slight increase or decrease in drug binding pocket of WT may affects protein and ligand interaction. Pocket volume of MTs such as V131F, Q141P, R154T, A170P, and V180F were measured, 406.761Å, 400.849Å, 480.475Å, 405.861Å, and 404.706Å in comparison with WT (585.736Å) is significantly lower, resulting a weak or no binding affinity to convert a pro-PZA into active form POA. Docking score of all MTs including V131F, Q141P, R154T, A170P, and V180F (-2.6, -3.9, -3.2, 4.7, and 4.5), is higher, compared to WT (-5.8) (Table. 4.16).

4.10.3.3 Root Means Square Deviation and Fluctuation

RMSF and RMSD are measured as a mean describing stability and flexibility differences among protein residues. Molecular dynamics simulation on high performance computing at Shanghai Jiao Tong University China, was run for 40 and 100ns without PZA bound (apo) and PZase complex with drug. WT structures attained RMSD value of 2.4 and 1.4 Å at 40 and 19ns in apo and complex state with drug and finally attained stable value while MTs, L19R, R140H and E144K in apo state showed a deviations and attained the RMSD value of 2.3Å, 2.4Å and 2.8 Å at 50, 54 and 100ns respectively. WT structure was found more stable and less deviated in comparison with MTs. R140H showed maximum deviation and remain unstable even at 100 ns. In complex form, WT PZase attained 1.4 Å of RMSD of at 10ns while MTs, R140H, L19R, and E144K have been demostrated maximum deviation and instability, attaining RMSD of 2.3 Å, 2.5 Å and 2.7 Å at 58, 100 and 90ns respectively. RMSF of WT and MTs has been found in variation in residues from 30 to 110 (Figure. 4.1). Similarly RMSD and RMSF of

MTs, D126N, N11K, and P69T showed instability throughout simulation period of 100ns and the residues are more fluctuated as compared to WT (Figure. 4.2). MTs, L19R, R140H and E144K exhibited more flexibility in comparison with WT, exhibiting RMSF of 0.4 to 2.4Å and 0.4-2.1Å both, apo and complex states. Flexibility were detected in residues from 15-115 while, L19R exhibited 0.4-2.9 and 0.4-2.4Å of RMSF in residues from 15 to 115 and 20 to 90. MTs, R140H attained the highest flexibility (3.1Å and 3.2Å) in residues 15 to 115 and 30 to 105. The highest RMSF value was demonstrated by E144K (3.0 and 1.7Å) in both states in residues from 15 to 115, 155 to 175 and 160 to 185 in apo state, then a sudden rise in fluctuation, indicating the destabilized effect of mutation on PZase structure. Similarly, L19R, R140H, and E144K also demonstrating higher RMSD and RMSF, causing a low drug binding affinity with PZase. Residues from 61-85, present in the conserved region of PZase have been altered in MTs. MTs, A46V, D129N,
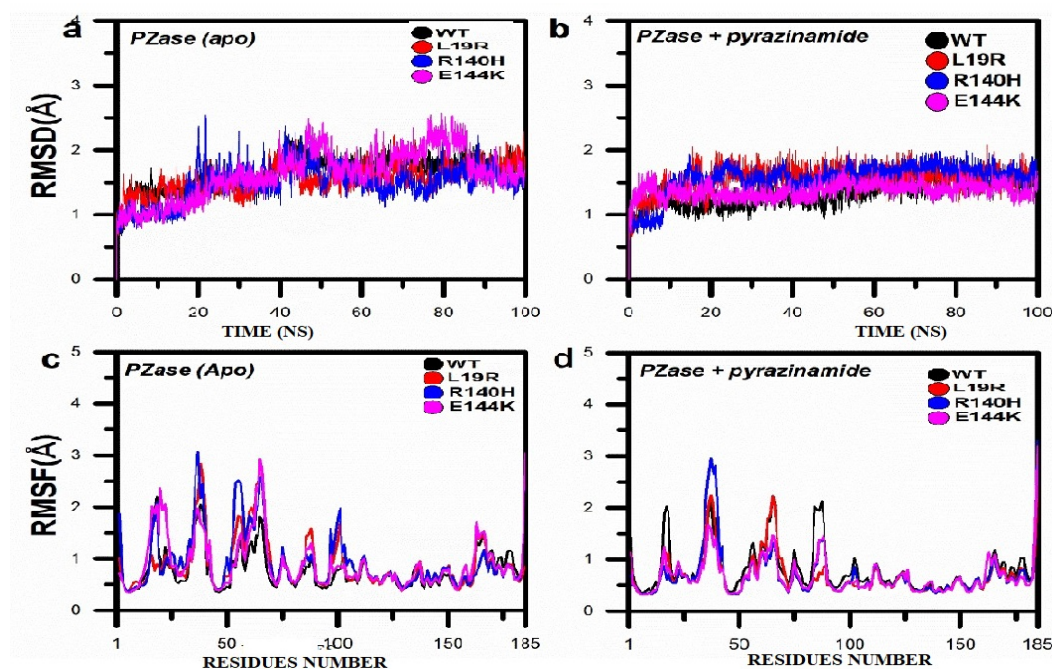
FIGURE 4.1: RMSD and RMSF of WT and MTs L19R, R140H, and E144K. The MTs ehibited more deviation (a,b) and the residues are more fluctuating (c,d) than WT in apo and drug bound state.

V131F, Q141P, G150A, R154T, A170P, S179G, and V180F may cause large deviation in comparison with WT PZase that may be involved in PZA-resistance. WT PZase attained RMSD values between 0.5Å and 1.3Å which seems stable after 15ns. MTs, V131F has a minimum RMSD of 1Å, however, it remains unstable
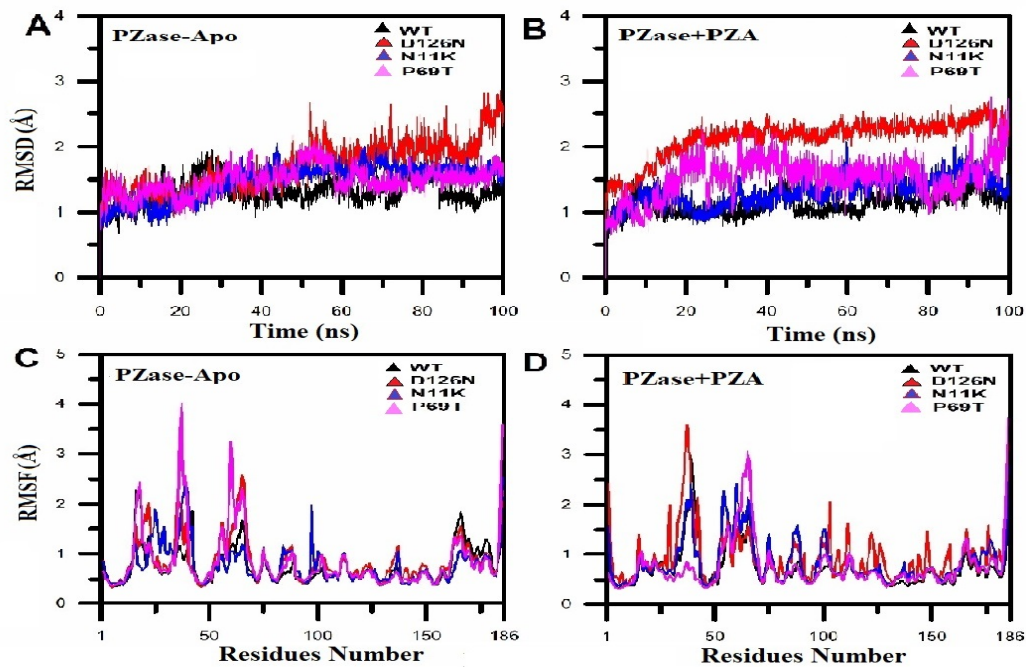
FIGURE 4.2: RMSD and RMSF of WT and variants, D126N, N11K, and P69T. The MTs exhibited high instability in deviations during whole simulation period (A,B). Residues of MTs demonstrated more flexibility than WT (C,D).

throughout simulations period. MTs, Q141P exhibited 0.5Å RMSD which become stable at a value of 1Å after 20ns but it has a little high deviation at 35ns and then looks like stable. Variant, R154T initially demonstared RMSD value of 1Å, however, a constantly increasing deviations have been seen after 5ns. At initial stage, MTs, A170P and V180F exhibited 1Å and 0.9 Å of RMSD and seems to be unstable after 5ns and 10ns respectively. With the aim to predict, whether these mutations affect the dynamic behavior of protein residues, the RMSF values of WT and MTs structures were compiled. The backbone RMSF of each residue of WT and MTs class, A46V, D129N, V131F, Q141P, G150A, R154T, A170P, A179P, and V180F have been calculated in order to analyze the flexibility of backbone structure (Figures. 4.5, 4.6). Higher RMSF value depicts more flexibility whereas low limit the movements during simulation in relation to its average position. WT exhibited the RMSF value between 0.3Å and 3Å. The residues 30 to 70 shows a little higher flexibility, however, overall fluctuations seems to be stable. In comparison with WT, MTs, V131F, Q141P, R154T, A170P, and V180F demonstrated a higher fluctuation in large number of residues. MTs V131F attained RMSF value from 0.5Å to 3.7Å, where residues at position 30 to 110 and 160 to 186 are seemed to be

more flexible. MTs Q141P demonstrated a slightly lower (0.3Å to 2.1Å), however, residues at position 18 to 90 were detected more flexible. MTs, R154T, A170P, and V180F exhibited RMSF values from 0.3Å to 3Å, 0.3Å to 2.7Å, and 0.3Å to 3.4Å respectively. Moreover, flexibility have been depicted at residues position, 25-80, 16-90, and 16-90 respectively. This high flexibility in MTs may cause the failure of PZase to convert pro-PZA into active form POA, resulting in resistance to interact with targets. RMSD of MTs, A46V, D129N, V131F, Q141P, G150A, R154T, A170P, S179G, and V180F may cause large deviation in comparison with WT PZase that may cause PZA-resistance as shown in (Figures. 4.4, 4.3).
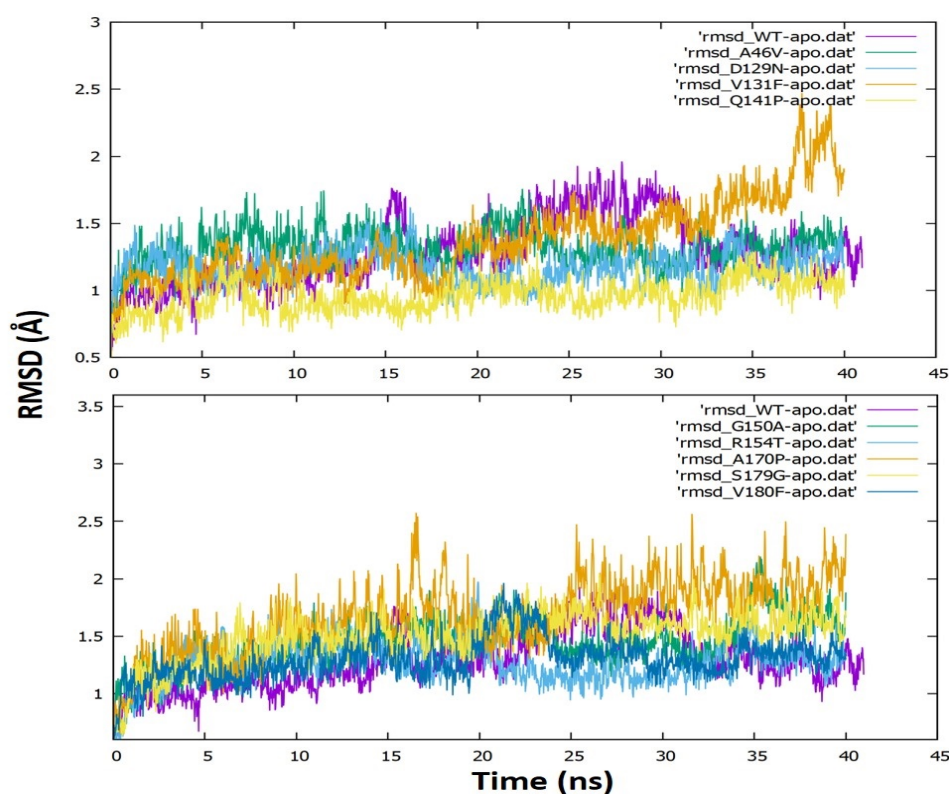
FIGURE 4.3: Comparison of WT and MTs PZase RMSDs in apo state.
The RMSD of WT is decreasing at 35ns to 40ns while MTs (A46V, D129N, V131F, Q141P, G150A, R154T, A170P, S179G, and V180F) are still attaining high value at the end of simulation period.

4.10.3.4   Folding Stability and Radius of Gyration

Radius of gyration (Rg) is a measure of degree of compactness and folding of proteins, plotted against time. The Rg of some MTs were calculated, showing a
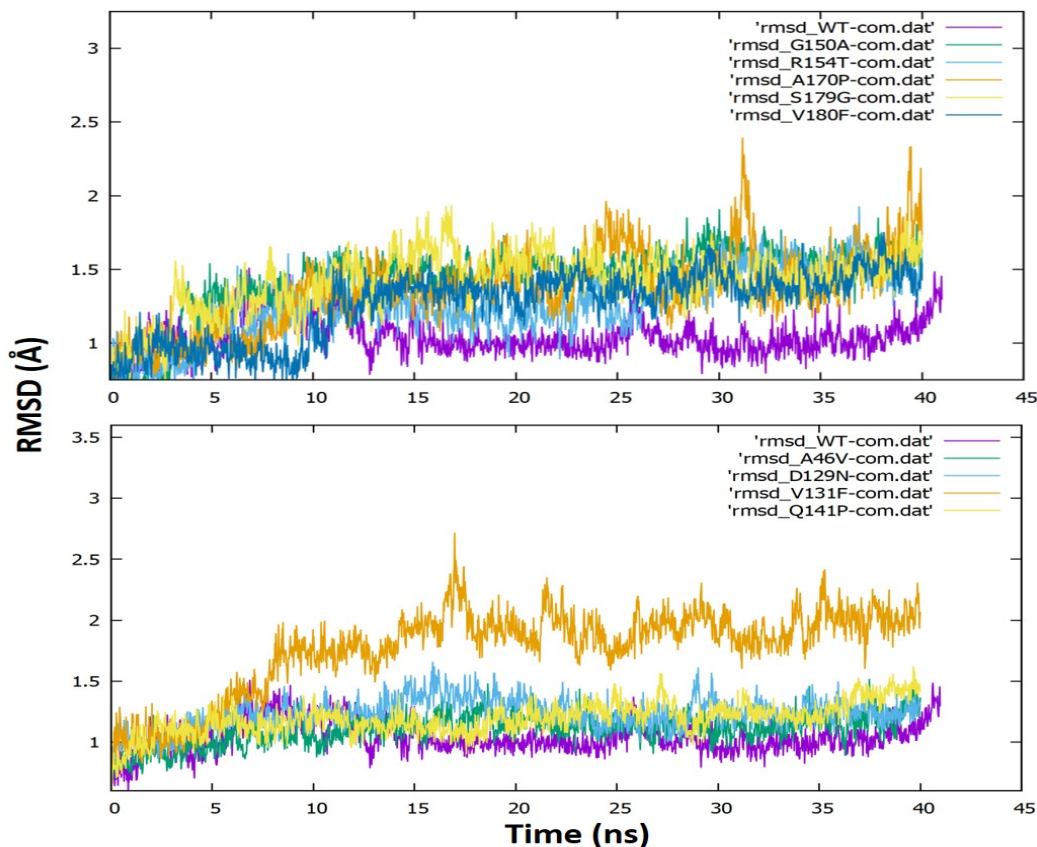
FIGURE 4.4: Comparison of WT and MTs PZase RMSDs.
The RMSD of WT was measured, lowest at 12 to 40ns while MTs (A46V, D129N, V131F, Q141P, G150A, R154T, A170P, S179G, and V180F) are rising still at the end in complex state (com).

variation between MTs, L19R, R140H, E144K, and WT (Figure. 4.7). The Apo states of MTs PZase (Figure. 4.7 c,e,g) seems to be more in variable states with respect to simulation period, attaining more deviation than WT (native), where as in drug bound, MTs PZase (Figure. 4.7 d,f,h) attained a little more Rg value.

Changes in folding and stability can be measured by observing the variations with respect to time, while a constant Rg value shows stability in folding during MD simulation. In the present investigation WT exhibited a more straight graph when compared with MTs. This straight plot during simulation period reveals a more stable behavior. The plot (Figure. 4.8) demonstrated a degree of variations, A degree of variations have been observed in MTs N11K, P69T, and D126N in comparison with WT in both, apo and complex states. MTs shows variation from 40 to 100ns simulation period when compared with WT. These finding suggests
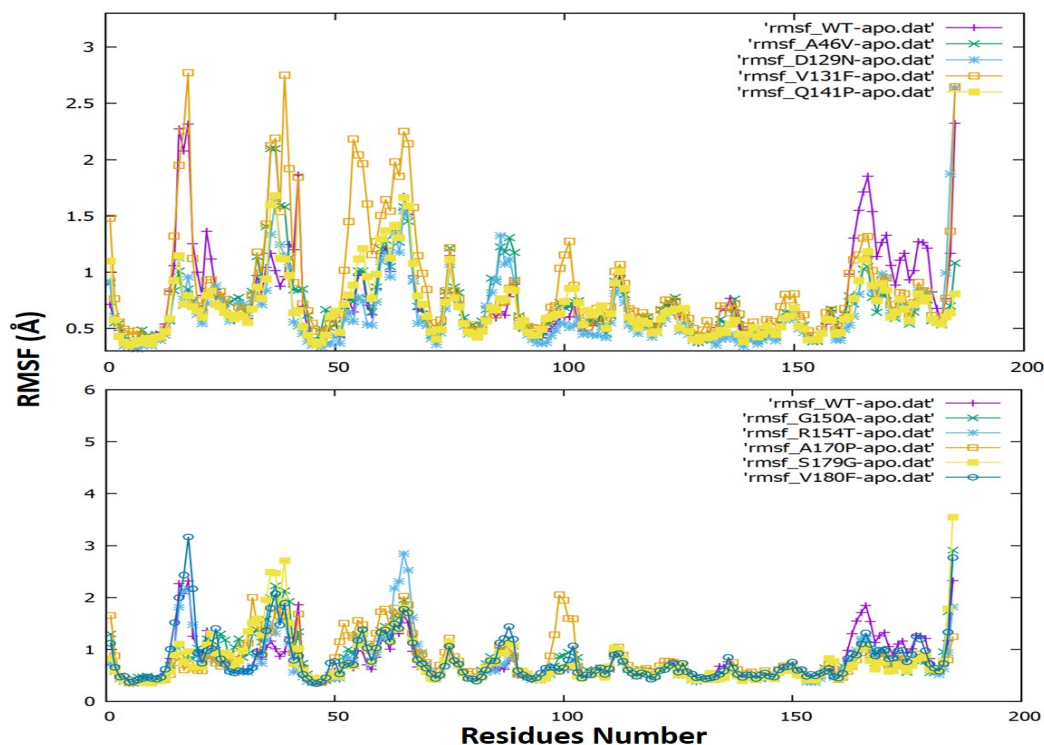
FIGURE 4.5: RMSF comparison of WT of MTs PZase in apo state. WT has been attaining less fluctuation than MTs (A46V, D129N, V131F, Q141P, G150A, R154T, A170P, S179G, and V180F).

that PZA-resistance might be due to folding defect.

4.10.3.5 Essential Dynamics

Principal Component analysis of WT and some selected MTs were plotted (Figures. 4.9, 4.10). A cluster type motion has been observed in WT PZase as compared to MTs, exhibiting dispersed type of motion in residues. MTs, L19R covering an area on PC1 and PC2 between -50 and 50, -50 and 40 in apo state, while in drug bound state, it covered an area between -58 and 35 on PC1 and -50 to 40 on PC2 (Figure. 4.9 c,d). A more scattered type of motion has been found in R140H along PC1 between -60 and 45, -60 and 25 while on PC2 it was dispersed between -30 and 40, -30 and 40. In apo state, E144K was scattered between -58 and 50 along PC1 while it was dissociated in complex state (Figure. 4.9 g,h). In apo state, the area covered by Q141P (-20 and 20, -50 and 30), R154T (-20 and 40, -38 and 42), V131F (-30, 50 and -40, 55), A170P (-35, 30 and -55, 35),
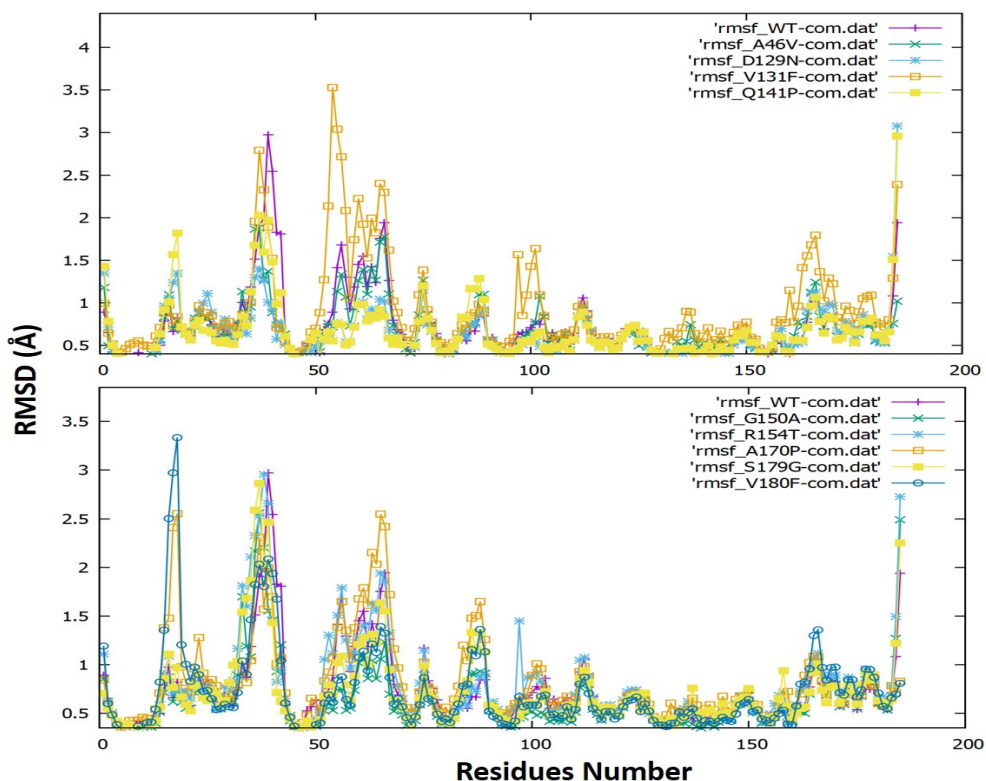
FIGURE 4.6: RMSFs comparison of WT and of MTs PZase in complex state. WT exhibited less flexibility than MTs (A46V, D129N, V131F, Q141P, G150A, R154T, A170P, S179G, and V180F) as shown by colored peaks of WT and MTs PZase.

and V180F (-32, 30 and -35, 33) on PCA-1 and PCA-2 is seemed to be high and more scattered type than WT as shown (Figure. 4.11). In drug bound state, WT exhibited a compact type motion, covering an area of -28 and 33 on PC1 while -34 and 38 on PC2. In apo state, WT exhibited more disperse type of motion on PC1 and PC2 (-28, 34 and -35, 42) than in drug bound state. MT exhibited a highest degree of dispersion in motion on PC1 and PC2, covering an overall area of -120 and 90, -140 and 102 respectively. MT A170P attained a motion between -120, 90 and -140, 102 on PC1 and PC2 respectively. The motion exhibited by MT Q141P (-29, 29 and -25, 28), R154T (-90, 90 and -82, 120), V131F (-140, 90 and -110, 110), and V180F (-30, 27 and -37, 28) on PC1 and PC2 is seemed to be more dispersed type than WT (Figure. 4.12).

These observations suggest that how a point mutation may affect the dynamics of molecules, make them a weak target to interact with specific drug. The disperse type of motion analyzed through principal components might be used to depict
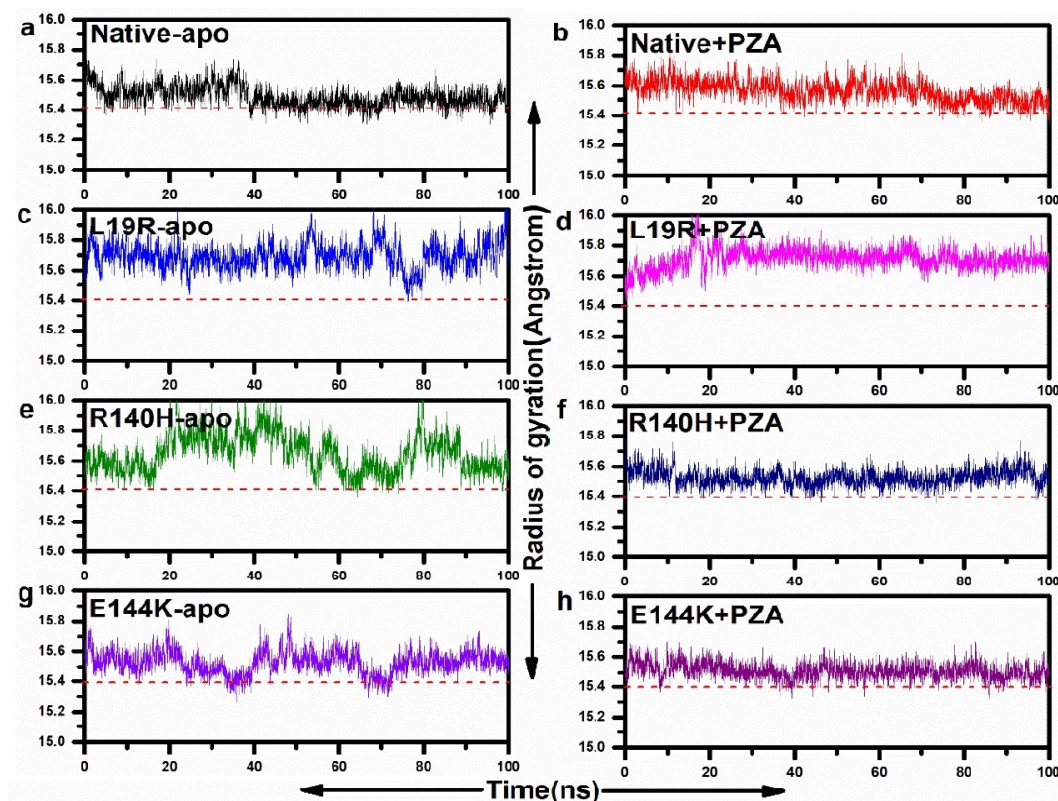
FIGURE 4.7: Radius of gyration of WT (a, b) and MTs (c, d, e, f, g, h). Stable folding in proteins is essential for proper function. A straight graph represent a stable folding of proteins structures. The graph of WT structure (a,b) seems more stable than MTs.

the residual motion in protiens for better understanding the effect. WT exhibited a normal behavior than MTs.

4.10.3.6 Projection of Motion (Eigenvectors)

A multidimensional linear least square fit of the trajectory is measured through eigenvectors which give a projection of motion of proteins. This multidimensional fitting represent the best fitting direction with respective to eigenvector number. The first four eigenvector attained variation at initial state and attained a stable value within ten eigenvectors. The graph in figures demonstrated that WT is occupying less phase space area than MTs, E144K, L19R, D126N, N11K, P69T, and R140H in apo and complexed with PZA (Figures. 4.13, 4.14). This mutation is present close to the active site resisdue 138, present in the ligand interacting pocket of target.
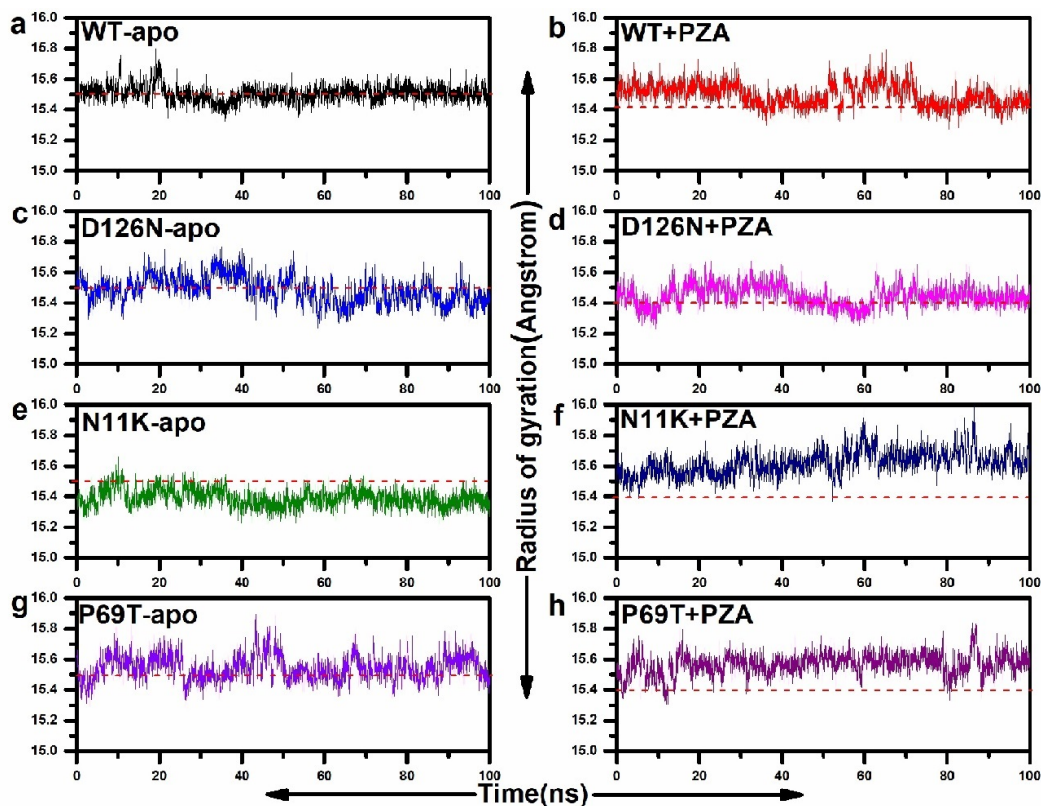
FIGURE 4.8: Comparison of Radius of gyration of WT and MTs.
WT attained a stable Rg (a,b) while MTs showing unstable folding. A smooth straight graph represent a stable folding of proteins structures.

4.10.3.7 Gibbs Free Energy

The amount of work done of closed system, exchanging heat with surrounding is known as gibbs free energy (GFE), which can be used to measure the relative stability of proteins. The differences in GFE values of WT and some selected MTs (L19R, R140H, E144K, P69T, N11K, and D126N) demonstrating the stability of PZase. A more blue peaks in plots represent more stablilty. WT demonstrated more stability in GFE as compared to MTs, indicated by the peak color of plot (Figures. 4.15, 4.16). WT is seemed to be more stable in both state.

4.10.3.8 Binding Pocket

Binding pocket volume is commonly measured by CASTp server. The pocket's volume may provide valuable surface topographic information, intercting with PZA
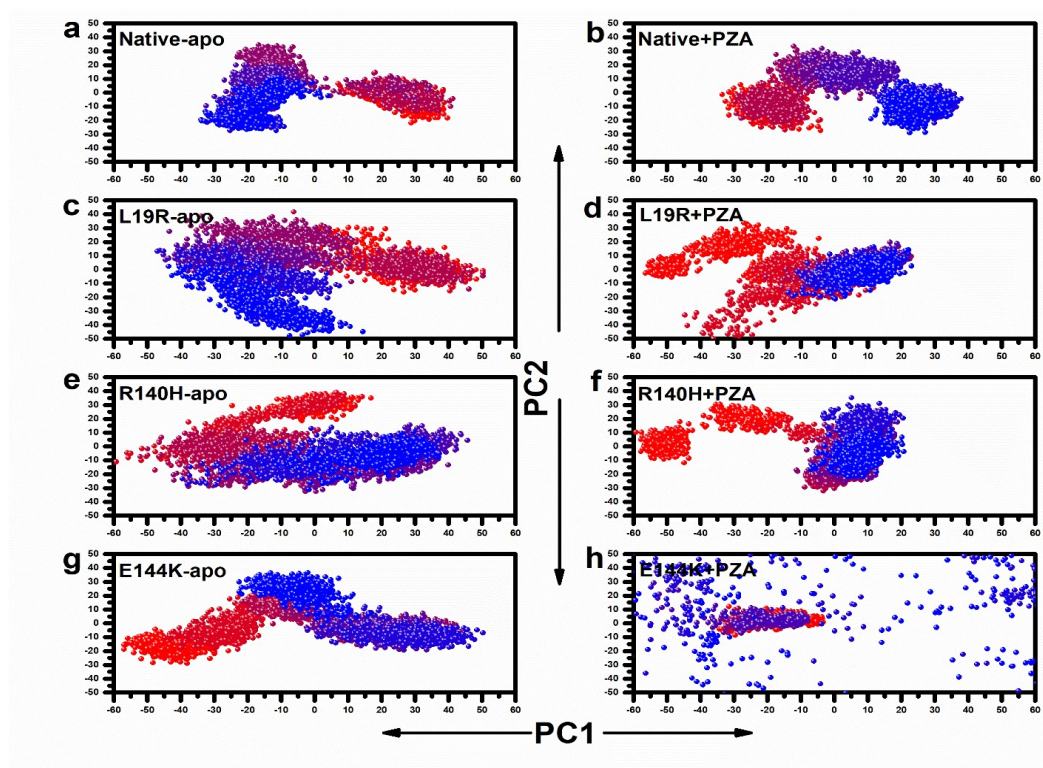
FIGURE 4.9: PCA of WT and MTs in apo and complex state of PZase. WT (a, b) and MT L19R, R140H, E144K (c,d,e,f,g,h) have been plotted on both axis as PC1 and PC2. The motion in MTs structure seems, more scattered than WT. E144K in complex state (h) has been dissociated.

to convert it into active form, POA. A decrease in pocket volume has been detected in L19R, R140H, and E144K as compared to WT (Table. 4.16). Pocket's volume of WT ($585.736Å^3$) and MTs, 556.236 $Å^3$, 437.966 $Å^3$, and 552.825 $Å^3$ respectively. This decrease in MT's pocket size may cause a weak binding of PZA with PZase to convert it into active form, POA.

4.10.3.9 Proteins and Ligand Interactions

Hydrogen and hydrophobic forces are important in ligand and protein interactions. These interactions were detected between residues Leu19, Asp49, His51, His57, His71, Ile133, Ala134, His137, Cys138 and PZA. Hydrogen bonds (H-bonds) have been found between PZA and residues, Leu19, His137, Ala134, Cys138, and Ile133 of PZase. Fewer H-bonds have been found between MTs and PZA drug as shown (Figure. 4.17). This weak interaction may cause drug resistance.
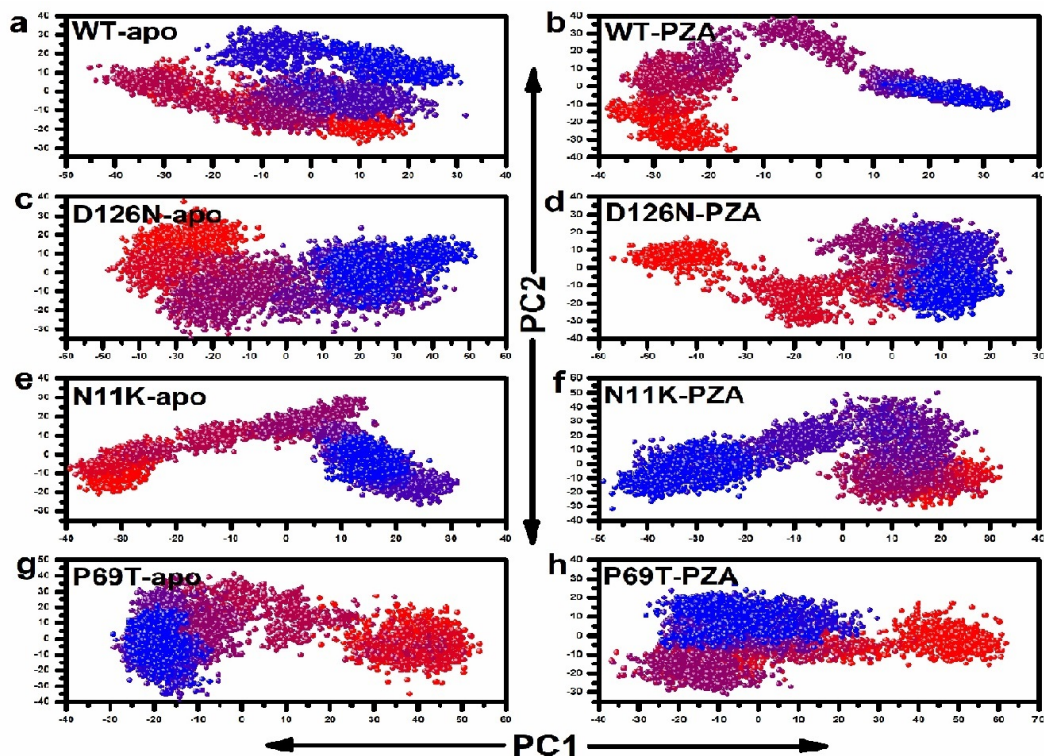
FIGURE 4.10: PCA of WT and D126N, N11K, and P69T in apo and complex state.

The motion in MTs (c,d,e,f,g,h) and WT (a,b) on PC1 and PC2 has been shown, signifying the effect of mutation on PZase dynamics.

4.10.3.10 Hydrogen Bonding Effect

To find the effect of mutations on fraction of hydrogen bonding, the residues at active site and its surrounding (Cys138, His137, Ala134, Leu19, and Asp49) have been investigated in some MTs. The number of H-bonds have been found significantly differ between WT and MTs PZase (Figure. 4.18). WT formed maximum H-bonds, especially in the PZA interaction and surrounding amino acids, D8, L19, Ile133, A134, H137, and C138 while MTs L19R has a fewer number of hydrogen bonding in comparison with WT (Figure. 4.18). The number of hydrogen bonding were significantly low in MTs R140H, E144K (Figure. 4.19).

4.10.3.11 Metal Ion (Fe^{+2}) Effect and Mutation

Metallic ions play important role in proper functioning of enzymes. WT PZase has Fe^{+2} metal ion coordinated by D49, H51, H57, and H71 (Figure. 4.21). The
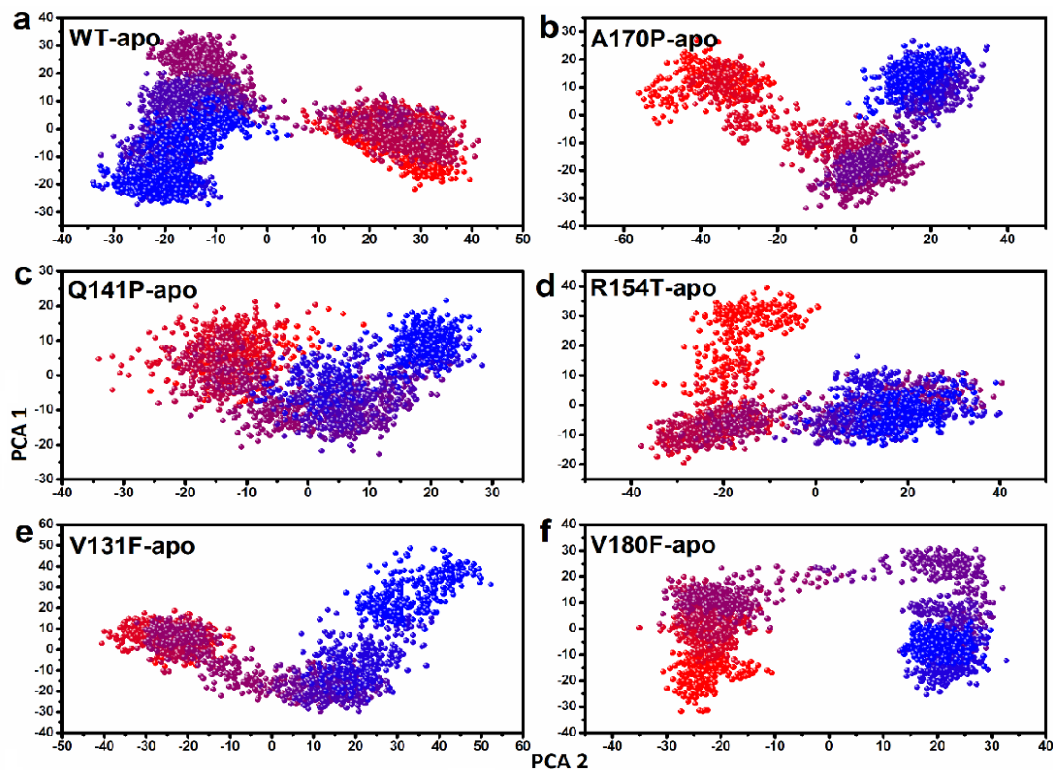
FIGURE 4.11: PCA of WT and MTs PZase in apo state.
WT (a) and MTs PZase A170P, Q141P, R154T, V131F, and V180F (b,c,d,e,f). Cluster type of motion exhibited by WT, while motion in MTs are dispersed, covering more area on both the axis in apo state.

RMSD and RMSF values of D49, H51, H57, and H71 has been found high in the MTs's metal Fe^{+2} (Figure. 4.20, 4.21). Iron binding site remains stable in WT PZase after 35ns while it is unstable in MTs (Figure. 4.20 a,b).

MTs complex with PZA exhibited more deviation and attained the RMSD value of 2.3Å (Figure. 4.20 a,b). Fluctuations have been detected in Fe^{+2} binding site residues (Figures. 4.20, 4.21 c,d). The highest fluctuation was observed in MTs as compared to WT, whereas MTs exhibited a high fluctuations from 0.7 to 2.1Å (Figures. 4.20, 4.21).

4.10.3.12 Mutation and Dynamic Cross-correlation Matrix

A large-scale motion of proteins can be measured through dynamic cross-correlation matrix (DCCM). Positive (correlate motions) and negative motion (anti-correlated motions) of residues are shown by red and blue regions. The red and blue are the
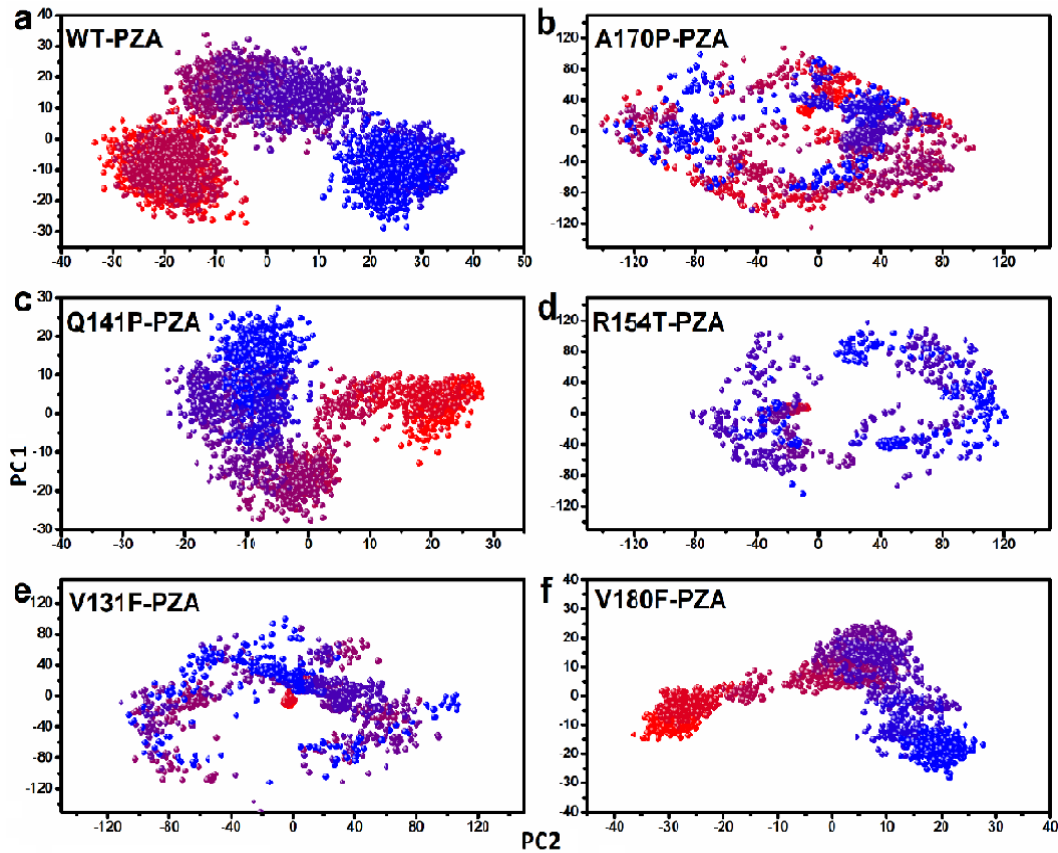
FIGURE 4.12: PCA of WT and MTs in complex state.
MTs, A170P, Q141P, R154T, V131F, and V180F (b,c,d,e,f) are more dispersed than WT (a) on both axis in complex state.

positive and negative correlated regions. WT residues were mostly exhibiting correlated motion than MTs, involving in more anti-correlated motions. Correlated motions were detected in both state of WT PZase, particularly in residues 130 to 180 while there were more anti-correlated motions in complex state of MTs. E144K, R140H, and L19R in apo and PZA bound form are seems to be involved in more negative correlated motion (Figure. 4.22). However, P69T, N11K, and D126N are slightly involved in more correlated motions than WT (Figure. 4.23).

The residues motion in PZase WT and MTs have been shown, colored coded with more correlated (red), medium (yellow), less (green), and anti-correlated (blue) (Figures. 4.24, 4.25). A positive correlation was observed at residues position 125-186 and 50-70 in WT. MT Q141P-apo exhibited more positive motion 50-70 and 160-186. MTs, A170P, R154T, V131F, and V180F have been shown, having a high degree of anti-correlated motion among residues. The difference in residues
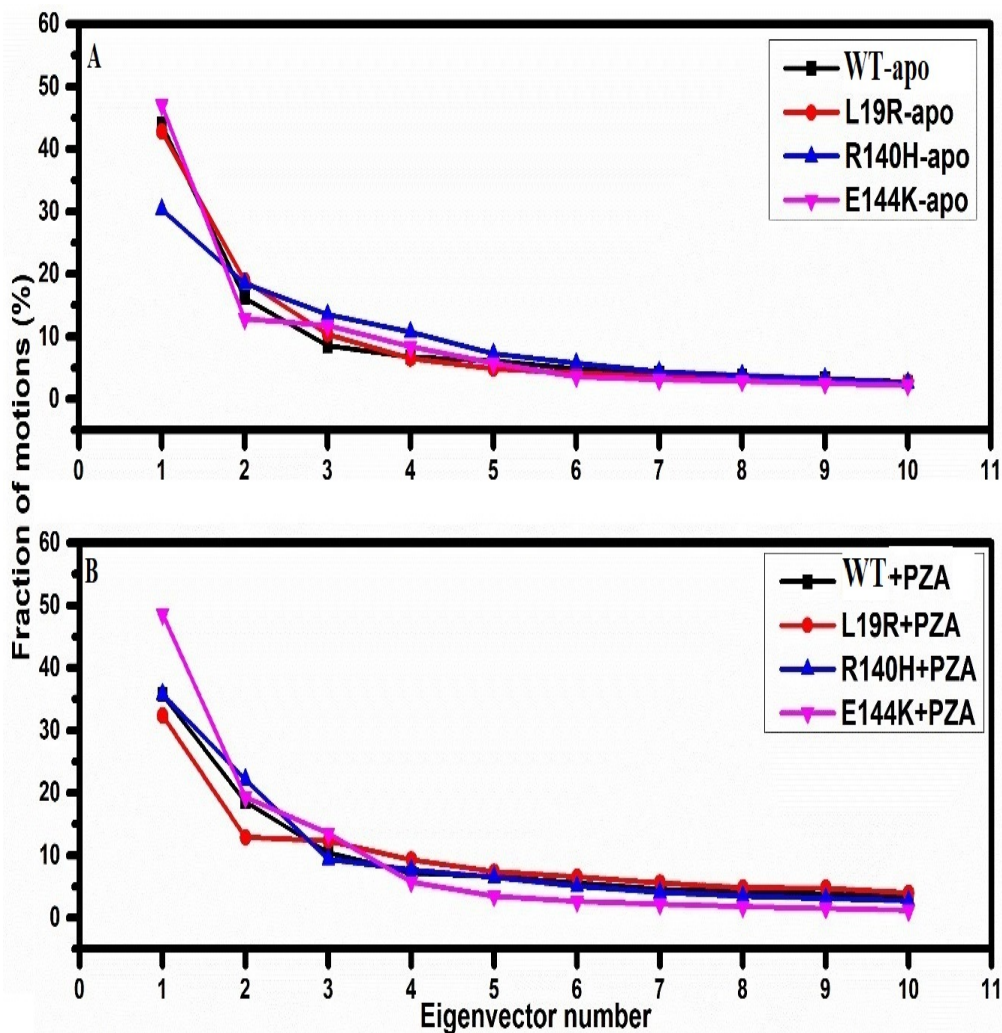
FIGURE 4.13: Projection of motions in WT and MTs (E144K, L19R, and R140H).

WT and MTs (E144K, L19R, and R140H) shows the projection of motions during the first ten eigenvalues. (A) Apo state. (B) complex with PZA. The WT (black) shows fitting best than MTs.

motions between WT and MT suggest that point mutation at far other than active site may affect the motion which is important for proper function of proteins.

The correlated and anti-correlated motion of residues have been found in great variation in bound state of PZA and PZase. MTs Q141P, R154T, and A170P retained more correlated motion in residues as compared to WT. The residues at position 61-68 exhibited correlated motion with 160-180 in WT, whereas this correlation is very strong in MTs, Q141P, R154T, and A170P. V131F and V180F exhibited a strong anti-correlated motion.
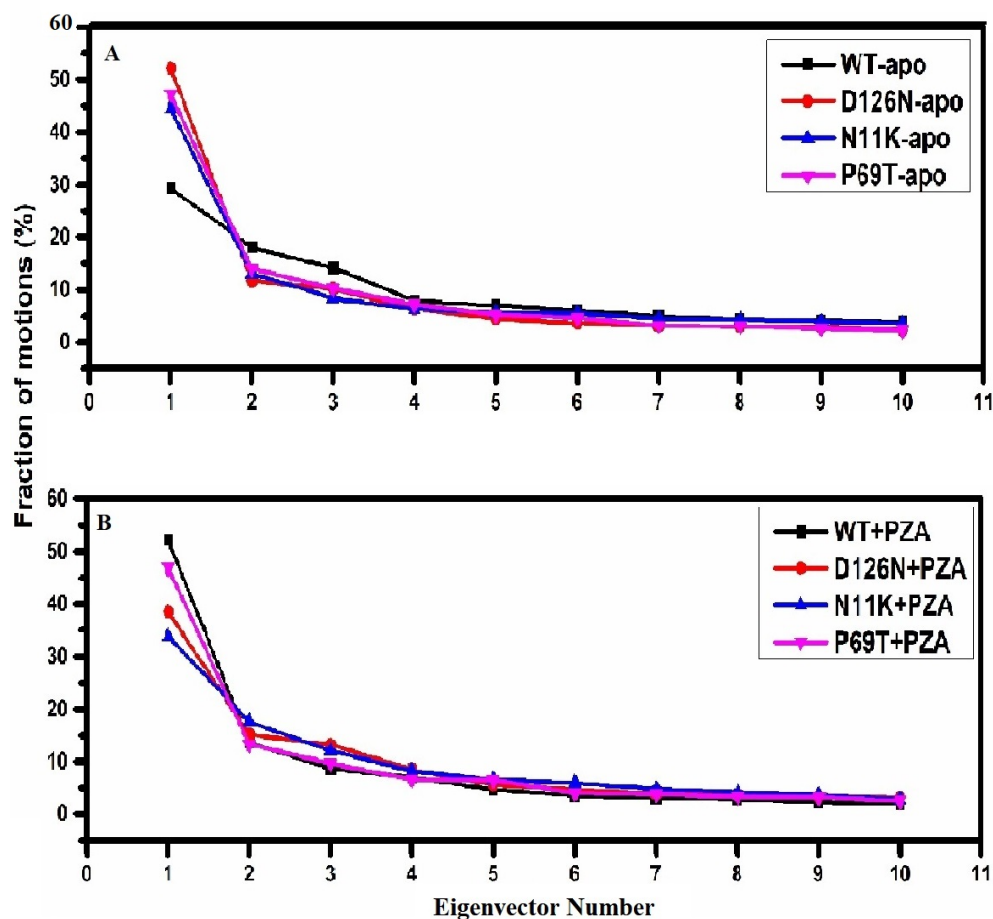
FIGURE 4.14: Projection of motions in WT and MTs PZase.
WT structure has been shown (black), occupying less space area and shows best fitting than MTs. (A) Apo state, (B) Complex with PZA.

These result suggest that a point mutation may cause significant alteration in residual motions that may affect the activation of PZA into POA for active elimination of latent MTB isolates (Figures. 4.24, 4.25).

4.10.3.13 Distance Matrix

The drug and PZase distance is commonly plotted through distance matrix. WT exhibited a constant matrix throughout simulation. However, the MTs E144K has been dissociated at 76ns. During the whole simulation period, The average distance between PZA and PZase was remained constant except E144K complex, exhibited fluctuation and dissociated at 76ns (Figure. 4.26). However, in MTs
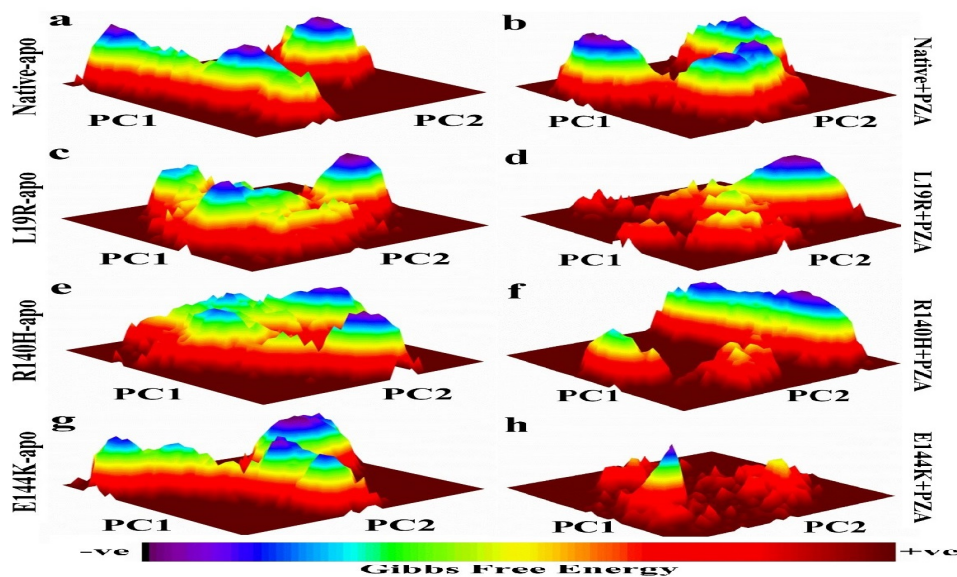
FIGURE 4.15: Gibbs free energy of WT and MTs in apo and complex state. GFE of WT (a,b) and MTs (c,d,e,f,g,h). A blue color (-ive) is more stable followed by green and yellow. Red color shows more unstable state. MTs, L19R, R140H, and E144K are seeming in unstable state.
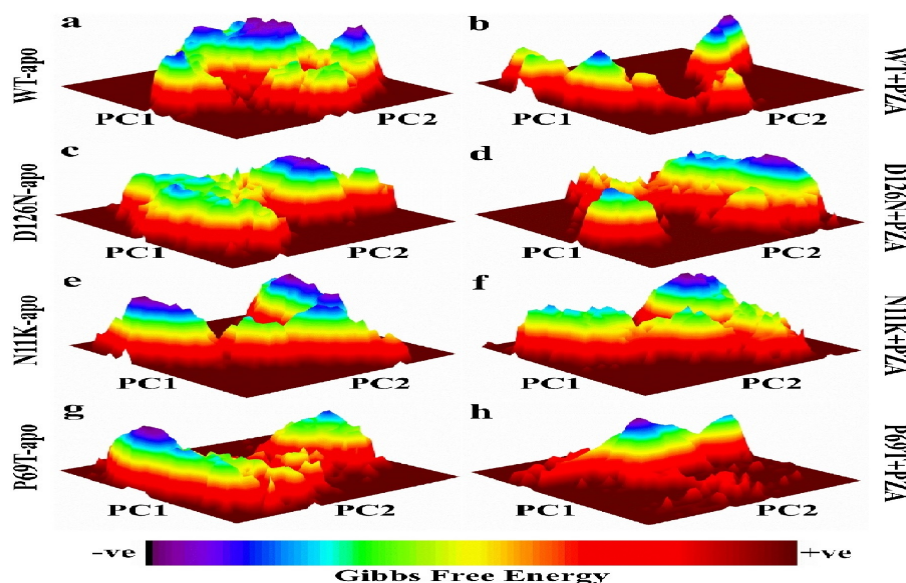
FIGURE 4.16: Gibbs free energy of WT and MTs (P69T, N11K, and D126N). Peak color are color coded with more -ive (blue) or more +ive (red). A more -ive is most stable structure.

P69T, N11K, and D126N the average distance between PZA and PZase is seem to be more fluctuated throughout simulations than WT (Figure. 4.27). N11K exhibited more distance between drug and proteins than D126N. The same results were obtained inspite the repitition of simulation suggesting that the E144K complex is unstable.
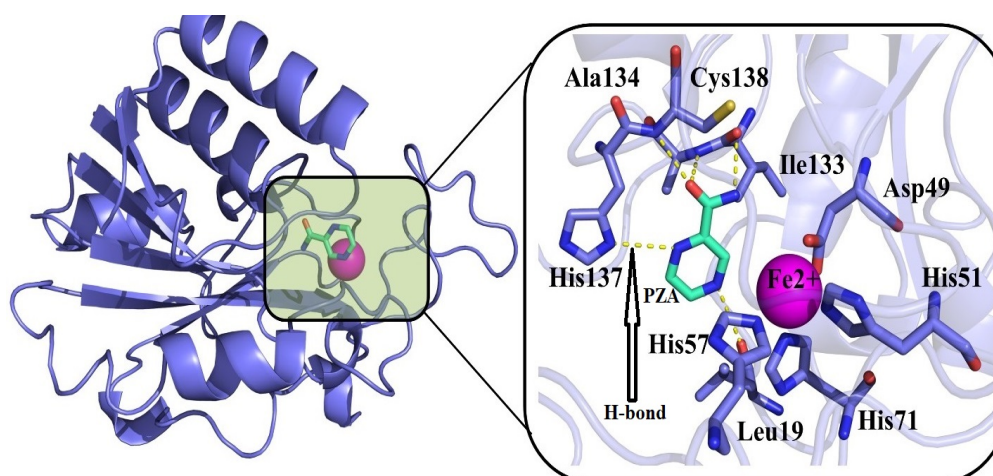
FIGURE 4.17: WT PZase interaction with PZA drug.
Residues, Asp49, His57, His51, and His71 are natural ligand (Fe^{+2}) binding residues in PZase. Hydrogen bonds (HB), have been shown in yellow dots, present between PZA and PZase residues, Leu19, Ala134, His137, Cys138, and Ile133.
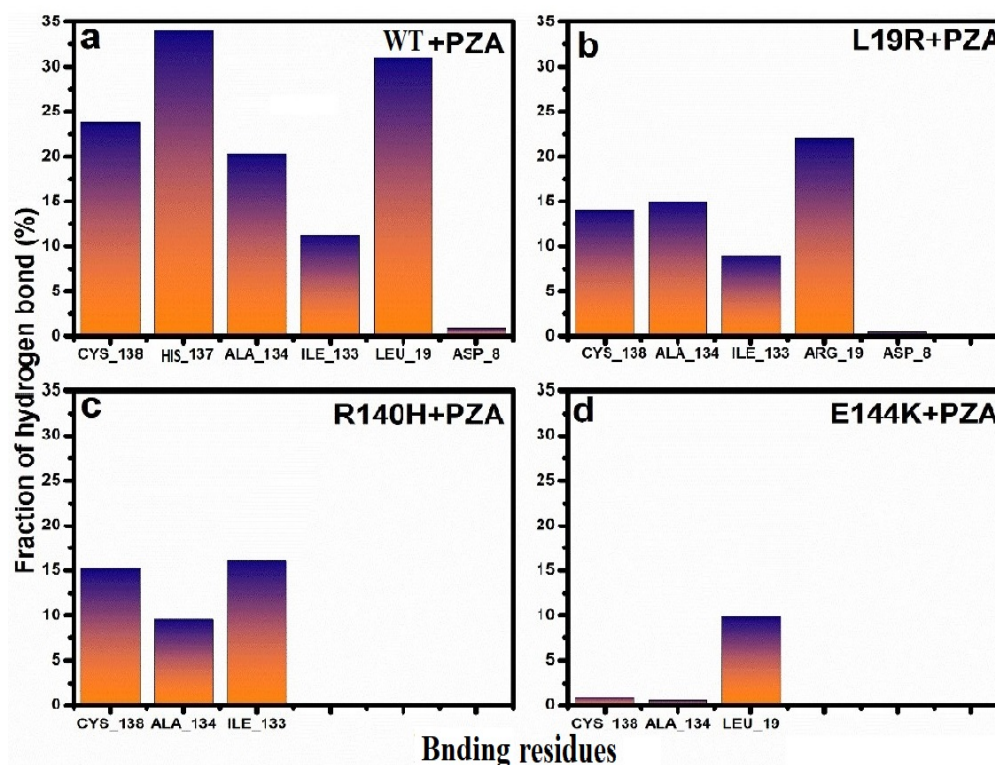
FIGURE 4.18: Effect of mutations (L19R, R140H, E144K) on H-bonds.
H-bonding frequency in drug interacting residues of WT (a) and MTs L19R, R140H, and E144K (c,d,e). The fraction of hydrogen bonding have been reduced to very few in MTs. WT have been found with maximum number of hydrogen bonding in active site residues.
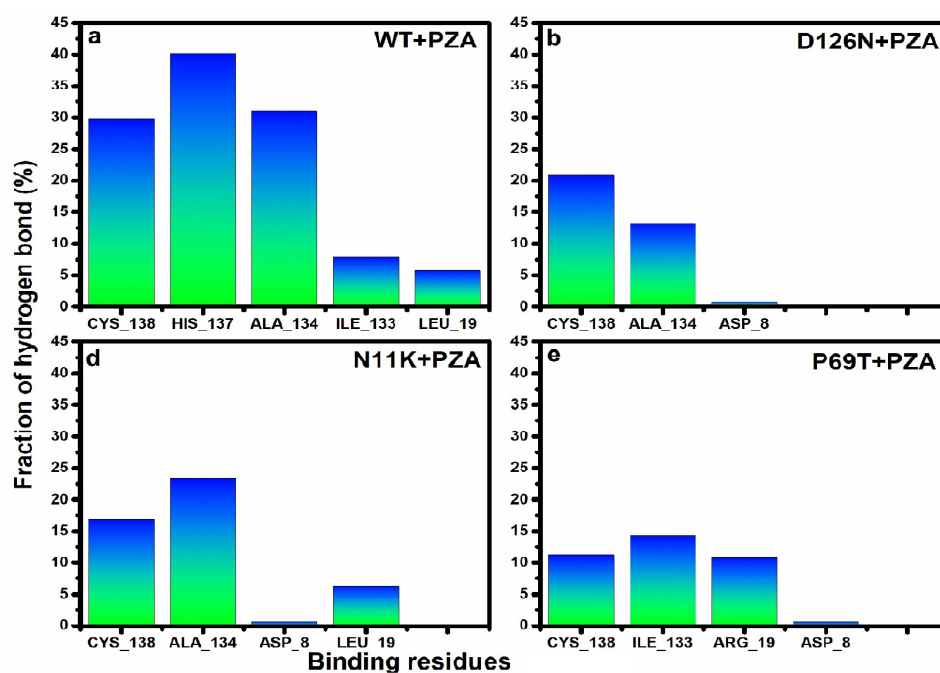
FIGURE 4.19: Effect of mutations (N11K, D126N, P69T) on H-bonds. H-bonding frequency in active site residues. WT (a) and MTs (b,d,e) N11K, D126N, and P69T. The fraction of H-bond is very low in MTs.
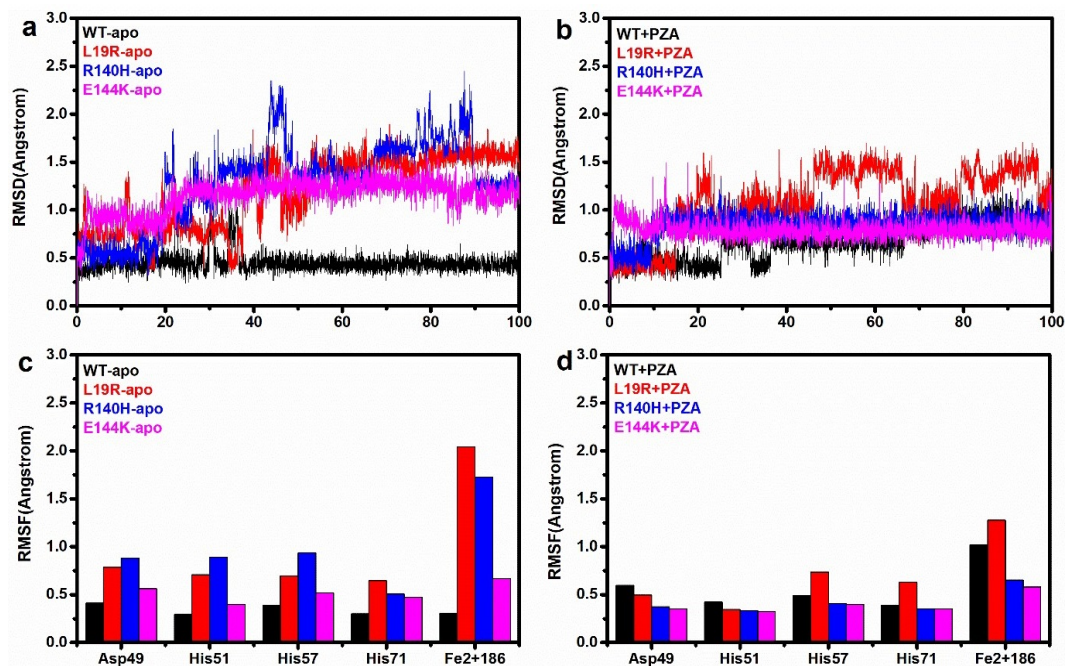
FIGURE 4.20: Mutations effect on Fe^{+2} binding residues. Mutations may cause high RMSD and RMSF on Fe^{+2} (Asp49,His51, His57, His71). WT retained low RMSD than MTs (a,b). RMSF of WT in apo (c) and complex with PZA (d), is lower as compared to the MTs (L19R, R140H, E144K).
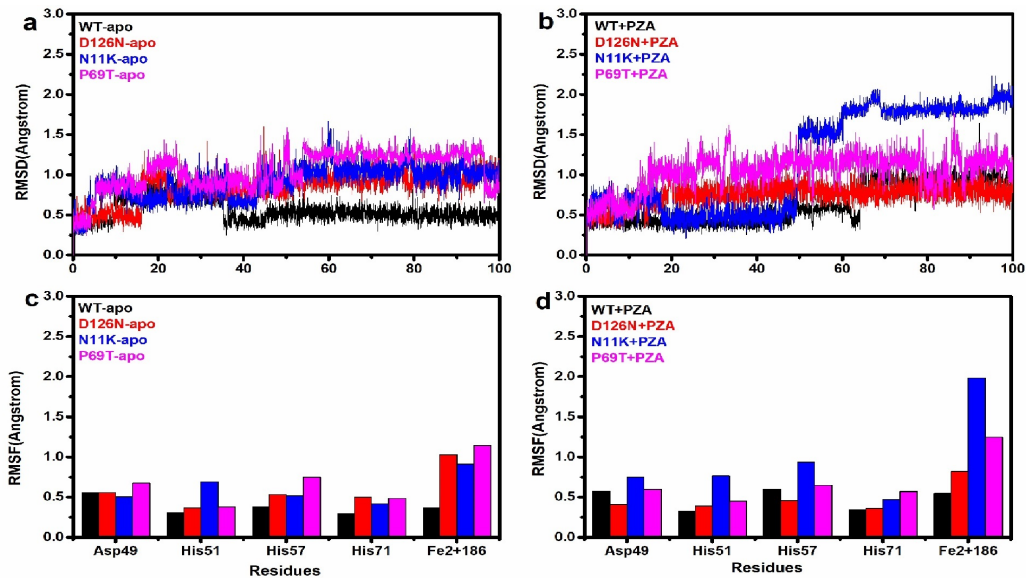
FIGURE 4.21: Mutations effect on binding residues of Fe^{+2} ion.
The effect causes high deviation (a,b) and fluctuation (c,d) in Fe^{+2} binding residues
of PZase. RMSD (a,b) and RMSF (c,d) at Fe^{+2} binding residues is significantly
different in WT and MTs (N11K, D126N, and P69T).
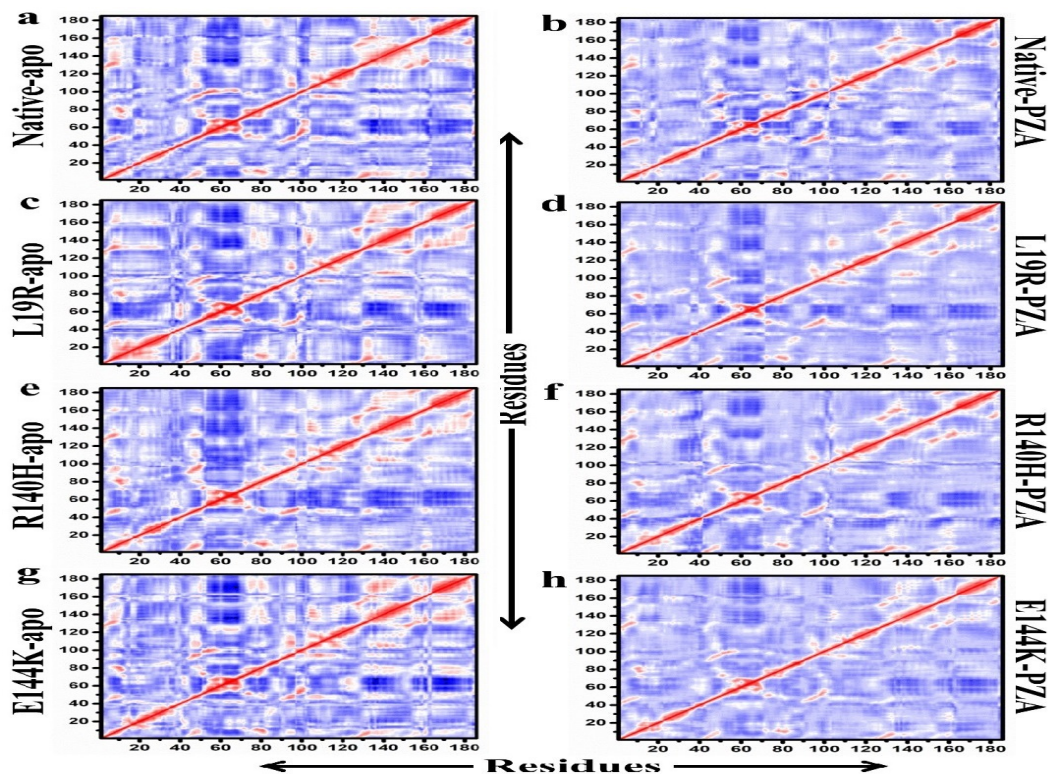
FIGURE 4.22: DCCM of WT and E144K, R140H, and L19R.
PZase with 186 residues, shown in red regions exhibiting more correlated motion
than blue region (anti-correlated motion). The correlated motion were mostly
found in drug bound state of PZase (b,d,f,h). MTs, E144K, R140H, L19R in apo
and PZA bound form, exhibiting more anti-correlated motion. In apo state, WT
exhibited more correlated motion than MT except Q141P.
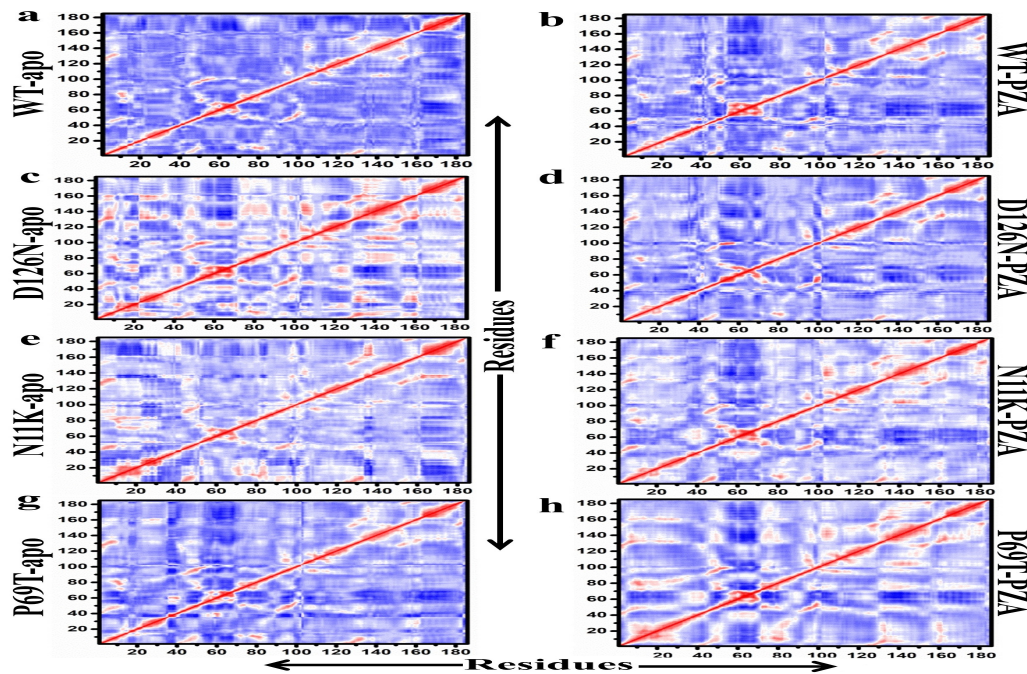
FIGURE 4.23: DCCM of WT and P69T, N11K, and D126N.
Red regions exhibiting more correlated motion than blue region (anti-correlated motion). More positive motions was observed in D126N-apo (c). Positive motions is seemed to be more prominent in apo state (a,c,e,g).
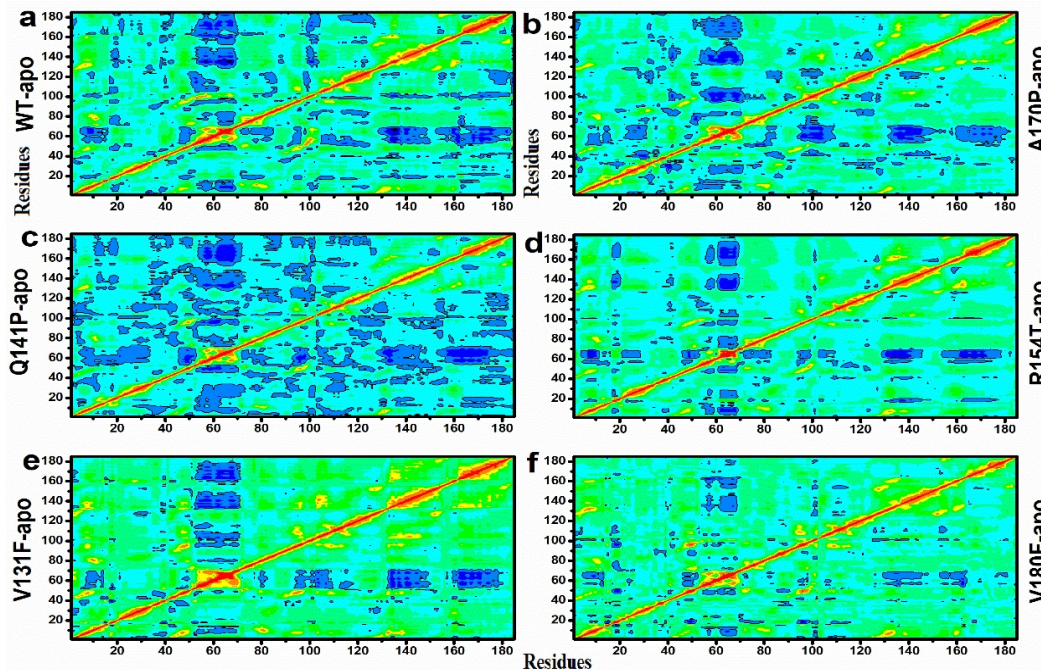
FIGURE 4.24: DCCM of WT and MTs in apo state.
The residue motion have been colored coded. More correlated (red), medium (yellow), less (green), and anti-correlated (blue). MTs, A170P, R154T, V131F, and V180F have been shown, exhibiting more anti-correlated motion.
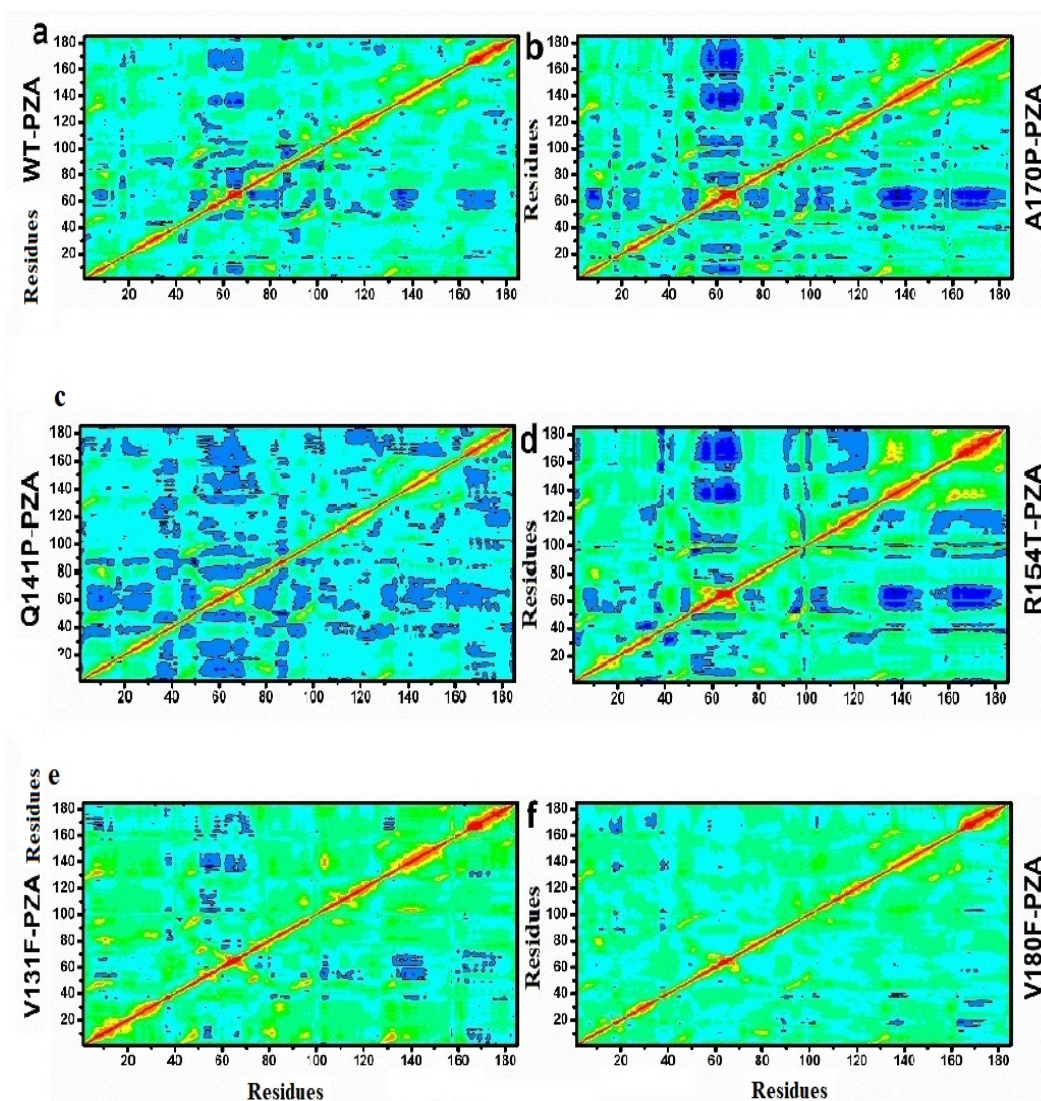
FIGURE 4.25: DCCM of WT and MTs in complex state.

The residue motion are colored coded with more correlated (red), medium (yellow), less (green), and anti-correlated (blue). The anti-correlated motion is more prominent in MTs, Q141P and R154E (c, d). DCCM in residues between 100 and 180 of WT seems in correlated motion as compared to MTs. A170P shows more anti-correlated motion at positions, 45-65, 140-180, and also some anti-correlation motion in residues at 10-30. MTs Q141P plot depict a more anti-correlated motion among all residues when compared with WT. Residues at postions 30-45, 50-70 and 100-180 seems in anti-correlation motion. This anti-correlation may alter the optimum function of enzyme, necessary for the biological function. In this case, PZase might be unable to convert PZA into POA for interaction with targets. MTs R154T also exhibited a more anti-correlated motion in comparison with WT and other MTs. However, V131F, and V180F seems, exhibiting a more correlated motion as compared to other MTs. Thus, a correlated motion is more favourable when a receptor interact with ligand.

4.11   Sequence of *RpsA* and Mutations

Among the 69 PZA-resistance isoates, 51 harbored mutations in *pncA* gene while 18 samples were PZA-resistance but *pncA* wild type (*pncA*^WT). All these 18 were repeated for DST using BACTEC MGIT 960 automated system. They were found as PZA-resistance and majority of these isolates were MDR (13/18) (Table. 4.17). To investigate the mutations in 1,544-bp fragment of *rpsA* gene, the resistance isolates along with sensitive and one H37Rv were also sequenced. Mutation in RpsA have been investigated in both, PZA-resistance and susceptible isolates in coding region (1446-bp fragment) of *rpsA*. Out of 18 PZA-resistance isolates, 11 (61%) isolate have fifteen different mutations while seven PZA-resistance were found WT for *rpsA* (*rpsA*^WT) (Table. 4.18). However, we did not find any mutation in PZA-resistance *panD* gene with *pncA*^WT gene and neither among sensitive isolates. We suggest that *rpsA* gene mutations should be considered along with *pncA* gene mutation for better development of new molecular methods of DST and TB management. The role of *rpsA* gene mutations in PZA-resistance should be evaluated from geographically diverse environment, specially TB high burden countries with more sample size to find the exact role of each gene in PZA-resistance. These mutations in the targets may also be useful in designing future biomarkers for early diagnosis of resistance in PZA-resistance isolates. The results may be compared with high burden countries for adopting a common strategy.

TABLE 4.17: Patients data of PZA-resistance pncA^WT

Type of resistance		resistance	Total
	1-MDR	13	13
	2-Poly_esistance	4	4
	3-XDR	1	1
Gender			
	1-Female	12	12
	2-Male	6	6
Treatment history			
	1-Diagnostics	14	14
	2-Follow Up	4	4

MDR: Multidrug resistance, XDR: extensively drug resistance
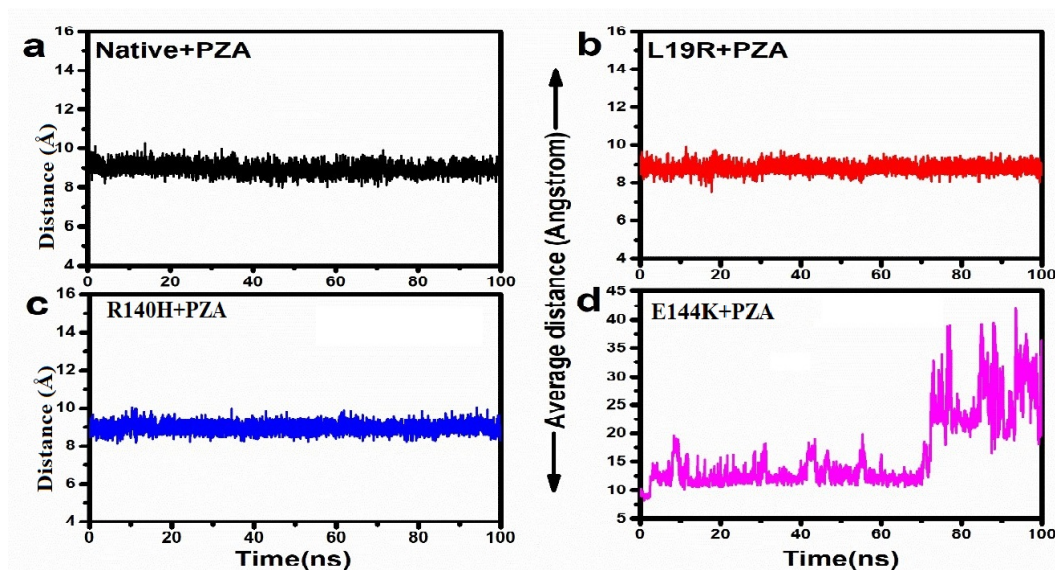
FIGURE 4.26: Distance matrix of WT (a), MTs (b,c,d) with PZA drug.
The average distance between WT (a) and MTs (b,c) is almost similar. E144K
(d) exhibited more distance between drug and protein from 76 to 100ns.
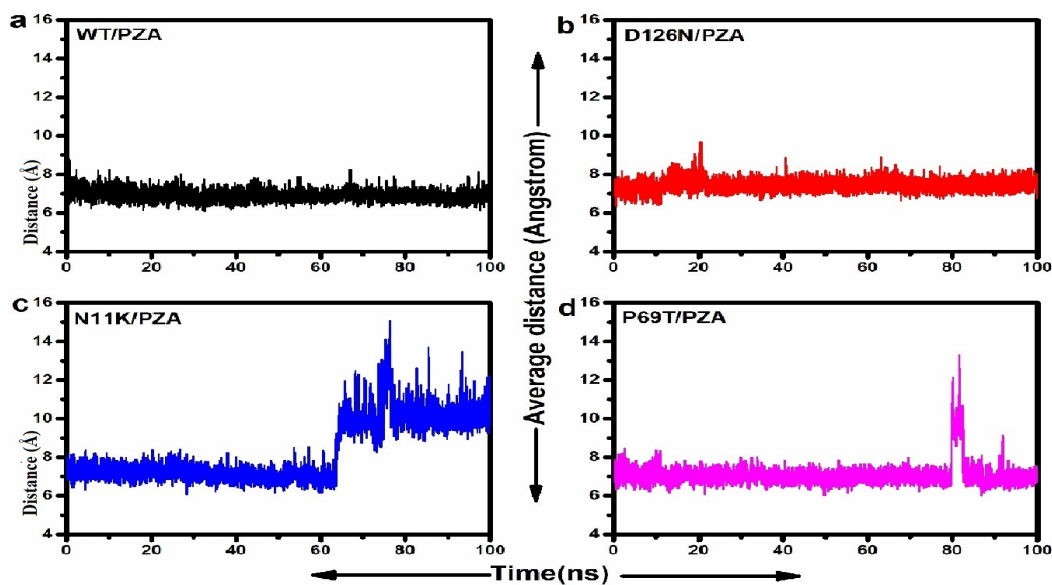
FIGURE 4.27: Distance matrix of WT and MTs with PZA drug.
A stable graph demonstrate a constant distance between PZA and PZase. WT
exhibited a constant distance (a). The distance between PZA and PZase increases
from 65 to 100ns (c) and 80-100ns (d) in MTs.

TABLE 4.18: Mutations detected in PZA-resistance *rpsA* gene

Mutation	Codon No.	Codon Change	*A.A Change	No.
76delA	26	ATA	Ile26FRAME	1
G220A	74	GTC-ATC	Val74Ile	1
A278G	93	AAG-AGG	Lys93Arg	1
G618A	206	TTG-TTA	Leu206Leu	2
A636C	212	CGA-CGC	Arg212Arg	2
A830G	277	AAG-AGG	Lys277Arg	1
C971T	324	TCC-TTC	Ser324Phe	1
G973A	325	GAG-AAG	Glu325Lys	3
G1021C	341	GGC-CGC	Gly341Arg	1
G1024A	342	GAC-AAC	Asp342Asn	4
G1027A	343	GAC-AAC	Asp343Asn	6
G1030C	344	GCG-CCG	Ala344Pro	6
A1051T	351	ATC-TTC	Ile351Phe	3
A1108C	370	ACC-CCC	Thr370Pro	1
T1207G	403	TGG-GGG	Trp403Gly	1

*A.A; Amino acid

4.11.1 Mutations Effect on RpsA Activity

4.11.1.1 Mutations in RpsA and Effect

MD simlations results, performed on all the RpsA variants in comparison with WT have been in significant variations with MTs. Mutations, Ile351Phe, Ser324Phe, Ala344Pro, Glu325Lys, Asp342Asn, Gly341Arg, Asp343Asn, Thr370Pro, and Trp4-03Gly present in *Mycobacterium tuberculosis* C-terminal domain (Mt-RpsA^{CTD}) also known as conserved region of RpsA. Molecular dynamics simulation was run on WT and MTs RpsA. WT RpsA exhibited RMSD of 2.0Å, 4.8Å, and 1.8Å at 0ns, 23ns, and 50ns respectively. After 50ns WT attained the stability. While MTs, S324F attained the RMSD value of 1.2Å, 4.2 Å, and 3.8Å at 0ns, 28, and 40ns respectively and then seemed to be a little stable at 3.8 Å (50ns). RMSD attained by E325K was found between 1.1Å and 4.8 Å at 9ns and 45ns respectively. However, the final RMSD (3.4 Å), was slightly higher than WT. The RMSD exhibited by G341R at 10ns and 25ns, was in between 1.2Å and 4.0Å respectively. A little stable RMSD has been observed (3.2 Å) at 50ns. Although the RMSD of MTs is low at initial period of simulation, however, at the end the RMSD of WT is looking

more stable. (Figure. 4.28). MTs D342N and D343N exhibited RMSD between 1.8Å and 3.7Å, 1.3Å and 3.6 Å respectively. Whereas MT D343N seemed to be consistent after 20ns. MTs A344P attained RMSDs between 1.7Å, 1Å while I351F exhibited 3.5Å and 4Å RMSDs seems highly unstable. WT RpsA demonstrated a stable RMSD (2.5-3.2Å) throughout the simulations. The other MTs RpsA, D342N (1-3.7Å), D343N (1.3-3.8Å), A344P (1-3.4 Å), and I351F (1.5Å-3.5Å) exhibiting variations during a 50ns simulation period. The D343N and I351F seems to be more deviated at 50ns. T370P and W403G attained RMSD between 2Å and 5.1Å, 2.5Å and 5Å respectively. These MTs exhibited deviations in RMSDs during 100ns simulation.
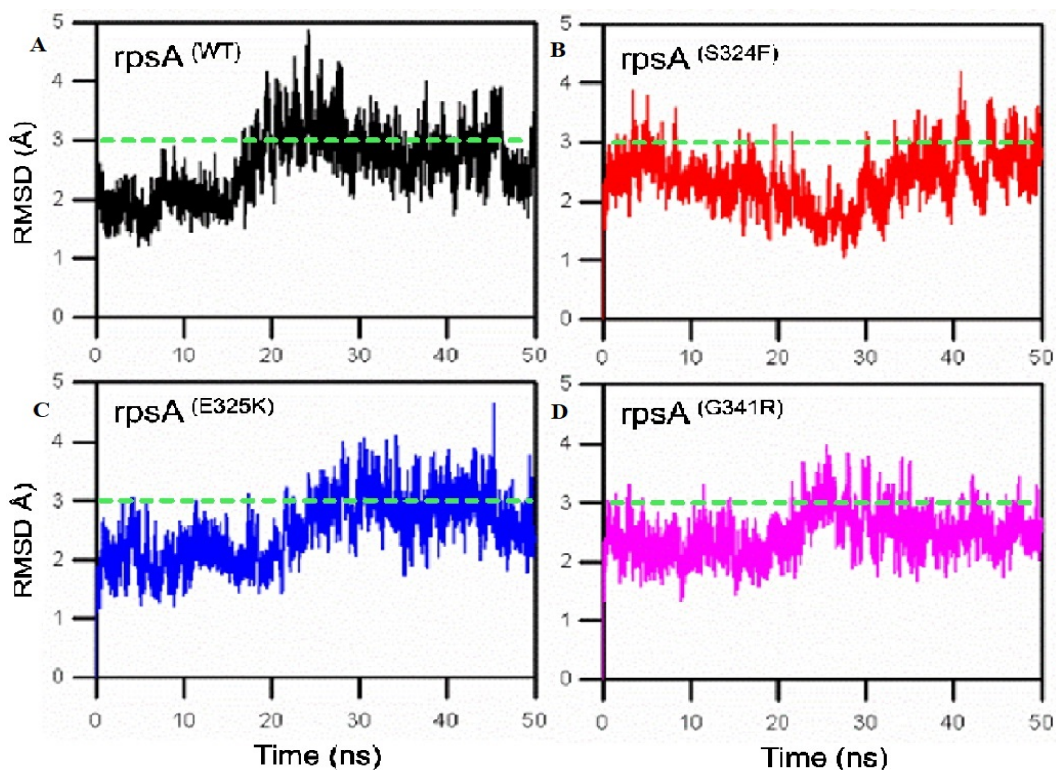
FIGURE 4.28: RMSD of WT and S324F, E325K, and G341R rpsA. RMSD of WT (A) is decreasing at the end of simulation period as compared to MTs (S324F, E325K, and G341R) (B, C, D).

4.11.1.2   Mutations in RpsA and Effect on Fluctuation

Flexibilities of WT and MTs were measured through RMSF. High RMSF values of MTs may result in weak affinity for interaction with POA. In combination with
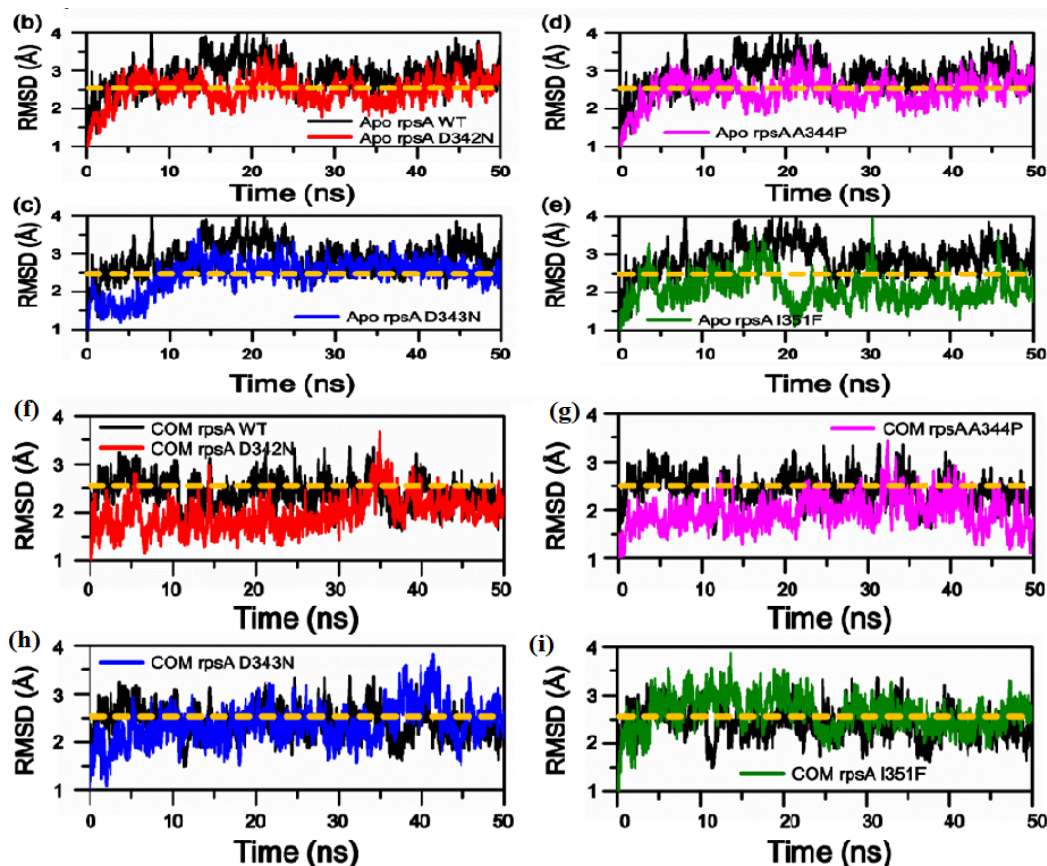
FIGURE 4.29: RMSD of WT and D342N, D343N, and A344P rpsA.
WT rpsA protein (black) attained a little high RMSD than D342N, D343N, and
A344P in apo (b,d,c) and complex (COM) state with PZA (f,g,h). While I351F
has a lower value in apo (e) and higher in complex state.

a drug, RpsA WT exhibited lower flexibility as compared to MTs. Fluctuations
in residues of S324F, E325K, and G341R were a little high than WT RpsA, ex-
hibiting RMSF between 0.3-3.8Å. These flexibilities were seemed in residues from
358 to 400. S324F exhibited RMSF from 0.4-.9Å, where residues 358-434 are more
flexible. E325K, exhibited RMSF between 0.7Å and 4.7Å in residues 358 to 434,
seems more flexibile. G341R attained RMSF between 0.8-5.2Å, in which residues
355-434 are more flexible (Figure. 4.31). The MTs, D342N exhibited high fluc-
tuation in residues 320-340, 355-360, and 370-390. Whereas a higher RMSF was
calculated for D343N at residues 324 and 340. A344P and I351F demonstrated
the highest flexibility at residues position 327-340 while 398-405 are more flexi-
ble in I351F. The MTs, T370P and W403G exhibited high fluctuation in residues
363-370, 370-380. In complex with a drug, WT exhibited lower flexibility as com-
pared to MTs. T370P and W403G attained more flexibility at residues 370-380
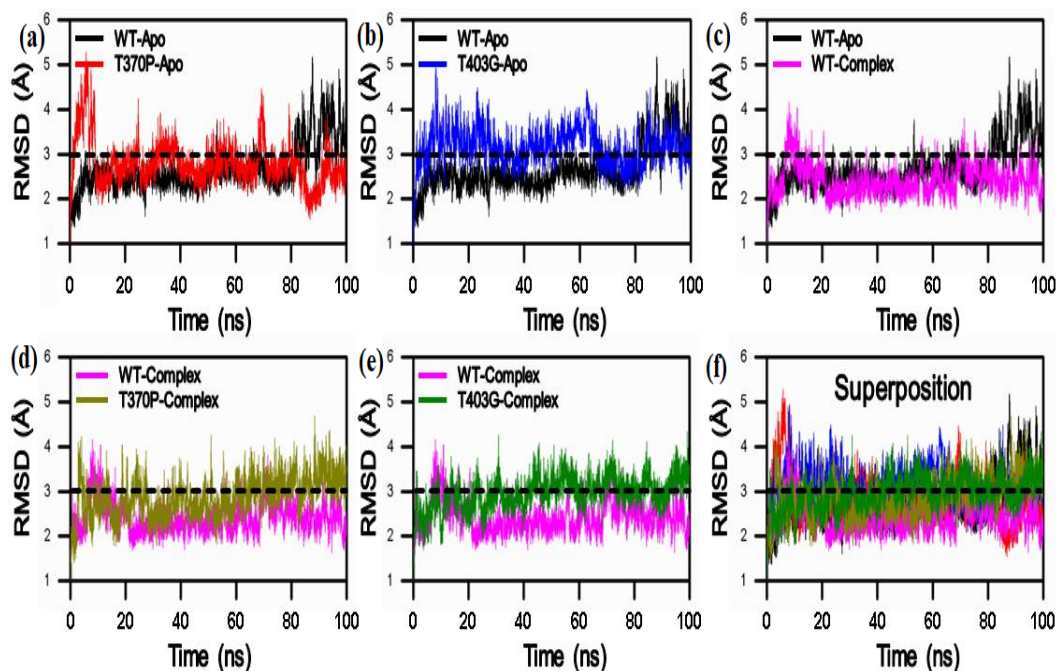
FIGURE 4.30: RMSD of WT and T370P and W403G.
In apo state (a,b) MTs are more deviated during the simulation period. (c); WT-apo and Wt-complex RMSDs comparison. (d,e); RMSDs of WT and MTs in complex with drug. (f); Superposition of all RMSDs.

(2.0-4.0Å and 2.0-5Å) (Figures. 4.32, 4.33). The effect of point mutation stability and flexibility may cause a drug resistance.

4.11.1.3   Radius of Gyration

The degree of compactness and folding can be measured through radius of gyration (Rg), plotted against time. The graphs showed a variation between MTs and WT RpsA. MTs RpsA (Figure. 4.34) is seemed to be more flexible and deviated in comparison with WT. Variations with respect to time represent changes in folding and stability while a constant Rg value shows no change in folding during MD simulation. The plot demonstrated a degree of variations in MTs S324F, E325K, and G341R in comparison with WT which has a stable Rg value of between 18.0Å and 19Å after 25ns but the Rg value MTs is smoothly increases during the whole simulation period from 0ns to 50ns. The MTs exhibited Rg value between 17 and 19 whereas the WT attained Rg values between 17.4 and 18. D342N, D343N, A344P, and I351F demonstrated a degree of variation in folding during
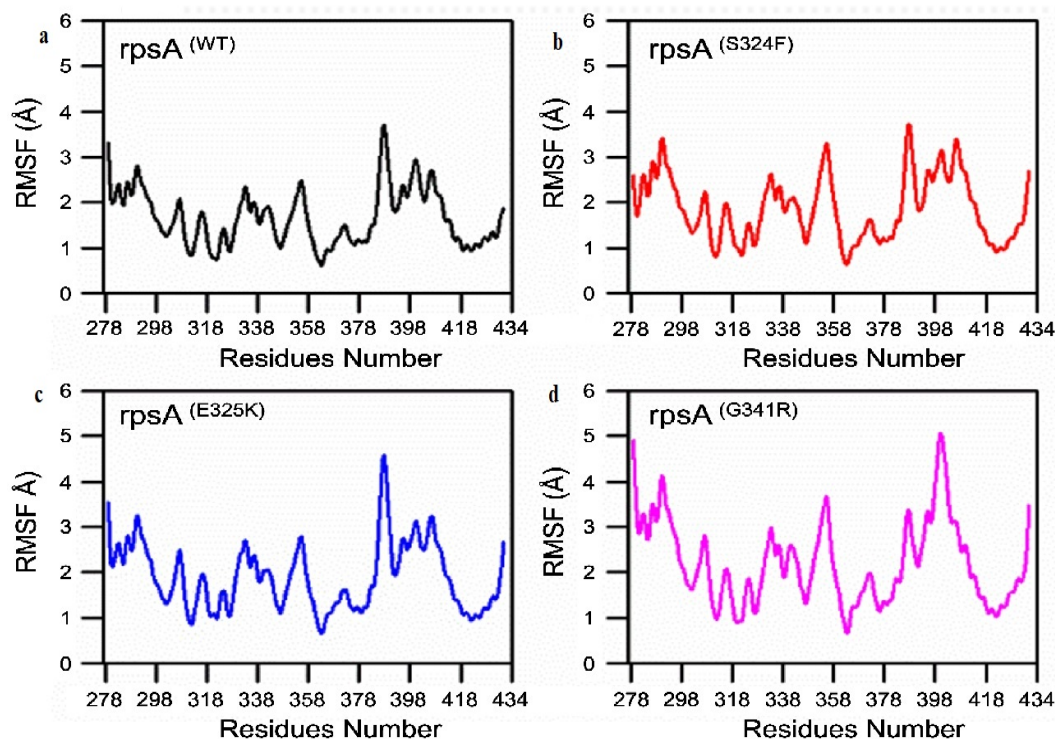
FIGURE 4.31: RMSF of WT and MTs (S324F, E325K, G341R) rpsA.
WT (a) attained a lower RMSF than MTs RpsA (b,c,d).

the simulation period, depicting unstable folding than WT (Figure. 4.35). In apo forms, T370P and W403G exhibited the Rg value between 17.5-19 and 17.3-19.4 respectively (Figure. 4.36). The structure W403G is seemed to be highly misfolded whereas the WT exhibited Rg values between 18 and 19. The plot (Figure. 4.36) demonstrated a degree of variation in T370P and W403G, showing unstable folding.

4.11.1.4 Essential Dynamics

The area of motion covered by MTs in apo and complex with the drug is more disperse type, showing its variation in dynamics of motions (uncorrelated). The dynamics of structure is commonly depicted in the form of principle component analysis (PCA) where WT and MTs are compared through a plot. WT RpsA showed a cluster type of motion while MTs exhibited a more dispersed type of motion except E325K. WT structure is scattered, covering an area on PC1 between -188 and 44, -125 and 144 (PC2). MTs S324F exhibited motion along -144 and
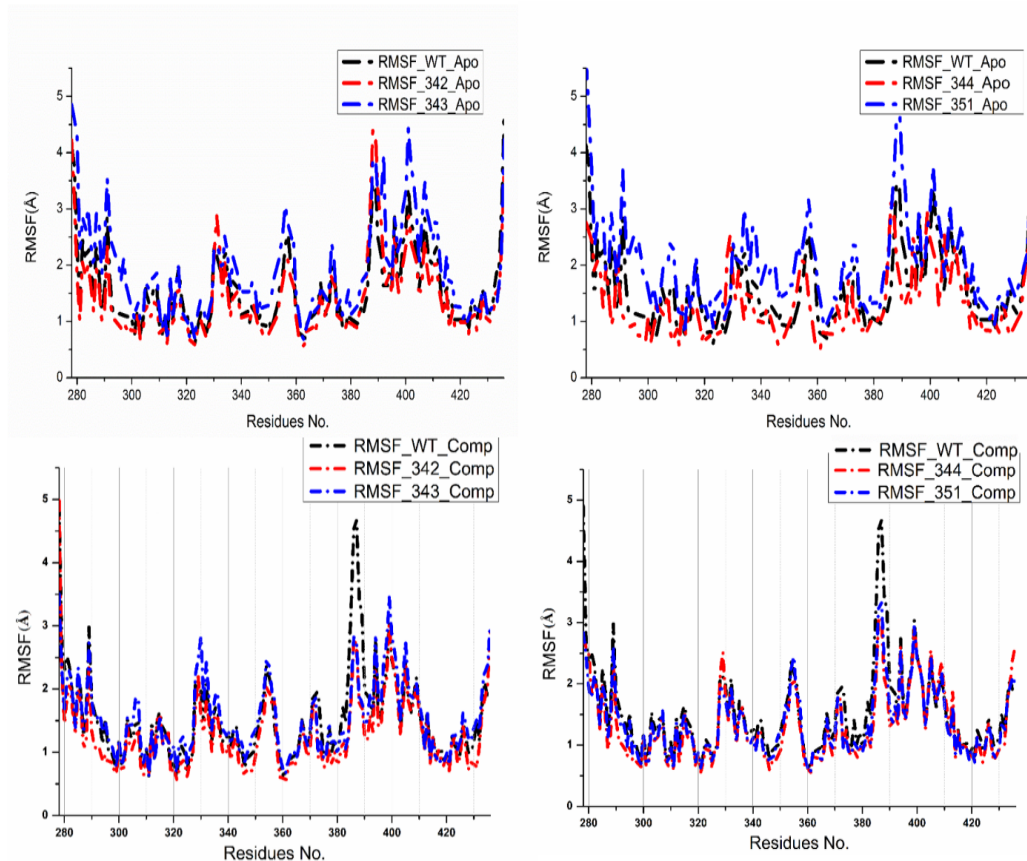
FIGURE 4.32: RMSF of WT and D342N, A343F, D344N, I351F RpsA$^{\text{CTD}}$.
WT (a) attained a lower RMSF than MTs (b,c,d).

144 (PC1), -125 and 150 (PC2)(Figure. 4.37). However, E325K was found to be less scattered in between PC1 and PC2, covering area between -144 and 140, -75 and 75 respectively. The area of motion covered by MTs G341R along PC1 has been recorded between -116 and 174 and -75 and 125 along PC2. A cluster type of motion was observed in WT, scattering over a small area along PC1 between -60 and 50, -90 and 60 along PC2. MTs RpsA, D342N, D343N, A344P, and I351F exhibited a more scatter type of motion on PC2 between -40 and 60, -40 and 90, -60 and 80, -100 and 60 respectively. The MTs's structures covered more area in both, apo and complex with the drug and is more disperse type, showing its variation in dynamics of motions (uncorrelated). T370P and W403G attained a scatter type of motion when compared with WT. A cluster type of motion was observed in WT scattering over a small area on PC1 between -75 and 75, -50 and 30 along PC2. T370P and T403G exhibited a more scattered type of motion on PC2 between -50 and 100, -100 and 100 respectively.
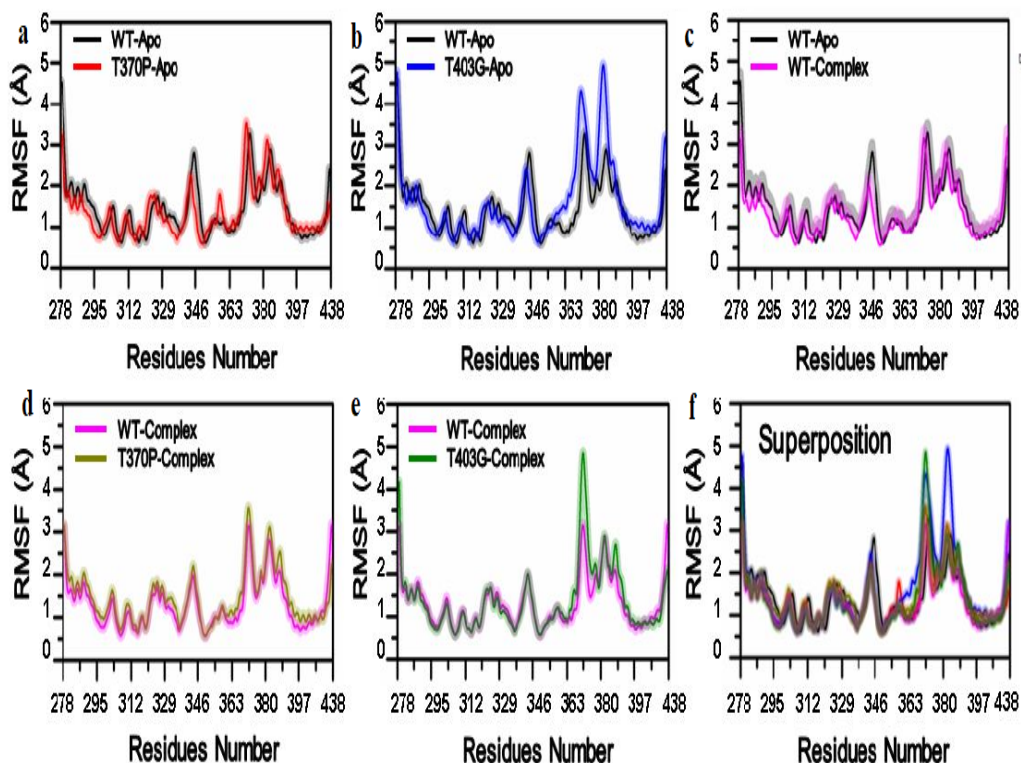
FIGURE 4.33: RMSF of WT and T370P and W403G RpsA$^{\text{CTD}}$.
(a,b); WT and MTs in apo state. (c); RMSF of WT in apo and complex state.
(d,e); RMSF of WT and MTs RpsA$^{\text{CTD}}$ in complex with drug (PZA).

4.11.1.5 Gibbs Free Energy

A protein with WT structure has the minimum GFE. The relative stability of WT and MTs can be measured using Gibbs Free Energy (GFE) which is the amount of work of closed system exchanging heat and work with surrounding. A more negative value shows the most stable structure. The differences in Gibbs free energy values of WT and MTs RpsA, S324F, E325K, G341R, D342N, D343N, A344P, I351F, T370P, and T403G showed that mutation may alter the stability of RpsA (Figures. 4.40, 4.41) and (4.42). WT has a significant GFE difference with that of MTs as indicated by the peak color of plot. The peak color in both state of WT is more stable in comparison of MTs. The differences in GFE values may have importance in the stability calculation. The color (red) in both states of the MTs is more unstable compared to the WT. The loop position is more open in T370P and T403G (Figure. 4.42 B,F,I) while GFE shows that WT is more stable than T370P and T403G.
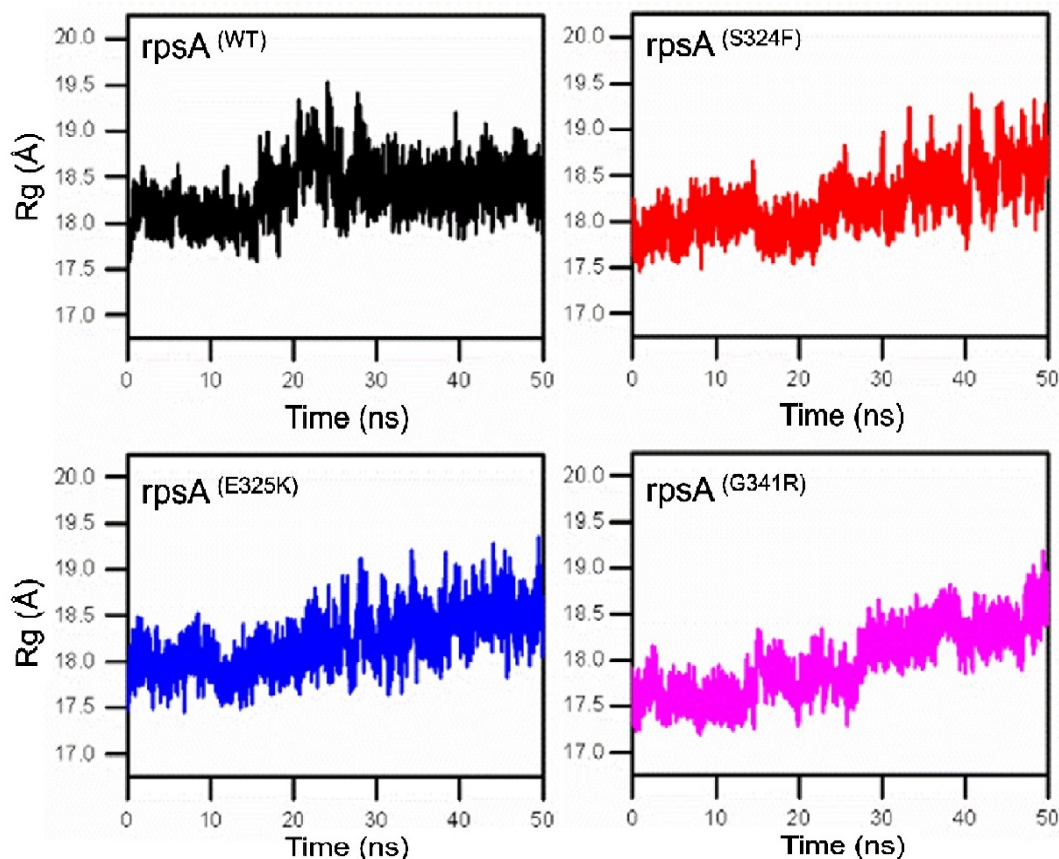
FIGURE 4.34: Rg of WT (rpsA$^{\text{WT}}$) and S324F, E325F, G341R.
WT (black) demonstrated more compactness and stable folding than MTs. WT
shows stability while folding from 25ns to 50ns of simulation period. MTs (S324F,
E325F, G341R) shows a rise and unstable plot during the same simulation period.

4.11.1.6 Distance Matrix

A stable distance matrix graph depicts a good binding affinity of drug and protein. Distance matrix of drug and RpsA were found to be almost similar, however, in apo state, the average distance in MTs was little higher than WT. The average distance of WT and POA is almost constant during the simulation period as compared to MTs, where a little fluctuation represent distance variation between drug and protein interactions. The MTs, S324F, E325K, G341R (Figure. 4.43) and D343N, I351F (Figure. 4.44) exhibited a high average distance between target and drug during interaction, signifying the effect on target binding affinity. However, no obvious effect has been seen in MTs D342N and A344P. T370P and T403G also exhibited a high average distance as compared to WT (Figure. 4.45). The difference in ligand and protein distance between WT and MTs may cause
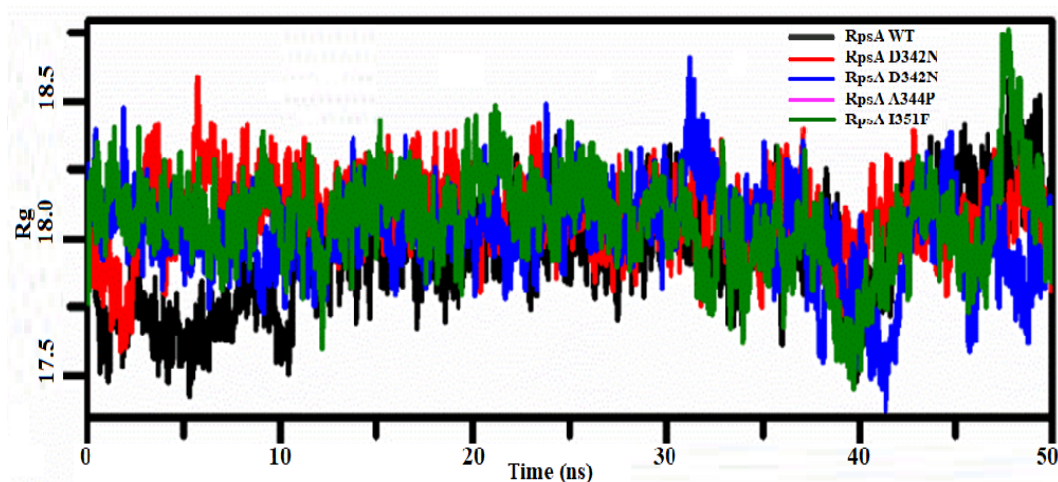
FIGURE 4.35: Rg of WT and D342N, D343N, A344P, I351F RpsA.
WT (black) demonstrated more compactness than MTs.
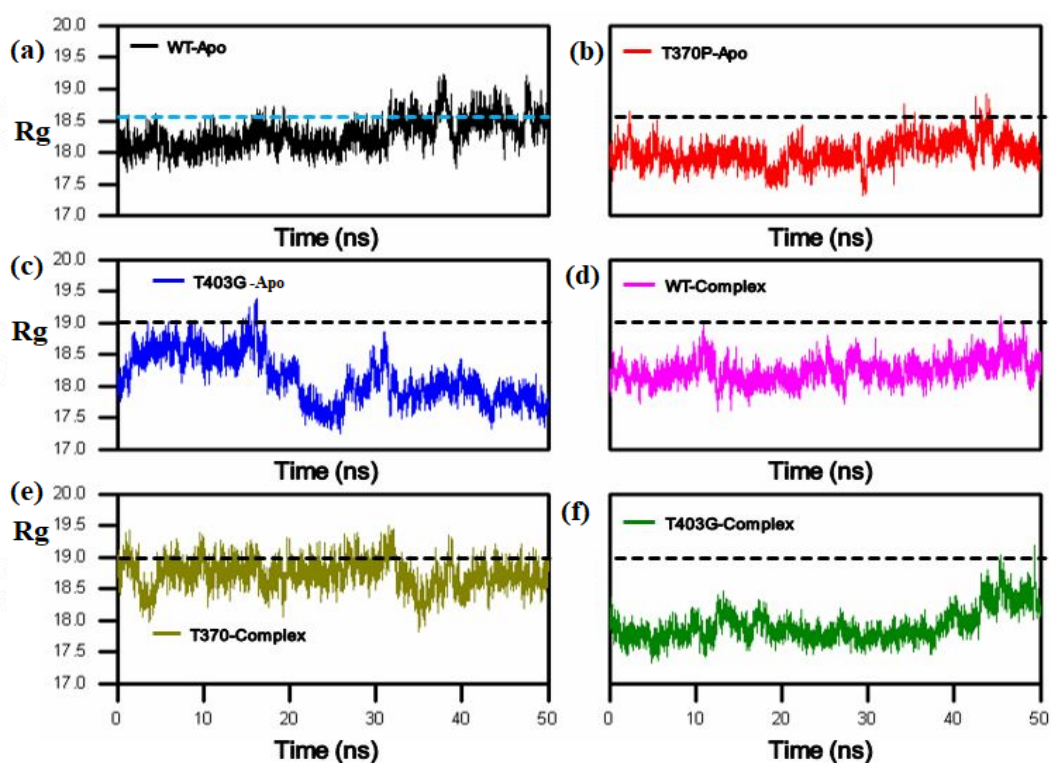
FIGURE 4.36: Rg of WT and MTs rpsA (T370P,T403G).
*(a,b,c); WT and MTs in apo state. (d,e,f); WT and MTs complex with drug

weak interaction. Inspite the distance matrix, the principal component analysis of E325K shows a little compactness in motion on PC1 and PC2. S324F is covering more area on PC2 than PC1, scattered between -145 and 145 on PC1, -125 and 150 on PC2. It has been observed that these mutation may affect the dynamic of enzymes, thus unable to perform its normal functions. In comparison with WT,
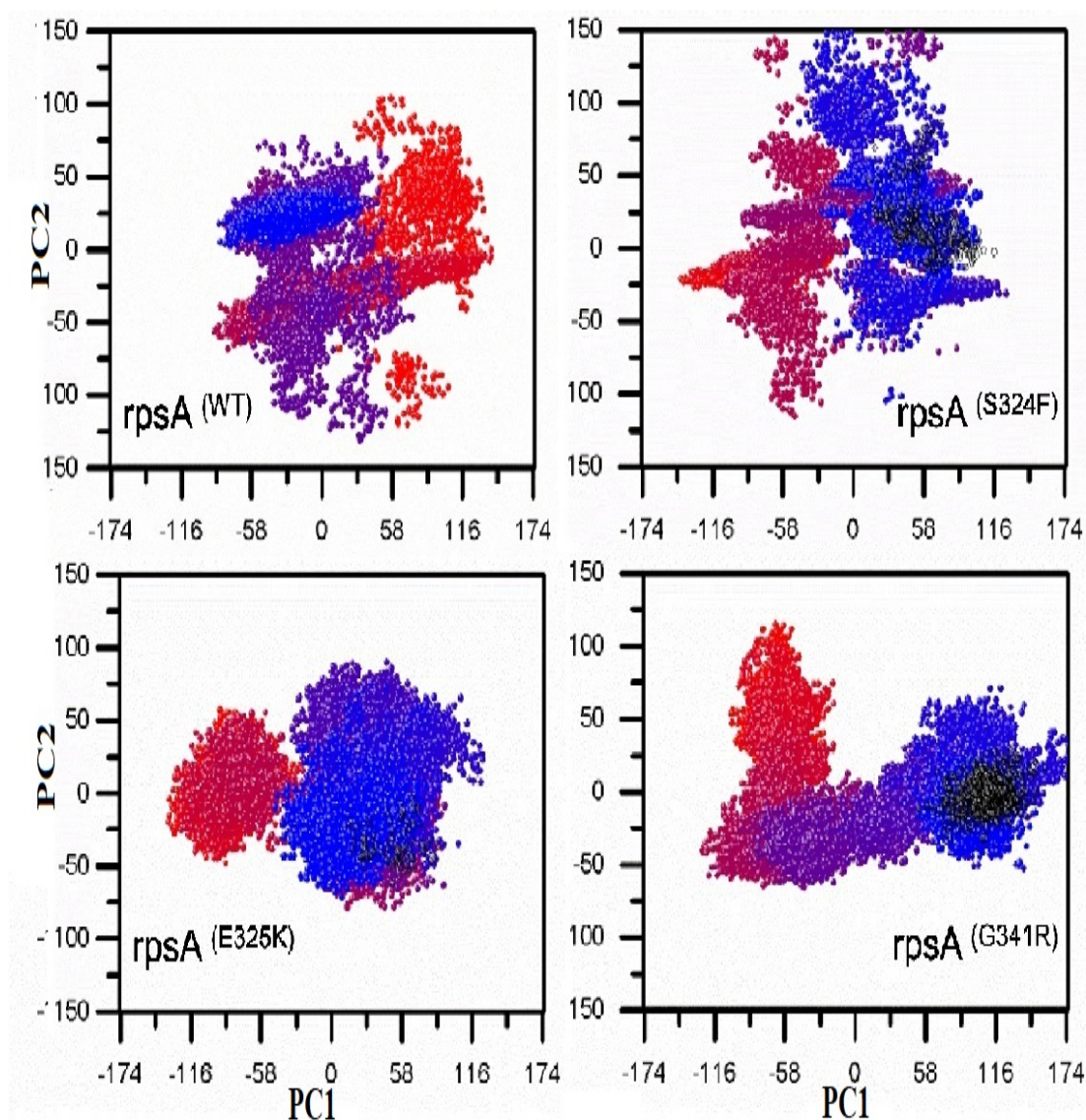
FIGURE 4.37: PCA of WT, S324F, E325K, and G341R RpsA.
MTs (S324F, E325K, and G341R RpsA) are more scattered on PC1 and PC2 than
WT RpsA. WT is less scattered on both axis, PC1 and PC2 than MTs. WT RpsA
scattered between -90 and 145 on PC1, -125 and 100 on PC2.

MTs are more scattered on both, PC1 and PC2, covering area of motion between
-125 and 174. MTs G341R is more scattered on PC1 when compared with other
MTs. The difference in residual motion between WT and MTs on PC1 and PC2
might be useful to infer the extent of effect and it interaction while converting
prodrug into active form. A more compact type of motion in WT may interacts
with drug forming maximum hydrogen bonds. Further, a dispersed type of motion
shows weak interaction, forming less or no hydrogen bonds, required for a good
binding affinity.
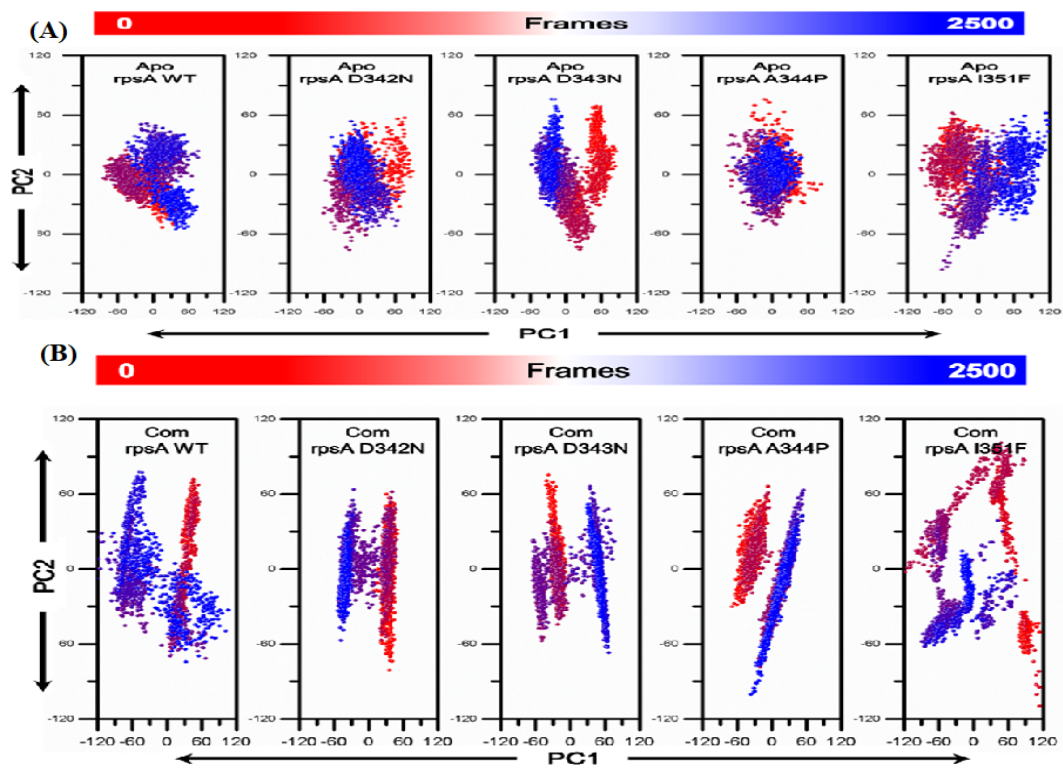
FIGURE 4.38: PCA of WT, D342N, D343N, A344P, and I351F rpsA.
(A); Apo state. (B); Complex with drug (POA).
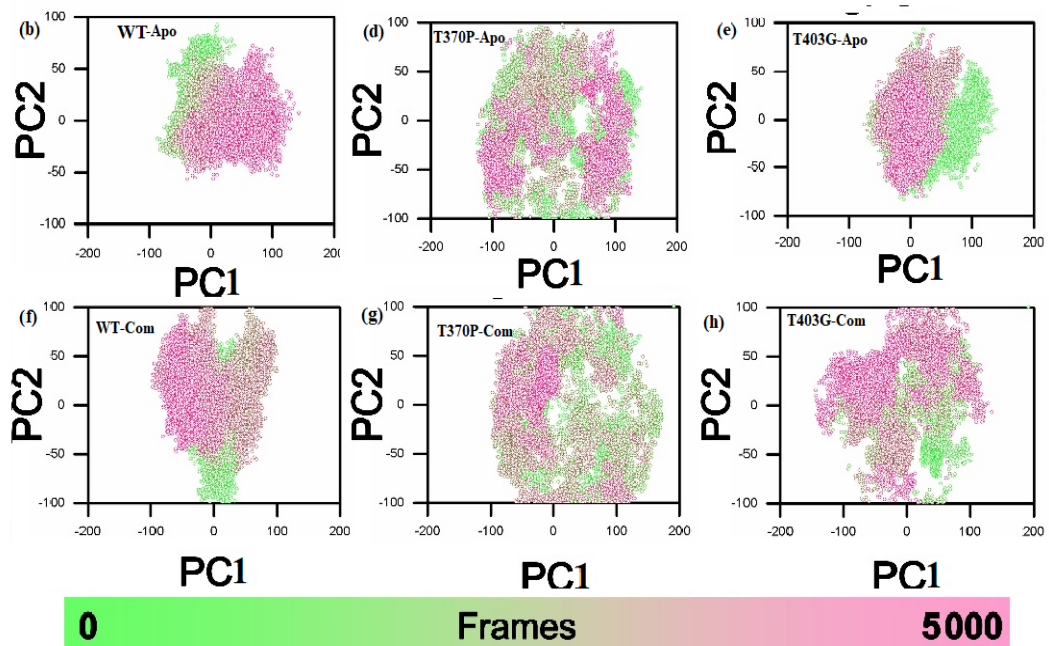
FIGURE 4.39: PCA of WT, T370P, and T403G.
Apo state (b,d,e). Complex with POA (f,g,h). WT (b,f) is less scattered on both
axis, PC1 and PC2 than MTs (d,e,g,h).
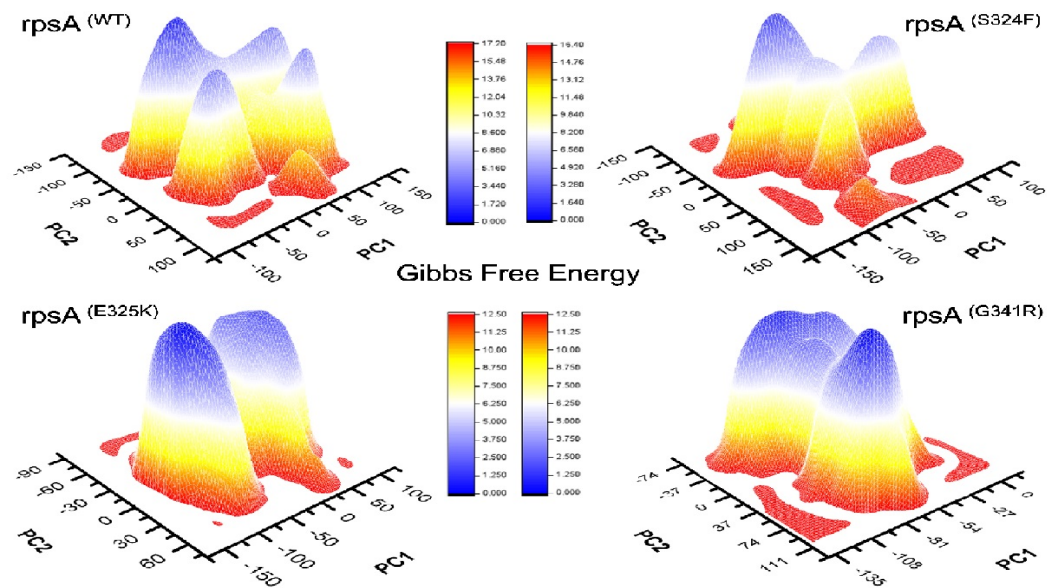
FIGURE 4.40: Gibbs free energy of WT and MTs (S324F, E325K, G341R). GFE is represented as low (blue), green (intermediate), yellow (high) and red (very high). Peak are color coded with more -ive (blue) or more +ive (red). A more -ive is most stable structure.
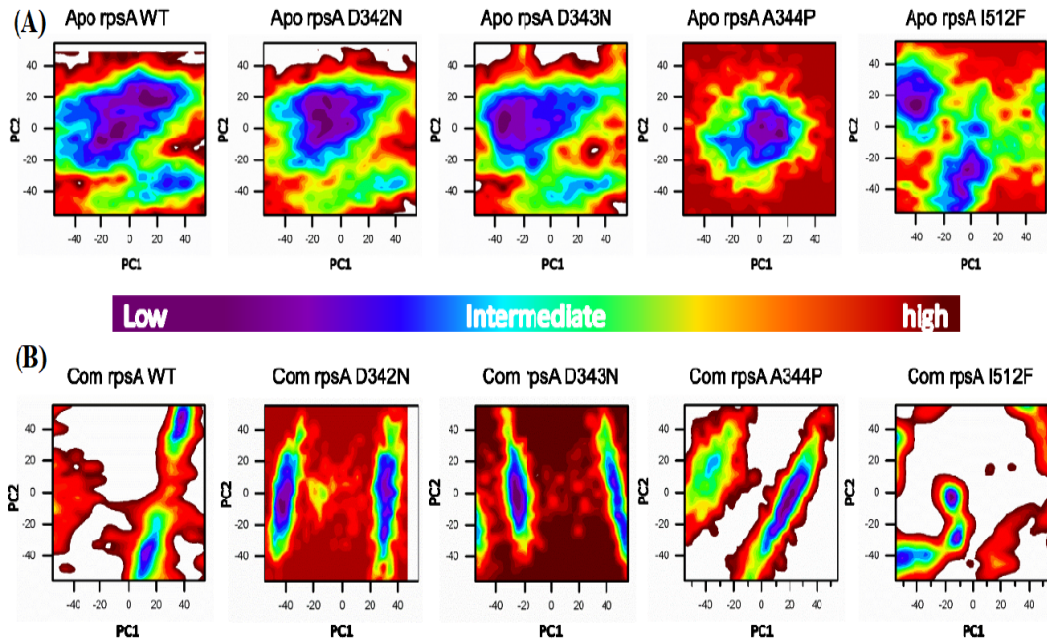
FIGURE 4.41: Gibbs free energy of WT and MTs (D342N, D343N, A344P, I351F).
(A); GFE in Apo state. WT in apo state has been detected in more stable state (B); GFE in Complex state (RpsA+POA). In complex state, the MTs are seemed to be in more energized state (unstable). Color coded with more -ive (blue) is stable or more +ive (red) is unstable.
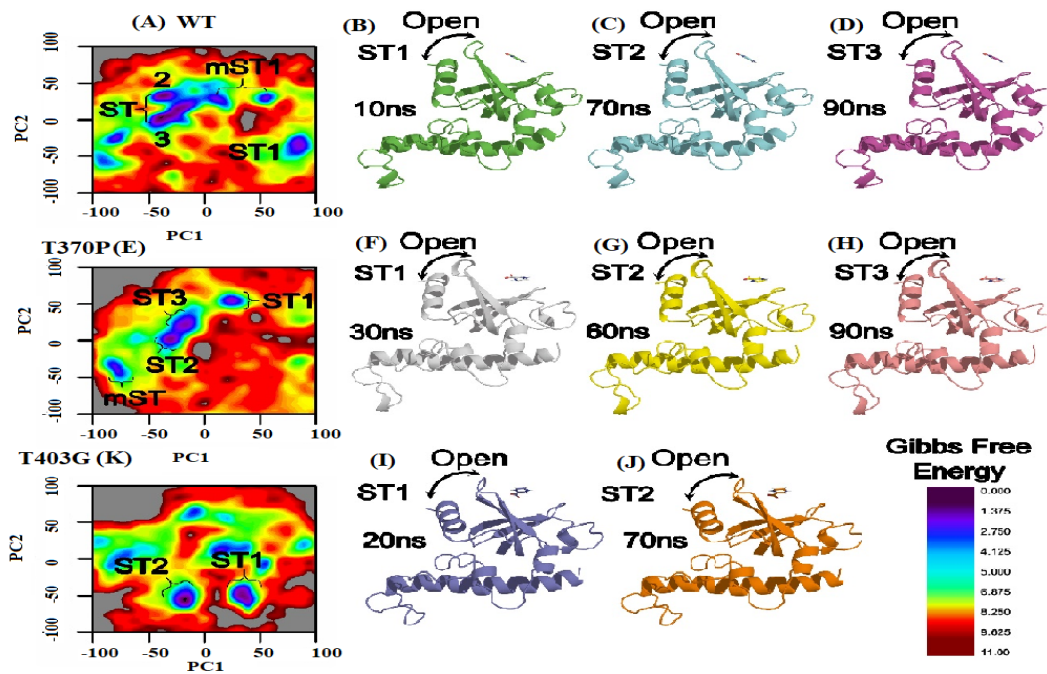
FIGURE 4.42: Gibbs free energy of WT T370P, T403G.
ST1 (simulation time 1), ST2 (simulation time 2), and ST3 (simulation time 3).
ST2, ST2, and ST3 represent the energy state during different simulation time in
WT and MTs (A,E,K). (B,C,D), RpsA loop position in WT. (F,G,H,I,J); Loop
position in MTs, T370P and T403G.
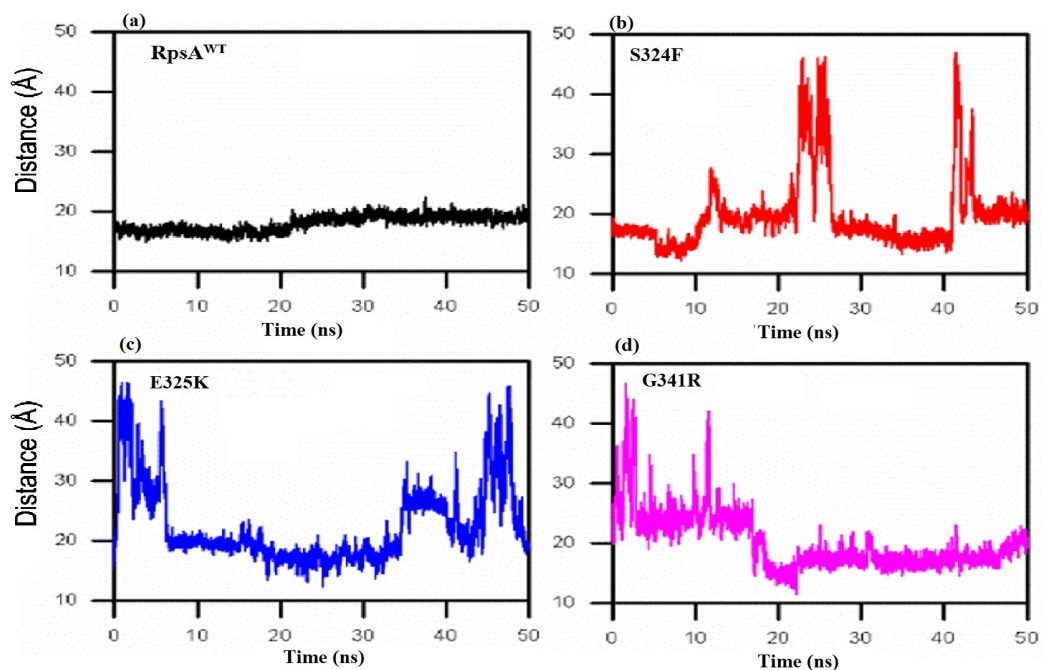
FIGURE 4.43: Distance matrix of WT and MTs (S324F, E325K, G341R).
WT (a) shows a constant average distance between RpsA and POA during the
whole simulation period. MTs (b, c, d) exhibited a high average distance with
POA.
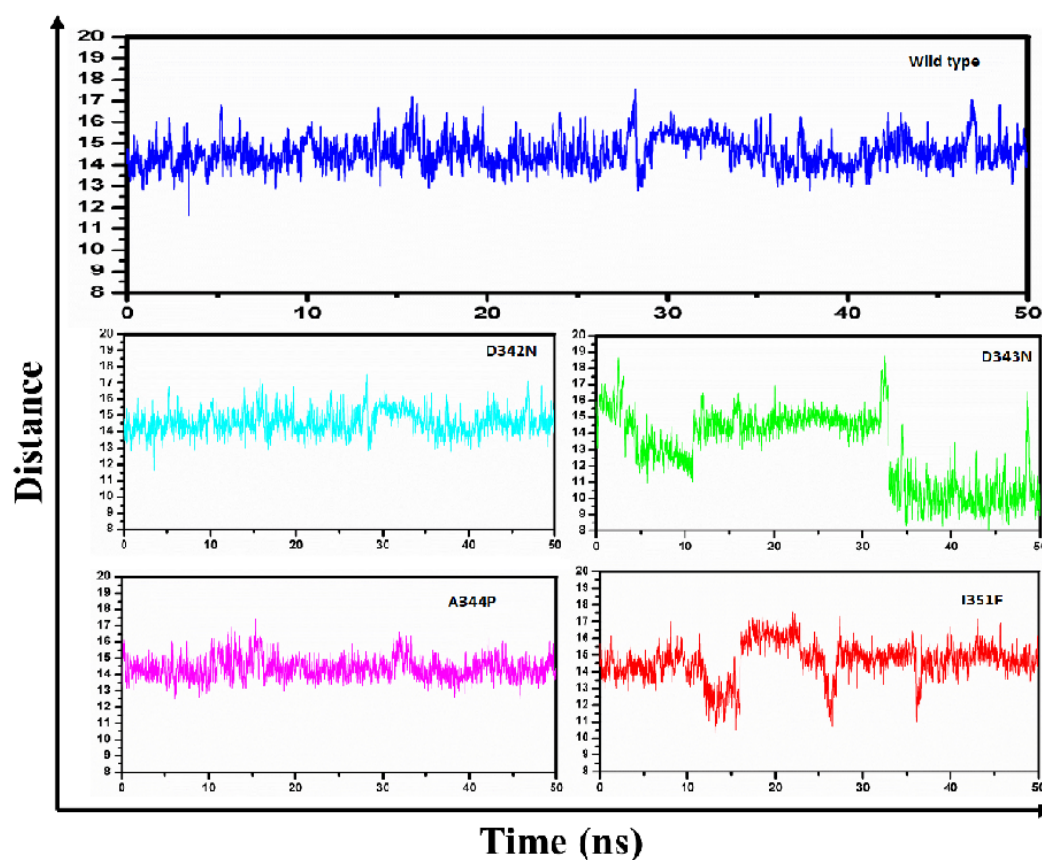
FIGURE 4.44: Distance matrix of WT and MTs (D342N, D343N, A344P, I351F).
WT (blue) shows a constant average distance between RpsA and Drug, during simulation period. MTs D343N and I351F have attained a degree of variations in distance between RpsA and POA drug during simulation time.
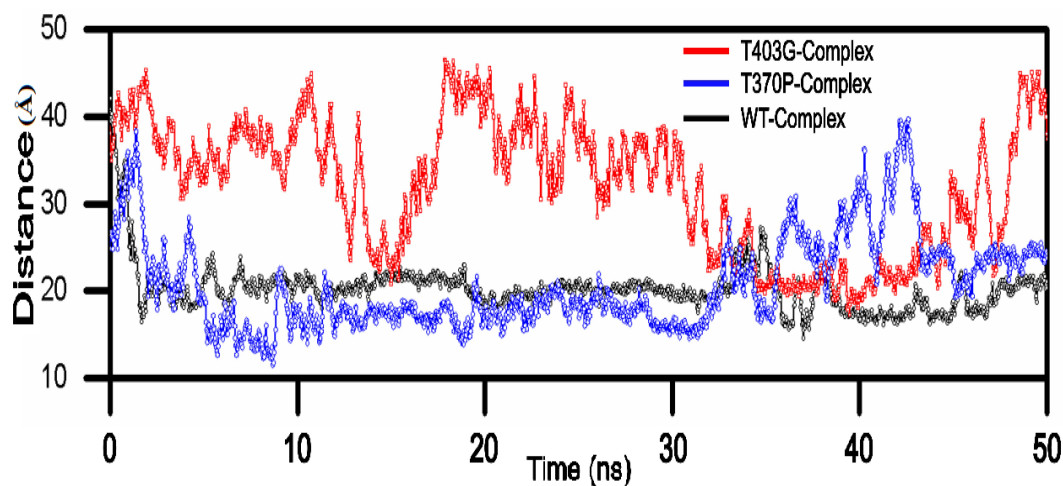
FIGURE 4.45: Distance matrix of WT and MTs (T370P and T403G).
WT (black), MTs, T370P (red) and T403G (blue).

4.12 Latent Tuberculosis and SigH Regulatory Pathway

The stress responder, sigH plays a critical function in controlling the response to heat, oxidative-stress, hypoxia and envelope damage. A sigH regulatory pathway mapped from literature has been shown (Figure. 4.46). The external signals in the forms of stress is sensed by membrane receptor protein, pknB, a key factor of a signal transduction pathway, regulating growth, shape and cell division via phosphorylation of target proteins including SigH and RshA complex. This causes the disintegration of sigH-rshA complex resulting in sigH to be set free to form a complex with RNA polymerase and activate a series of networking pathways called stress responders. Upon activation, the sigH and rshA are also synthesized but rshA is continuously inhibited in making any complex with sigH until the stress signal is ceased. The pathway is negatively regulated by rshA and positively by rshA-P, depending on stress signal (Figure. 4.46). To confirm the regulatory
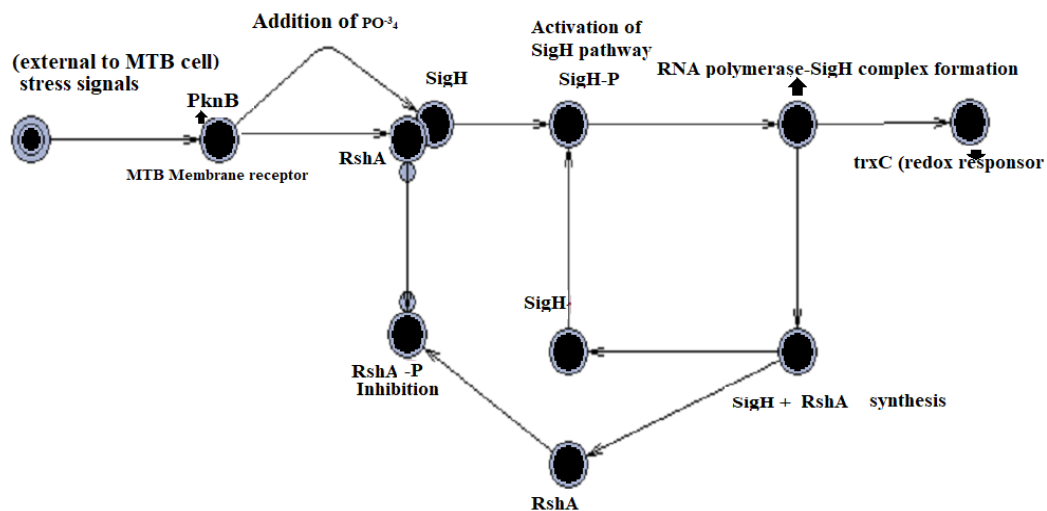
FIGURE 4.46: SigH regulatory pathway under latent stage of MTB.
PknB functions as membrane sensor of stress, by phosphorylating the SigH-RshA complex to initiate the pathway. Phosphorylation of sigH and rshA is causing the activation of SigH to form a complex with RNA polymerase (RNA Pol-sigH complex) while rshA is being inhibited to initiate the regulatory pathway under stress. RNA Pol-sigH complex causes the transcription of of sigH and rshA. Upon activation, sigH may further activate the other gene network (trxC), functioning as redox responder.

pathway of figure (4.46), a network was generated in the string database (Figure. 4.47) and the file was imported to cytoscape, where a total of 12 paths have been identified from the network in cytoscape, using Pathlinker plugin. The longest path (Figure. 4.48) was similar to the mapped pathway of literature (Figure 4.46). The longest path linked all the essential genes regulated in sigH regulation. The path also linked with a thioredoxins, trxC, constituting a dynamic response to oxidative stress. System biology aspires to build biological systems that implement dynamic
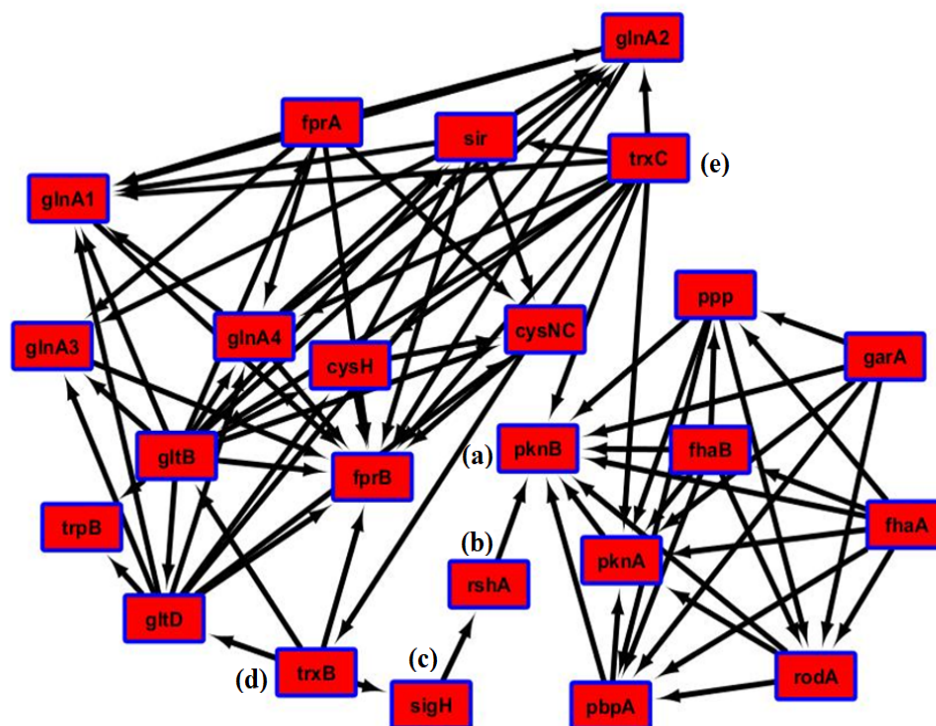
FIGURE 4.47: SigH-network generated in string database.
The network shows all the major stress responders (a,b,c,d,e) found in literature. This network of sigH was increased in string database to link the major stress responders.

of biological regulatory pathway. Biological system via computational modeling and simulation will reduce the costly wet lab experiments. Here we investigated the use of biological system in MTB under latent stage. A total of six regulators (nodes), pknB, sigH-rshA complex, sigH-P, sigH-RNA polymerase complex, and rshA-P while stress signal and RNA-polymerase are the external inputs in model construction. The two-control input of MTB signaling may be the potent target under dormant stage in sigH regulatory pathway. If both the control inputs (stress,
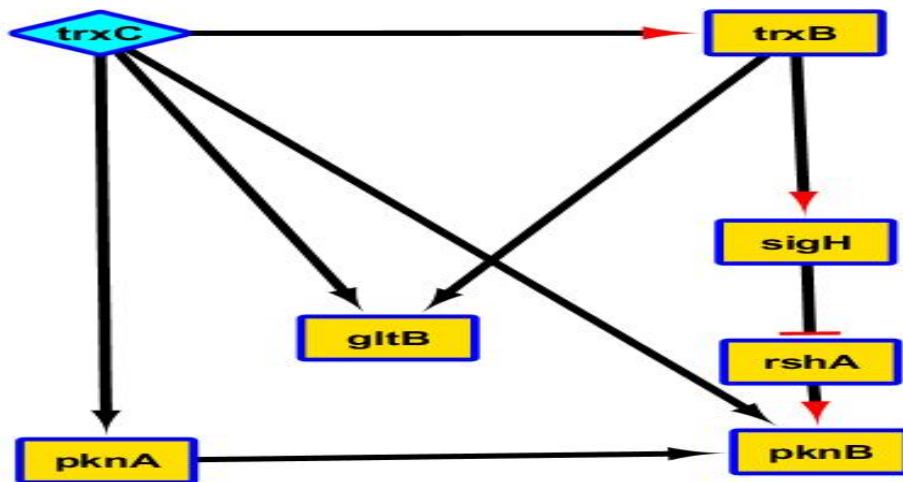
FIGURE 4.48: Path generated from string network through Pathlinker.
The longest path linked all the major stress responders in SigH regulation. The
major regulators (pknB, sigH, and trxC are linked in the path.)
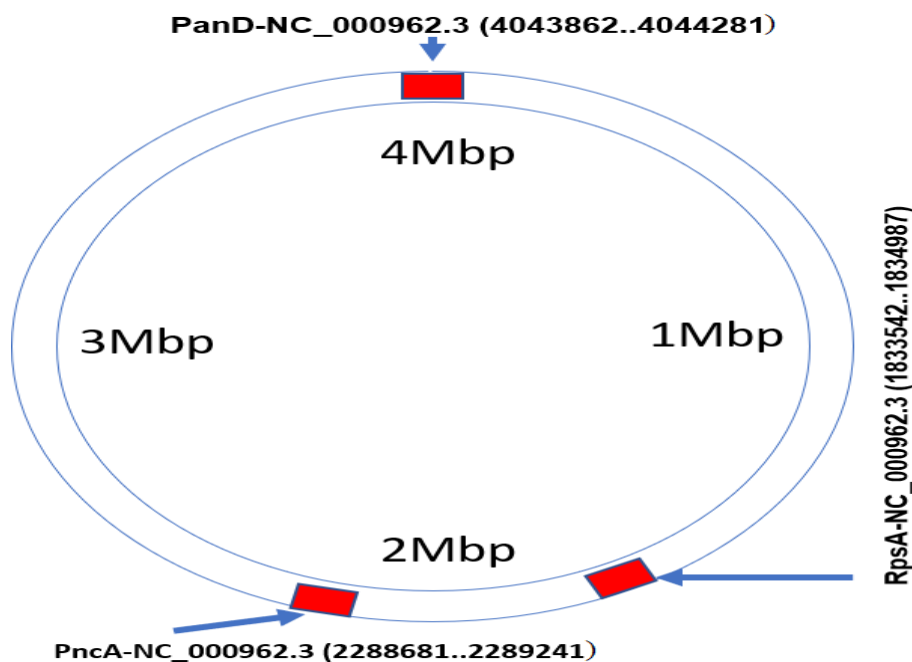

FIGURE 4.49: Genes PncA, RpsA, and PanD location on MTB genomes.
PncA (2288681-2289241), RpsA (1833542-1834987), and PanD (4043862-4044281)
encodes PZase, ribosomal protein S1, and aspartate decarboxilase respectively.
Mutations in PncA has been associated in more than 70% MTB cases.

RNA polymerase) remains OFF. Some other nodes, pknB, sigH and trxC may be
potent drug targets under latent stage.

Chapter 5

Discussion

The effective TB therapy recommends the use of first-line drugs that include, Rifampicin (RIF), Isoniazid (INH), and Pyrazinamide (PZA) [173, 174]. However, the appearance of drug failure due to large number of mutations in targets caused a global burden of treatment. Information is scarce about the main mechanism that leads to the first-line drug resistance. However, resistance has been associated with mutations in the targets proteins. RIF-resistance has been associated with mutations in the hot-spot region (96%) from 507-533 codons of *rpoB* gene [31]. Isoniazid (INH) resistance has been strongly linked with alteration in katG and inhA or its promoter region [33]. PZA is a distinct anti-tuberculosis drug, playing a key role in shortening of TB treatment from six to nine months. It kills non-replicating persistent MTB under different stress conditions where other drugs are not effective. After conversion into its active form, POA by pyrazinamidase (PZase), the drug remains active at low pH during acidic stress [21, 36, 74, 93, 175]. However, in a large number of isolates, MTB develops resistance against PZA that led to the survival of persistent bacteria. Drug resistance emerges due to inappropriate therapy and negligence of WHO treatment guidlines. Further, majority of geographic regions also lack information about the prevalence of PZA-resistance, causing mismanagement of resistance TB. Data regarding the prevalence of PZA-resistance should be investigated in distinct geographic regions of high burden countries for better management of TB.

Among the circulating MTB isolates in this geographic distinct area, the current investigation found a significat number of PZA-resistance (7.7%) using drug susceptibility testing during the first phase of the study (Table.4.10). These findings show that persistent bacilli, which is the main target of PZA, survive in PZA-resistance isolates, increasing the risk of transmission which may adopt the active form. Moreover, the resistance level of PZA increases with increase in resistance to other drugs, particularly the two important first line drugs, INH (90% to 91.6%) and RIF (80% to 80.7%). MDR was also found in 63 (76%) of PZA-resistance whereas the second phase of this study detected more than half of the tested isolates were also MDR (52/69 (75.35%)), consistent with previous studies [176, 177]. The prevalence of PZA-resistance has been associated with resistance to INH, RIF, STR, and OFX (Table. 4.12). A large number of PZA-resistant isolates are also MDR and XDR, affecting the treatment outcomes. The resistance level of some other drugs, OFX 40(48.2%) and STR 41 (49.4%) is also seemed high among PZA-resistant isolates. We suggest that, inclusion of PZA in a TB treatment regimen appears to be essential in susceptible cases, however, in case of MDR, susceptibility of PZA must be performed prior to its inclusion in the treatment. Therefore, PZA DST must regularly be performed along with other first line drugs. Previous studies have also shown a correlation between PZA and RIF resistance through molecular detection of mutations in *pncA* [43]. In the study of Zignol 2016 [178], a total of 4972 patients were screened in order to find the prevalence of PZA-resistance from five countries (3.0-42.1% in the surveyed settings). However, the levels of resistance for patients in all countries correlated with RIF-resistance except Pakistan, where RIF-resistance level is higher than PZA in all patients groups (p<0.0001). Previous study investigated the resistance level of PZA in MDR patients where 37 of 71 (52.1%) were resistant to PZA while 6 out of 59 (10.2%) among fully susceptible cases [179]. These findings suggest that there is approximately half a chance to successfully eradicate persistent bacilli in MDR patients. More studies with a large sample size should be conducted for better estimation of PZA prevalence in high burden countries. Therefore, PZA inclusion to treat MDR should be linked after susceptibility test.

Unlike the DST of other drugs, PZA sensitivity testing requires acidic pH for action. The result is sometimes interpreted as false positive due to buffering issues in media. These conventional methods of PZA DST may increase the level of false resistance that may be resulted from media buffering issues or inoculum sizes, where the low pH environment is required for drug action but inhibits the growth of MTB [180, 181]. Therefore, molecular detection of PZA-resistance are the most reliable methods, involving sequencing of *pncA* gene to appraise mutations in the 561 bp coding region [182]. The earlier studies [41, 114, 177, 183] have also shown a correlation between mutations in the *pncA* gene and phenotypic PZA-resistance. In correlation to these findings, we also reported mutations in *pncA* among 51(74%) of PZA-resistant isolates that harbored 36 mutations in the coding region of *pncA* (Table. 4.13) with sensitivity and specificity of 79.31% (95% CI, 69.29% to 87.25%) and 86.67% (95% CI, 69.28% to 96.24%), respectively. Some studies reported a better sensitivity and specificity in *pncA* sequencing compared with that of MGIT 960 DST (90.9, 100%) [184–186] and 95.0 (95% CI 92.1 - 98.0), 99.1 (95% CI 98.4>99.9) [182]. Miotto et al. (2014) identified 280 mutations in 1,950 clinical strains [92], categorized into four groups: (1) very high confidence resistance mutations (2) high-confidence resistance mutations (3) mutations with an unclear role (4) mutations not associated with phenotypic resistance, based on confidence level. We detected 12 mutations with very high confidence resistance, while the rest of mutations have been found in Miotto unclear category. Mutations 211C>T, 212A>G, 226A>C, 286A>C, and 422A>C in the present study (Table. 4.13) were previously shown as very high confidence resistance mutations [92, 176, 187]. Molecular biomarkers that could specifically target the first two categories may be developed [92] for early diagnosis PZA-resistance. Moreover, molecular methods of PZA susceptibility testing should regularly be performed along with other frequently used drugs for better management of TB treatment.

Tan et al. (2014) reported that each geographical region has a specific type of variations in *pncA*. Isolates from Southern China exhibited a scattered type of mutations, which remains a complex target in the development of diagnostic

biomarkers involved in PZA-resistance [114]. Some strains, which were PZA-resistance by conventional DST, but lacking mutations in *pncA* and its regulatory gene, suggesting other targets of drug and issues concerning PZA DST. Residues, Cys138, Asp8, Lys96 and Asp49, His51, His57, and His71 are present in the active and metal binding sites [99, 128] of the *pncA*-encoded enzyme, PZase. We identified mutations, dispersed throughout the *pncA* gene (35A>C—538G>T), nearby the area of metal binding and active site amino acids (46-76 and 133-146), important for enzyme activity. Mutations 33C>A, 53C>A, 194-203 Del CCTCGTCGTG, 205C>A, 317-18 Del TC, 331G>T, 376G>A, 419G>A, 430G>A, 449G>C, 508G>C, 519G>A, 522G>A, 530DEL C and 535A>G were not found in the GMTV, TBDRM databases and neither in previous studies. However, we did not detect any mutations in the 18 PZA-resistant MTB isolates, suggesting the involvement of other genes *rpsA* and *panD* (aspartate decarboxylase) [43, 112, 188, 189]. These findings may be helpful to design biomarkers in TB high burden countries for rapid testing of PZA-resistance. In a more recent study, four new efflux proteins Rv0191, Rv1667c, Rv3756c, and Rv3008 were implicated in PZA/POA resistance [190]. These findings suggest a new mechanism of PZA-resistance in MTB. However, further investigations are needed to identify the quantitative role of all these targets in high burden countries and the mechanisms behind PZA-resistance for better management of drug-resistant TB. Molecular methods to investigate PZA-resistance by screening mutations in *pncA* gene in distinct epidemiological regions, offer a much more rapid alternative, compared to that of conventional bacteriology. Further studies are needed to identify the mutations in PZA-resistant isolates specific to certain geographical areas for the better management.

The lack of mutations in *pncA* eighteen PZA-resistant isolates, suggest the involvement of other targets like *rpsA*, encoding the 30S ribosomal protein S1 (*rpsA*) and *panD*, encoding aspartate decarboxylase. However, the role of *rpsA* mutations in PZA-resistance is accounted in a small number of cases [116, 191, 192]. We detected fifteen mutations in 11 (61%) isolates (Table. 4.18), while seven isolates were PZA-resistance *pncA*^WT and *rpsA*^WT. However, no *panD* gene mutation was

detected among the seven PZA-resistant $pncA^{\text{WT}}$. In association to this study, Gu et al., also found 6 isolates lacking any mutations in $panD$ among $pncA$ and $rpsA$ wild types PZA-resistant strains [112]. These findings suggest the role of some other targets including efflux in PZA-resistance. Further investigations are needed to find the quantitative role of all these targets and mechanisms in PZA-resistance. Very limited information reported from previous studies about $rpsA$ mutations in $pncA^{\text{WT}}$ PZA-resistance strains. Alexander et al. (2012) reported majority of synonymous mutation in $rpsA$ among PZA-resistant isolates [41], while Bhuju et al., did not reported any mutations in PZA-resistant $pncA^{\text{WT}}$ $rpsA$ gene [116]. Similarly Tan et al., found 3 mutations in PZA-resistant $pncA^{\text{WT}}$ $rpsA$ gene and one in susceptible strain [114]. All the above reports showed a weak correlation between $rpsA$ gene mutations and PZA-resistance. However, Gu et al., [112] found 26 mutations dispersed along the whole coding region of $rpsA$, a very different pattern of mutations than previously reported [41, 116] in $rpsA$ gene. In the current study we also found 14 nonsynonymous and one synonymous mutations, a different pattern of mutations in 11 strains out of 18 PZA-resistant $pncA^{\text{WT}}$ $rpsA$ gene. Further, all these mutations has not been reported in previous studies and scattered in whole $rpsA$ gene but not concentrated to C-terminal as reported earlier [41, 111].

In conclusion, $rpsA$ gene mutations should be considered along with $pncA$ gene mutations for better development of new molecular methods of DST and TB management. The role of $rpsA$ gene mutations in PZA-resistance should be evaluated from geographically diverse environment specially TB high burden countries with more sample size to find the exact role of $rpsA$ gene mutations in PZA-resistance along with treatment and development of geographically specific biomarkers.

Drug resistance is most commonly develop due to mutations in the target structure. However, how this resistance develop, may help in our understanding to find some alternative. The mechanism of resistance behind mutation may be investigated using X-rays crytallography, NMR and computer simulations. However, MD simulation also termed as computer simulations, an alternative of conventional in vivo and vitro experimental approaches, have been applied in exploring

the properties at molecular level among the atoms. We can find a deep inside mechanism of dynamics among molecules behind mutations in macromolecules. MD simulations are very useful in the sense when a test is difficult or impossible in the laboratory [44, 193, 194]. For better management of major public health issues, inside mechanism has been investigated to define some control strategies. Drug resistance TB has been found a major obstacle towards the global TB control programm. Here, we explored the mechanism of PZA-resistance behind mutations in target proteins, PZase and RpsA. A comprehensive study was performed by comparing mutiple factors of MTs and WT including, RMSD, RMSF, Rg, GFE, distance matrix, total energy, pocket volume, docking scores etc. Mutations have been found, effecting the fexibility and stability of proteins, making them a weak target to interact with drugs, resulting in drug resistance. RMSD and RMSF of MTs and WT have been compared, indicating imbalance stability. These findings support the earlier studies on PZase MTs W68R, W68G, and K96R [195, 196]. Although majority of these mutation were not detected in active site but still they conferred resistance, may be due to allosteric effect, leading to PZA-resistance. A stable Rg value in simulaton period signifies the folding stability [197, 198]. Compared to MTs exhibited variations in Rg (Figures. 4.7, 4.8) throughout the whole simulation period. These results support the findings of Yoon et al., [107] that mutations may result in folding effect in proteins structures. Yoon and colleagues [107] investigated the consequences of *pncA* mutations on its function. They identified nineteen PZA-resistant strains, harboring eight point mutations, in which C14R, H51P, W68S, and A146V were insoluble, K48E and G97D exhibited a low expression and solubility. However, MTs, Y99D and T135P showed high expression and solubility comparable to those of the WT PZase. All the mutant structures were predicted through CUPSAT program. Only Y99D and T135P showed high solubility and expression, resulted a stabilizing effect. The remaining MTs appeared to be low or have no stabilizing effect. However, K48E and Y99D retained WT activity, demonstrating that residues, C14, H51, W68, G97, T135, and A146 might be significant for PZase activity and folding. Vats et al., explored the insight mechanism behind PZA-resistance using molecular dynamic

simulation. Mutation K96R affected the cavity volume, significantly large in MT in comparison with WT. The docking score, Glide, Electrostatic, Van der Waal energies were also found in variations between WT and MTs. Proteins and PZA binding affinity may also be affected due to change in binding pockets [199, 200]. Hydrogen bonding play a key role in three dimensional structure of proteins, especially antibodies and enzymes. In the current research, a significant difference has been detected while measuring the hydrogen bonding in MTs and WT, offering most of interactions in protein folding, stability and molecular recognition. Hydrogen bonding support the core composed of α-helix and β-sheet [201–205]. The primary forces in protein-ligand interactions are hydrogen bonds along with Van der Waals and electrostatic forces, [204–206]. Hydrogen bonding ploted in WT, are significant in number in comparison with MTs. The hydrogen bonding effect in interaction site residues, Cys138, Ile133, Arg19 and Asp8, indicating the effect of mutation on ligand binding site residues (Figures. 4.18, 4.19).

Catalytic proteins may contain cations, providing coordination ability and redox activity [207, 208]. A specific ligand's combination with the surrounding hydrogen bonding system have a central metal like redox potential [146]. PZase has Fe^{+2} metal ion coordinated by Asp49, His51, His57, and His71 (Figures. 4.20, 4.21). The RMSD and RMSF values of metal binding residues exhibited less stability and more lexibility in MTs metal Fe^{+2} (Figures. 4.20, 4.21). These results have strengthened the importance of residues in non-active site, whose mutation may result in PZA-resistance. Dynamic cross correlations and PCA are oftenly measured in MD simulations to depict the mutations effect on protein motion [45, 195]. Positive and negative motion (correlate motions and anti-correlated motions) of residues are important for proper function of enzymes. In the present study, these motions have been found in variations between WT and MTs PZase and RpsA. WT have been exhibiting more correlated and less scattered type motion, covering less area than MTs, involved more in anti-correlated motions as shown (Figures. 4.22, 4.23). A more scattered type of motion in protein made them weak target represent (Figure. 4.9). The structural difference between WT and MTs may compared through distance matrix which is commonly applied to

quantify the structural changes [209]. A significant difference have been detected while comparing the distance matrices of WT and MTs. These findings suggest that mutations may affect the average distance of alpha carbon by residue number. Further, the drug binding pocket have been also investigated in our recent studies, affected by mutations [67, 210, 211]. Such changes may cause a weak binding affinity, resulting in PZA-resistance.

Currently one-third of the world world's population harbors dormant bacilli where the risk of reactivation of bacilli in latent TB is estimated to be 5-10% [6, 212]. Along with the investigation of mutations in the targets that confer resistance in distinct geographical locations, a focus should be kept on latent TB. These are latent reservoir for recurrence and transmission of TB in populations. Host body generate different types of stress, oxidative, nitrosative, acidic and heat to eradicate the causative agent but such factors also mediate MTB growth by many sensor genes but the role of sigH in oxidative stress was first established on the experiments *M. smegmatis* sigH MTs by Fernandes et al., [49]. They confirmed that sigH has a central role in the defense of MTB from reactive oxygen species and oxidative thiol stress [213]. The SigH protects MTB against oxidative stress by regulating the expression of stress-responsive factor SigE, thioredoxins (trxB1 and trxC). stress-responsive s factor SigB is also regulated by SigE and SigH.

In the current study we found that sigH is activated by pknB after sensing the external stress while rshA is inactivated (Figure. 4.46). This phenomenon suggests that the main regulator in sensing the external signal is pknB, a cell membrane receptor. The pknB has been also connected with these main stress responders in the network, generated by string database and pathlinker in cytoscape. However, the activation of pathway is mediated by external factor, stress only. These findings suggest that targeting the stress sensor, pknB and sigH will cause disintegration of the whole pathway, ultimately resulting in a lack of conversion into latent stage. Thus MTB survival under latent TB can be controlled efficiently by the application of system biology, to understand the regulation of essential genes in certain phenomena. However, modelling biological signaling pathways give only qualitative knowledge. One of these is Boolean network models, the simplest kind

of dynamic model that can be applied only on qualitative data. However, these models are able to summarize complex biological signaling pathways for identification of potential targets.

Chapter 6

Conclusion and Recommendation

6.1   Conclusion

In conclusion, the prevalence of pyrazinamide resistance in Khyber pakhtunkhwa province of Pakistan is high and have been significantly associated with other 1st and 2nd line drug resistance. Therefore, pyrazinamide sensitivity should regularly be performed, prior to include in tuberculosis theraphy. However, due to buffering issues in pyrazinamide drug susceptibility testing, molecular methods to access pyrazinamide resistance are better, especially in tuberculosis high-burden countries. Our novel mutations in resistance isolates may be used as geographic specific biomarkers. Mechanism of pyrazinamide resistance behind mutations have been accessed through molecular dynamic simulations, where drug binding pocket, docking score, root means square deviation, root means square fluctuations, essential dynamics, principal component analysis, and hydrogen bonding at different simulation periods of mutants have been altered in comparison with wild type. In comparative analysis of interaction energy, van der waals and electrostatics between wild type and mutants, a significant difference have been detected in electrostatic energies. The principal component analysis of wild type showed a cluster type of motion as compared to mutants. Further, hydrogen bonding in

metal, Fe^{+2} binding residues shows more deviation in mutants. The overall analysis supports the hypothesis that these mutations might be involved in pyrazinamide resistance. Wild type exhibited positive (correlate motions) than mutants (anti-correlated motions) among residues. Molecular dynamic simulations of wild type and mutants explored a significant variations in the characteristics, resulting in pyrazinamide resistance. The regulatory pathways analysis revealed some more potent drug targets, pknB and sigH, essential for the survival of *Mycobacterium tuberculosis* under stress conditions. SigH regulons are the successful regulatory network, activating complex system for survival in stress environment. Drug designing against these regulons might be useful to eliminate the latent isolates. Our results unveil the insight mechanism of drug resistance and therefore may be helpful for better management of tuberculosis.

6.2 Future Work

The major challenge in control of TB is raising in high burden countries. Owing to these mutational effects that results in drug resistance is considered as an obstacle in course of TB treatment. As we identified geographical specific mutations, the researchers may design specific biomarkers in high burden countries for rapid access of PZA-resistance. Further, the mutation effect may also be tested through in vitro studies on mutants. The SigH Network and regulatory pathway of genes under latent stage may be more elaborated and drug may be designed, active under latent MTB isolates, especially, targeting the SigH regulon for better control strategies in future. High throughput computational technologies can be integrated in diagnosis of disease to give minimum time for transmission and early initiation of treatment. Synthetic and system biology may reduce the efforts in understanding and identification of potent drug targets in complex interactive system under latent stage of MTB and can be applied for the effective management of TB and drug resistance mechanism. Further studies are needed on the application of such approaches to unravel the hidden regulatory pathways under latent TB

that may assist for more accurate identification of drug targets and reducing the relapse occurrence of TB.

Funding Source

Bibliography

[1] Y. Zhang and D. Young, "Strain variation in the katG region of *Mycobacterium tuberculosis*," *Molecular Microbiology*, vol. 14, no. 2, pp. 301–308, 1994.

[2] WHO, "WHO publishes global tuberculosis report 2013," *Eurosurveillance*, vol. 18, no. 43, pp. 1–214, 2013.

[3] K. Floyd, P. Glaziou, A. Zumla, and M. Raviglione, "The global tuberculosis epidemic and progress in care, prevention, and research: an overview in year 3 of the end TB era," *The Lancet Respiratory Medicine*, vol. 6, no. 4, pp. 299–314, 2018.

[4] WHO, "WHO Global tuberculosis report 2013," *Euro surveillance: bulletin Européen sur les maladies transmissibles, European Communicable Disease Bulletin*, vol. 18, pp. 1–306, 2013.

[5] WHO, "Global tuberculosis report 2018," vol. 55, no. 33, pp. 1–243, 2018.

[6] WHO, "Global tuberculosis report 2017," vol. 12, no. 23, pp. 1–147, 2017.

[7] J. W. Ai, Q. L. Ruan, Q. H. Liu, and W. H. Zhang, "Updates on the risk factors for latent tuberculosis reactivation and their managements," *Emerging Microbes and Infections*, vol. 5, pp. 10–10, 2016.

[8] J. M. Grange, "Koch's tubercle bacillus:a centenary reappraisal," *Infektionskrankheiten und Parasitologie*, vol. 251, pp. 297–307, 1982.

[9] C. Dye, A. Harries, D. Maher, S. Hosseini, W. Nkhoma, and F. Salaniponi, "Chapter 13: Tuberculosis," *Disease and Mortality in Sub-Saharan Africa*, pp. 2000–2006, 2006.

[10] B. A. Brown-Elliott, D. E. Griffith, and J. R. Wallace, "Diagnosis of nontuberculous mycobacterial infections." *Clinics in Laboratory Medicine*, vol. 22, no. 4, pp. 911–25, 2002.

[11] D. Wagner and L. S. Young, "Nontuberculous mycobacterial infections: a clinical review," *Infection*, vol. 32, pp. 257–270, 2004.

[12] R. W. Merritt, E. D. Walker, P. L. Small, J. R. Wallace, P. D. Johnson, M. E. Benbow, and D. A. Boakye, "Ecology and transmission of Buruli ulcer disease: a systematic review," *PLOS Neglected Tropical Diseases*, vol. 4, pp. 4–12, 2010.

[13] G. Weiss and U. E. Schaible, "Macrophage defense mechanisms against intracellular bacteria," *Immunological Reviews*, vol. 264, no. 1, pp. 182–203, 2015.

[14] S. Basu, S. K. Pathak, A. Banerjee, S. Pathak, A. Bhattacharyya, Z. Yang, S. Talarico, M. Kundu, and J. Basu, "Execution of macrophage apoptosis by pe-pgrs33 of *Mycobacterium tuberculosis* is mediated by toll-like receptor 2-dependent release of tumor necrosis factor-α," *Journal of Biological Chemistry*, vol. 282, no. 2, pp. 1039–1050, 2007.

[15] S. Cole, R. Brosch, J. Parkhill, T. Garnier, C. Churcher, D. Harris, S. V. Gordon, K. Eiglmeier, S. Gas, and C. r. Barry, "Deciphering the biology of *Mycobacterium tuberculosis* from the complete genome sequence," *Nature*, vol. 393, pp. 537–544, 1998.

[16] J. C. Camus, M. J. Pryor, C. Médigue, and S. T. Cole, "Re-annotation of the genome sequence of *Mycobacterium tuberculosis* H37rv," *Microbiology*, vol. 148, pp. 2967–2973, 2002.

[17] J. W. Dale, "Mobile genetic elements in mycobacteria," *The European Respiratory Journal*, vol. 20, pp. 633–648, 1995.

[18] B. Wiedenheft, S. H. Sternberg, and J. A. Doudna, "RNA-guided genetic silencing systems in bacteria and archaea," *Nature*, vol. 482, pp. 331–338, 2012.

[19] D. van Soolingen, M. W. Borgdorff, P. E. de Haas, M. M. Sebek, J. Veen, M. Dessens, K. Kremer, and J. D. van Embden, "Molecular epidemiology of tuberculosis in the Netherlands: a nationwide study from 1993 through 1997," *The Journal of Infectious Diseases*, vol. 180, no. 3, pp. 726–736, 1999.

[20] M. Gengenbacher and S. H. Kaufmann, "*Mycobacterium tuberculosis*: success through dormancy," *FEMS Microbiology Reviews*, vol. 36, pp. 514–532, 2012.

[21] O. Zimhony, C. Vilchèze, M. Arai, J. T. Welch, and W. R. Jacobs, "Pyrazinoic acid and its n-propyl ester inhibit fatty acid synthase type I in replicating tubercle bacilli," *Antimicrobial Agents and Chemotherapy*, vol. 51, pp. 752–754, 2007.

[22] P. J. Brennan, "Structure, function, and biogenesis of the cell wall of Mycobacterium," *Tuberculosis*, vol. 83, no. 1, pp. 91–97, 2003.

[23] T. J. Beveridge, "Use of the Gram stain in microbiology," *Biotechnic and Histochemistry*, vol. 76, pp. 111–118, 2001.

[24] A. J. Wolf, B. Linas, G. J. Trevejo-Nuñez, E. Kincaid, T. Tamura, K. Takatsu, and J. D. Ernst, "*Mycobacterium tuberculosis* infects dendritic cells with high frequency and impairs their function in vivo," *The Journal of Immunology*, vol. 179, pp. 2509–2519, 2007.

[25] J. Bacon, B. W. James, L. Wernisch, A. Williams, K. A. Morley, G. J. Hatch, J. A. Mangan, J. Hinds, N. G. Stoker, and P. D. Butcher, "The influence of reduced oxygen availability on pathogenicity and gene expression in *Mycobacterium tuberculosis*," *Tuberculosis*, vol. 84, pp. 205–217, 2004.

[26] S. Sturgill-Koszycki, P. H. Schlesinger, P. Chakraborty, P. L. Haddix, H. L. Collins, A. K. Fok, R. D. Allen, S. L. Gluck, J. Heuser, and D. G. Russell, "Lack of acidification in Mycobacterium phagosomes produced by exclusion of the vesicular proton-ATPase," *Science*, vol. 263, pp. 678–681, 1994.

[27] M. K. Balcewicz-Sablinska, J. Keane, H. Kornfeld, and H. G. Remold, "Pathogenic *Mycobacterium tuberculosis* evades apoptosis of host macrophages by release of tnf-r2, resulting in inactivation of tnf-α," *The Journal of Immunology*, vol. 161, no. 5, pp. 2636–2641, 1998.

[28] A. M. Cooper, "Cell-mediated immune responses in tuberculosis," *Annual Review of Immunology*, vol. 27, pp. 393–422, 2009.

[29] A. N. J. Malik and P. Godfrey-Faussett, "Effects of genetic variability of *Mycobacterium tuberculosis* strains on the presentation of disease," *The Lancet Infectious Diseases*, vol. 5, no. 3, pp. 174–183, 2005.

[30] WHO, "Drug-resistant TB: surveillance and response: supplement to global tuberculosis report 2014," *WHO*, pp. 1–214, 2014.

[31] S. D. Parsons, J. A. Drewe, N. C. Gey van Pittius, R. M. Warren, and P. D. van Helden, "Novel cause of tuberculosis in meerkats, South Africa," *Emerging Infectious Diseases*, vol. 19, pp. 2004–2007, 2013.

[32] C. Vilchèze and W. R. Jacobs, Jr, "The mechanism of isoniazid killing: clarity through the scope of genetics," *Annual Review of Microbiology*, vol. 61, pp. 35–50, 2007.

[33] D. A. Rozwarski, G. A. Grant, D. H. Barton, W. R. Jacobs, and J. C. Sacchettini, "Modification of the NADH of the isoniazid target (InhA) from *Mycobacterium tuberculosis*," *Science*, vol. 279, pp. 98–102, 1998.

[34] M. H. Larsen, C. Vilchèze, L. Kremer, G. S. Besra, L. Parsons, M. Salfinger, L. Heifets, M. H. Hazbon, D. Alland, and J. C. Sacchettini, "Overexpression of inhA, but not kasA, confers resistance to isoniazid and ethionamide in

Mycobacterium smegmatis, *Mycobacterium bovis* BCG and *Mycobacterium tuberculosis*," *Molecular Microbiology*, vol. 46, pp. 453–466, 2002.

[35] R. Yeager, W. Munroe, and F. I. Dessau, "Pyrazinamide (aldinamide) in the treatment of pulmonary tuberculosis," *American Review of Tuberculosis*, vol. 65, no. 5, pp. 523–546, 1952.

[36] A. Scorpio and Y. Zhang, "Mutations in pncA, a gene encoding pyrazinamidase/nicotinamidase, cause resistance to the antituberculous drug pyrazinamide in tubercle bacillus," *Nature Medicine*, vol. 2, no. 6, pp. 662–667, 1996.

[37] T. British and Others, "Short-course chemotherapy in pulmonary tuberculosis." *Lancet*, pp. 119–24, 1975.

[38] B. T. Association, "A controlled trial of six months chemotherapy in pulmonary tuberculosis: second report: results during the 24 months after the end of chemotherapy," *American Review of Respiratory Disease*, vol. 126, no. 3, pp. 460–462, 1982.

[39] R. M. McCune, R. Tompsett, and W. McDermott, "The fate of mycobacterium tuberculosis in mouse tissues as determined by the microbial enumeration technique: Ii. the conversion of tuberculous infection to the latent state by the administration of pyrazinamide and a companion drug," *Journal of Experimental Medicine*, vol. 104, no. 5, pp. 763–802, 1956.

[40] A. S. Kalokhe, M. Shafiq, J. C. Lee, S. M. Ray, Y. F. Wang, B. Metchock, A. M. Anderson, and M. L. T. Nguyen, "Multidrug-resistant tuberculosis drug susceptibility and molecular diagnostic testing: a review of the literature," *The American Journal of the Medical Sciences*, vol. 345, pp. 143–145, 2013.

[41] D. C. Alexander, J. H. Ma, J. L. Guthrie, J. Blair, P. Chedore, and F. B. Jamieson, "Gene sequencing for routine verification of pyrazinamide resistance in *Mycobacterium tuberculosis*: a role for pncA but not rpsA," *Journal of Clinical Microbiology*, vol. 50, pp. 3726–3728, 2012.

[42] W. Shi, X. Zhang, X. Jiang, H. Yuan, J. S. Lee, C. E. Barry, H. Wang, W. Zhang, and Y. Zhang, "Pyrazinamide inhibits trans-translation in *Mycobacterium tuberculosis*," *Science*, vol. 333, no. 6049, pp. 1630–1632, 2011.

[43] S. Zhang, J. Chen, W. Shi, W. Liu, W. Zhang, and Y. Zhang, "Mutations in pand encoding aspartate decarboxylase are associated with pyrazinamide resistance in *Mycobacterium tuberculosis*," *Emerging Microbes and Infections*, vol. 2, no. 6, pp. 34–40, 2013.

[44] H. Kumar and P. K. Maiti, "Introduction to molecular dynamics simulation," in *Computational Statistical Physics.* Springer, 2011, pp. 161–197.

[45] M. C. Childers and V. Daggett, "Insights from molecular dynamics simulations for computational protein design," *Molecular Systems Design and Engineering*, vol. 2, no. 1, pp. 9–33, 2017.

[46] A. Kumar, A. Farhana, L. Guidry, V. Saini, M. Hondalus, and A. Steyn, "Redox homeostasis in mycobacteria: the key to tuberculosis control Expert Review." *Molecular Medicine*, vol. 13, pp. 13–20, 2011.

[47] A. Trivedi, N. Singh, S. Bhat, P. Gupta, and A. Kumar, "Redox biology of tuberculosis pathogenesis." *Advanced Microbial Physiology*, vol. 60, pp. 263–324, 2012.

[48] M. Bashyam and S. Hasnain, "The extracytoplasmic function sigma factors: role in bacterial pathogenesis." *Infection, Genetics and Evolution*, vol. 4, pp. 301–308, 2004.

[49] N. Fernandes, Q. Wu, D. Kong, X. Puyang, S. Garg, and R. Husson, "A mycobacterial extracytoplasmic sigma factor involved in survival following heat shock and oxidative stress." *Journal of Bacteriology*, vol. 181, pp. 4266–4274, 1999.

[50] J. E. Graham and J. E. Clark-Curtiss, "Identification of *Mycobacterium tuberculosis* RNAs synthesized in response to phagocytosis by human

macrophages by selective capture of transcribed sequences (SCOTS)," *Proceedings of the National Academy of Sciences of the United States*, vol. 96, no. 20, pp. 11 554–11 559, 1999.

[51] D. Kaushal, B. G. Schroeder, S. Tyagi, T. Yoshimatsu, C. Scott, C. Ko, L. Carpenter, J. Mehrotra, Y. C. Manabe, R. D. Fleischmann, and W. R. Bishai, "Reduced immunopathology and mortality despite tissue persistence in a *Mycobacterium tuberculosis* mutant lacking alternative factor, SigH," *Proceedings of the National Academy of Sciences*, vol. 99, pp. 8330–8335, 2002.

[52] T. Song, S. L. Dove, K. H. Lee, and R. N. Husson, "RshA, an anti-sigma factor that regulates the activity of the mycobacterial stress response sigma factor SigH," *Molecular Microbiology*, vol. 50, no. 3, pp. 949–959, 2003.

[53] S. T. Park, C. M. Kang, and R. N. Husson, "Regulation of the SigH stress response regulon by an essential protein kinase in *Mycobacterium tuberculosis*," *Proceedings of the National Academy of Sciences of the United States*, vol. 105, pp. 13 105–13 110, 2008.

[54] C. Kenyon, "The first long-lived mutants: discovery of the insulin/IGF-1 pathway for ageing," *Philosophical Transaction of the Royal Society B, Biological Sciences*, vol. 366, no. 1561, pp. 9–16, 2011.

[55] H. Liu, M. M. Fergusson, R. M. Castilho, J. Liu, L. Cao, J. Chen, D. Malide, I. I. Rovira, D. Schimel, C. J. Kuo, J. S. Gutkind, P. M. Hwang, and T. Finkel, "Augmented Wnt signaling in a mammalian model of accelerated aging," *Science*, vol. 317, no. 5839, pp. 803–806, 2007.

[56] S. C. Manolagas and M. Almeida, "Gone with the Wnts: beta-catenin, T-cell factor, forkhead box O, and oxidative stress in age-dependent diseases of bone, lipid, and glucose metabolism," *Molecular Endocrinology*, vol. 21, no. 11, pp. 2605–2614, 2007.

[57] A. Richardson, F. Liu, M. L. Adamo, H. Van Remmen, and J. F. Nelson, "The role of insulin and insulin-like growth factor-I in mammalian ageing,"

Best Practice and Research: Clinical Endocrinology and Metabolism, vol. 18, no. 3, pp. 393–406, 2004.

[58] WHO, "WHO global tuberculosis report 2011," vol. 18, no. 43, pp. 1–213, 2011.

[59] G. X. He, Y. L. Zhao, G. L. Jiang, Y. H. Liu, H. Xia, S. F. Wang, L. X. Wang, M. W. Borgdorff, M. J. van der Werf, and S. van den Hof, "Prevalence of tuberculosis drug resistance in 10 provinces of China," *BMC Infectious Disease*, vol. 8, pp. 166–170, 2008.

[60] WHO, "WHO Global tuberculosis report 2016," vol. 18, no. 31, pp. 1–214, 2016.

[61] WHO, "WHO towards universal access to diagnosis and treatment of multidrug-resistant and extensively drug-resistant tuberculosis by 2015: Progress report 2011," Geneva: World Health Organization, Tech. Rep., 2011.

[62] WHO, "WHO Global tuberculosis report 2013," vol. 11, no. 40, pp. 1–214, 2013.

[63] L. Heifets, M. Higgins, and B. Simon, "Pyrazinamide is not active against *Mycobacterium tuberculosis* residing in cultured human monocyte-derived macrophages, unresolved issues," *The international Journal of Tuberculosis and Lung Disease*, vol. 4, pp. 491–495, 2000.

[64] A. Scorpio and Y. Zhang, "Mutations in pncA, a gene encoding pyrazinamidase/nicotinamidase, cause resistance to the antituberculous drug pyrazinamide in tubercle bacillus," *Nature Medicine*, vol. 2, no. 6, pp. 662–670, 1996.

[65] P. J. Claus, S. Diamond, and M. A. Mills, *South Asian Folklore: An Encyclopedia: Afghanistan, Bangladesh, India, Nepal, Pakistan, Sri Lanka.* Taylor and Francis, 2003.

[66] M. A. Khan, A. Basit, A. Javaid, M. A.-U.-R. Adnan, F. Ahmad, N. Khan, A. Khattak, H. Sajjad, and M. A. Khattak, "Outcome of community based therapy of multi drug resistant tuberculosis patients treated in a tertiary care hospital of khyber pakhtunkhwa," *Pakistan Journal of Chest Medicine*, vol. 20, no. 3, pp. 1463–1470, 2015.

[67] M. T. Khan, S. I. Malik, S. Ali, A. Sheed Khan, T. Nadeem, M. T. Zeb, N. Masood, and M. T. Afzal, "Prevalence of pyrazinamide resistance in khyber pakhtunkhwa, pakistan," *Microbial Drug Resistance*, vol. 24, no. 9, pp. 1417–1421, 2018.

[68] M. Coscolla, A. Lewin, S. Metzger, K. Maetz-Rennsing, S. Calvignac-Spencer, A. Nitsche, P. W. Dabrowski, A. Radonic, S. Niemann, and J. Parkhill, "Novel *Mycobacterium tuberculosis* complex isolate from a wild chimpanzee," *Emerging Infectious Diseases*, vol. 19, pp. 969–976, 2013.

[69] P. Supply, M. Marceau, S. Mangenot, D. Roche, C. Rouanet, V. Khanna, L. Majlessi, A. Criscuolo, J. Tap, and A. Pawlik, "Genomic analysis of smooth tubercle bacilli provides insights into ancestry and pathoadaptation of *Mycobacterium tuberculosis*," *Nature Genetics*, vol. 45, pp. 172–179, 2013.

[70] Y. Blouin, G. Cazajous, C. Dehan, C. Soler, R. Vong, M. O. Hassan, Y. Hauck, C. Boulais, D. Andriamanantena, C. Martinaud *et al.*, "Progenitor "*Mycobacterium canettii*" clone responsible for lymph node tuberculosis epidemic, djibouti," *Emerging Infectious Diseases*, vol. 20, no. 1, pp. 21–30, 2014.

[71] R. Brosch, S. V. Gordon, M. Marmiesse, P. Brodin, C. Buchrieser, K. Eiglmeier, T. Garnier, C. Gutierrez, G. Hewinson, and K. Kremer, "A new evolutionary scenario for the *Mycobacterium tuberculosis* complex," *Proceedings of the National Academy of Sciences*, vol. 99, pp. 3684–3689, 2002.

[72] M. B. Reed, V. K. Pichler, F. McIntosh, A. Mattia, A. Fallow, S. Masala, P. Domenech, A. Zwerling, L. Thibert, and D. Menzies, "Major *Mycobacterium tuberculosis* lineages associate with patient country of origin," *Journal of Clinical Microbiology*, vol. 47, pp. 1119–1128, 2009.

[73] B. C. de Jong, M. Antonio, and S. Gagneux, "*Mycobacterium africanum*, review of an important cause of human tuberculosis in West Africa," *PLOS Neglected Tropical Diseases*, vol. 4, pp. 744–750, 2010.

[74] K. A. Alexander, P. N. Laver, A. L. Michel, M. Williams, P. D. van Helden, R. M. Warren, and N. C. G. van Pittius, "Novel *Mycobacterium tuberculosis* complex pathogen, M. mungi," *Emerging Infectious Diseases*, vol. 16, pp. 1296–1300, 2010.

[75] D. D. Kang, Y. Lin, J.-R. Moreno, T. D. Randall, and S. A. Khader, "Profiling early lung immune responses in the mouse model of tuberculosis," *PLoS One*, vol. 6, pp. 1–6, 2011.

[76] R. Blomgran, L. Desvignes, V. Briken, and J. D. Ernst, "*Mycobacterium tuberculosis* inhibits neutrophil apoptosis, leading to delayed activation of naive CD4 T cells," *Cell Host and Microbe*, vol. 11, pp. 81–90, 2012.

[77] J. M. Davis and L. Ramakrishnan, "The role of the granuloma in expansion and dissemination of early tuberculous infection," *Cell*, vol. 136, pp. 37–49, 2009.

[78] M. Divangahi, D. Desjardins, C. Nunes-Alves, H. G. Remold, and S. M. Behar, "Eicosanoid pathways regulate adaptive immunity to *Mycobacterium tuberculosis*," *Nature Immunology*, vol. 11, pp. 751–758, 2010.

[79] B. N. Mohapatra and C. Mohanty, "Treatment of tuberculosis WHO guidelines 2010," *Tersedia dari: Http://www. apiindia. org/pdf/medicine_update_2011/81_treatment_of_tuberculosi s. pdf.*

[80] J. A. Caminero, G. Sotgiu, A. Zumla, and G. B. Migliori, "Best drug treatment for multidrug-resistant and extensively drug-resistant tuberculosis," *The Lancet Infectious Diseases*, vol. 10, no. 9, pp. 621–629, 2010.

[81] Centers for Disease Control and Prevention (CDC), "Trends in tuberculosis incidence–United States, 2006," *Morbidity and Mortality Weekly Report*, vol. 56, no. 11, pp. 245–250, 2007.

[82] B. Müller, S. Borrell, G. Rose, and S. Gagneux, "The heterogeneous evolution of multidrug-resistant *Mycobacterium tuberculosis*," *Trends in Genetics*, vol. 29, no. 3, pp. 160–169, 2013.

[83] B. Müller, S. Borrell, G. Rose, and S. Gagneux, "The heterogeneous evolution of multidrug-resistant *Mycobacterium tuberculosis*," *Trends in Genetics*, vol. 29, pp. 160–169, 2013.

[84] D. C. Perlman, Y. Segal, S. Rosenkranz, P. M. Rainey, R. P. Remmel, N. Salomon, R. Hafner, C. A. Peloquin, and A. C. T. G. . Team, "The clinical pharmacokinetics of rifampin and ethambutol in HIV-infected persons with tuberculosis," *Clinical Infectious Diseases*, vol. 41, pp. 1638–1647, 2005.

[85] I. Abubakar, M. Zignol, D. Falzon, M. Raviglione, L. Ditiu, S. Masham, I. Adetifa, N. Ford, H. Cox, and S. D. Lawn, "Drug-resistant tuberculosis: time for visionary political leadership," *The Lancet Infectious Diseases*, vol. 13, pp. 529–539, 2013.

[86] WHO, "Management of drug-resistant tuberculosis: training for staff working at dr-tb management centres: training modules," World Health Organization, Tech. Rep., 2014.

[87] J. P. Lanoix, F. Betoudji, and E. Nuermberger, "Sterilizing activity of pyrazinamide in combination with first-line drugs in a c3heb/fej mouse model of tuberculosis," *Antimicrobial Agents and Chemotherapy*, vol. 60, no. 2, pp. 1091–1096, 2016.

[88] S. M. Ramirez-Busby and F. Valafar, "Systematic review of mutations in pyrazinamidase associated with pyrazinamide resistance in *Mycobacterium tuberculosis* clinical isolates," *Antimicrobial Agents and Chemotherapy*, vol. 59, no. 9, pp. 5267–5277, 2015.

[89] J. Yang, Y. Liu, J. Bi, Q. Cai, X. Liao, W. Li, C. Guo, Q. Zhang, T. Lin, Y. Zhao *et al.*, "Structural basis for targeting the ribosomal protein S1 of *Mycobacterium tuberculosis* by pyrazinamide," *Molecular Microbiology*, vol. 95, no. 5, pp. 791–803, 2015.

[90] Y. Zhang, W. Shi, W. Zhang, and D. Mitchison, "Mechanisms of pyrazinamide action and resistance," *Microbiology Spectrum*, vol. 2, pp. 1–12, 2013.

[91] K. Konno, F. M. Feldmann, and W. McDermott, "Pyrazinamide Susceptibility and Amidase Activity of Tubercle Bacilli 1, 2," *American Review of Respiratory Disease*, vol. 95, pp. 461–469, 1967.

[92] P. Miotto, A. M. Cabibbe, S. Feuerriegel, N. Casali, F. Drobniewski, Y. Rodionova, D. Bakonyte, P. Stakenas, E. Pimkina, and E. Augustynowicz-Kope, "*Mycobacterium tuberculosis* pyrazinamide resistance determinants: a multicenter study," *MBio*, vol. 5, pp. e01 819–14, 2014.

[93] Y. Zhang, M. M. Wade, A. Scorpio, H. Zhang, and Z. Sun, "Mode of action of pyrazinamide: disruption of *Mycobacterium tuberculosis* membrane transport and energetics by pyrazinoic acid," *Journal of Antimicrobial Chemotherapy*, vol. 52, pp. 790–795, 2003.

[94] Y. Zhang and D. Mitchison, "The curious characteristics of pyrazinamide: a review," *The International Journal of Tuberculosis and Lung Disease*, vol. 7, pp. 6–21, 2003.

[95] S. Sreevatsan, X. Pan, Y. Zhang, B. N. Kreiswirth, and J. M. Musser, "Mutations associated with pyrazinamide resistance in pncA of *Mycobacterium tuberculosis* complex organisms," *Antimicrobial Agents and Chemotherapy*, vol. 41, pp. 636–640, 1997.

[96] M. Chen, H. Gan, and H. G. Remold, "A mechanism of virulence: virulent *Mycobacterium tuberculosis* strain H37Rv, but not attenuated H37Ra, causes significant mitochondrial inner membrane disruption in macrophages leading to necrosis," *The Journal of Immunology*, vol. 176, no. 6, pp. 3707–3716, 2006.

[97] S. Zhang, J. Chen, W. Shi, P. Cui, J. Zhang, S. Cho, W. Zhang, and Y. Zhang, "Mutation in clpC1 encoding an ATP-dependent ATPase involved in protein degradation is associated with pyrazinamide resistance in *Mycobacterium tuberculosis*," *Emerging Microbes and Infection*, vol. 6, no. 2, pp. 8–10, 2017.

[98] N. Lemaitre, I. Callebaut, F. Frenois, V. Jarlier, and W. Sougakoff, "Study of the structure activity relationships for the pyrazinamidase (PncA) from *Mycobacterium tuberculosis*," *Biochemical Journal*, vol. 353, pp. 453–458, 2001.

[99] S. Petrella, N. Gelus-Ziental, A. Maudry, C. Laurans, R. Boudjelloul, and W. Sougakoff, "Crystal structure of the pyrazinamidase of *Mycobacterium tuberculosis*: insights into natural and acquired resistance to pyrazinamide," *PLoS One*, vol. 6, pp. 1–6, 2011.

[100] O. H. Vandal, L. M. Pierini, D. Schnappinger, C. F. Nathan, and S. Ehrt, "A membrane protein preserves intrabacterial pH in intraphagosomal *Mycobacterium tuberculosis*," *Nature Medicine*, vol. 14, pp. 849–854, 2008.

[101] T. Zhang, S.-Y. Li, and E. L. Nuermberger, "Autoluminescent *Mycobacterium tuberculosis* for rapid, real-time, non-invasive assessment of drug and vaccine efficacy," *PLoS One*, vol. 7, pp. e29 774–e29 774, 2012.

[102] H. Kim, K. Shibayama, E. Rimbara, and S. Mori, "Biochemical characterization of quinolinic acid phosphoribosyltransferase from *Mycobacterium tuberculosis* H37rv and inhibition of its activity by pyrazinamide," *PLoS One*, vol. 9, pp. e100 062–e100 062, 2014.

[103] L. E. Via, R. Savic, D. M. Weiner, M. D. Zimmerman, B. Prideaux, S. M. Irwin, E. Lyon, P. O Brien, P. Gopal, and S. Eum, "Host-mediated bioactivation of pyrazinamide: implications for efficacy, resistance, and therapeutic alternatives," *ACS Infectious Diseases*, vol. 1, pp. 203–214, 2015.

[104] X. Du, W. Wang, R. Kim, H. Yakota, H. Nguyen, and S.-H. Kim, "Crystal structure and mechanism of catalysis of a pyrazinamidase from pyrococcus horikoshii," *Biochemistry*, vol. 40, no. 47, pp. 14 166–14 172, 2001.

[105] N. Lemaitre, Isabelle, F. Callebaut, V. Frenois, W. Jarlier, and Sougakoff, "Study of the structure' activity relationships for the pyrazinamidase (*pncA*) from *Mycobacterium tuberculosis*," pp. 453–458, 2001.

[106] P. Sheen, P. Ferrer, R. H. Gilman, J. López-Llano, P. Fuentes, E. Valencia, and M. J. Zimic, "Effect of pyrazinamidase activity on pyrazinamide resistance in *Mycobacterium tuberculosis*," *Tuberculosis*, vol. 89, pp. 109–113, 2009.

[107] J. H. Yoon, J.-S. Nam, K.-J. Kim, and Y.-T. Ro, "Characterization of pncA mutations in pyrazinamide-resistant *Mycobacterium tuberculosis* isolates from Korea and analysis of the correlation between the mutations and pyrazinamidase activity," *World Journal of Microbiology and Biotechnology*, vol. 30, pp. 2821–2828, 2014.

[108] M. Bycroft, T. J. Hubbard, M. Proctor, S. M. Freund, and A. G. Murzin, "The solution structure of the S1 rna binding domain: a member of an ancient nucleic acid–binding fold," *Cell*, vol. 88, no. 2, pp. 235–242, 1997.

[109] G. Gopalan, S. Chopra, A. Ranganathan, and K. Swaminathan, "Crystal structure of uncleaved l-aspartate-α-decarboxylase from *Mycobacterium tuberculosis*," *Proteins: Structure, Function, and Bioinformatics*, vol. 65, no. 4, pp. 796–802, 2006.

[110] H. Zhang, J.-Y. Deng, L.-J. Bi, Y.-F. Zhou, Z.-P. Zhang, C.-G. Zhang, Y. Zhang, and X.-E. Zhang, "Characterization of *Mycobacterium tuberculosis* nicotinamidase/pyrazinamidase," *FEBS Journal*, vol. 275, pp. 753–762, 2008.

[111] W. Shi, J. Chen, J. Feng, P. Cui, S. Zhang, X. Weng, W. Zhang, and Y. Zhang, "Aspartate decarboxylase (PanD) as a new target of pyrazinamide in *Mycobacterium tuberculosis*," *Emerging Microbes and Infections*, vol. 3, pp. 1–8, 2014.

[112] Y. Gu, X. Yu, G. Jiang, X. Wang, Y. Ma, Y. Li, and H. Huang, "Pyrazinamide resistance among multidrug-resistant tuberculosis clinical isolates in a national referral center of China and its correlations with pncA, rpsA, and panD gene mutations," *Diagnostic Microbiology and Infectious Disease*, vol. 84, no. 3, pp. 207–211, 2016.

[113] M. J. Keiser, V. Setola, J. J. Irwin, C. Laggner, A. I. Abbas, S. J. Hufeisen, N. H. Jensen, M. B. Kuijer, R. C. Matos, T. B. Tran *et al.*, "Predicting new molecular targets for known drugs," *Nature*, vol. 462, no. 7270, pp. 175–180, 2009.

[114] Y. Tan, Z. Hu, T. Zhang, X. Cai, H. Kuang, Y. Liu, J. Chen, F. Yang, K. Zhang, and S. Tan, "Role of pncA and rpsA gene sequencing in detection of pyrazinamide resistance in *Mycobacterium tuberculosis* isolates from southern China," *Journal of Clinical Microbiology*, vol. 52, pp. 291–297, 2014.

[115] T. S. Huang, S. S.-J. Lee, H.-Z. Tu, W.-K. Huang, Y.-S. Chen, C.-K. Huang, S.-R. Wann, H.-H. Lin, and Y.-C. Liu, "Correlation between pyrazinamide activity and pncA mutations in *Mycobacterium tuberculosis* isolates in Taiwan," *Antimicrobial Agents and Chemotherapy*, vol. 47, pp. 3672–3673, 2003.

[116] S. Bhuju, L. de Souza Fonseca, A. G. Marsico, G. B. de Oliveira Vieira, L. F. Sobral, M. Stehr, M. Singh, and M. H. F. Saad, "*Mycobacterium tuberculosis*

isolates from Rio de Janeiro reveal unusually low correlation between pyrazinamide resistance and mutations in the pncA gene," *Infection, Genetics and Evolution*, vol. 19, pp. 1–6, 2013.

[117] K. Bishop, L. Blumberg, A. Trollip, A. Smith, L. Roux, D. York, and P. Kiepiela, "Characterisation of the pncA gene in *Mycobacterium tuberculosis* isolates from Gauteng, South Africa," *The International Journal of Tuberculosis and Lung disease*, vol. 5, pp. 952–957, 2001.

[118] C. Miyagi, N. Yamane, B. Yogesh, H. Ano, and T. Takashima, "Genetic and phenotypic characterization of pyrazinamide-resistant *Mycobacterium tuberculosis* complex isolates in japan," *Diagnostic microbiology and infectious disease*, vol. 48, no. 2, pp. 111–116, 2004.

[119] S. Rodrigues, Vívian, M. A. Telles, M. O. Ribeiro, P. I. Cafrune, M. L. R. Rossetti, and A. Zaha, "Characterization of pncA mutations in pyrazinamide-resistant *Mycobacterium tuberculosis* in Brazil," *Antimicrobial Agents and Chemotherapy*, vol. 49, pp. 444–446, 2005.

[120] R. C. Chan, M. Hui, E. W. Chan, T. K. Au, M. L. Chin, C. K. Yip, C. K. AuYeang, C. Y. Yeung, K. M. Kam, and P. C. Yip, "Genetic and phenotypic characterization of drug-resistant *Mycobacterium tuberculosis* isolates in Hong Kong," *Journal of Antimicrobial Chemotherapy*, vol. 59, pp. 866–873, 2007.

[121] S. Pandey, S. Newton, A. Upton, S. Roberts, and D. Drinkovi, "Characterisation of pncA mutations in clinical *Mycobacterium tuberculosis* isolates in New Zealand," *Pathology*, vol. 41, pp. 582–584, 2009.

[122] J. Jonmalung, T. Prammananan, M. Leechawengwongs, and A. Chaiprasert, "Surveillance of pyrazinamide susceptibility among multidrug-resistant *Mycobacterium tuberculosis* isolates from Siriraj Hospital, Thailand," *BMC Microbiology*, vol. 10, p. 1, 2010.

[123] G. E. Louw, R. M. Warren, P. R. Donald, M. B. Murray, M. Bosman, P. D. Van Helden, D. B. Young, and T. C. Victor, "Frequency and implications

of pyrazinamide resistance in managing previously treated tuberculosis patients," *The International Journal of Tuberculosis and Lung Disease*, vol. 10, pp. 802–807, 2006.

[124] L. Hou, D. Osei-Hyiaman, Z. Zhang, B. Wang, A. Yang, and K. Kano, "Molecular characterization of pncA gene mutations in *Mycobacterium tuberculosis* clinical isolates from China," *Epidemiology and Infection*, vol. 124, pp. 227–232, 2000.

[125] K. Hirano, M. Takahashi, Y. Kazumi, Y. Fukasawa, and C. Abe, "Mutation in pncA is a major mechanism of pyrazinamide resistance in *Mycobacterium tuberculosis*," *Tubercle and Lung Disease*, vol. 78, pp. 117–122, 1998.

[126] K. W. Lee, J. M. Lee, and K. S. Jung, "Characterization of pncA mutations of pyrazinamide-resistant *Mycobacterium tuberculosis* in Korea," *Journal of Korean medical science*, vol. 16, pp. 537–537, 2001.

[127] S. O. Simons, J. van Ingen, T. van der Laan, A. Mulder, P. R. Dekhuijzen, M. J. Boeree, and D. van Soolingen, "Validation of pncA gene sequencing in combination with the mycobacterial growth indicator tube method to test susceptibility of *Mycobacterium tuberculosis* to pyrazinamide," *Journal of Clinical Microbiology*, vol. 50, pp. 428–434, 2012.

[128] Y. Zhang and W. W. Yew, "Mechanisms of drug resistance in *Mycobacterium tuberculosis* [State of the art series. Drug-resistant tuberculosis. Edited by CY. Chiang. Number 1 in the series]," *The International Journal of Tuberculosis and Lung disease*, vol. 13, pp. 1320–1330, 2009.

[129] A. Akhmetova, U. Kozhamkulov, V. Bismilda, L. Chingissova, T. Abildaev, M. Dymova, M. Filipenko, and E. Ramanculov, "Mutations in the pncA and rpsA genes among 77 *Mycobacterium tuberculosis* isolates in Kazakhstan," *The International Journal of Tuberculosis and Lung Disease*, vol. 19, pp. 179–184, 2015.

[130] Z. Dundas, J. B. , and Y. L. , "Joe Tseng Turpaz CASTp: computed atlas of surface topography of proteins with structural and topographical mapping

of functionally annotated resiudes." *Nucleic Acids Research*, vol. 34, pp. 116–118, 2006.

[131] H. F. Tippmann, "Analysis for free: comparing programs for sequence analysis," *Briefings in Bioinformatics*, vol. 5, no. 1, pp. 82–87, 2004.

[132] M. Machado, W. C. Magalhães, A. Sene, B. Araújo, A. C. Faria-Campos, S. J. Chanock, L. Scott, G. Oliveira, E. Tarazona-Santos, and M. R. Rodrigues, "Phred-phrap package to analyses tools: a pipeline to facilitate population genetics re-sequencing studies," *Investigative Genetics*, vol. 2, no. 1, pp. 3–3, 2011.

[133] T. Hall, "Bioedit version 5.0. 6," *North Carolina State University, Department of Microbiology, Raleigh, North Carolina*, vol. 192, 2001.

[134] J. D. Thompson, T. J. Gibson, and D. G. Higgins, "Multiple sequence alignment using clustalw and clustalx," *Current protocols in Bioinformatics*, no. 1, pp. 2–3, 2003.

[135] C. Dong and B. Yu, "Mutation surveyor: an in silico tool for sequencing analysis," *Springer*, pp. 223–237, 2011.

[136] A. Nayeem, D. Sitkoff, and S. Krystek, "A comparative study of available software for high-accuracy homology modeling: From sequence alignments to structural models," *Protein Science*, vol. 15, no. 4, pp. 808–824, 2006.

[137] B. Webb and A. Sali, "Comparative protein structure modeling using modeller," *Current Protocols in Protein Science*, vol. 86, no. 1, pp. 2–9, 2016.

[138] Y. Choi and A. P. Chan, "PROVEAN web server: a tool to predict the functional effect of amino acid substitutions and indels," *Bioinformatics*, vol. 31, no. 16, pp. 2745–2747, 2015.

[139] C. W. Chen, J. Lin, and Y.-W. Chu, "istable: off-the-shelf predictor integration for predicting protein stability changes," *BMC Bioinformatics*, vol. 14, pp. S5–S5, 2013.

[140] S. Kulshreshtha, V. Chaudhary, G. K. Goswami, and N. Mathur, "Computational approaches for predicting mutant protein stability," *Journal of Computer-aided Molecular Design*, vol. 30, no. 5, pp. 401–412, 2016.

[141] A. Kume, S. Kawai, R. Kato, S. Iwata, K. Shimizu, and H. Honda, "Exploring high-affinity binding properties of octamer peptides by principal component analysis of tetramer peptides," *Journal of Bioscience and Bioengineering*, vol. 123, no. 2, pp. 230–238, 2017.

[142] Z. Ouaray, K. M. ElSawy, D. P. Lane, J. W. Essex, and C. Verma, "Reactivation of mutant p53: Constraints on mechanism highlighted by principal component analysis of the dna binding domain," *Proteins: Structure, Function, and Bioinformatics*, vol. 84, no. 10, pp. 1443–1461, 2016.

[143] S. Tripathi, G. Srivastava, and A. Sharma, "Molecular dynamics simulation and free energy landscape methods in probing l215h, l217r and l225m βi-tubulin mutations causing paclitaxel resistance in cancer cells," *Biochemical and Biophysical Research Communications*, vol. 476, no. 4, pp. 273–279, 2016.

[144] Y. Sugita and A. Kitao, "Dependence of protein stability on the structure of the denatured state: free energy calculations of i56v mutation in human lysozyme," *Biophysical Journal*, vol. 75, no. 5, pp. 2178–2187, 1998.

[145] T. A. Binkowski, S. Naghibzadeh, and J. Liang, "CASTp: Computed Atlas of Surface Topography of proteins," *Nucleic Acids Research*, vol. 31, no. 13, pp. 3352–3355, 2003.

[146] K. Salazar-Salinas, P. A. Baldera-Aguayo, J. J. Encomendero-Risco, M. Orihuela, P. Sheen, J. M. Seminario, and M. Zimic, "Metal-ion effects on the polarization of metal-bound water and infrared vibrational modes of the coordinated metal center of *Mycobacterium tuberculosis* pyrazinamidase via quantum mechanical calculations," *The Journal of Physical Chemistry*, vol. 118, no. 34, pp. 10 065–10 075, 2014.

[147] Y. Zhang, W. Shi, W. Zhang, and D. Mitchison, "Mechanisms of pyrazinamide action and resistance," *Microbiology Spectrum*, vol. 2, no. 4, pp. 1–4, 2013.

[148] P. T. Kent and G. P. Kubica, *Public health mycobacteriology: a guide for the level III laboratory.* US Department of Health and Human Services, Public Health Service, Centers for Disease Control, 1985.

[149] G. E. Pfyffer and F. Wittwer, "Incubation time of mycobacterial cultures: how long is long enough to issue a final negative report to the clinician?" *Journal of Clinical Microbiology*, vol. 50, no. 12, pp. 4188–4189, 2012.

[150] J. Arora, G. Kumar, A. K. Verma, M. Bhalla, R. Sarin, and V. P. Myneedu, "Utility of mpt64 antigen detection for rapid confirmation of *Mycobacterium tuberculosis* complex," *Journal of Global Infectious Diseases*, vol. 7, no. 2, pp. 66–70, 2015.

[151] A. Aono, K. Hirano, S. Hamasaki, and C. Abe, "Evaluation of BACTEC MGIT 960 PZA medium for susceptibility testing of *Mycobacterium tuberculosis* to pyrazinamide (PZA): compared with the results of pyrazinamidase assay and Kyokuto PZA test," *Diagnostic Microbiology and Infectious Disease*, vol. 44, pp. 347–352, 2002.

[152] J. Hosek, P. Svastova, M. Moravkova, I. Pavlik, and M. Bartos, "Methods of mycobacterial dna isolation from different biological material: A review," *Veterinarni Medicina*, vol. 51, no. 5, pp. 180–192, 2006.

[153] G. E. Buck, L. C. O'Hara, and J. T. Summersgill, "Rapid, simple method for treating clinical specimens containing *Mycobacterium tuberculosis* to remove dna for polymerase chain reaction." *Journal of Clinical Microbiology*, vol. 30, no. 5, pp. 1331–1334, 1992.

[154] P. Kirschner, B. Springer, U. Vogel, A. Meier, A. Wrede, M. Kiekenbeck, F. C. Bange, and E. C. Böttger, "Genotypic identification of mycobacteria by nucleic acid sequence determination: report of a 2-year experience in a

clinical laboratory." *Journal of Clinical Microbiology*, vol. 31, no. 11, pp. 2882–2889, 1993.

[155] Q. Xia, L.-l. Zhao, F. Li, Y.-m. Fan, Y.-y. Chen, B.-b. Wu, Z.-w. Liu, A.-z. Pan, and M. Zhu, "Phenotypic and Genotypic Characterization of Pyrazinamide Resistance among Multidrug-Resistant *Mycobacterium tuberculosis* Isolates in Zhejiang, China," *Antimicrobial Agents Chemotherapy*, vol. 59, no. 3, pp. 1690–1695, 2015.

[156] J. Sambrook, E. F. Fritsch, T. Maniatis *et al.*, *Molecular cloning: A laboratory manual.* Cold Spring Harbor Laboratory Press, 1989, no. Ed.2.

[157] J. A. Minton, S. E. Flanagan, and S. Ellard, "Mutation surveyor: software for dna sequence analysis," *Springer*, pp. 143–153, 2011.

[158] J. Lauritsen, "Epidata data entry, data management and basic statistical analysis system," *Odense Denmark: EpiData Association*, 2008.

[159] S. K. Burley, H. M. Berman, C. Christie, J. M. Duarte, Z. Feng, J. Westbrook, J. Young, and C. Zardecki, "RCSB protein data bank: Sustaining a living digital data resource that enables breakthroughs in scientific research and biomedical education," *Protein Science*, vol. 27, no. 1, pp. 316–330, 2018.

[160] W. L. DeLano, "The pymol molecular graphics system (2002)," *http://www. pymol. org*, 2002.

[161] S. Kim, J. Chen, T. Cheng, A. Gindulyte, J. He, S. He, Q. Li, B. A. Shoemaker, P. A. Thiessen, B. Yu *et al.*, "Pubchem 2019 update: improved access to chemical data," *Nucleic Acids Research*, vol. 47, no. D1, pp. 1102–1109, 2018.

[162] T. A. Halgren, "Merck molecular force field. i. basis, form, scope, parameterization, and performance of mmff94," *Journal of Computational Chemistry*, vol. 17, no. 5-6, pp. 490–519, 1996.

[163] S. Vilar, G. Cozza, and S. Moro, "Medicinal chemistry and the molecular operating environment (moe): application of qsar and molecular docking to drug discovery," *Current Topics in Medicinal Chemistry*, vol. 8, no. 18, pp. 1555–1572, 2008.

[164] T. Darden, D. York, and L. Pedersen, "Particle mesh ewald: An Nlog (n) method for ewald sums in large systems," *The Journal of Chemical Physics*, vol. 98, no. 12, pp. 10 089–10 092, 1993.

[165] J. Allwright, "Conjugate gradient versus steepest descent," *Journal of Optimization Theory and Applications*, vol. 20, no. 1, pp. 129–134, 1976.

[166] A. H. Aytenfisu, A. Spasic, A. Grossfield, H. A. Stern, and D. H. Mathews, "Revised rna dihedral parameters for the amber force field improve rna molecular dynamics," *Journal of Chemical Theory and Computation*, vol. 13, no. 2, pp. 900–915, 2017.

[167] V. Parthiban, M. M. Gromiha, and D. Schomburg, "Cupsat: prediction of protein stability upon point mutations," *Nucleic Acids Research*, vol. 34, no. suppl_2, pp. W239–W242, 2006.

[168] C. L. Worth, R. Preissner, and T. L. Blundell, "Sdm: A server for predicting effects of mutations on protein stability and malfunction," *Nucleic Acids Research*, vol. 39, no. suppl_2, pp. 215–222, 2011.

[169] D. Szklarczyk, J. H. Morris, H. Cook, M. Kuhn, S. Wyder, M. Simonovic, A. Santos, N. T. Doncheva, A. Roth, P. Bork, L. J. Jensen, and C. von Mering, "The STRING database in 2017: quality-controlled protein-protein association networks, made broadly accessible," *Nucleic Acids Research*, vol. 45, pp. 362–368, 2017.

[170] P. Shannon, A. Markiel, O. Ozier, N. S. Baliga, J. T. Wang, D. Ramage, N. Amin, B. Schwikowski, and T. Ideker, "Cytoscape: a software environment for integrated models of biomolecular interaction networks," *Genome Research*, vol. 13, no. 11, pp. 2498–2504, 2003.

[171] M. H. Kabir, R. Patrick, J. W. Ho, and M. D. Connor, "Identification of active signaling pathways by integrating gene expression and protein interaction data," *BMC Systems Biology*, vol. 12, no. 9, pp. 120–125, 2018.

[172] Y. Rodriguez, C. Alejo, I. Alejo, and A. Viguria, "Animo, framework to simplify the real-time distributed communication," *Springer*, pp. 77–92, 2016.

[173] R. Bansal, D. Sharma, and R. Singh, "Tuberculosis and its treatment: An overview," *Mini Reviews in Medicinal Chemistry*, vol. 18, no. 1, pp. 58–71, 2018.

[174] C. Timire, C. Sandy, A. M. Kumar, M. Ngwenya, B. Murwira, K. C. Takarinda, and A. D. Harries, "Access to second-line drug susceptibility testing results among patients with rifampicin resistant tuberculosis after introduction of the hain® line probe assay in southern provinces, zimbabwe," *International Journal of Infectious Diseases*, vol. 81, pp. 236–243, 2019.

[175] S. Srivastava, J. G. Pasipanodya, and T. Gumbo, "ph conditions under which pyrazinamide works in humans," *Antimicrobial Agents and Chemotherapy*, vol. 61, no. 9, pp. e00 854–17, 2017.

[176] S. Sengstake, I. L. Bergval, A. R. Schuitema, J. L. de Beer, J. Phelan, R. de Zwaan, T. G. Clark, D. van Soolingen, and R. M. Anthony, "Pyrazinamide resistance-conferring mutations in *pncA* and the transmission of multidrug resistant TB in Georgia," *BMC Infectious Disease*, vol. 17, pp. 491–491, 2017.

[177] Y. Pang, D. Zhu, H. Zheng, J. Shen, Y. Hu, J. Liu, and Y. Zhao, "Prevalence and molecular characterization of pyrazinamide resistance among multidrug-resistant mycobacterium tuberculosis isolates from southern china," *BMC Infectious Diseases*, vol. 17, no. 1, pp. 711–711, 2017.

[178] M. Zignol, A. S. Dean, N. Alikhanova, S. Andres, A. M. Cabibbe, D. M. Cirillo, A. Dadu, A. Dreyer, M. Driesen, C. Gilpin, and others, "Population-based resistance of *Mycobacterium tuberculosis* isolates to pyrazinamide and

fluoroquinolones: results from a multicountry surveillance project," *The Lancet Infectious Diseases*, vol. 16, no. 10, pp. 1185–1192, 2016.

[179] M. Mphahlele, H. Syre, H. Valvatne, R. Stavrum, T. Mannsåker, T. Muthivhi, K. Weyer, P. B. Fourie, and H. M. Grewal, "Pyrazinamide resistance among South African multidrug-resistant *Mycobacterium tuberculosis* isolates," *Journal of Clinical Microbiology*, vol. 46, pp. 3459–3464, 2008.

[180] S. Hoffner, K. Angeby, E. Sturegård, B. Jönsson, A. Johansson, M. Sellin, and J. Werngren, "Proficiency of drug susceptibility testing of *Mycobacterium tuberculosis* against pyrazinamide: the Swedish experience," *International Journal of Tuberculosis and Lung Disease*, vol. 17, no. 11, pp. 1486–1490, 2013.

[181] C. Piersimoni, A. Mustazzolu, F. Giannoni, S. Bornigia, G. Gherardi, and L. Fattorini, "Prevention of false resistance results obtained in testing the susceptibility of *Mycobacterium tuberculosis* to pyrazinamide with the Bactec MGIT 960 system using a reduced inoculum," *Journal of clinical microbiology*, vol. 51, no. 1, pp. 291–294, 2013.

[182] M. G. Whitfield, H. M. Soeters, R. M. Warren, T. York, S. L. Sampson, E. M. Streicher, P. D. Van Helden, and A. Van Rie, "A global perspective on pyrazinamide resistance: systematic review and meta-analysis," *PloS One*, vol. 10, no. 7, pp. e0 133 869–e0 133 869, 2015.

[183] N. Q. Huy, C. Lucie, T. T. T. Hoa, N. V. Hung, N. T. N. Lan, N. T. Son, N. V. Nhung, D. D. Anh, B. Anne-Laure, and N. T. Van Anh, "Molecular analysis of pyrazinamide resistance in mycobacterium tuberculosis in vietnam highlights the high rate of pyrazinamide resistance-associated mutations in clinical isolates: Pnca mutations and pza resistance in m. tuberculosis in vietnam," *Emerging Microbes and Infections*, vol. 6, no. 1, pp. 1–7, 2017.

[184] E. M. Streicher, K. Maharaj, T. York, C. Van Heerden, M. Barnard, A. Diacon, C. M. Mendel, M. E. Bosman, J. A. Hepple, A. S. Pym *et al.*, "Rapid sequencing of the *Mycobacterium tuberculosis pncA* gene for detection of pyrazinamide susceptibility," *Journal of Clinical Microbiology*, vol. 52, no. 11, pp. 4056–4057, 2014.

[185] W. Liu, J. Chen, Y. Shen, J. Jin, J. Wu, F. Sun, Y. Wu, L. Xie, Y. Zhang, and W. Zhang, "Phenotypic and genotypic characterization of pyrazinamide resistance among multidrug-resistant mycobacterium tuberculosis clinical isolates in hangzhou, china," *Clinical Microbiology and Infection*, vol. 24, no. 9, pp. 1016–e1, 2018.

[186] S. Andres, M. I. Gröschel, D. Hillemann, M. Merker, S. Niemann, and K. Kranzer, "A diagnostic algorithm to investigate pyrazinamide and ethambutol resistance in rifampin-resistant mycobacterium tuberculosis isolates in a low-incidence setting," *Antimicrobial Agents and Chemotherapy*, vol. 63, no. 2, pp. e01 798–18, 2019.

[187] P. Xu, J. Wu, C. Yang, T. Luo, X. Shen, Y. Zhang, C. A. Nsofor, G. Zhu, B. Gicquel, and Q. Gao, "Prevalence and transmission of pyrazinamide resistant *Mycobacterium tuberculosis* in China," *Tuberculosis*, vol. 98, pp. 56–61, 2016.

[188] X. Wu, W. Lu, Y. Shao, H. Song, G. Li, Y. Li, L. Zhu, and C. Chen, "pnca gene mutations in reporting pyrazinamide resistance among the mdr-tb suspects," *Infection, Genetics and Evolution*, vol. 72, pp. 147–150, 2019.

[189] W. Shi, P. Cui, H. Niu, S. Zhang, T. Tønjum, B. Zhu, and Y. Zhang, "Introducing rpsa point mutations δ438a and d123a into the chromosome of mycobacterium tuberculosis confirms their role in causing resistance to pyrazinamide," *Antimicrobial Agents and Chemotherapy*, vol. 63, no. 6, pp. e02 681–18, 2019.

[190] Y. Zhang, J. Zhang, P. Cui, W. Zhang, and Y. Zhang, "Identification of novel efflux proteins Rv0191, Rv3756c, Rv3008 and Rv1667c involved in pyrazinamide resistance in *Mycobacterium tuberculosis*," *Antimicrobial Agents and Chemotherapy*, pp. AAC.00 940–17, 2017.

[191] W. Liu, J. Chen, Y. Shen, J. Jin, J. Wu, F. Sun, Y. Wu, L. Xie, Y. Zhang, and W. Zhang, "Phenotypic and genotypic characterization of pyrazinamide resistance among multidrug-resistant *Mycobacterium tuberculosis* clinical isolates in Hangzhou, China," *Clinical Microbiology and Infection*, vol. 24, no. 9, pp. 1016–e1, 2017.

[192] K. K.-G. Tam, K. S.-S. Leung, G. K.-H. Siu, K.-C. Chang, S. S.-Y. Wong, P.-L. Ho, E. K.-C. Leung, and W.-C. Yam, "Direct detection of pyrazinamide resistance of mycobacterium tuberculosis using pnca pcr sequencing," *Journal of Clinical Microbiology*, pp. e00 145–19, 2019.

[193] A. Prakash, V. Kumar, P. Pandey, D. R. Bharti, P. Vishwakarma, R. Singh, M. I. Hassan, and A. M. Lynn, "Solvent sensitivity of protein aggregation in cu, zn superoxide dismutase: A molecular dynamics simulation study," *Journal of Biomolecular Structure and Dynamics*, vol. 36, no. 10, pp. 2605–2617, 2018.

[194] S. A. Hollingsworth and R. O. Dror, "Molecular dynamics simulation for all," *Neuron*, vol. 99, no. 6, pp. 1129–1143, 2018.

[195] M. Aggarwal, A. Singh, S. Grover, B. Pandey, A. Kumari, and A. Grover, "Role of pnca gene mutations w68r and w68g in pyrazinamide resistance," *Journal of Cellular Biochemistry*, vol. 119, no. 3, pp. 2567–2578, 2018.

[196] M. He, W. Li, Q. Zheng, and H. Zhang, "A molecular dynamics investigation into the mechanisms of alectinib resistance of three alk mutants," *Journal of Cellular Biochemistry*, vol. 119, no. 7, pp. 5332–42, 2018.

[197] M. Y. Lobanov, N. Bogatyreva, and O. Galzitskaya, "Radius of gyration as an indicator of protein structure compactness," *Molecular Biology*, vol. 42, no. 4, pp. 623–628, 2008.

[198] D. Smilgies and E. Folta-Stogniew, "Molecular weight–gyration radius relation of globular proteins: a comparison of light scattering, small-angle x-ray scattering and structure-based data," *Journal of Applied Crystallography*, vol. 48, no. 5, pp. 1604–1606, 2015.

[199] L. Swier, L. Monjas, F. Reeßing, R. Oudshoorn, T. Primke, M. Bakker, E. van Olst, T. Ritschel, I. Faustino, S. Marrink *et al.*, "Insight into the complete substrate-binding pocket of thit by chemical and genetic mutations," *MedChemComm*, vol. 8, no. 5, pp. 1121–1130, 2017.

[200] C. Vats, J. K. Dhanjal, S. Goyal, A. Gupta, N. Bharadvaja, and A. Grover, "Mechanistic analysis elucidating the relationship between lys96 mutation in *Mycobacterium tuberculosis* pyrazinamidase enzyme and pyrazinamide susceptibility," vol. 16, no. 2, pp. 14–20, 2015.

[201] J. A. Gerlt, M. M. Kreevoy, W. Cleland, and P. A. Frey, "Understanding enzymic catalysis: the importance of short, strong hydrogen bonds," *Chemistry and biology*, vol. 4, no. 4, pp. 259–267, 1997.

[202] R. E. Hubbard, "Hydrogen bonds in proteins: role and strength," *eLS*, 2001.

[203] C. N. Pace, H. Fu, K. Lee Fryar, J. Landua, S. R. Trevino, D. Schell, R. L. Thurlkill, S. Imura, J. M. Scholtz, K. Gajiwala *et al.*, "Contribution of hydrogen bonds to protein stability," *Protein Science*, vol. 23, no. 5, pp. 652–661, 2014.

[204] D. Shi, Q. Bai, S. Zhou, X. Liu, H. Liu, and X. Yao, "Molecular dynamics simulation, binding free energy calculation and unbinding pathway analysis on selectivity difference between fkbp51 and fkbp52: Insight into the molecular mechanism of isoform selectivity," *Proteins: Structure, Function, and Bioinformatics*, vol. 86, no. 1, pp. 43–56, 2018.

[205] R. Shukla, H. Shukla, P. Kalita, A. Sonkar, T. Pandey, D. B. Singh, A. Kumar, and T. Tripathi, "Identification of potential inhibitors of fasciola gigantica thioredoxin1: computational screening, molecular dynamics simulation,

and binding free energy studies," *Journal of Biomolecular Structure and Dynamics*, vol. 36, no. 8, pp. 2147–2162, 2018.

[206] N. Nagasundaram, H. Zhu, J. Liu, V. Karthick, C. Chakraborty, L. Chen *et al.*, "Analysing the effect of mutation on protein function and discovering potential inhibitors of cdk4: Molecular modelling and dynamics studies," *PLoS One*, vol. 10, no. 8, pp. e0 133 969–82, 2015.

[207] K. Kumar, S. M. Woo, T. Siu, W. A. Cortopassi, F. Duarte, and R. S. Paton, "Cation interactions in protein-ligand binding: Theory and data-mining reveal different roles for lysine and arginine," *Chemical Science*, vol. 9, no. 10, pp. 2655–2665, 2018.

[208] C. D. Okafor, J. C. Bowman, N. V. Hud, J. B. Glass, and L. D. Williams, "Folding and catalysis near life's origin: Support for fe 2+ as a dominant divalent cation," in *Prebiotic Chemistry and Chemical Evolution of Nucleic Acids*. Springer, 2018, pp. 227–243.

[209] Y. Xu, J. Lee, Y.-D. Park, J.-M. Yang, J. Zheng, and Q. Zhang, "Molecular dynamics simulation integrating the inhibition kinetics of hydroxysafflor yellow a on α-glucosidase," *Journal of Biomolecular Structure and Dynamics*, vol. 36, no. 4, pp. 830–840, 2018.

[210] M. T. Khan, M. Junaid, X. Mao, Y. Wang, A. Hussain, S. I. Malik, and D.-Q. Wei, "Pyrazinamide resistance and mutations l19r, r140h, and e144k in pyrazinamidase of mycobacterium tuberculosis," *Journal of Cellular Biochemistry*, vol. 120, no. 5, pp. 7154–7166, 2019.

[211] M. Junaid, M. T. Khan, S. I. Malik, and D.-Q. Wei, "Insights into the mechanisms of the pyrazinamide resistance of three pyrazinamidase mutants n11k, p69t, and d126n," *Journal of Chemical Information and Modeling*, vol. 59, no. 1, pp. 498–508, 2018.

[212] W. H. Organization *et al.*, "Global tuberculosis report 2018. 2018," *Geneva: World Health*, pp. 1–243, 2019.

[213] S. Raman, T. Song, X. Puyang, S. Bardarov, J. Jacobs, and R. N. Husson, "The alternative sigma factor sigh regulates major components of oxidative and heat stress responses in *Mycobacterium tuberculosis*," *Journal of Bacteriology*, vol. 183, no. 20, pp. 6119–6125, 2001.

Appendix A
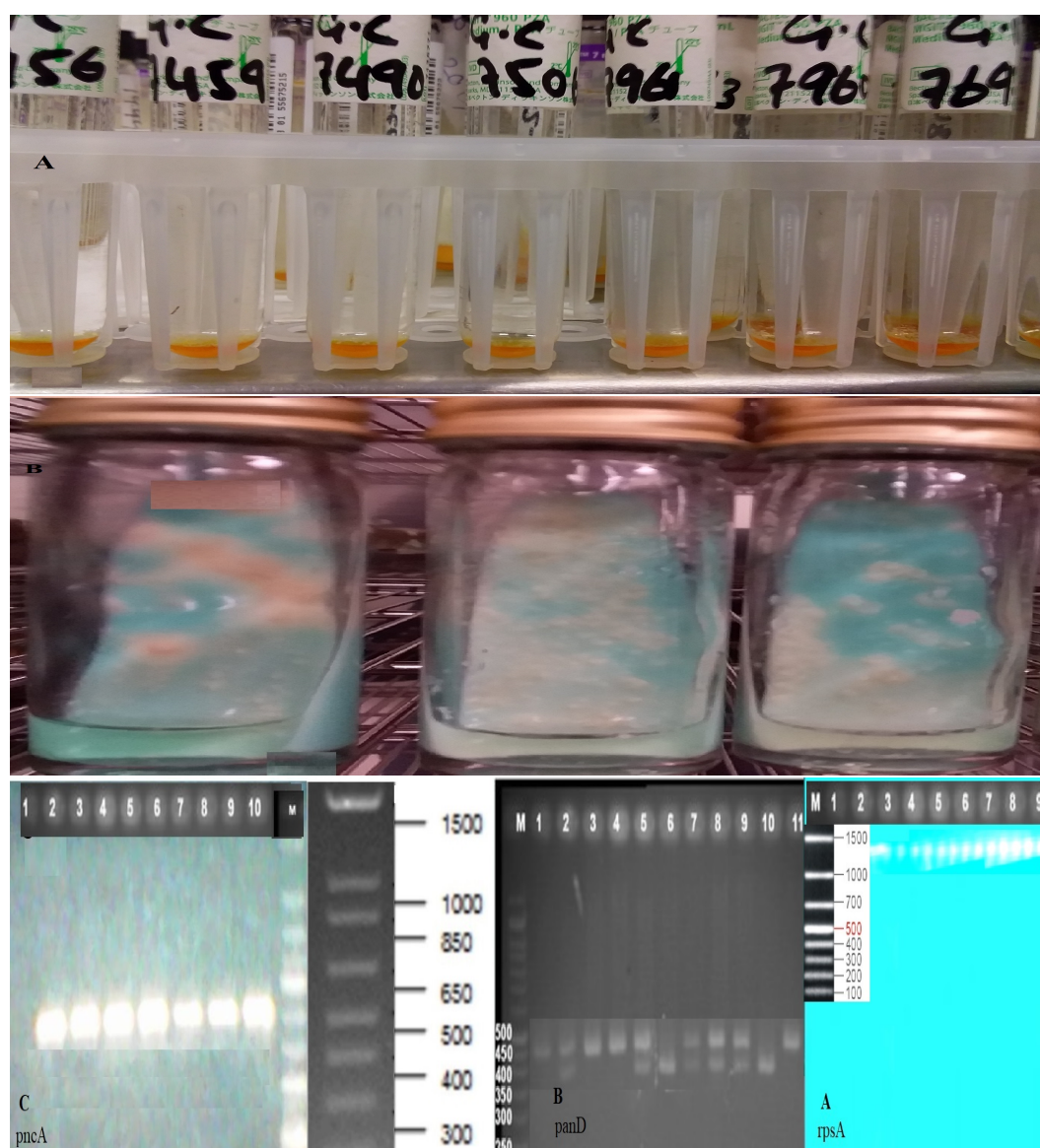
Figure A1: MTB growth on MGIT and LJ media and PCR product.
A: MTB growth in MGIT, B: MTB growth on LJ, C:PCR product of *pncA*,
panD, and *rpsA* on gel.
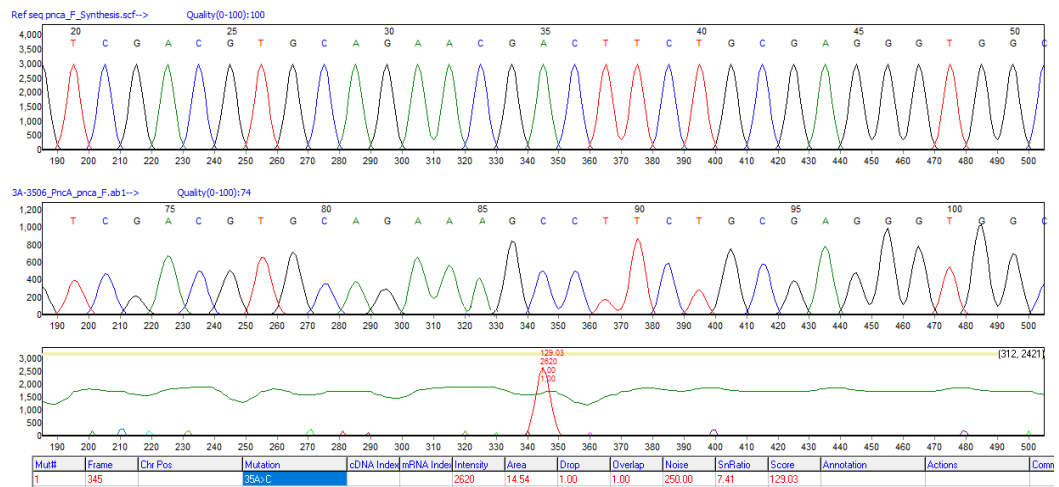
FIGURE A2: Mutation at position 33C-A of *pncA* gene
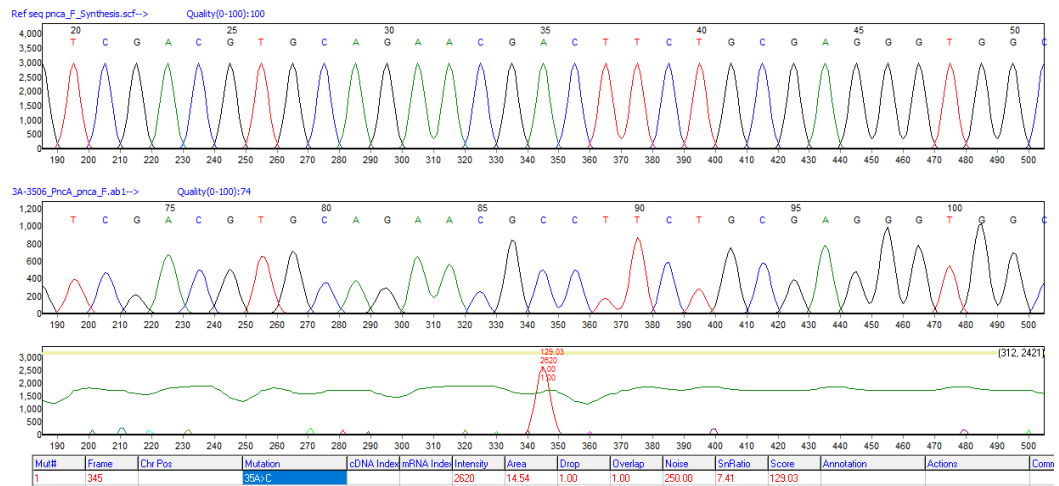
FIGURE A3: Mutation at position 35A-C of *pncA* gene
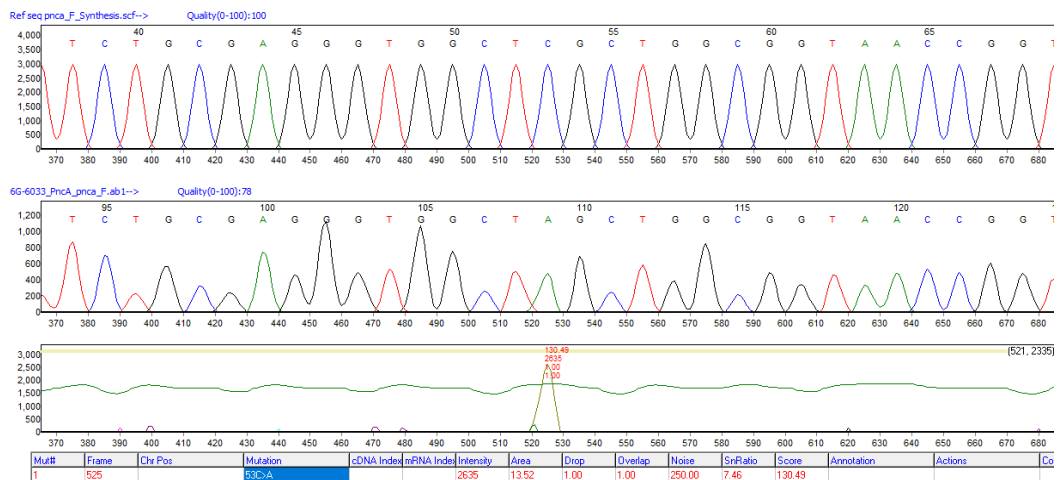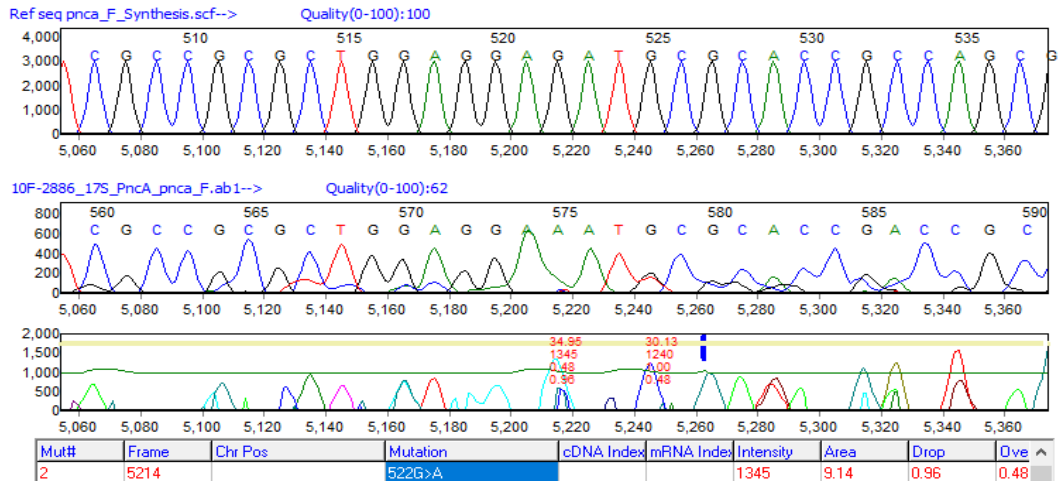

FIGURE A4: Mutation at position 53C-A of *pncA* gene
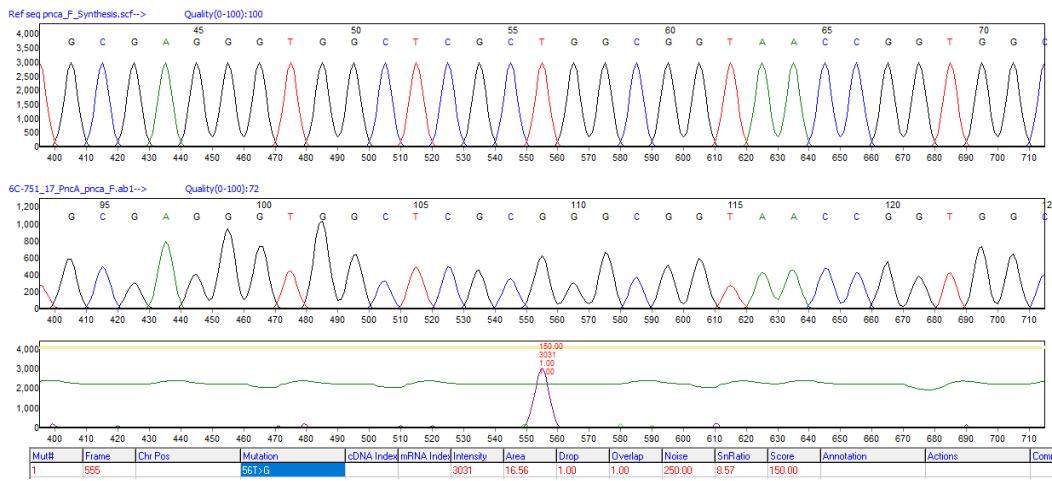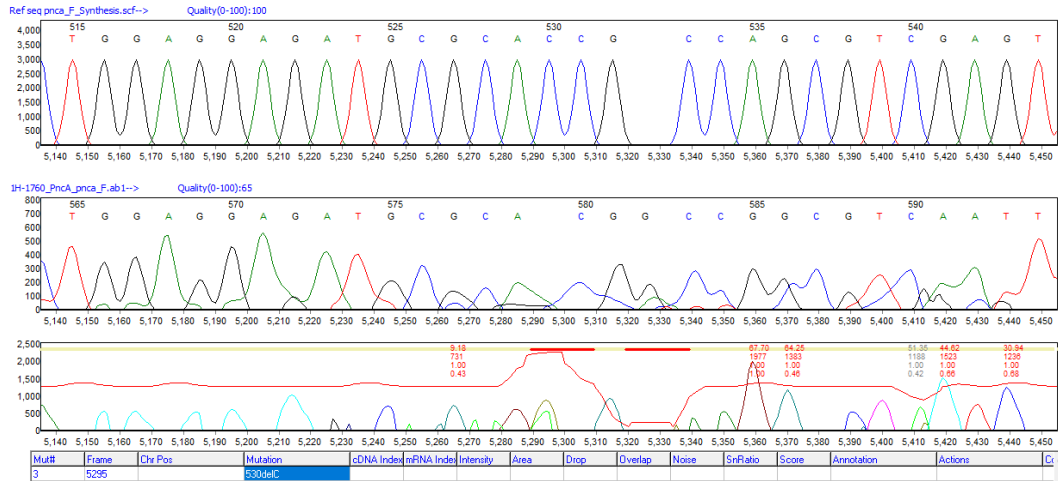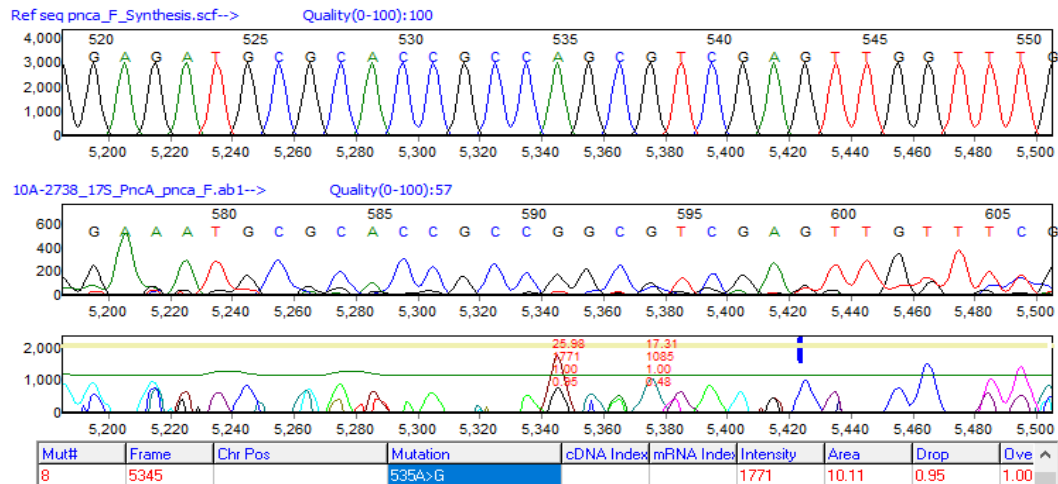
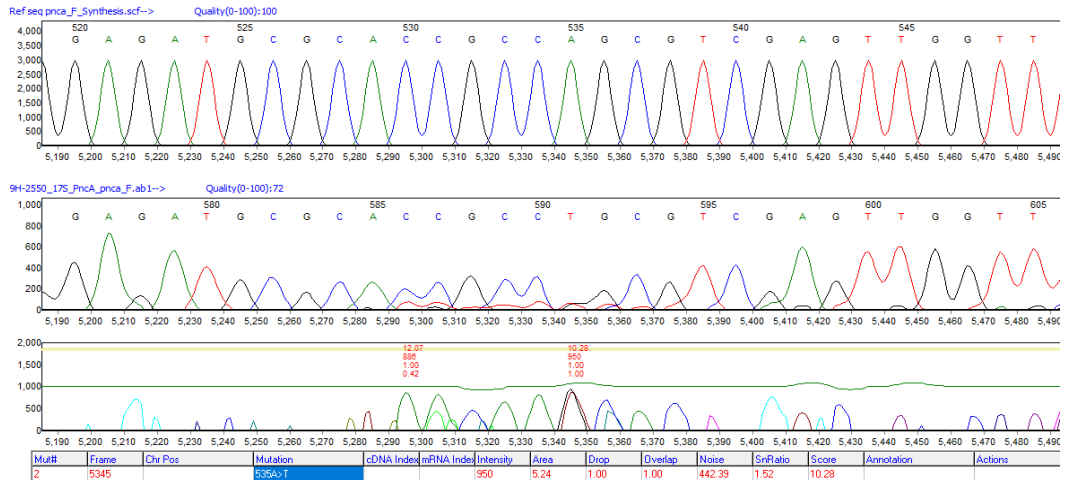FIGURE A5: Mutation at position 56T-G of *pncA* gene
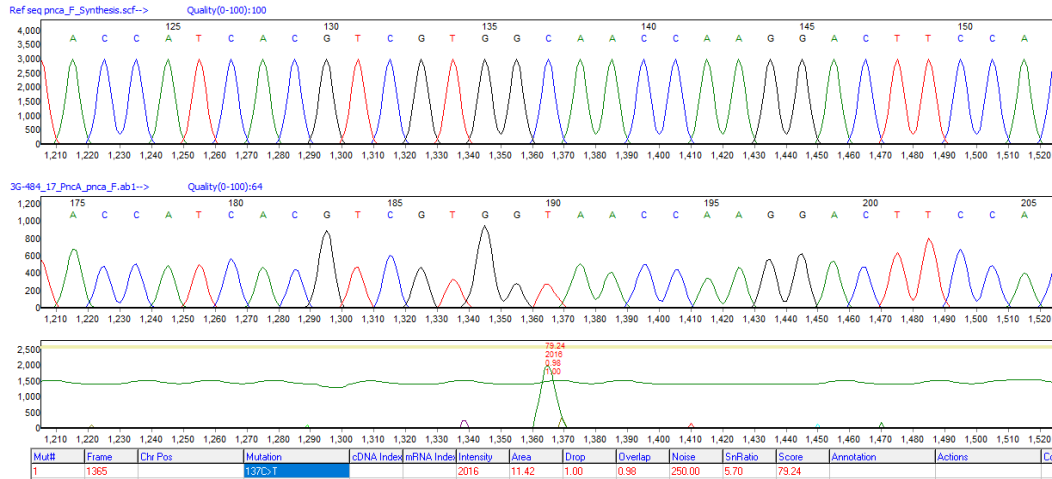
FIGURE A6: Mutation at position 137C-T of *pncA* gene
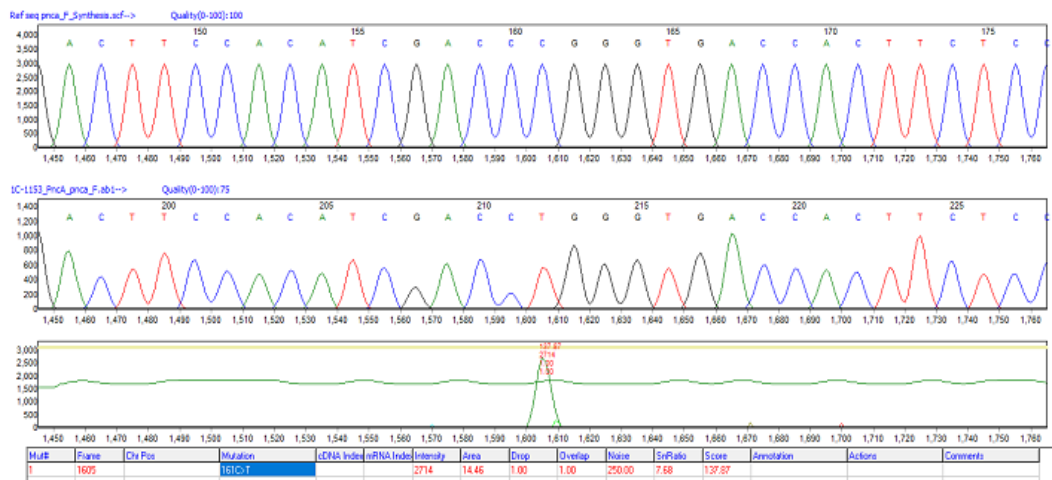
FIGURE A7: Mutation at position 161C-T of *pncA* gene
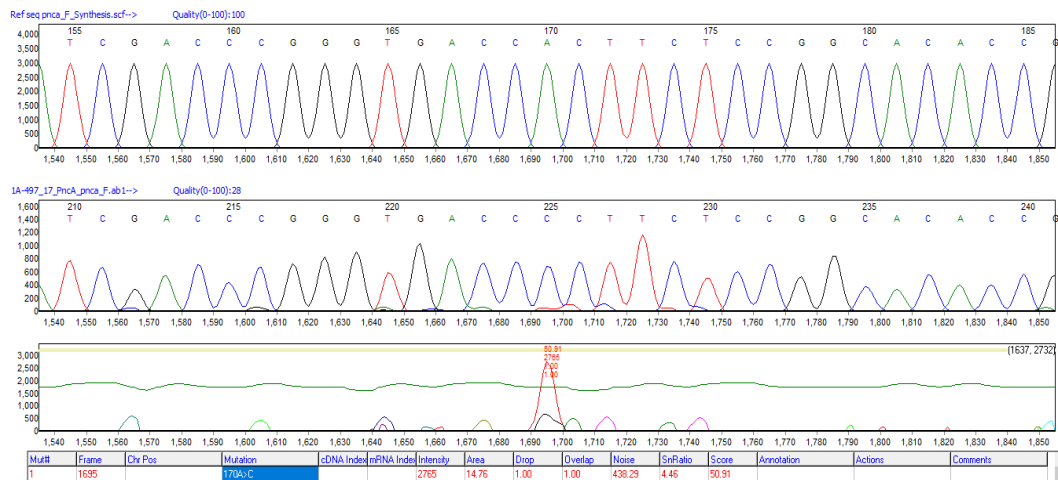
FIGURE A8: Mutation at position 170A-C of *pncA* gene
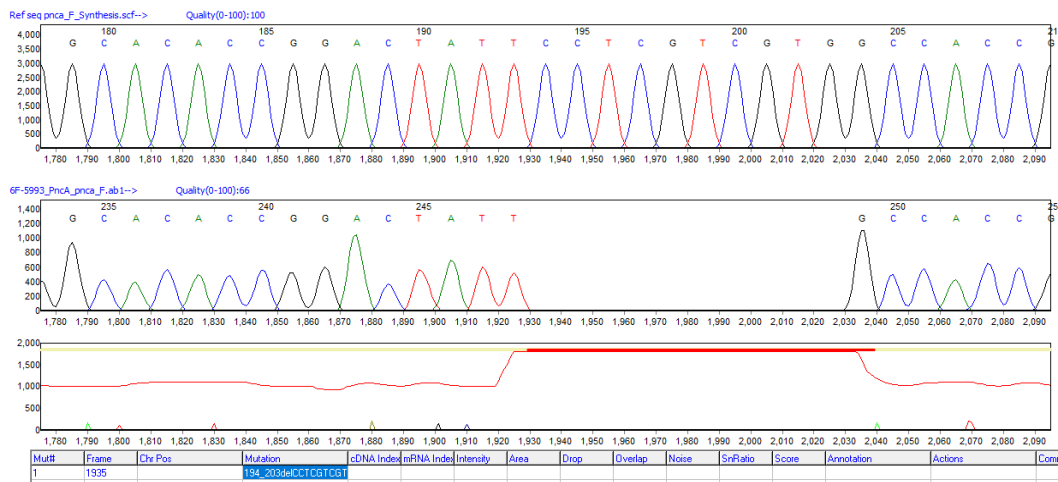
FIGURE A9: Mutation at position 194-203DELCCT of *pncA* gene
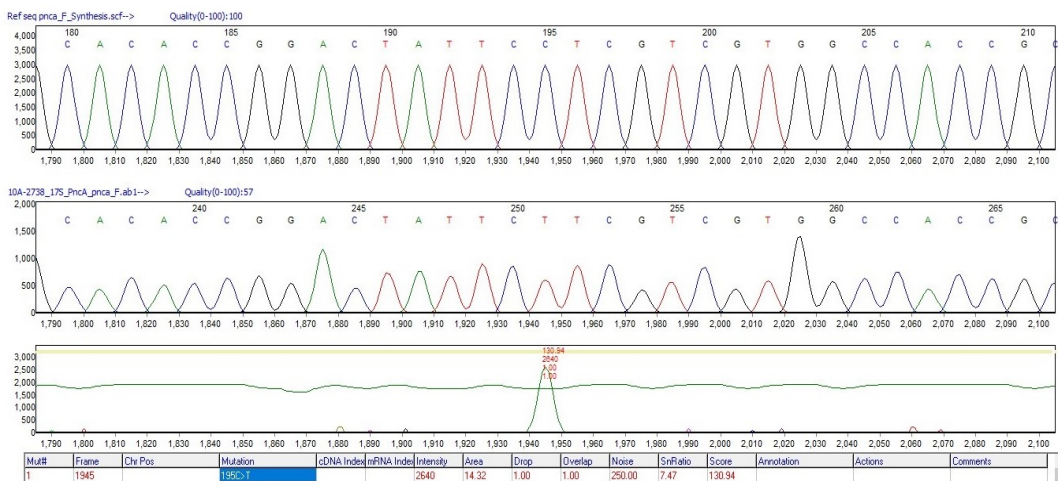
FIGURE A10: Mutation at position 195C-T of *pncA* gene
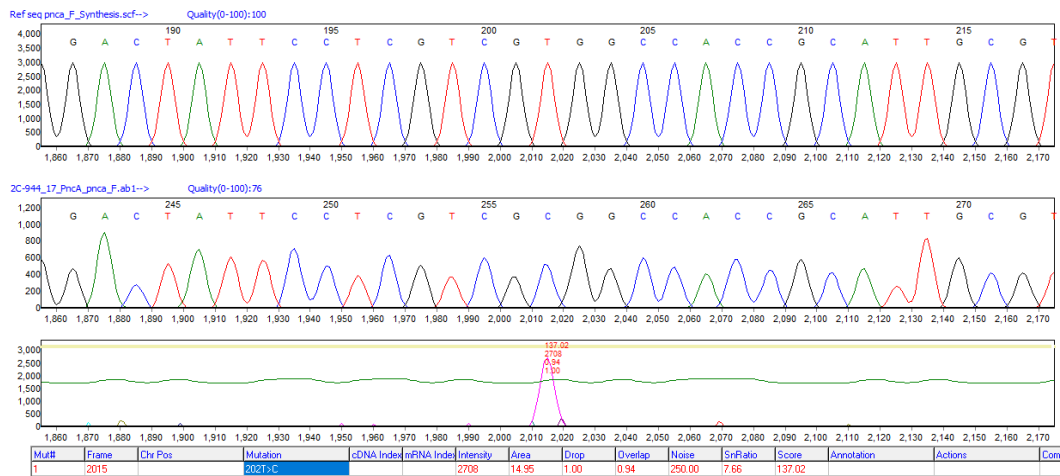
FIGURE A11: Mutation at position 202T-C of *pncA* gene
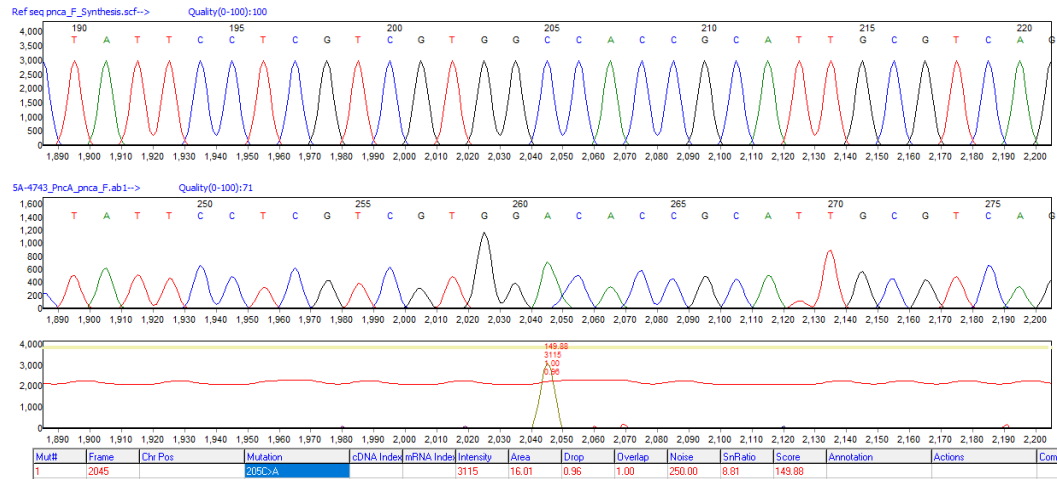
FIGURE A12: Mutation at position 205C-A of *pncA* gene
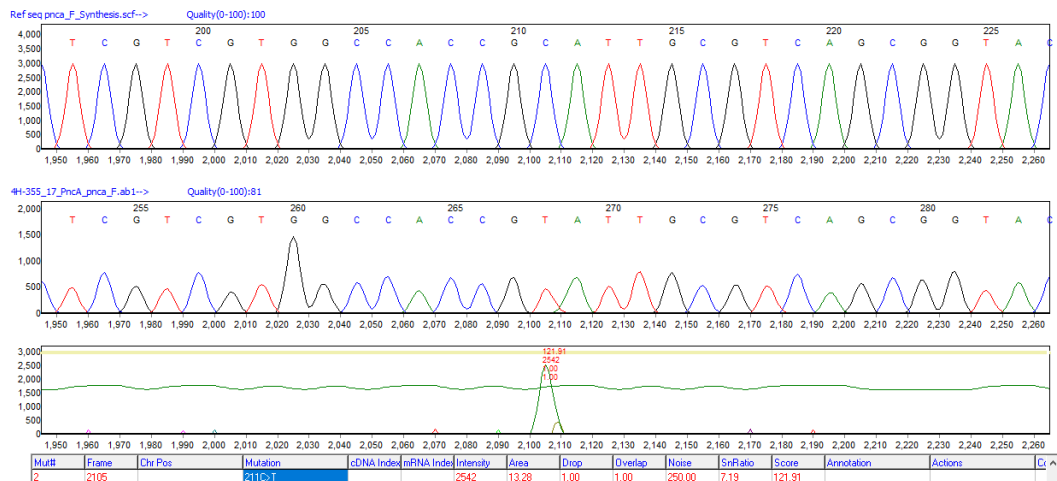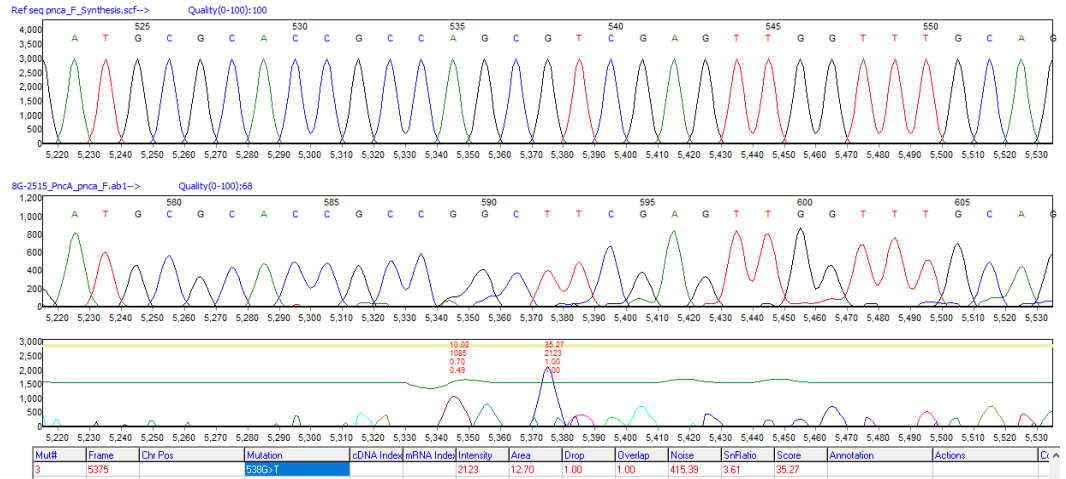

FIGURE A13: Mutation at position 211C-T of *pncA* gene
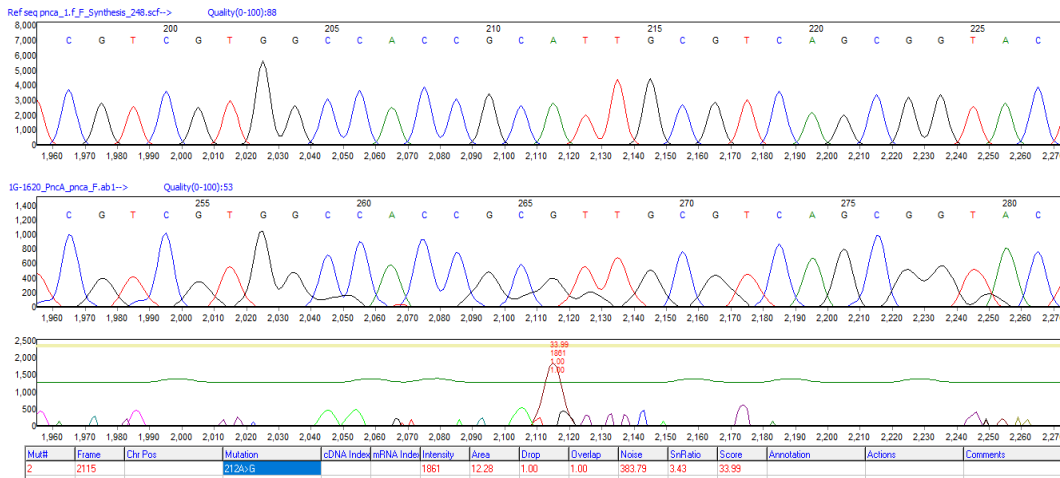
FIGURE A14: Mutation at position 212A-G of *pncA* gene
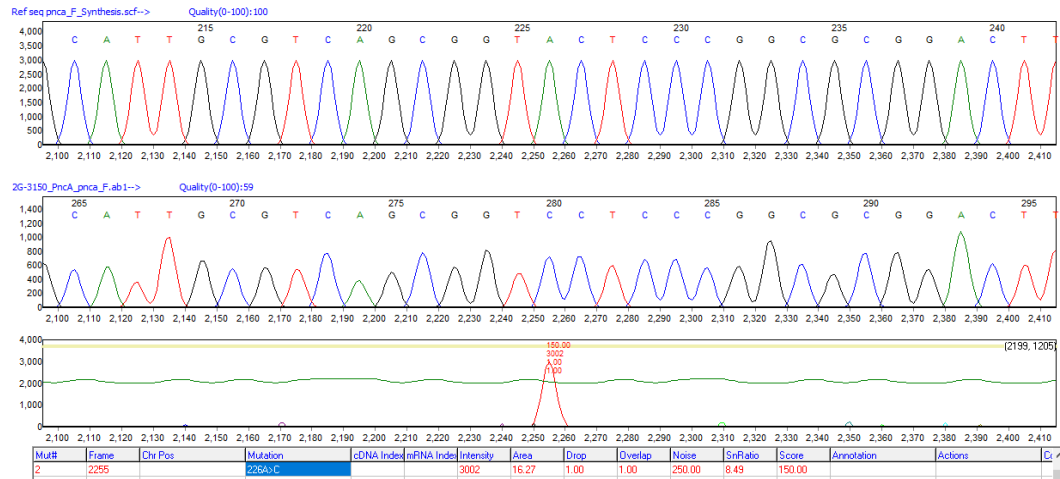
FIGURE A15: Mutation at position 226A-C of *pncA* gene
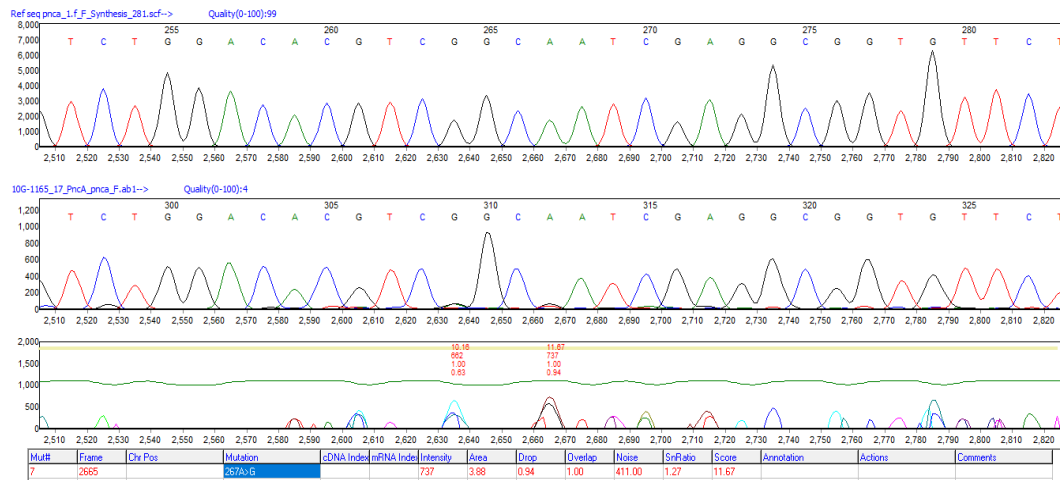
FIGURE A16: Mutation at position 267A-G of *pncA* gene
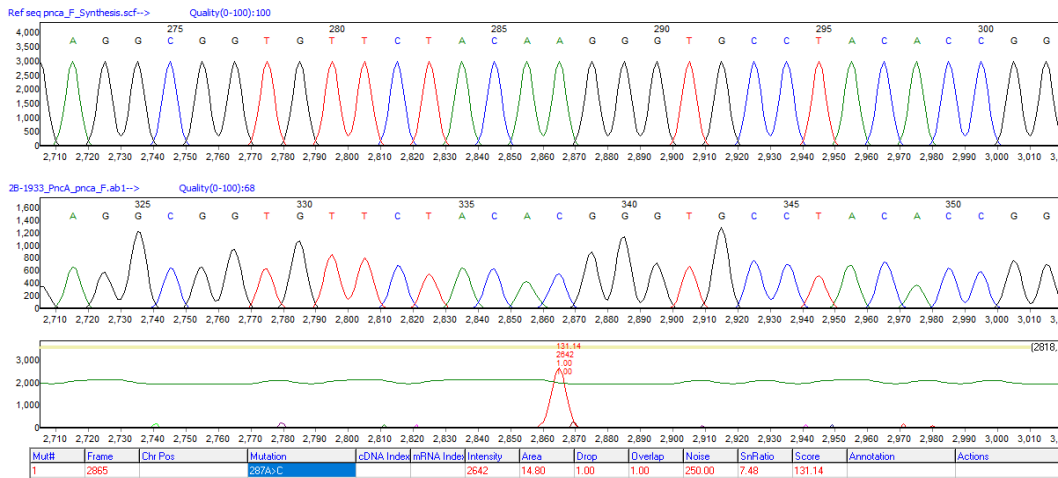
FIGURE A17: Mutation at position 287A-C of *pncA* gene
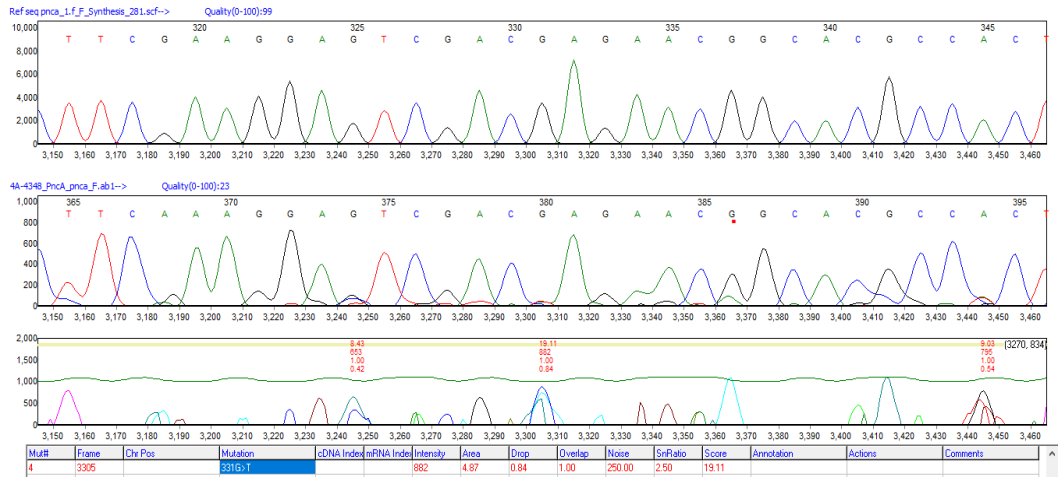
FIGURE A18: Mutation at position 331G-T of *pncA* gene
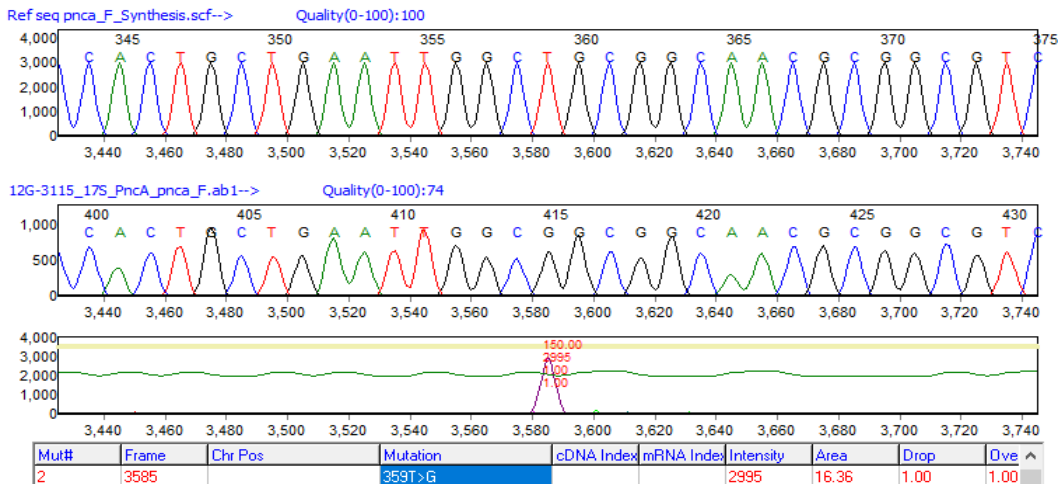
FIGURE A19: Mutation at position 359T-G of *pncA* gene
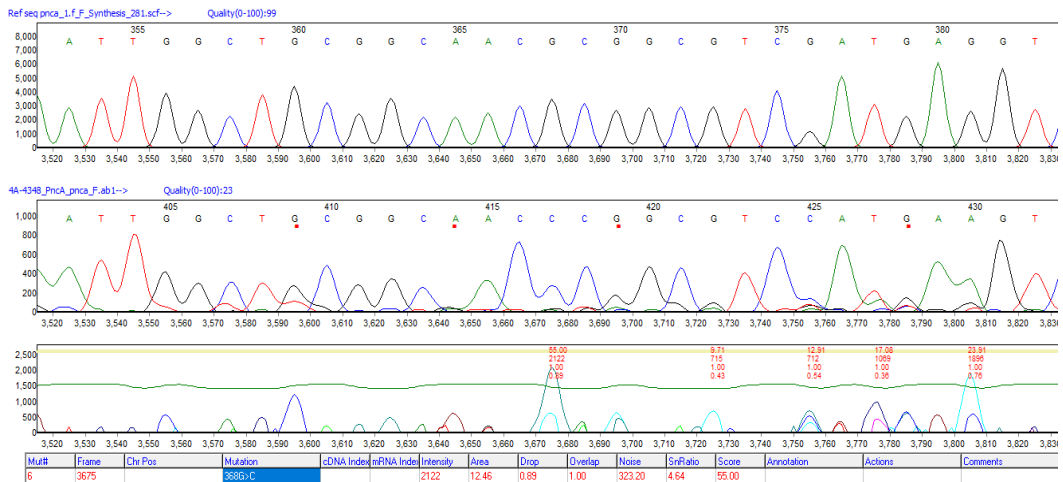
FIGURE A20: Mutation at position 368G-C of *pncA* gene
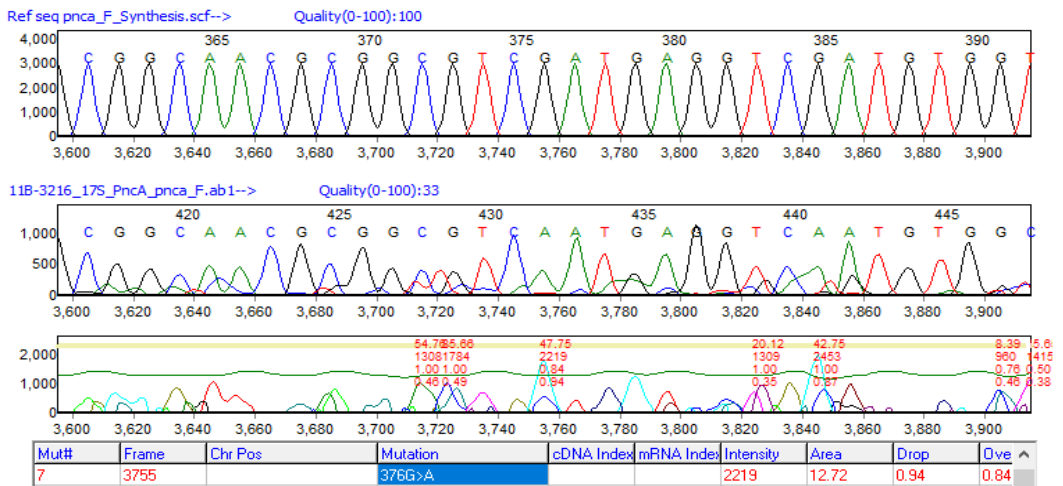
FIGURE A21: Mutation at position 376G-A of *pncA* gene
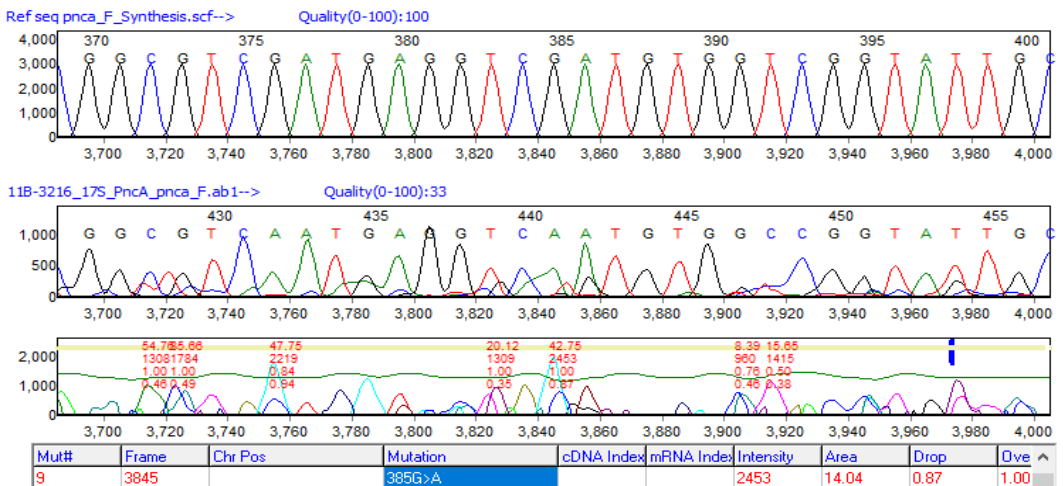
FIGURE A22: Mutation at position 385G-A of *pncA* gene
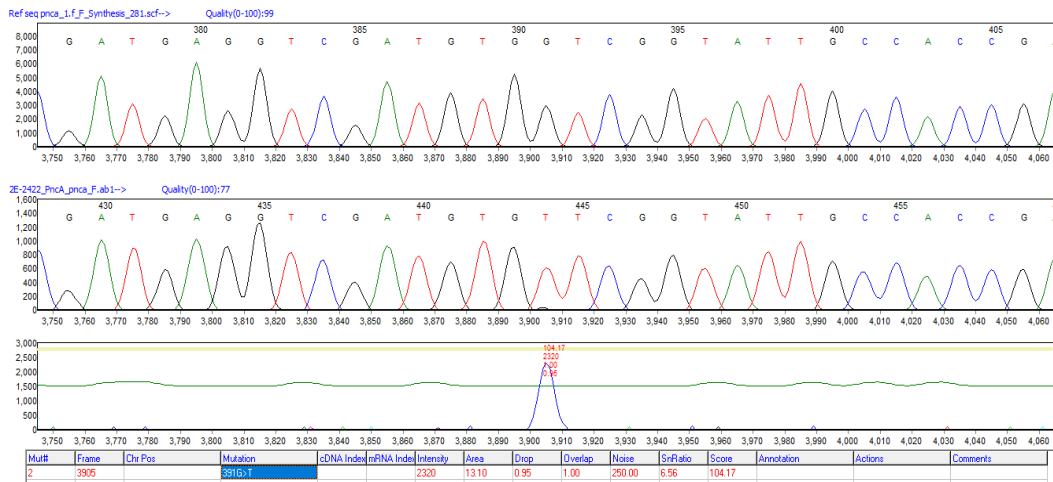
FIGURE A23: Mutation at position 391G-T of *pncA* gene
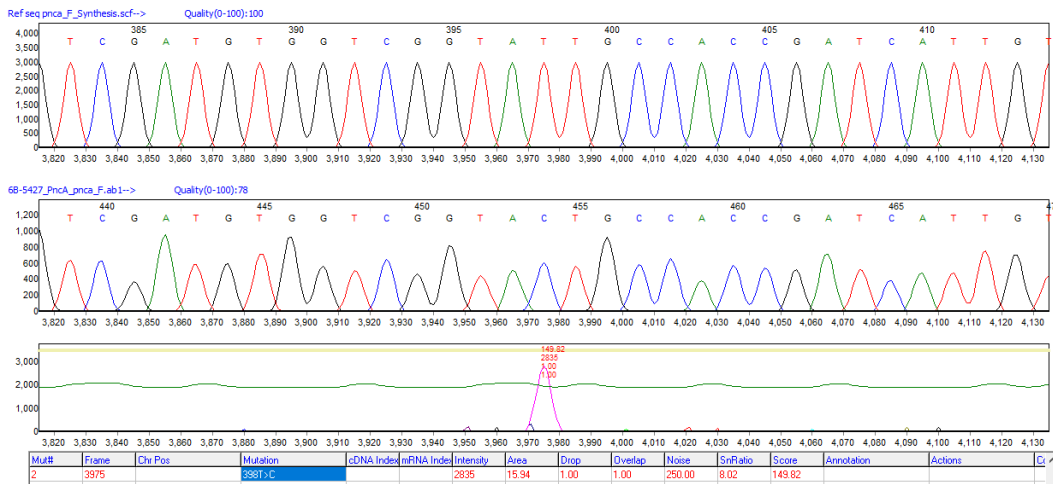
FIGURE A24: Mutation at position 398T-C of *pncA* gene
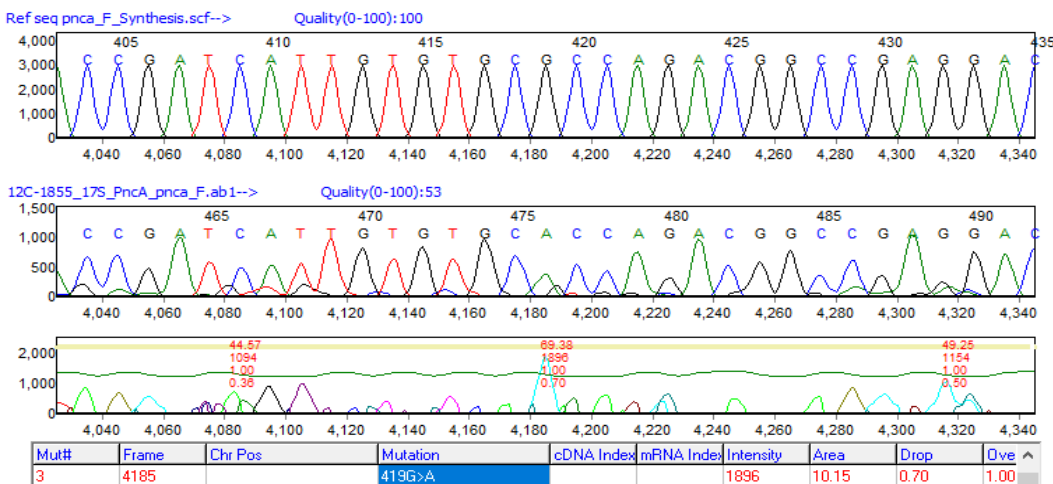
FIGURE A25: Mutation at position 419G-A of *pncA* gene
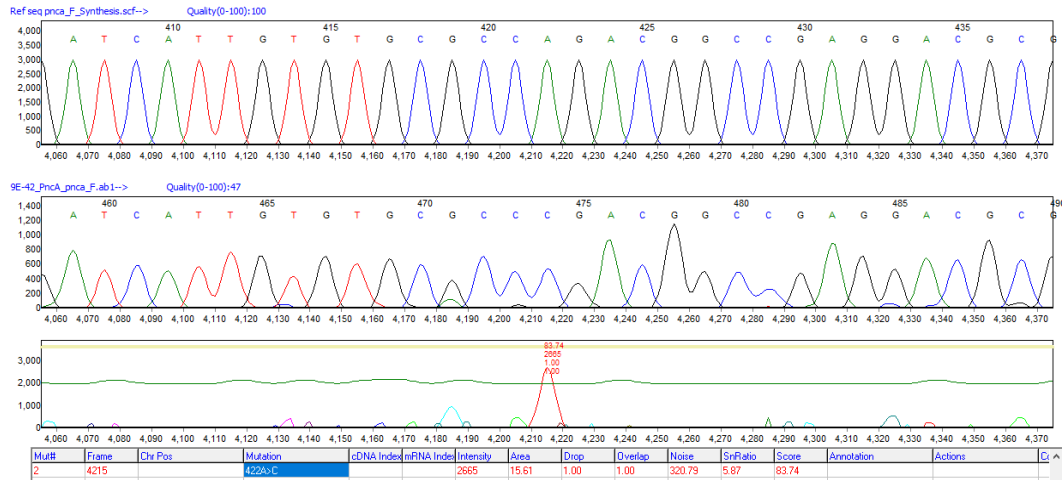
FIGURE A26: Mutation at position 422A-C of *pncA* gene
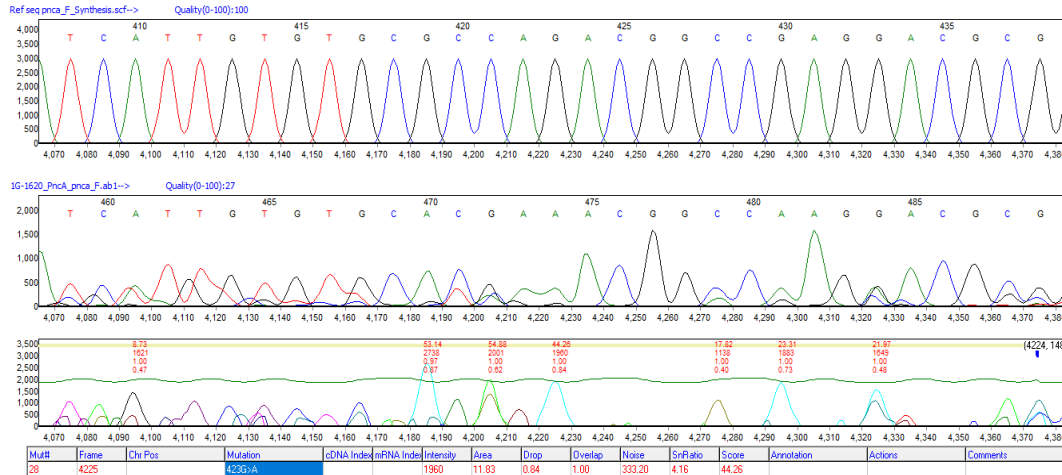
FIGURE A27: Mutation at position 423G-A of *pncA* gene
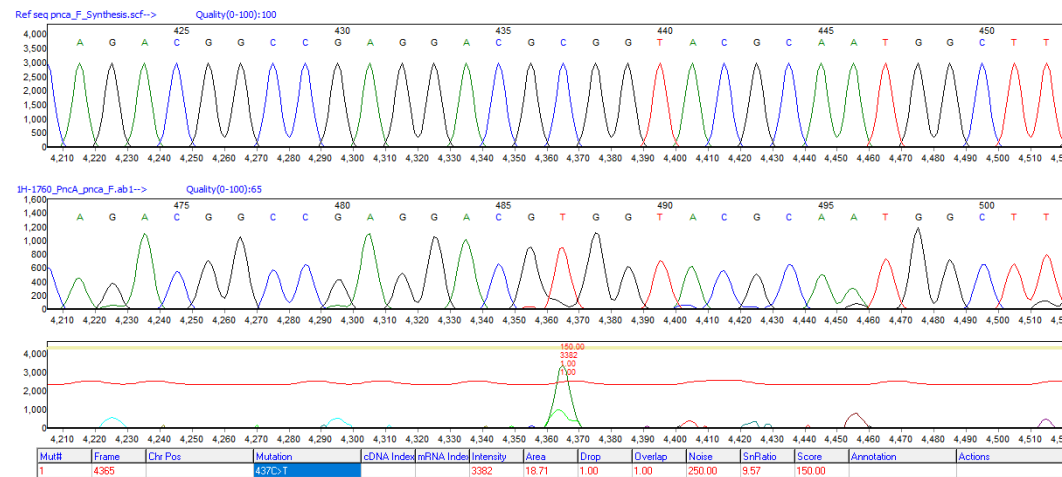
FIGURE A28: Mutation at position 437C-T of *pncA* gene
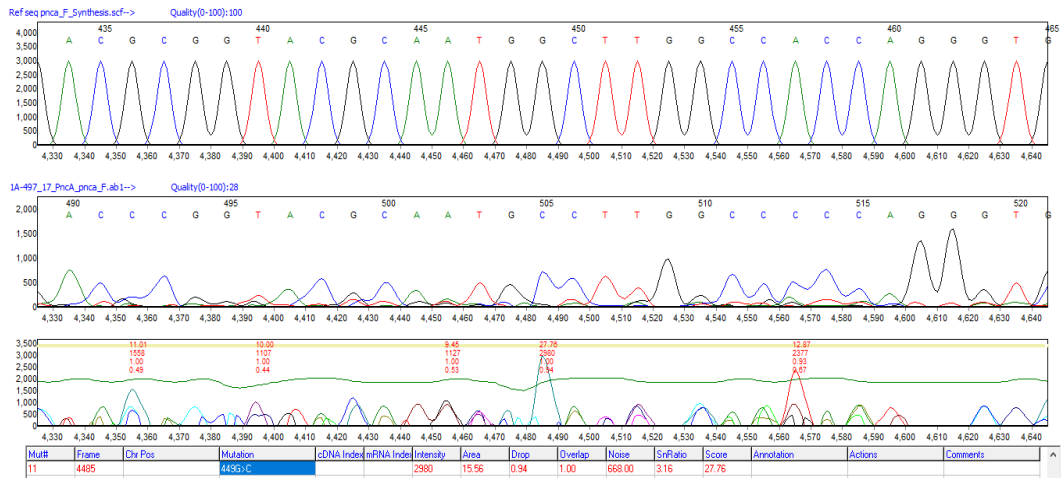
FIGURE A29: Mutation at position 449G-C of *pncA* gene
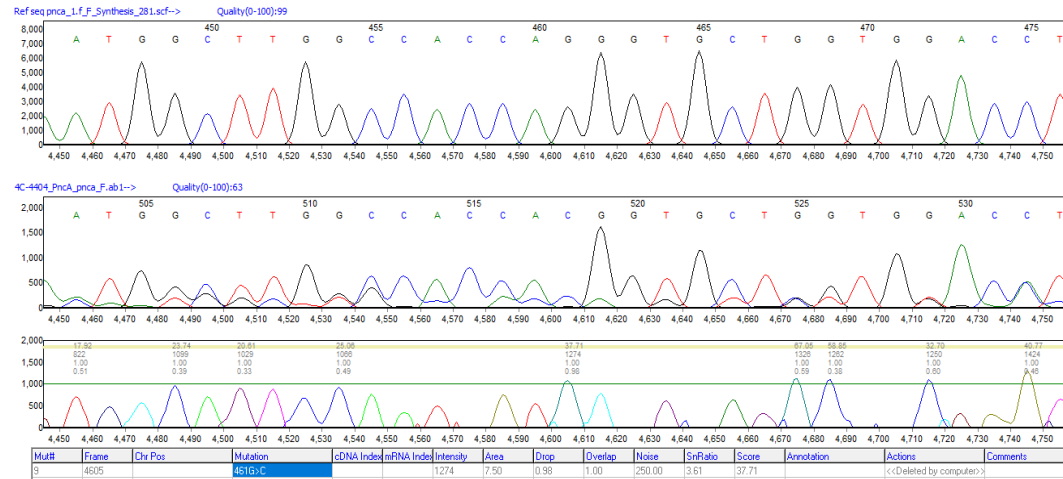
FIGURE A30: Mutation at position 461-C of *pncA* gene
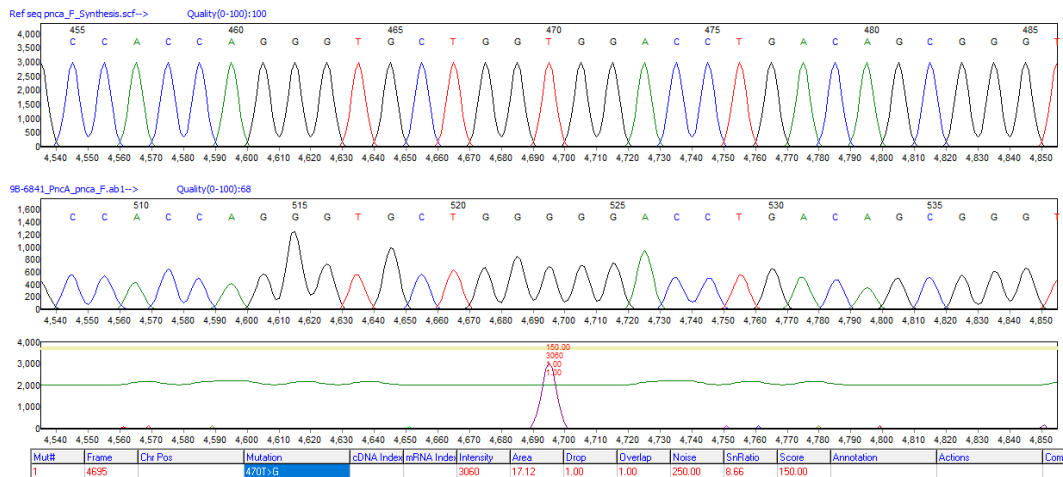
FIGURE A31: Mutation at position 470T-G of *pncA* gene
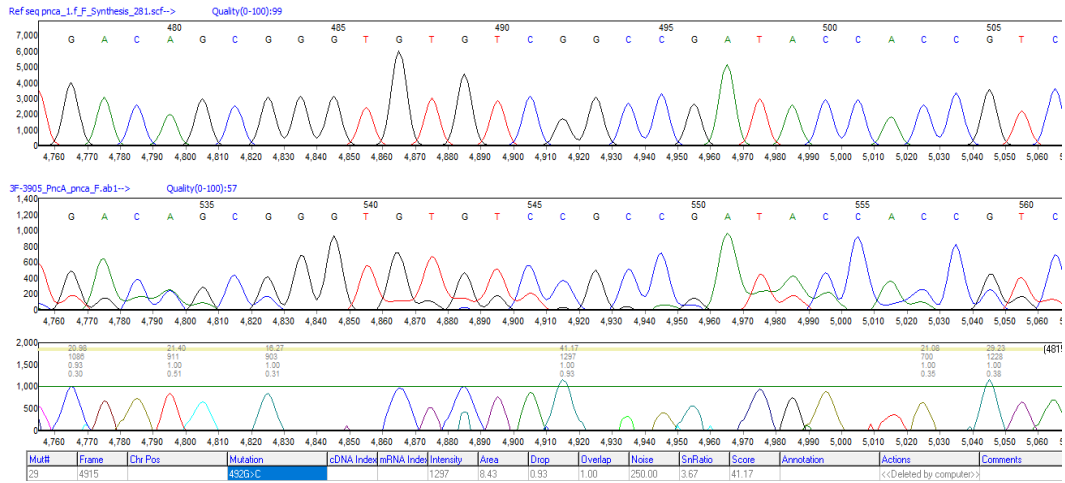
FIGURE A32: Mutation at position 492G-C of *pncA* gene
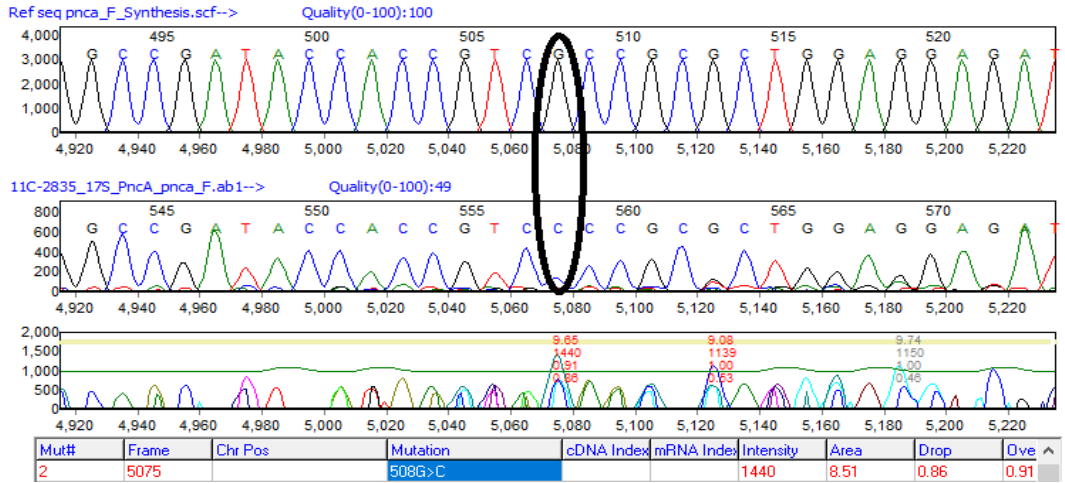
FIGURE A33: Mutation at position 508G-C of *pncA* gene
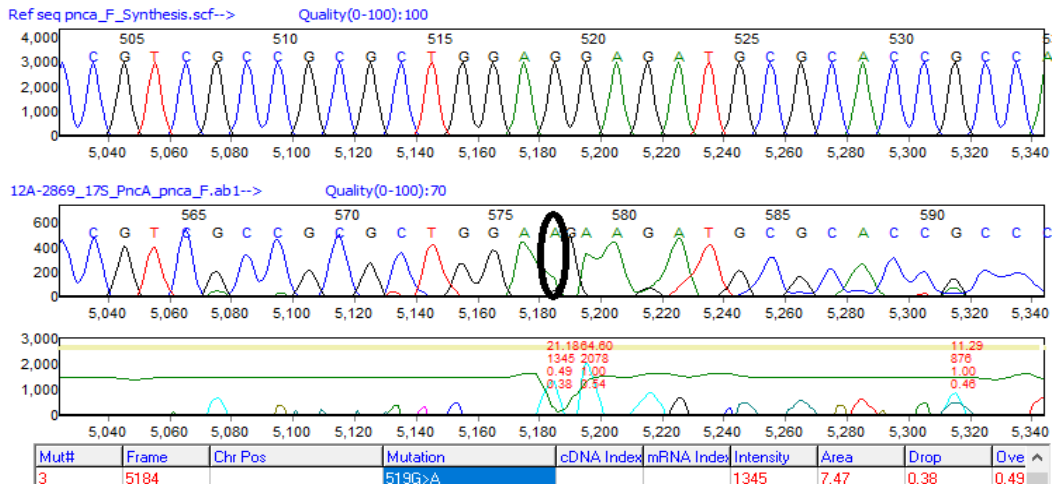

FIGURE A34: Mutation at position 519G-A of *pncA* gene

FIGURE A35: Mutation at position 522G-A of *pncA* gene

FIGURE A36: Mutation at position 530-DEL-C of *pncA* gene

FIGURE A37: Mutation at position 535A-G of *pncA* gene

FIGURE A38: Mutation at position 535A-T of *pncA* gene

FIGURE A39: Mutation at position 538G-T of *pncA* gene
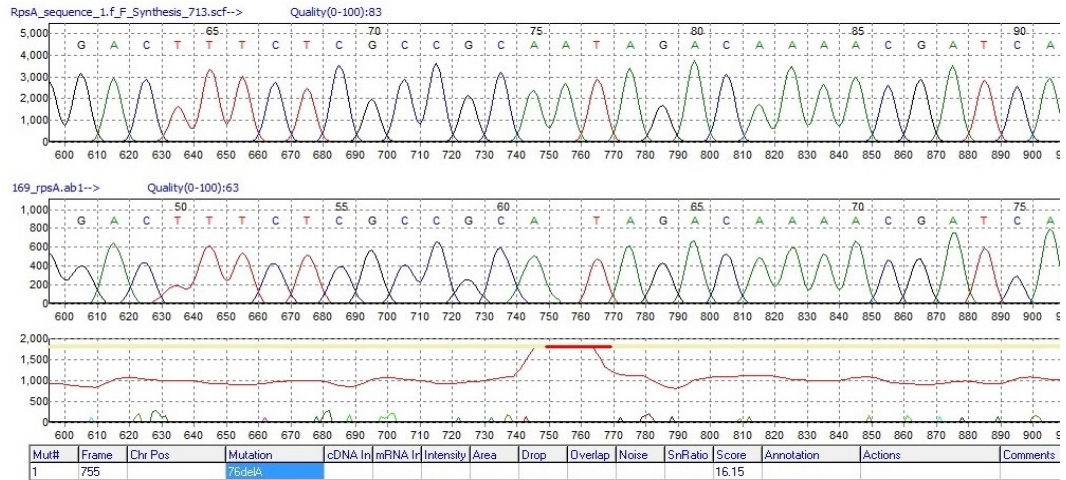
FIGURE A40: Mutation at position 76DelA of *rpsA* gene
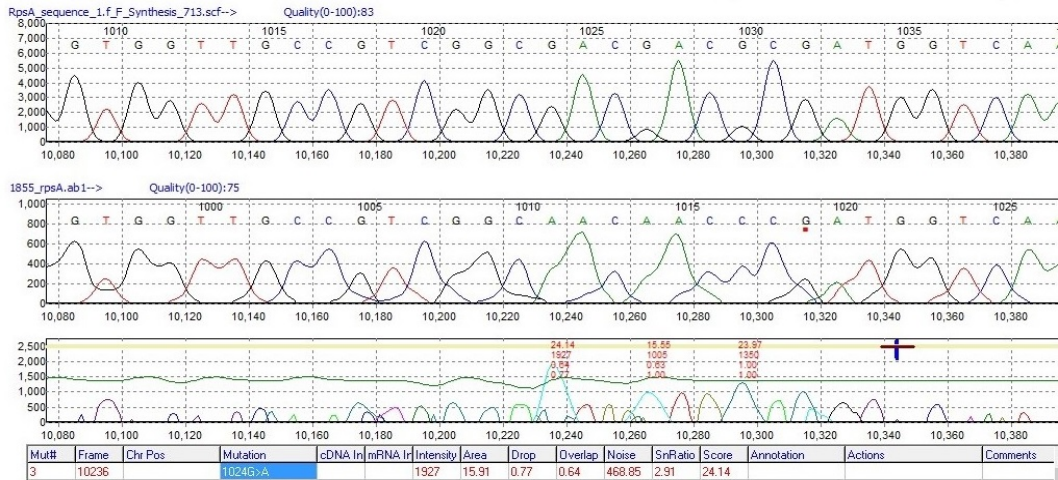
FIGURE A41: Mutation at position 1024G-A of *rpsA* gene
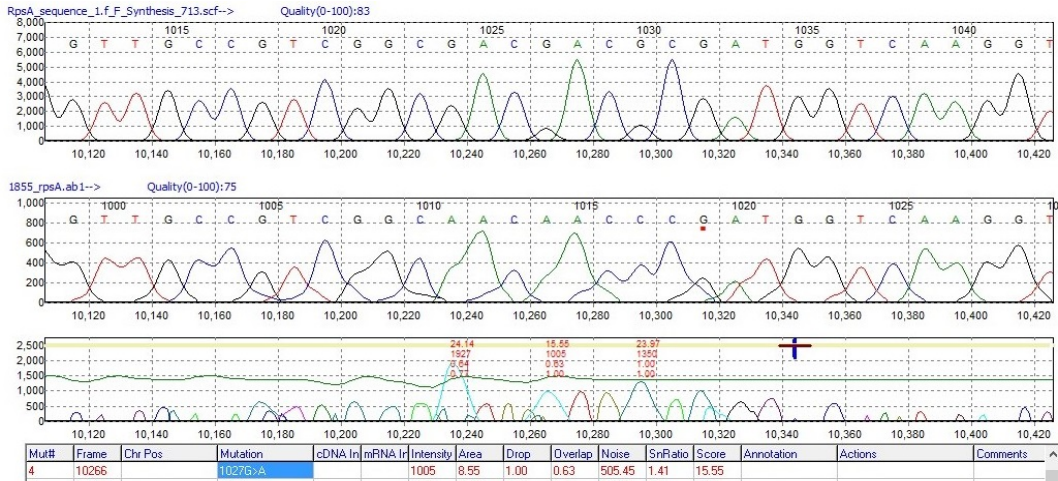
FIGURE A42: Mutation at position 1027G-A of *rpsA* gene
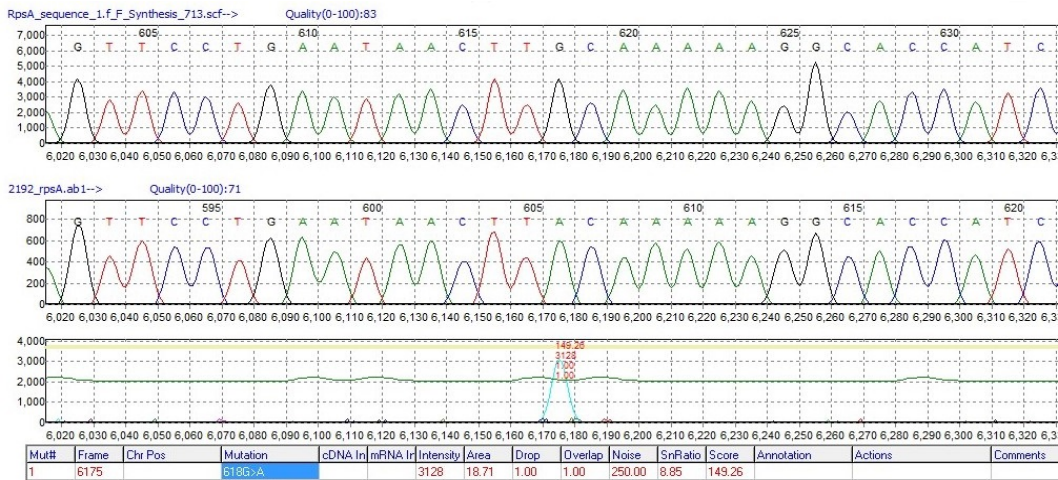
FIGURE A43: Mutation at position 618G-A of *rpsA* gene
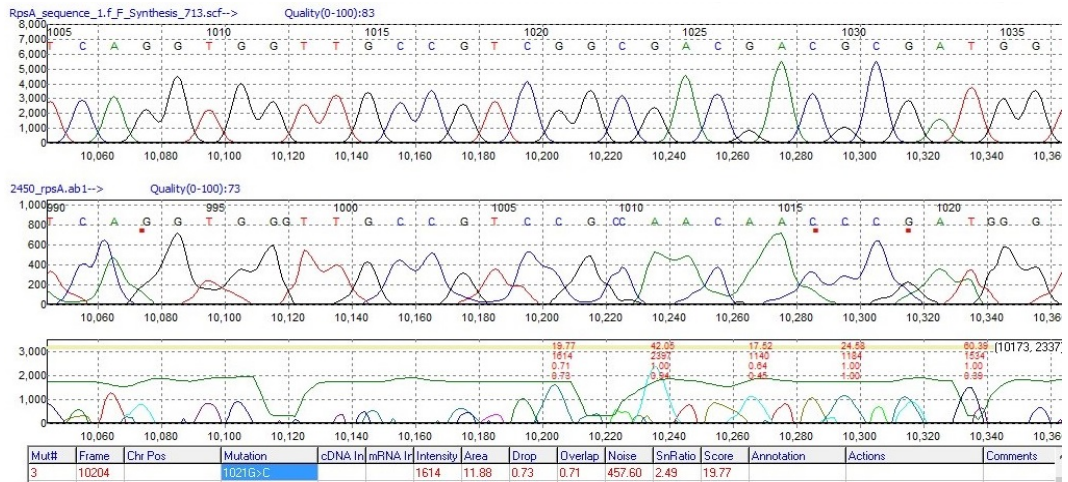
FIGURE A44: Mutation at position 1021G-C of *rpsA* gene
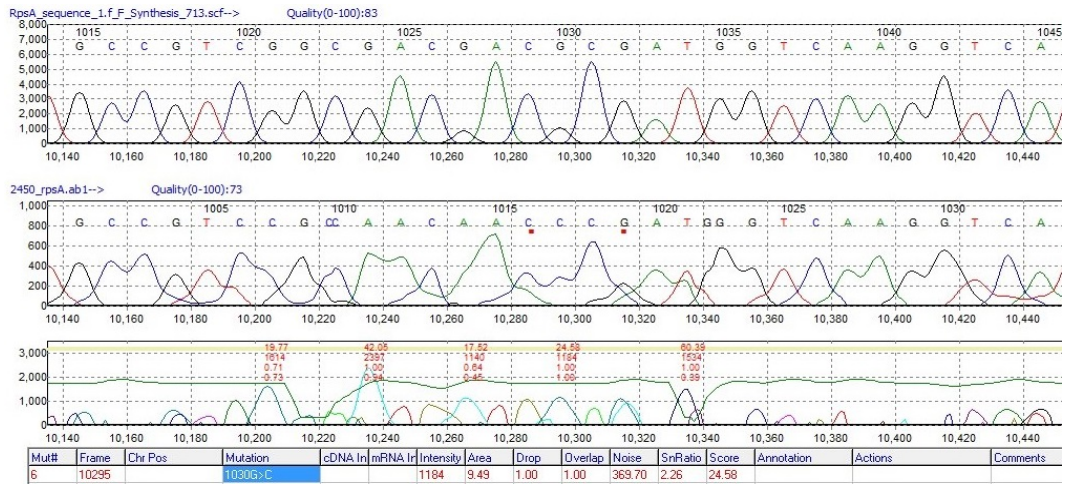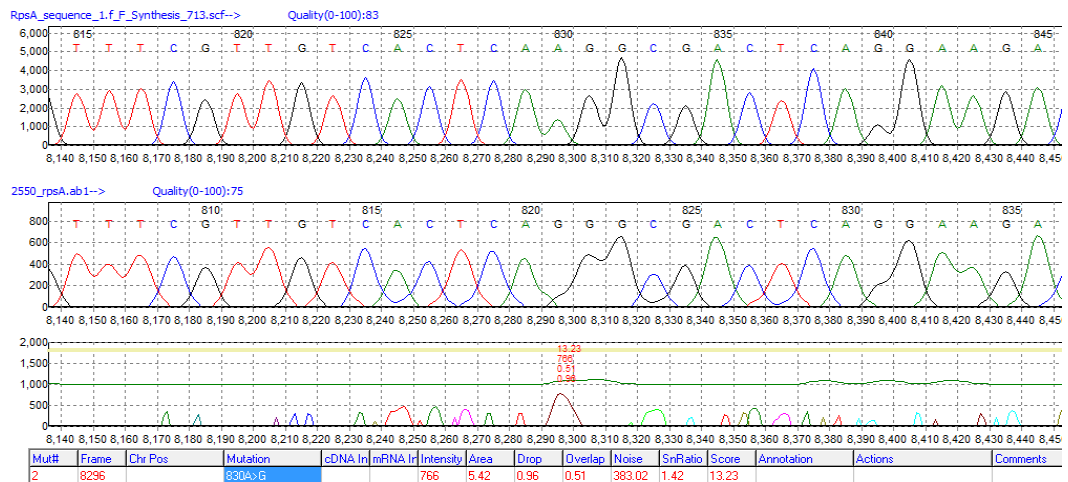

FIGURE A45: Mutation at position 1030G-C of *rpsA* gene

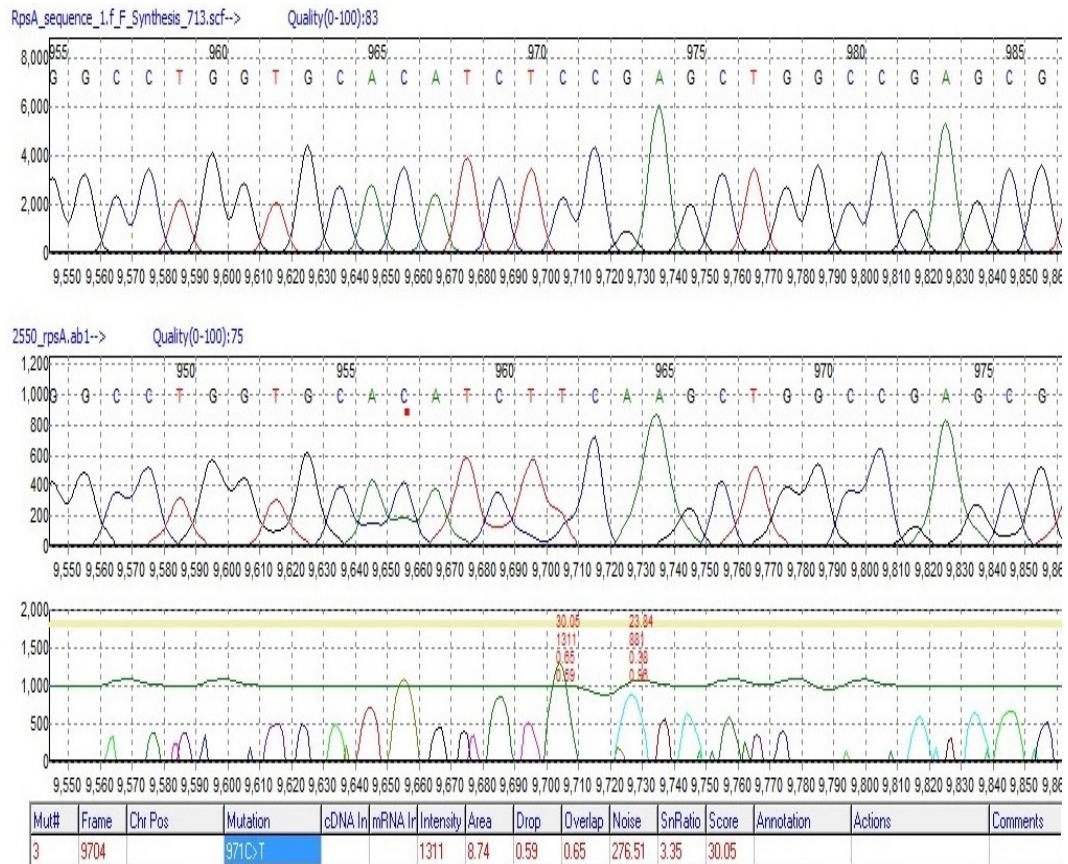FIGURE A46: Mutation at position 830A-G of *rpsA* gene

FIGURE A47: Mutation at position 971C-T and 973G-A of *rpsA* gene
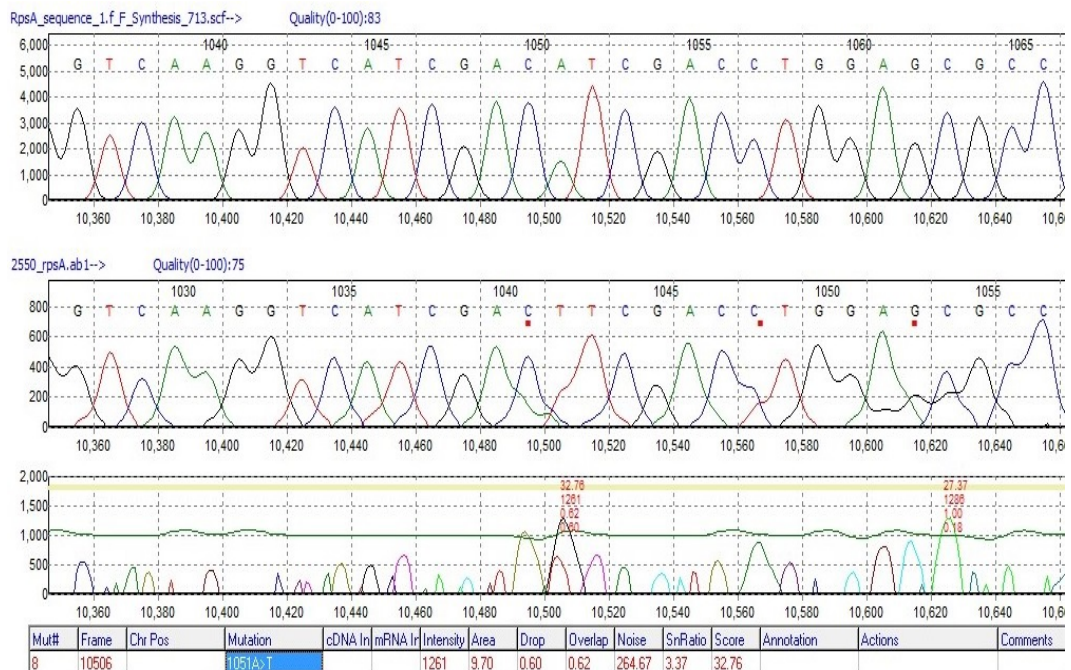

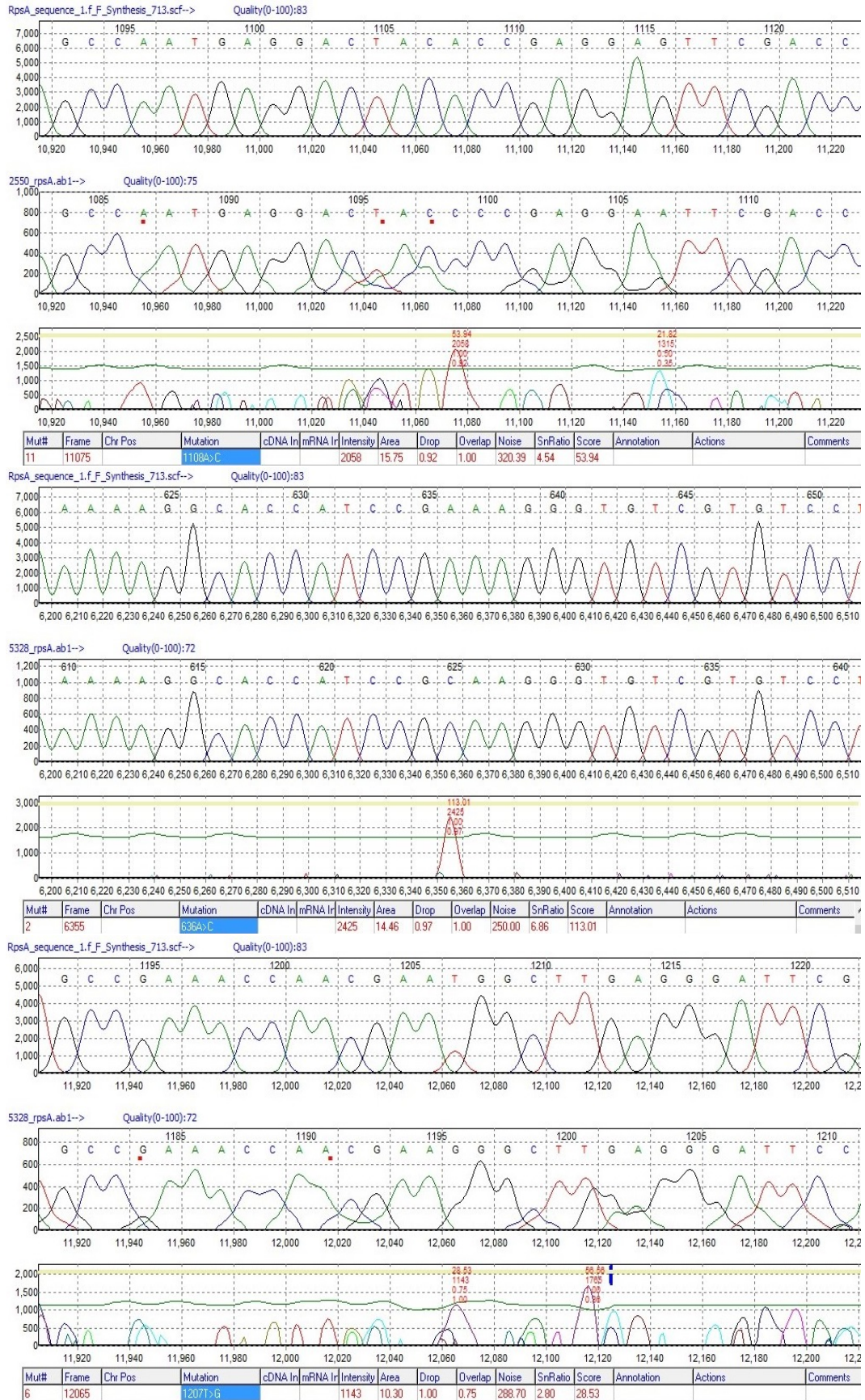FIGURE A48: Mutation at position 1051A-T of *rpsA* gene

FIGURE A49: Mutation at position 636A-C, 1108A-C, and 1207T-G of *rpsA* gene